Thesis presented for the degree of Doctor of Philosophy

Synthesis of heterocyclic analogues of Benzo-TCNQ

Colm Crean
Dublin City University
School of Chemical Sciences

Supervisor: Prof. Albert Pratt

July 2002

Dedicated to my family and friends.

Without whom none of this would have been possible.

I hereby certify that this material, which I now submit for the assessment on the programme of study leading to the award of a Doctor of Philosophy is entirely my own work and has not been taken from the work of others save and to the extent that such work has been cited and acknowledged within the text of my work.

Signed: _____ I.D. No: 96970596

Date: 17/09/02

I would like to thank my supervisor Prof. Albert Pratt for the advice and encouragement he gave me throughout the course of my postgraduate study. Similarly I thank Dr. John Gallagher and Dr. Alan J. Lough (University of Toronto) for the X-ray crystallographic data and Dr. Conor Hogan for his help with the cyclic voltammetry experiments. I would also like to thank the technical staff of the chemistry department, Mick, Damien, Maurice, Veronica, Vinnie, Ambrose and Ann for all their help.

My colleagues both past and present I thank you all very deeply for the support, kindness and patience you have shown me over the years, in particular those who had the misfortune to share a lab with me Ben, Ollie, Mairead, Bronagh, Peter, Davnat, Collette, Orla, Siobhan, Ger, Ray, Ciaran, Cathal, Dave, Darragh, Andrea, Robbie and Nameer. Members of the HVRG from the old days and also from more recent times Christine, Luke, Adrian, Scott, Helen and Marco. Respect to all the lads who played committed indoor football Tuesday and Thursday lunchtimes especially the hardcore Darren, Paddy, Karl, Robbie, Ray, Declan, Cathal, Adrian and Dave. Sundry others include Jenny, Darren, Richard, Rachel, Fran, Lorraine, Mary and Kevin.

I thank all my friends form the Borough for being sound and keeping the good times rolling, in spite of it all. I am eternally grateful to my family Brendan, Carmel, Donal, Declan and Clare for supporting and encouraging me without question over the years. Finally I would like to thank Carol for putting up with me.

Thanks to everybody who deserves a mention but I have forgotten to mention but it is getting late and I just can't think.

All the best,
Colm.

Abbreviations

TCNQ	Tetracyano-p-quinodimethane
TTF	Tetrathiafulvalene
TMDA	N,N,N',N'-tetramethyl-p-phenylenediamine
BEDT-TTF	Bis(ethylenedithio)tetrathiafulvalene
BEDO-TTF	Bis(ethylenedioxy)tetrathiafulvalene
DTEDT	2-(1,3-Dithiol-2-ylidene)-5-(2-ethanediylidene-1,3-dithiol-1,3,4,6-tetrathiopentalene
DDQ	2,3-Dichloro-5,6-dicyano-3,4-benzoquinone
TMTSF	Tetramethyltetraselenafulvalene
TSeF	Tetraselenafulvalene
BETS	Bis(ethylenedithio)tetraselenafulvalene
HMTTeF	Hexamethylenetetratellurafulvalene
TCNEO	Tetracyanoethyleneoxide
CPDT	4-Oxo-2,6-bis(dicyanomethylene)-2,6-dihydrocylopentadithiophene
HMPA	hexamethylphosphoramide
TCNDQ	13,13,14,14-Tetracyanodiphenoquinodimethane
BTDA	Bis(1,2,5)-(thiadiazolo)-tetracyanoquinodimethane
TSDA	Bis(1,2,5)-(thiadiazolo)-(selenadiazolo)-tetracyanoquinodimethane
BSDA	Bis(1,2,5)-(selenadiazolo)-tetracyanoquinodimethane
DCNQI	Dicyano-p-quinodiimine
DEAD	Diethylazodicarboxylate
DIAD	Diisopropylazodicarboxylate

Table of contents

The combination of electron deficient and electron rich species to form charge transfer complexes has led to the observation of conductivity and superconductivity in organic and organometallic systems. Heterocyclic electron acceptors analogous to TCNQ are of particular interest, since heteroatoms can lead to greater planarity, which can increase dimensionality and ultimately improve conductivity.

The reaction of phthalonitrile and aqueous methylamine formed 2-methyl-3-methylimino-2,3-dihydroisoindol-1-one. Analogous reactions with aqueous ethylamine and benzylamine did not yield corresponding products. 1,3-Dialkyliminoisoindolines resulted from the reaction of ethylamine and benzylamine with phthalonitrile. Treatment of 2-methyl-3-methylimino-2,3-dihydroisoindol-1-one in ethanol with malononitrile produced a methylammonium salt while a similar reaction in acetic acid yielded a mono-condensation product 2-(2-methyl-3-oxo-2,3-dihydro-isoindol-1-ylidene)-malononitrile. An analogous mono-condensation product was obtained from 1,3-diethyliminoisoindoline and malononitrile in acetic acid.

The Mitsunobu reaction of 2-(3-dicyanomethylene-2,3-dihydro-isoindol-1-ylidene)-malononitrile with activated primary alcohols generated the desired N-alkylated tetra-cyano isoindolines. Similarly the Mitsunobu reaction of 2-(3-oxo-2,3-dihydro-isoindol-1-ylidene)-malononitrile with various alcohols produced the desired N-alkylated products. The presence of a carbonyl group meant that 2-(3-oxo-2,3-dihydro-isoindol-1-ylidene)-malononitrile would react with more alcohols than its tetra-cyano analogue. Treatment of 2-(3-oxo-2-pentyl-2,3-dihydro-isoindol-1-ylidene)-malononitrile and 2-(3-oxo-2-decyl-2,3-dihydro-isoindol-1-ylidene)-malononitrile with titanium tetrachloride and bis(trimethylsilyl)carbodiimide gave compounds that possessed both a dicyanomethylene group and a cyanoimino group.

Cyclic voltammetric analysis of these three families of compounds showed that they were all electrochemically reducible. Solid charge transfer complexes were formed between TTF and the N-alkylated tetra-cyano isoindolines and between TTF and N-alkylated isoindolines that contained a dicyanomethylene and a cyanomino group. X-ray crystallography showed that the CT complex between 2-(2-allyl-3-dicyanomethylene-2,3-dihydro-isoindol-1-ylidene)-malononitrile and TTF had a mixed stack arrangement.

Chapter 1
Introduction

1.1 General Introduction

Lightweight materials with reasonable electrical conductivity and relatively high temperature superconductivity are of great synthetic interest. Superconductivity is conductance without resistance. This phenomenon if properly harnessed could yield the perfect engine, providing a driving force that is not dissipated over time.

An area which has shown some promise is that of organic metals. Organic metals are conducting polymers or conducting charge transfer (C-T) complexes. These compounds share one important property with metals; they have partially filled delocalised bands. However they have conductivities which are very small compared to copper metal (circa 10^6 Scm^{-1}).

The first organic compound to show interesting electrical properties, was the bromine-perylene complex (1).[1]

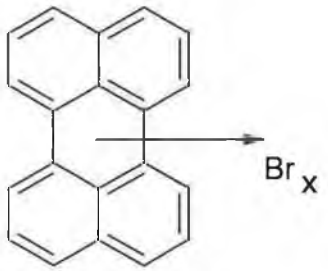

(1)

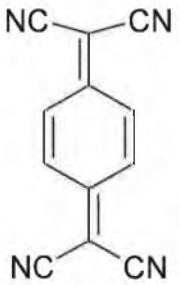

TCNQ (2)

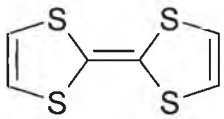

TTF (3)

This was the first time that metallic properties were observed in a material without a metal atom in it. The instability of complex (1) meant that the truly ground breaking discovery was not made until 1973,[2] when the C-T complex of TCNQ (2)[3] with TTF (3) was synthesised.[4]

Superconductivity was eventually achieved in an organic system by Bechgaard and Jerome (more detailed discussion later).[5] More recently the discovery of buckminsterfullerene C_{60} (4)[6] has stimulated a lot of interest. Metallic properties were found when alkali-earth metals were used to dope C_{60} solids in order to introduce electron carriers with superconductivity being achieved with potassium doped C_{60}.[7]

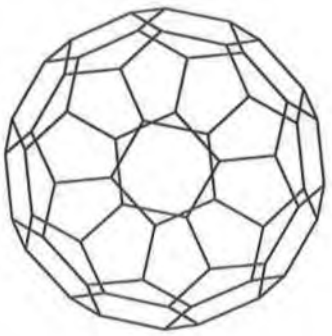

C_{60} Buckminster fullerene.

1.2 Conductivity in a solid

Band theory provides a vital insight into how crystalline materials behave when subjected to an electric field. Consider a large number (N) of identical atoms, far enough apart so their interactions are negligible. Every atom has the same energy level diagram. This energy level diagram shows the possible quantum states for the electrons and their associated energy levels. Each energy level is filled according to the Pauli exclusion principle (lowest levels filled first).

If the atoms are pushed together, because of the electronic interactions and the exclusion principle the energy levels change. Some move to higher energy and some move to lower energy. Each valence electron state for the system, formerly a sharp energy level that could accommodate N electrons, becomes spread out into a band containing N closely spaced levels. Since N is usually very large (circa 10^{23}), the energy levels form a continuous distribution of energies within a band. The higher energy levels form the conduction band (LUMO), while the lower energy levels form the valence band (HOMO). The highest energy state in the valence band is the Fermi level, E_f. The size of the energy gap between these 2 bands governs the conducting ability in crystalline materials.

If the energy gap is large (3-6 eV) between a filled valence band and an empty conduction band the material is considered to be an insulator. If the energy gap is smaller (0.1-1.0 eV) the material is a semi-conductor. If there is overlap between the bands (as in a metal) the material is a conductor. In conjunction with these energy considerations it is

necessary for the material to possess partially filled bands to permit the electrons to move.

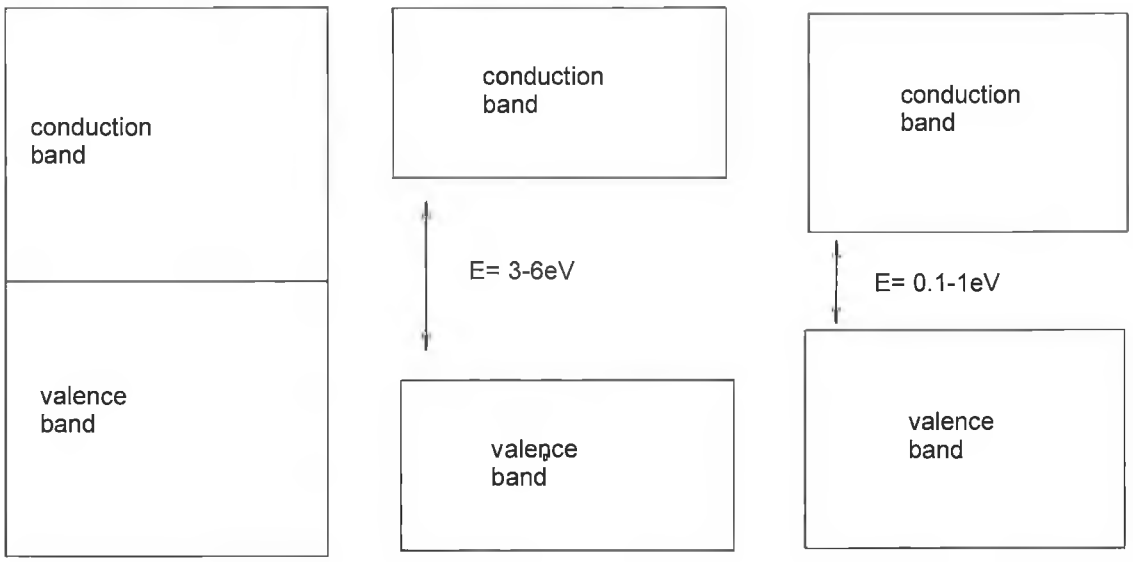

Figure 1.1 Band structure of (a) a metal, (b) an insulator and (c) a semi-conductor

The extent of occupation of the energy levels and the size of the band gap regulate the electrical properties of a crystalline material. This means that target materials to be designed and synthesised need to possess partially filled delocalised bands, similar to those found in a metal. This situation arises on occasion when planar conjugated molecules crystallise in a stack as with charge transfer complexes. In these complexes the transfer of electrons between donor and acceptor stacks provide the means for the formation of partially filled bands.

1.3 Charge Transfer Complexes

C-T complexes are a special case where metallic-like conductivites are obtained from essentially non-metallic, covalent, organic molecules. A C-T complex is formed by the interaction of an electron donor (D) and an electron acceptor (A). Electron donors are

compounds with low ionization potential, while electron acceptors are compounds with high electron affinity. The donor and acceptor are bound together by an electrostatic attraction, not a chemical bond. Partial electron transfer between the donor molecule and the acceptor molecule generates this electrostatic attraction. The "bonding" in these complexes can be expressed satisfactorily by equation 1.

$$D + A \rightarrow [A, D] \leftrightarrow [A^-, D^+].$$ Equation 1

The structure of C-T complexes was explored by Mulliken.[8] The ground state for a complex, $\Psi_N(D, A)$ is a combination of "no-bond" structure, $\Psi_N(D, A)$ and a dative bond structure, $\Psi_N(D^+, A^-)$. The "no-bond" structure describes dipole-dipole interactions and other intermolecular interactions. The "dative bond" structure arises when there is complete electron transfer from the donor to the acceptor. Therefore the ground state of the complex, $\Psi_N(D, A)$, can described by equation 2.

$$\Psi_N(D, A) = a\Psi_N(D, A) + b\Psi_N(D^+, A^-).$$ Equation 2.

Similarly the excited state of the complex can be described by equation 3.

$$\Psi_E(D, A) = a^*\Psi_E(D, A) + b^*\Psi_E(D^+, A^-).$$ Equation 3.

Some C-T complexes exhibit distinctive electronic absorptions in the ultraviolet/visible region. The fact that these new uv-vis absorptions are very different to either of the component molecules means that uv-vis spectroscopy is widely used as a means of testing for charge transfer. Mulliken proposed that the absorptions were due to the transfer of electrons from the HOMO of the donor to the LUMO of the acceptor.

The ionization potential of the donor and the electron affinity of the acceptor govern the degree of charge transfer. The ideal situation is to have partial electron transfer. This can be achieved when both the electron acceptor and electron donor constituents have moderate electron affinity and ionization potential respectively. When TCNQ reacts with alkali earth metals semi-conducting radical ion salts of general

formula $M^{+}TCNQ^{-}$ result. The low ionization potential of the metal means that there is complete electron transfer leading to an ionic ground state. An ionic ground state favours an insulator state. Therefore it is desirable to avoid compounds with extreme values of either ionization potential or electron affinity. Torrance[9] has catalogued the ionization potentials and electron affinities of numerous donors and acceptors.

Ionization potential (I) is not directly measurable experimentally, but is proportional to the measurable, electrochemical reduction potential (Ep) in solution

Another major requirement for C-T complexes to be conductive is that the constituent donor and acceptor molecules must crystallise as solids made up of segregated stacks of donors and acceptors. It is also possible for complexes to form mixed stacks. When this is the case the material will be a semi-conductor at best. Both systems are shown below.

A D A D	A D A D
A D A D	D A D A
A D A D	A D A D
A D A D	D A D A
(a) segregated stacks.	(b) mixed stacks.

These molecular complexes are considered to be one-dimensional conductors, the electrons finding a path through the partially filled delocalised π-orbitals between molecules down a stack. There is very little interaction between the stacks for these particular complexes

To conduct electricity down a mixed stack, an unpaired electron would have to jump from an acceptor molecule to a donor molecule. By definition electron acceptors have high electron affinity and would be reluctant to lose an unpaired electron. This acts as a large activation barrier to conduction. It is possible to raise the conductivity of mixed stack materials to a maximum value by providing extra thermal energy, increasing conductivity with increasing temperature being classic semi-conducting behaviour.

On the other hand, when a complex is made up of segregated stacks, there is no major energy barrier for the unpaired electrons to overcome and it is relatively easy for

charge to move down an acceptor stack. However if charge transfer is complete, coulombic repulsion U may affect the conductivity of the complex. Coulombic repulsion U is the repulsive force between the indigenous electrons of the acceptor's π-orbital and the newly arrived unpaired electron. If U>>4t (where 4t is the bandwidth of the conduction band) the molecule is said to be a Mott-Hubbard insulator. This situation arises when it is energetically unfavourable for 2 electrons to occupy a particular energy level and all available energy levels are therefore singly occupied. With partial electron transfer, the valency of the molecules within a stack is effectively mixed and there will be neutral acceptor molecules, which can readily accommodate an extra electron.

1.4 Stoichiometry

C-T complexes also have definite stoichiometric ratios between donor and acceptor molecules. For example TCNQ (2) forms a 1:1 complex with TTF (3) and a 2:1 salt with N,N,N',N'-tetramethyl-p-phenylenediamine (TMDA) (5).[10]

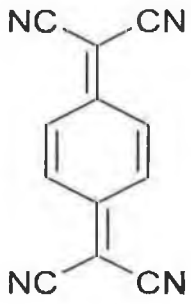

TCNQ (2)

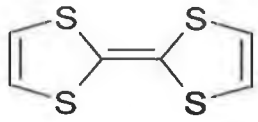

TTF (3)

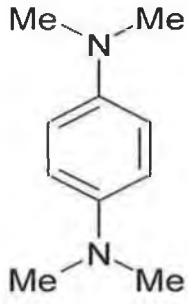

TMDA (5)

1.5 Unidimensionality and inherent lattice instabilities

Partially filled delocalised bands are responsible for conduction in organic C-T complexes. For complexes of segregated stacks, the overlap of the π-orbitals provides the necessary pathway for the movement of electrons. This means that the propagation of charge is inherently one-dimensional, unlike in a metal with electrons in this system unable to move in 3-dimensions. Organic C-T complexes are therefore sometimes referred to as pseudo or quasi one-dimensional conductors.

Lattice instabilities and lattice defects play a large role in dictating how the conductivity is affected by changes in temperature and pressure. There are 2 main lattice instabilities associated with organic C-T complexes; charge density waves (CDW) and spin density waves (SDW).

1.5.1 Charge density waves

Peierls distortions[11] or charge density waves[12] ruin the degeneracy of the Fermi level, E_f. The subsequent energy gap ends metallic conduction. This lattice instability is very similar to the Jahn-Teller effect experienced by cyclobutadiene. The Huckel π molecular orbitals for cyclobutadiene can be seen below.

Figure 1.2

Having two degenerate singly occupied orbitals is not the most energetically favourable state. The symmetry lowering deformation breaks the orbital degeneracy, stabilising one and destabilising another and the newly stabilised orbital contains two electrons. The new situation can be seen in figure1.2.

This distortion localises the double bonds. When this type of distortion occurs in a C-T complex it can open a band gap at the Fermi level, and hence impede conduction. When a material is cooled the frequency of the lattice vibration decreases, reducing the repulsion between electrons and making it easier for electrons to doubly occupy a certain orbital. If this situation is repeated throughout the crystalline material, regions of higher and lower charge density occur. These regions generate charge density waves (CDW).

The interaction of electrons and phonons (lattice vibrations) increases lattice strain and therefore increases the energy of the system. The Peierls transition analogous to the Jahn-Teller effect lowers the energy of the system at a cost of reducing the conductivity of the material. This behaviour means organic C-T transfer complexes have a "temperature window" through which they behave as conductors. This window is bounded by T_{M-I}, the metal to insulator transition temperature. Coincidentally the formation of "electron pairs" at low temperatures is a vital prerequisite for materials to exhibit superconductivity.

1.5.2 Spin density waves (SDW)

A Metal-Insulator transition is also caused by spin density waves. Electrons with the same spin oppose one another but pair up with electrons of opposite spin. When electrons arrange themselves in such a way (spin up, spin down) they are ordered, anti-ferromagnetically. The anti-ferromagnetic phase is insulating, due to its periodicity, which destroys the Fermi surface. Spin density waves are responsible for metal to insulator transition in some Bechgaard salts[13] formed with octahedral anions

1.6 Superconductivity

Superconductivity is the ability of a material to conduct electricity without resistance. A current set up in a superconductor is not dissipated as heat, but will continue forever. Onnes first discovered superconductivity in 1911 when mercury was cooled to circa 4K. Superconductors exhibit perfect diamagnetism. This means that

superconductors are impermeable to an external magnetic field, for example a magnet will float over a superconductor.

1.7 BCS Theory of superconductivity

Bardeen, Cooper and Schrieffer proposed the BCS Theory for superconductivity.[14] This theory states that below a certain critical temperature (T_c) electrons form Cooper pairs and a superconducting state ensues. More energy is required to impede Cooper pairs compared with single electrons. At low temperatures there is insufficient energy available to scatter these Cooper pairs, therefore electrical resistance disappears.

As an electron passes through the extended molecular orbitals of a solid material, it can exert an attractive force on an atom bound within the lattice. This attraction causes the lattice to distort. As the large positive lattice atoms move closer together a region of excessive positive charge is created. This transient region of positive charge attracts a further electron. The lattice vibration has linked these 2 electrons. They now form a Cooper pair.

The lattice atoms will then move apart under the influence of a restorative force. A region with a lower density of charge is then created that Cooper pairs tend to avoid. Consequently the Cooper pair electrons oscillate back and forth. For superconductivity to occur it is essential that a large number of pairs are formed.

Metallic-alloy superconductors only become superconducting at very low temperatures. It was thought that organic superconducting materials could considerably raise the critical temperature. Since the distance travelled by the displaced ions in the lattice is inversely proportional to the square root of the mass of the ion, if the ion is heavy the displacement will be small, whereas with a light ion the converse is true. This should lead to greater lattice distortion, which in turn should lead to greater attraction between electrons in a Cooper pair. Therefore the binding energy, which determines the transition temperature, should be inversely proportional to the square root of the mass of

the ion[15] and that lighter ions should lead to superconductors with higher transition temperatures.

1.8 The design of an organic metal

In order to maximise the chances of attaining a metallic state for an organic C-T complex a number of useful guidelines can be noted.

1. Molecules should be planar and be of similar size. They should also have delocalised π-molecular orbitals so donor HOMO and acceptor LUMO can overlap.
2. Stable free radical species are needed to create partially filled bands.
3. There should be no periodic distortion that destroys the Fermi level.
4. Mixed valency is necessary along a particular stack and the coulombic repulsion U should be less than the bandwidth.
5. Segregated stacks are needed.

Donor Molecules

1.9 Donor molecules

TTF (3) and its ability to form charge transfer complexes have led to a new area of research, the design and synthesis of electron donors. The synthesis of electron donors derived from TTF has followed 3 main trends:

1. Extension of the π-electron system in order to reduce the coulombic repulsion experienced in the doubly ionised cation.
2. Replacement of the sulphur with either selenium or tellurium should increase the bandwidth and there should also be increased inter and intra stack interactions.
3. Addition of various substituents to the TTF skeleton can fine-tune the donating properties of various TTF derivatives.

1.10 Synthetic Developments

TTF (3) was first synthesised by Wudl and co-workers.[16] The synthesis involved the deprotonation of 1,3-dithiolium hydrogen sulphate (6), scheme 1.

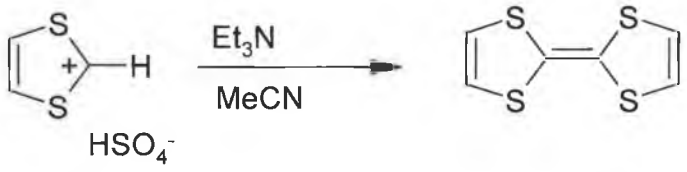

(6) (3)

Scheme 1

Key steps in the synthesis of TTF type electron donors are:

1. The formation of the tetraheterosubstituted double bond (π-bond formation).
2. Functionalization of the TTF skeleton.

1.11 π-Bond formation

These methods are the most widespread. A summary of these types of reactions can be seen in scheme 2.

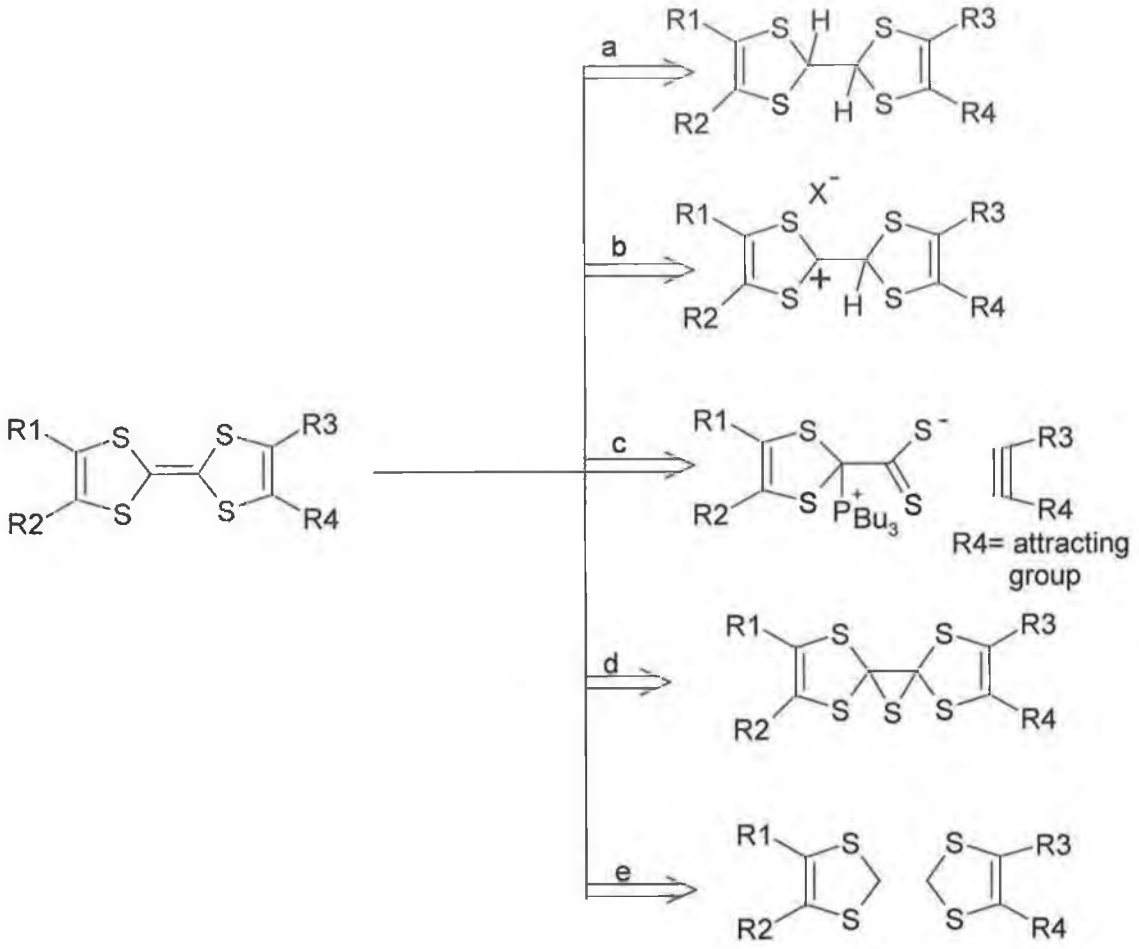

Scheme 2

1,3-Dithioles can be oxidatively dimerized to TTF derivatives electrochemically, scheme 3.[17]

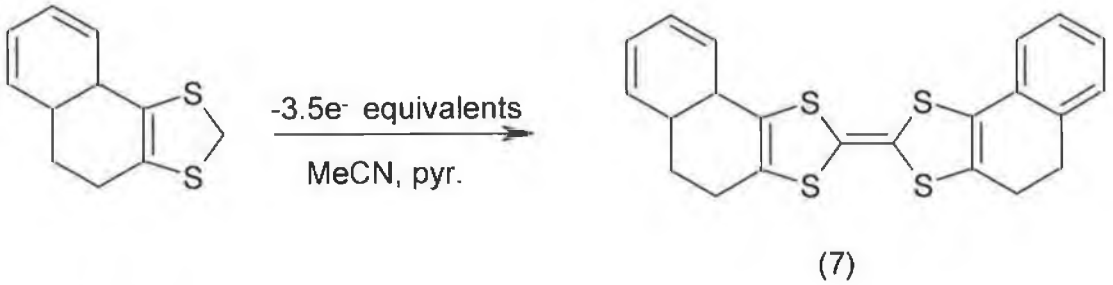

(7)

Scheme 3

This reaction is only effective in the presence of pyridine. TTF derivatives are also synthesised from the coupling of 1,3-dithiolium salts (8). The reaction takes place when a carbene is generated by base attack on a 1,3-dithiolium salt. The carbene can then react with another 1,3-dithiolium ion to form adduct (9), followed by removal of a proton to yield the TTF derivative, scheme 4.

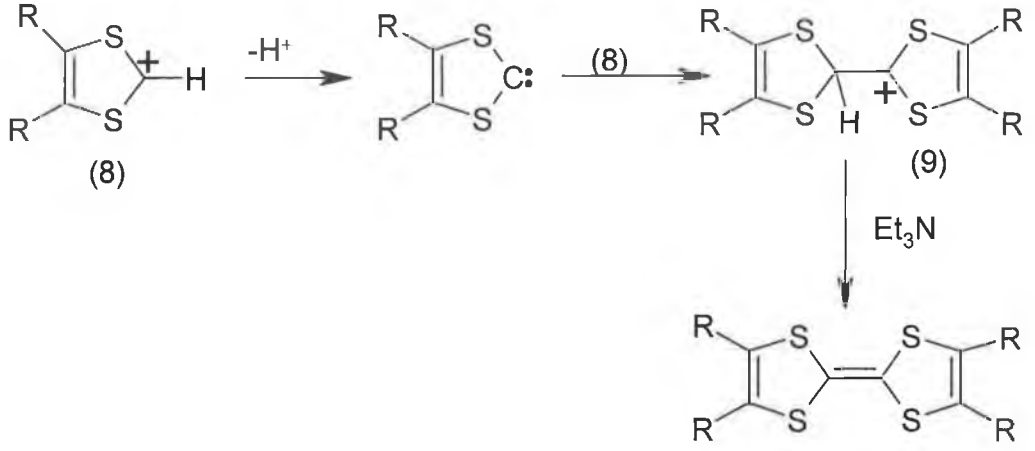

Scheme 4

1,3-Dithiolium salts (8) with a hydrogen at the 2-position can be prepared from 2-thioxo-1,3-dithiole (10) according to scheme 5.

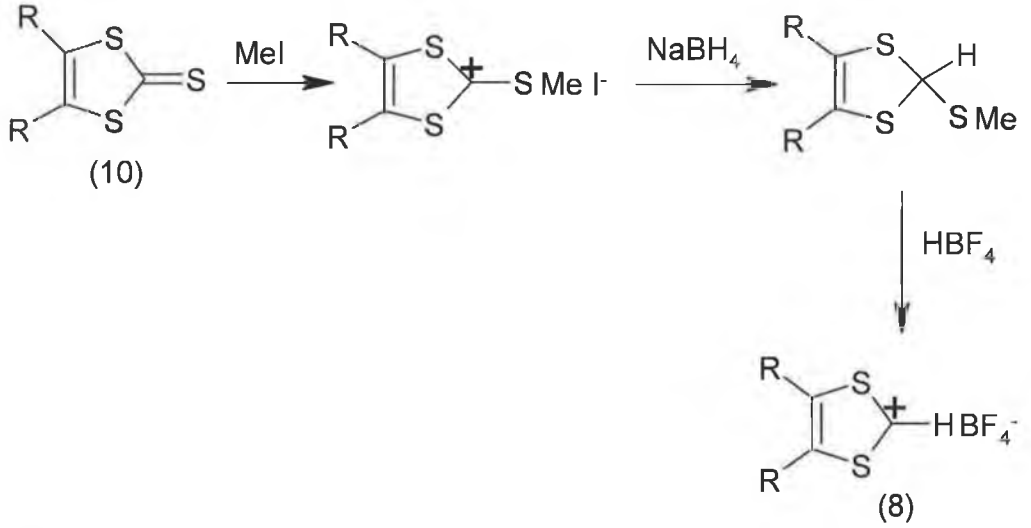

Scheme 5

Treatment of 2-thioxo-1,3-dithioles with methyl iodide, followed by reduction of the product salt with sodium borohydride yields a 2-alkylthio-1,3-dithiole. Reaction with a strong acid, generally fluoroboric acid, yields the desired 1,3-dithiolium salt (8). Subsequent reaction in the presence of base yields the corresponding TTF derivative.[4]

2-Oxo (11a), 2-thioxo (11b), 2-selenoxo (11c) 1,3-dithioles of general formula (11) react with various trivalent phosphorous compounds to give the corresponding TTF derivatives.

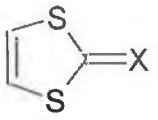

(11a): X=O.
(11b): X=S.
(11c): X=Se.

Triphenylphosphine (PPh_3) and various phosphites ($P(OR)_3$) have been used as desulphurizing agents. The latter are the more efficient reagents. Dibenzotetrathiafulvalene (DBTTF) (12)[18] was synthesised in this manner, scheme 6.

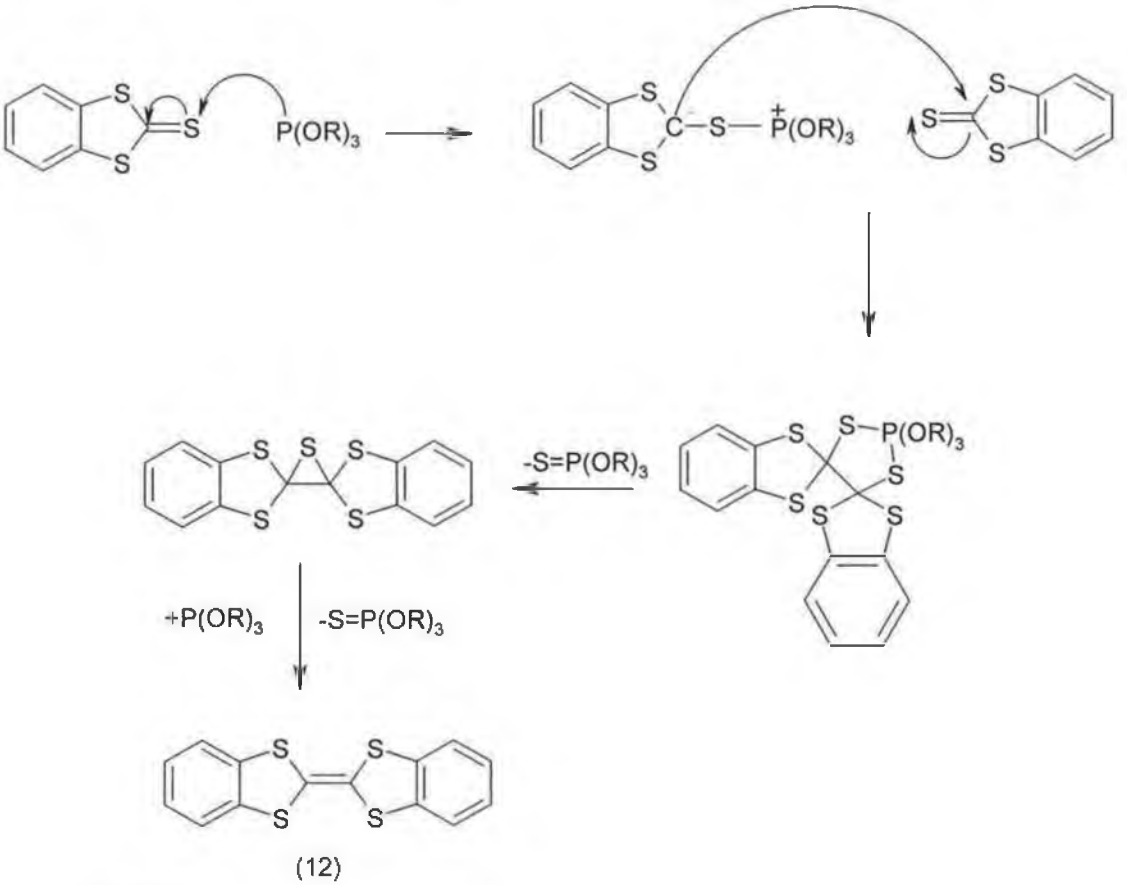

(12)

Scheme 6

Dicobaltoctacarbonyl $Co_2(CO)_8$ can be used instead of either PPh_3 or $P(OR)_3$ allowing a wider number of peripheral substituents.[19]

1.12 π-Extended TTF Derivatives

Charge transfer complexes are formed when there is charge transfer between a donor molecule and an acceptor molecule. Therefore radical ions, dications and dianions can be formed. Consequently stabilisation of the positive charge in a radical cation and reduction of the intramolecular coulombic repulsion in the dication state becomes very important. Extending the π-conjugation accomplishes both, the positive charge of the radical cation being stabilised by increased delocalisation of the charge in the π-system. Similarly coulombic repulsion is also reduced. π-Conjugation can be increased by placing a vinylic or an aromatic spacer between the 1,3-dithiole rings. Increasing π-conjugation should decrease the oxidation potential of the molecule and hence make it a better donor.

Bis(benzo-1,3-dithiafulvenyl) vinylogue (13)[20] was prepared in three steps from o-benzenedithiol and 2,5-dimethoxytetrahydrofuran, scheme 7.

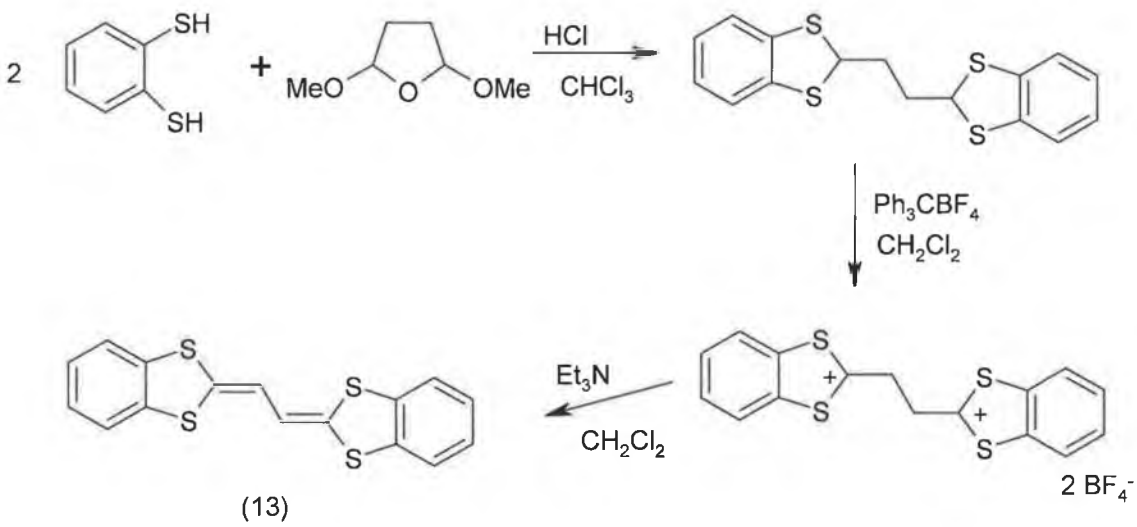

(13)

Scheme 7

The cyclic voltammogram of (13) displays two reversible one-electron oxidation waves at $E^1_{1/2}$= 0.47V and $E^2_{1/2}$= 0.64V. These values are both smaller than those of dibenzo-TTF ($E^1_{1/2}$= 0.61V and $E^2_{1/2}$= 0.93V). Comparison of the data clearly shows that (13) is a better electron donor than dibenzo-TTF (12).

Ethanediylidene-2,2'-bis(1,3-dithiole) (EDBDT) (14) was synthesised in 1983.[21] The phosphonium salt (15a) was reacted with glyoxal (16) in the presence of base to yield aldehyde (17a). Further reaction of (17a) with another molecule of (15a) and triethylamine yielded carbomethoxy derivative (18). Compound (18) was then treated with lithium bromide/hexamethylphosphoramide to yield EDBDT (14), scheme 8.

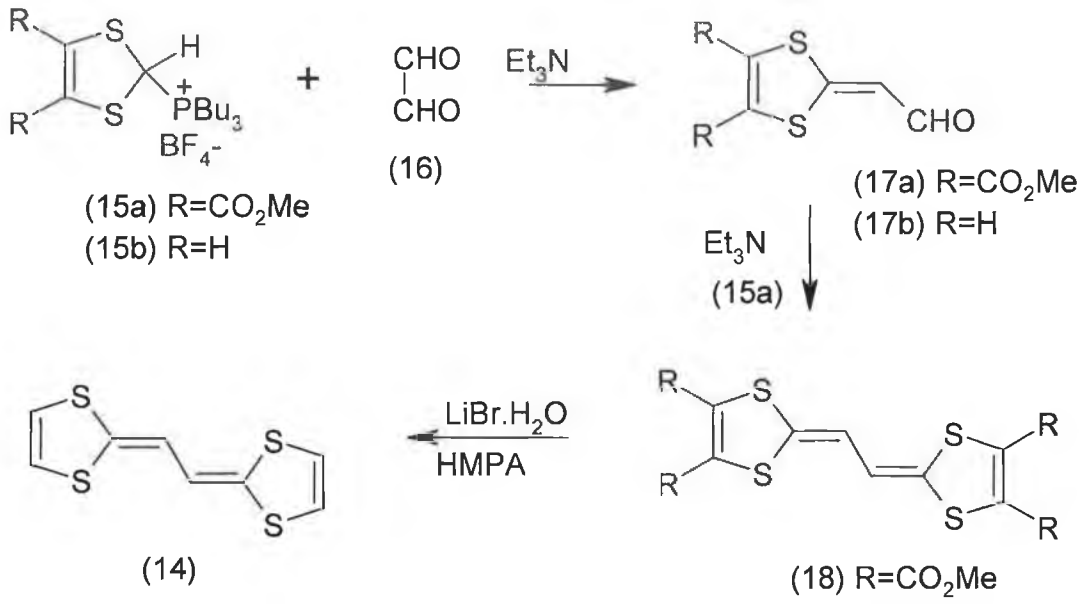

Scheme 8

The same group have synthesised 1,4-butenediylidene-2,2'-bis(1,3-dithiole) (BDBDT) (19) using a McMurry type reductive coupling reaction of aldehyde (17b).[22]

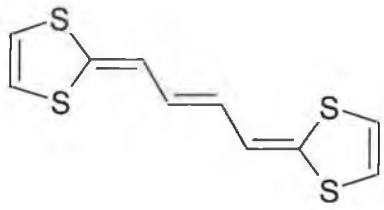

BDBDT (19).

Compound (14) has half-wave reduction potentials of $E^1_{1/2}$= 0.20V and $E^2_{1/2}$= 0.36V. TTF (3) has half-wave reduction potentials of $E^1_{1/2}$= 0.34V and $E^2_{1/2}$= 0.71V.

BDBDT has a single 2-electron redox wave at 0.22V. This situation arises because $\Delta E=(E^{1}_{1/2} - E^{2}_{1/2})$ is very small due to the decreased coulombic repulsion.

From scheme 8 it is clear that the key reagents are phosphonium salt (15) and unsaturated aldehyde (17). Variation of the heterocycle attached to either reagent will lead to new unsymmetrical compounds. Application of this rationale lead to the synthesis of (20) and a vinylic derivative of (BEDT-TTF) (21).[23]

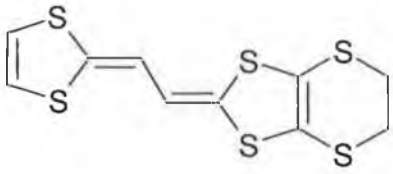

(20)

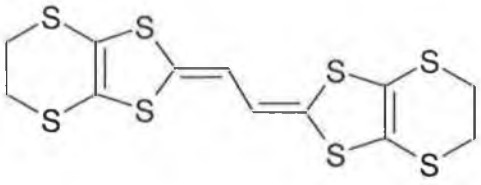

(21)

Compound (20) has two reversible redox waves at 0.40V and 0.57V, while (21) has two reversible redox waves at 0.46V and 0.66V.

It is also possible to use Wittig-Horner phosphonate reagents (23) in place of phosphonium salt (15). These phosphonates are formed when a 1,3-dithiolium salt (22) reacts with an alkyl phosphite $P(OR_3)$, scheme 9.

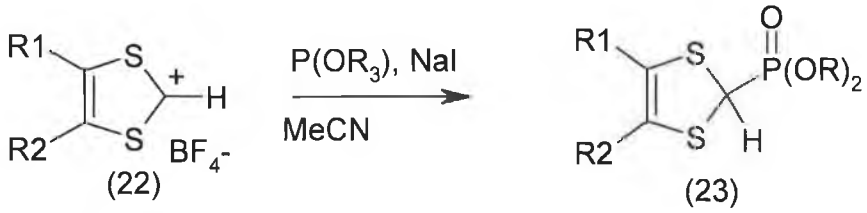

(22) (23)

Scheme 9

Using various Wittig-Horner reagents, donors (24), (25) and (26) have been synthesised.[24]

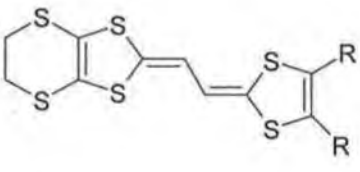

(24a): R=SMe.
(24b): R-R=-S-$(CH_2)_3$-S

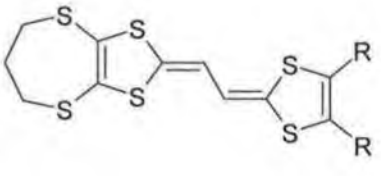

(25a): R=H.
(25b): R=Me. (25c): R=SMe.
(25d): R-R=-S-$(CH_2)_3$-S.

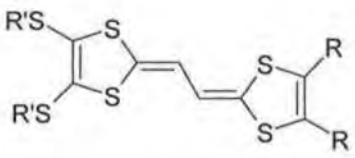

(26a): R=H, R'=Me.
(26b): R=R'=Me.
(26c): R=SMe, R'=Me.

All these compounds possess two reversible redox waves, except (24b) and (25d) where the second oxidation is irreversible. The values obtained for $E^1_{1/2}$and $E^2_{1/2}$ are lower than for the parent fulvalene and ΔE has also been reduced. All the donors form 1:1 C-T complexes with TCNQ. Room temperature conductivities of these complexes are in the range of 5 x 10^{-4} to 6 x 10^{-8} Scm^{-1}.

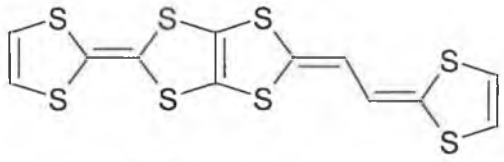

(27)

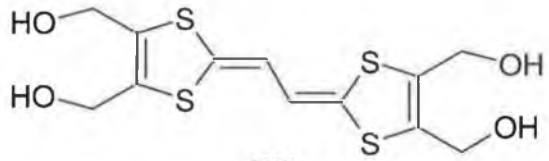

(28)

Similar synthetic routes were used to synthesise DTEDT (27)[25] and (28).[26] DTEDT (27) is of particular interest because it produces a superconducting $Au(CN)_2$ salt as well as many metallic cation radical salts stable to liquid helium temperature. $(DTEDT)(Au(CN)_2)_{0.4}$ has a superconducting transition temperature T_c= 4K. The donors form conducting sheets parallel to the ac plane. They are stacked face to face in a ring over bond type overlap.

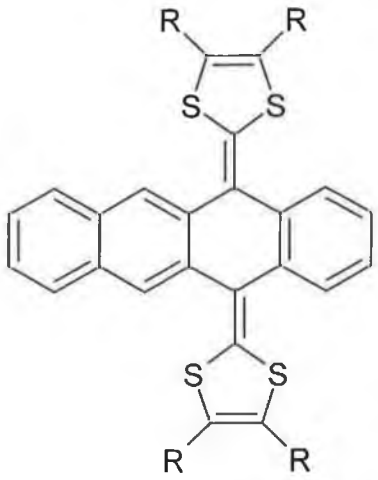

(29a): R=H.
(29b): R=Me.

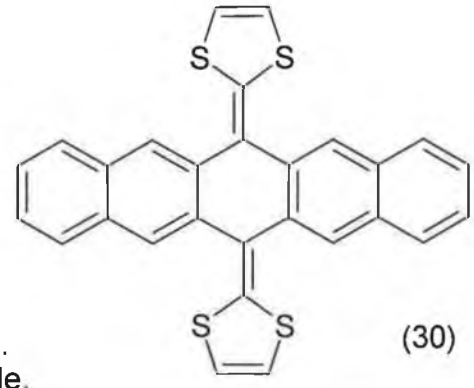

(30)

Derivatives of TTF in which there is a cyclic conjugated π-framework between the 1,3-dithiole rings are also of interest. Compounds (29),[27] (30),[28] (31)[29] and (32)[30] have all been prepared from the reaction of a Wittig-Horner reagent and a suitable quinone.

Compounds (29a) and (29b) have single two-electron oxidation waves at 0.44V and 0.41V respectively. Both undergo reduction at very low potentials, 0.12V and 0.09V, demonstrating the stability of the dication state in both compounds. Similarly compound (30) has a quasi-reversible oxidation wave at 0.50V corresponding to formation of the dication. There is also an irreversible oxidation due to the formation of the trication, which involves the hydrocarbon rings.

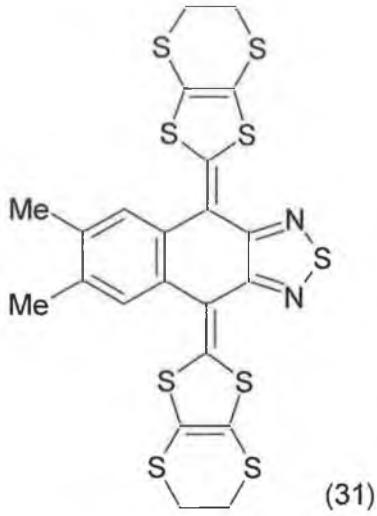

(31)

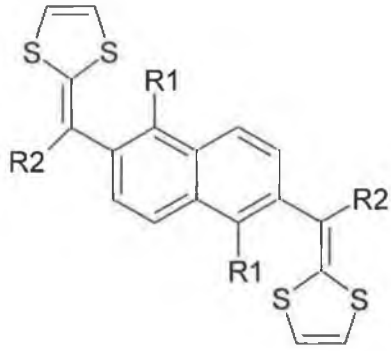

(32a): R1=R2=H. (32b): R1=H, R2=Ph
(32c): R1=OCH_3, R2=H.

Compound (31) gave cation radical salts that incorporate solvent molecules, of general formula $(31)_2(PF_6)$(solvent). When a THF solvent molecule was incorporated into the complex the resulting material showed metallic behaviour down to ca. 180K. Only (32b) exhibits reversible oxidation. It possesses two single electron oxidation waves at 0.29V and 0.52V. The replacement of the vinylic hydrogens with a phenyl group seems to have facilitated reversible behaviour.

Heteroaromatic spacers have also been introduced in an effort to enhance donor ability. Heteroaromatics were synthesised by Wittig-Horner reactions between appropriate aromatic dialdehydes (33) and the corresponding ylides generated from various phosphonate esters (34) and (35).

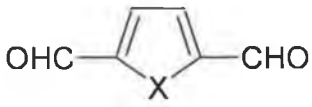

(33a): X=O.
(33b): X=S.
(33c): X=NMe.

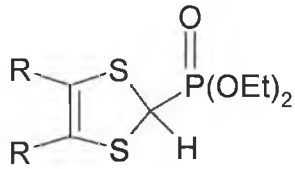

(34a): R=H.
(34b): R=COOMe.

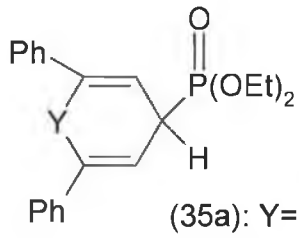

(35a): Y=O.
(35b): Y=S.

Coupling of (33a) and (33b) with (34a) and (34b) yielded compounds (36).[31]

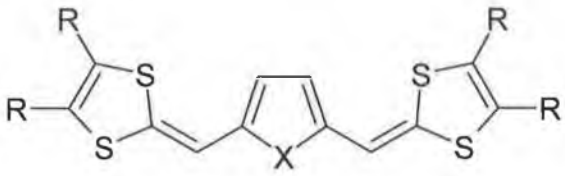

(36a): R=H, X=O. (36b): R=H, X=S. (36c): R=COOMe, X=S.

Compound (36a) has two one-electron oxidation waves at 0.29V and 0.36V. Similarly (36c) also has two reversible redox waves at 0.67V and 0.78V whereas (36b) has a single two-electron oxidation wave at 0.43V. This behaviour can be ascribed to the decreased coulombic repulsion experienced in the dication state and the formation of a less stable radical cation in which the conjugative interaction between the terminal 1,3-dithiole rings and central heterocyclic ring is not significantly enhanced due non-rigid conformations of (36a), (36b), and (36c). Compound (36b) forms semi-conducting complexes with TCNQ and DDQ.

Coupling of compounds (33) and (35) result in donors of general formula (37).[32]

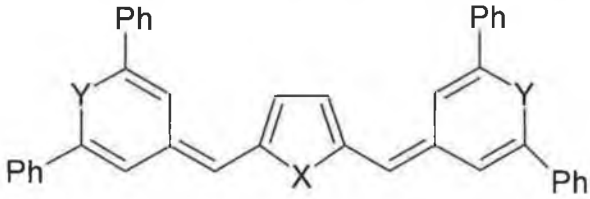

(37a): X=Y=O. (37b): X=S, Y=O. (37c): X=NMe, Y=O. (37d): X=O, Y=S.
(37e): X=Y=S. (37f): X=NMe, Y=S.

The best donors in the series were (37c) and (37f). Both of these compounds formed conductive charge transfer complexes with TCNQ. Both complexes were 1:1 donor:acceptor. The conductivities of these complexes were of the order of 0.0-1.0Scm^{-1}.

Extra rigidity can be introduced by removing the intercyclic single bonds, which hamper the ability of compounds (36) to form conductive complexes. This meant joining heterocyclic components together with double bonds only. Compounds (38) achieved this.[33]

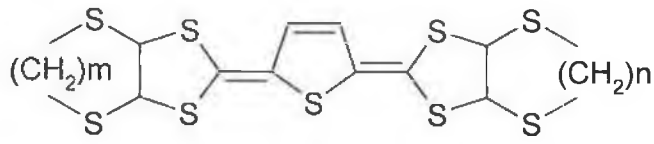

(38a): m=n=2; (38b):m=2, n=3; (38c): m=n=3.

The synthetic route to these compounds again involved Wittig-Horner coupling. All three have two single-electron reversible redox waves, (38a) at 0.26V and 0.34V, with (38b) at 0.24V and 0.42V and (38c) at 0.26V and 0.34V. Compound (38a) forms a highly conductive 1:1 C-T complex with TCNQ. The most conductive of these complexes was the one containing (38a) and TCNQ. Its conductivity was 16.0Scm^{-1} at 298K. It behaved in a metallic fashion down to 248K.

1.13 Substituted TTF derivatives

The addition of substituents is a very effective way of tailoring the donor ability of a TTF molecule. Addition of an electron withdrawing or donating group can have a marked effect on the strength of a particular donor. The introduction of substituents containing extra chalcogen atoms can increase dimensionality through increased inter and intra stack interactions. This increased dimensionality should diminish lattice distortions and therefore increase the conductivity of any subsequently formed C-T complexes.

Modification of the TTF skeleton can be achieved through lithiation and then reaction with an electrophile to yield compounds (39), scheme 10.[34] The reaction needs strict temperature control and uses butyl lithium or lithium diisopropylamide as lithiating agent.

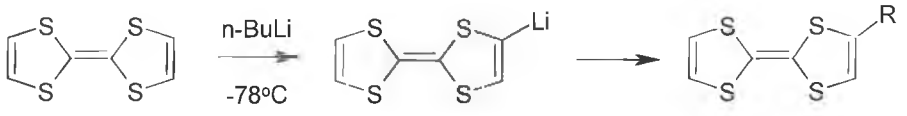

(39a): R=COOMe
(39b): R=Et.

Scheme 10

If the temperature becomes too high multi lithiation occurs. Green[35] synthesised a wide range of monosubstituted TTF derivatives using LDA at -70°C in ether. The presence of substituents on TTF exerts a strong directional force on position of lithiation. For example, an alkyl group on the heterocycle diminishes the acidity of the adjacent proton. Therefore metallation is more likely to occur at the other ring. The converse is true if an ester group is attached to the TTF skeleton.

Similar reaction conditions led to the synthesis of numerous mono-substituted TTFs, for example (40),[36] (41)[37] and (42).[38]

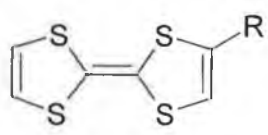

(40a): R=$COC_{15}H_{31}$.
(40b): R=$CO(CH_2)_3Br$.
(40c): R=$SiMe_3$.

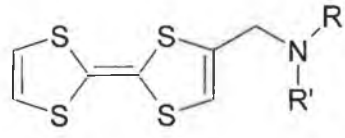

(41a): R=R'=Me.
(41b): R=Me, R'=Benzyl.

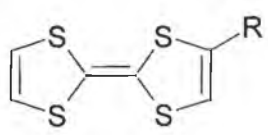

(42): R=Br.

Compounds (41a) and (41b) both formed 1:1 C-T complexes with TCNQ. These complexes were found to be mildly conductive. Compounds (40) were synthesised in order to investigate electroactive Langmuir-Blodgett (LB) films of amphiphilic TTF systems.

Mono-functionalised TTF derivatives are generally synthesised to provide building blocks for larger more elaborate systems. Compound (42) was used to synthesise a number of symmetric and unsymmetric assemblies (43).[39]

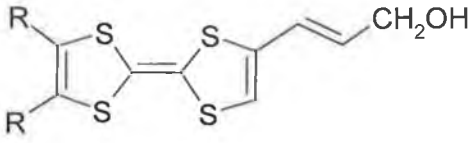

(42a): R-R=S$(CH_2)_2$S.
(42b): R=H.

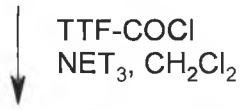

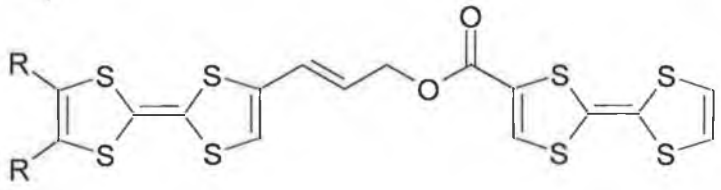

(43a): R-R=S$(CH_2)_2$S.
(43b): R=H.

Scheme 11

Compound (43a) has only two broadened oxidation peaks. The two TTF portions of the molecule have very similar oxidation potentials and are oxidised almost simultaneously. Lithiation has also been used as a way of producing alkyl and aryl chalcogenated derivatives of TTF.[40,41] Addition of LDA to TTF at -78°C produced tetra anion (44), which reacts with dialkyl or diaryl disulphide or diselenide electrophiles, scheme 12.

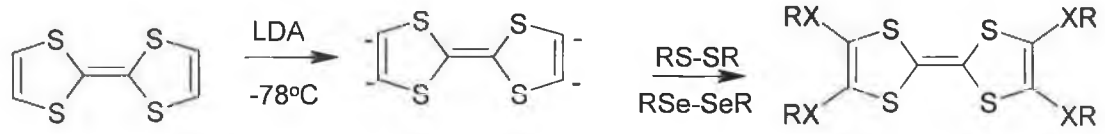

(44)

X=S.
(45a): R=Me.
(45b): R=Ph.

X=Se.
(46a): R=Me.
(46b): R=C_3H_7.
(46c): R=C_4H_9.
(46d): R=Ph.

Scheme 12

All the compounds had two single electron reversible redox waves. Lithiation also yielded N-methylthiocarbamoyl TTF derivatives (47).[42]

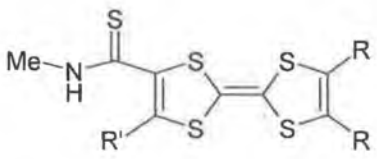

(47a): R=R'=H.
(47b): R=SMe, R'=H.
(47c): R-R=S(CH$_2$)$_2$S, R'=H.

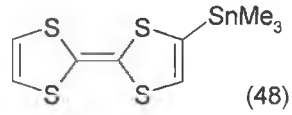

(48)

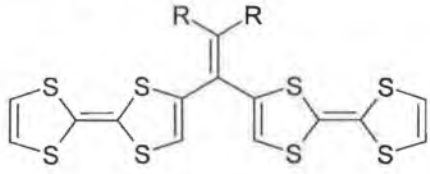

(49a): R=Ph.
(49b): R=Me.

These compounds are darker than TTF, due mainly to intramolecular charge transfer between the TTF moiety and the N-methylthiocarbamoyl moiety. All the compounds form 1:1 C-T complexes with TCNQ. It is also possible to trap mono-lithiated TTF with trimethylstannyl chloride, to yield trimethylstannyl-TTF (48), a shelf stable alternative to the mono-lithiated species. Application of this process led to the synthesis of dimeric TTF (49).[43]

Functionalised TTF derivatives are also used as building blocks for much larger molecules containing many TTF units. Chalcogenate anions are more reactive towards electrophiles than lithiated TTF precursors. Bis-functionalised TTF derivatives with two thiolate groups in the 2- and 3-positions can be protected with 2-cyanoethyl groups and have been used as building blocks for larger assemblies.[44] Deprotection takes place readily and selectively, scheme 13.

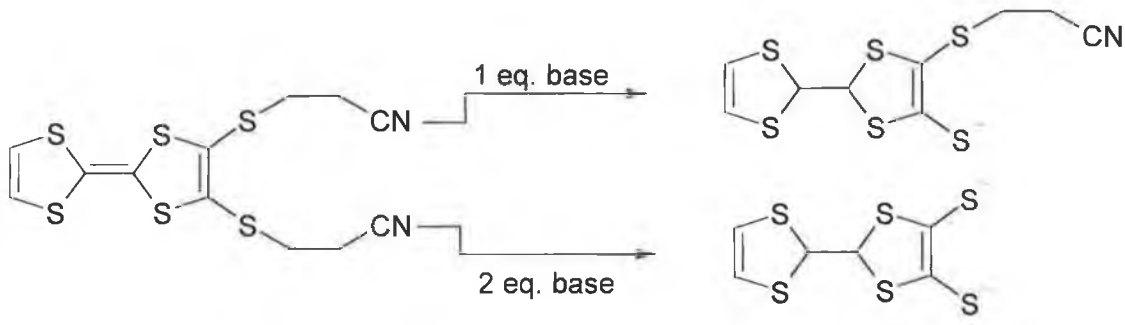

Scheme 13

Application of this strategy led to the synthesis of compound (50).[45] Four redox couples were observed. The data obtained was consistent with no significant interaction between the charged states of the TTF units. The redox waves that correspond to the strained 4,4'-disubstituted TTF unit occur at higher potential. Compound (50) formed a 1:2 perchlorate salt, which is a semiconductor.

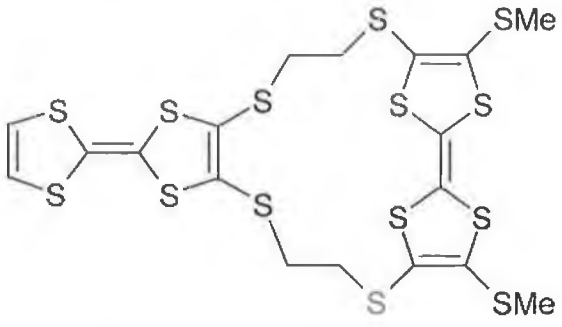

(50).

An enormous number of substituted TTF derivatives have been synthesised in the last 20 years. Major reviews of the various synthetic routes used to obtain both symmetrical and unsymmetrical TTF derivatives have been published.[46,47] In an attempt to focus the scope of this review, there will be no further elaboration on the majority of compounds mentioned in these reviews. Instead, efforts will be concentrated on electron donors that yielded superconducting complexes.

1.14 Synthesis of BEDT-TTF derivatives

In an effort to increase the likelihood of forming segregated stacks of electron donors and electron acceptors in C-T complexes, bis(ethylenedithio)tetrathiafulvalene (BEDT-TTF) or (ET) (52) was synthesised via phosphite coupling of two intermediate thione molecules (51) or from the reaction of tetrathiolate anion (53) and 1,2-dibromoethane.[48,49]

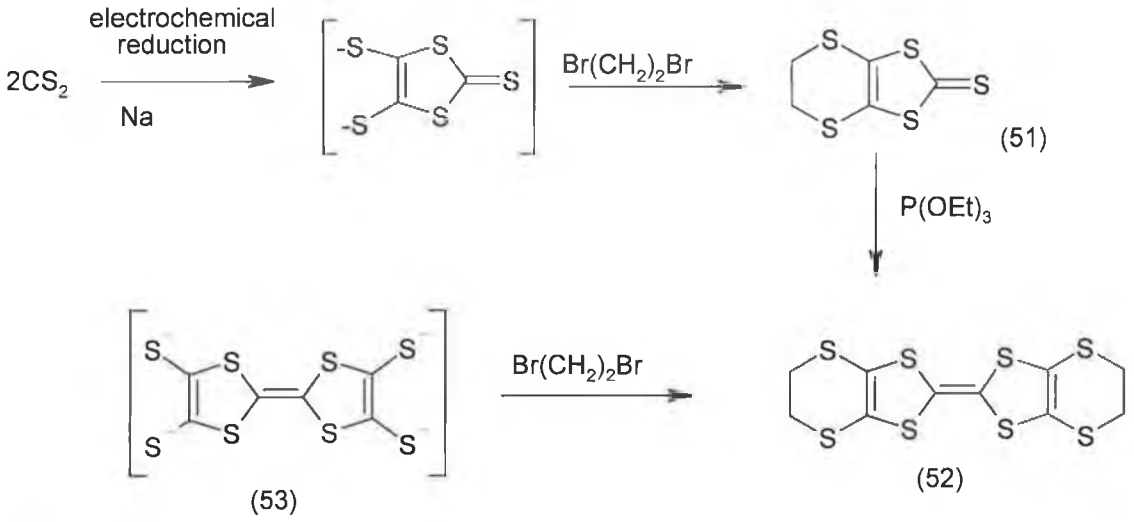

Scheme 14

1,4,5,8-Tetrathianaphthalene (TTN) (54) isomerises to TTF upon treatment with LDA and this rearrangement has been developed as a synthetic route to (BEDT-TTF) (52), scheme 15.[50,51]

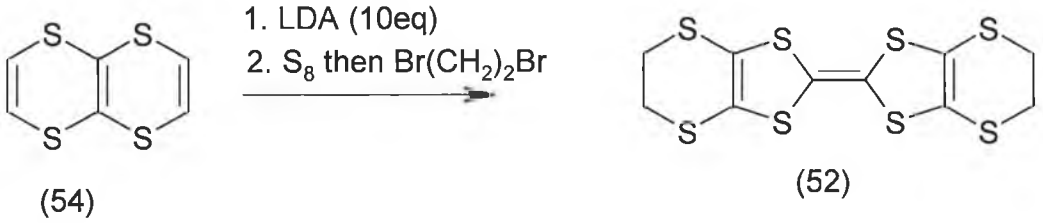

Scheme 15

BEDT-TTF forms superconducting salts with inorganic and organometallic anions. The salts crystallise in a number of different ways. The most important salts are β-phase and κ-phase salts. In β-phase salts the BEDT-TTF layers are made up of loose

stacks that are parallel to each other. This arrangement leads to a corrugated sheet network of donors. The donor layer has a honeycomb appearance. The interstack S-S contacts are shorter than the intrastack S-S contacts. The donor layer is bounded above and below by layers of anions.

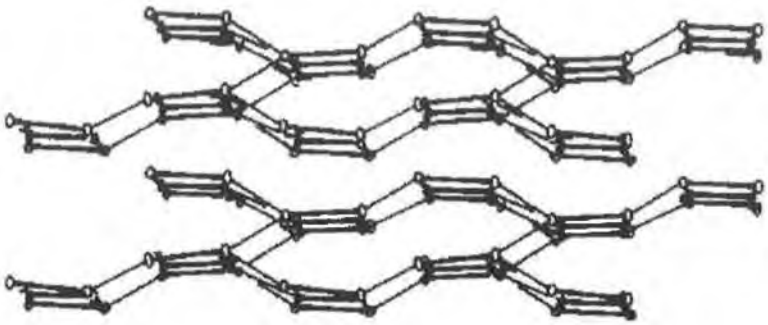

Figure 1.3. The corrugated sheet network of donor molecules in β-phase BEDT-TTF radical ion salts.

In κ-phase salts the donors form dimers. These dimers are arranged perpendicular to each other. The S-S intermolecular contacts within the dimer are longer than the sum of the van der Waals radii but the S-S contacts between dimers are shorter. Insulating layers of V-shaped anions bound the conducting layer of donor dimers.

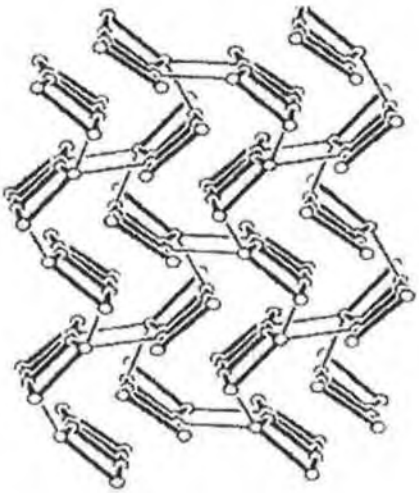

Figure 1.4. Donor arrangement in κ-phase BEDT-TTF radical ion salts

The first superconducting salt featuring BEDT-TTF was β-(BEDT-TTF)$_2$ReO$_4$.[52] This salt has a transition temperature T_c of 4K, at a pressure of > 4kbar. The introduction of linear poly halide anions led to the synthesis of β-(BEDT-TTF)$_2$I$_3$[53] which was the first sulphur based ambient pressure superconductor. T_c for this salt is 1.4-1.6K. The interstack S-S contacts provide the main conducting pathway in these quasi 2-D systems. Minimising this distance should raise the transition temperature. This rationale led to the synthesis of β-(BEDT-TTF)$_2$IBr$_2$ (T_c= 2.7 K).[54] The IBr_2^- anion is ≅ 7% shorter than I_3^-. In fact the average decrease in the interstack S-S contact distances was 0.02Å. For β-phase salts with linear anions, it has been observed that asymmetry of the counter anion tends to destroy the superconductivity.

Another ambient pressure superconductor is κ-(BEDT-TTF)$_2$Cu(SCN)$_2$.[55] This salt has a T_c value of 10.4K. In this salt two BEDT-TTF molecules form a dimer which is linked to another dimer by short S-S contacts, to form a BEDT-TTF sheet. Anions are located in the plane between BEDT-TTF sheets. Three N-C-S groups coordinate to a copper cation with two nitrogen and one sulphur atom to construct a one-dimensional zig-zag polymer along the b axis. Two organic superconductors with high transition temperatures are κ-(BEDT-TTF)$_2$Cu(N(CN)$_2$)Br, (T_c= 11.8K at ambient pressure)[56] and κ-(BEDT-TTF)$_2$Cu(N(CN)$_2$)Cl, (T_c= 12.8K at pressure of 0.3kbar).[57]

A κ-phase superconductor has been synthesised incorporating the organometallic anion $Cu(CF_3)_4^-$.[58] The new superconductor has general formula of κ-(BEDT-TTF)$_2$Cu(CF$_3$)$_4$.(TCE). The salt crystallised as both needles and plates. The needle shaped crystals yielded T_c= 9.2K and the plates had T_c= 4.0K.

BEDT-TTF also formed 1:1 charge transfer complexes with substituted derivatives of TCNQ (55) and (56).[59] Highly conductive 1:1 donor:acceptor complexes were obtained between BEDT-TTF and mono-halogenated TCNQs (55a) (R_1'= F, Cl, Br and R1= H). The room temperature conductivities were in the region of 30Scm^{-1}. These C-T complexes form segregated molecular stacks. However C-T complexes formed between BEDT-TTF and Me$_2$TCNQ and ClMeTCNQ crystallise in mixed molecular stacks. The C-T complex between (BEDT-TTF) and (56a) showed metallic behaviour to

T= 2K while (BEDT-TTF):(56b) and (BEDT-TTF):(56c) showed insulating behaviour because they crystallise in mixed stacks.

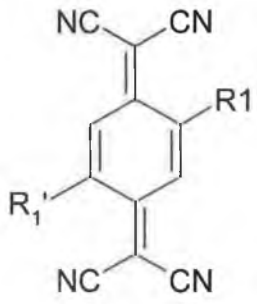

(55a): R1=H, F, Cl, Br, Me, R_1'=H.
(55b): R1=F, Cl, Br, Me, R_1'=Me.

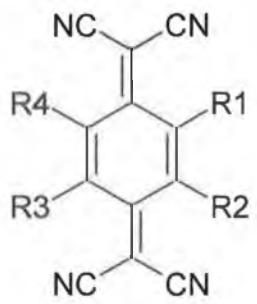

(56a): R1=F, R2=R3=R4=H.
(56b): R1=R3=F, R2=R4=H.
(56c): R1=R2=R3=R4=F.

Replacement of the outer sulphur atoms with oxygen atoms led to the synthesis of bis(ethylenedioxy)tetrathiafulvalene BEDO-TTF (57), scheme 16.[60]

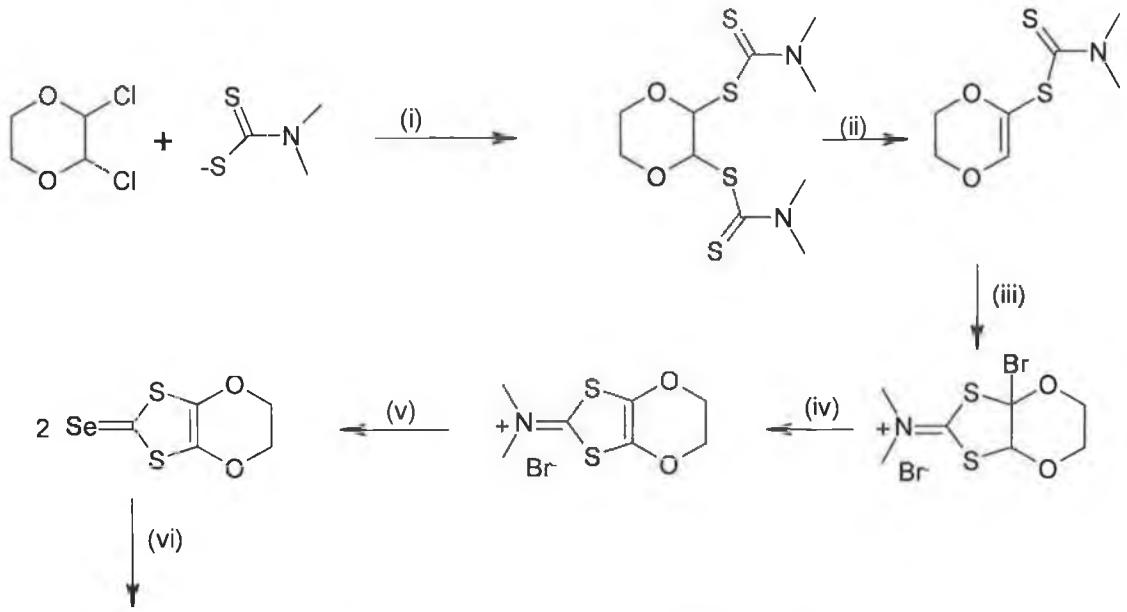

(57)

(i): CH_3CN/ reflux
(ii): 110°C/ DMSO
(iii): Br_2/ CH_2Cl_2 0°C
(iv):110°C/ 25 Torr
(v): H_2Se/ MeOH, rt
(vi):$(MeO)_3P$/ benzene, reflux

Scheme 16

Two superconductors based on BEDO-TTF have been synthesised to date. Both $(BEDO\text{-}TTF)_3Cu_2(NCS)_3$[61] and $(BEDO\text{-}TTF)_2ReO_4.(H_2O)$[62] are β-phase salts. A possible explanation for the occurrence of a single donor packing mode for BEDO-TTF salts is the existence of short C-H-O intermolecular hydrogen bonding contacts, which appear to favour a single intermolecular donor packing arrangement.

1.15 Selenium compounds

Replacement of sulphur with selenium was expected to increase interstack interactions, increase the bandwidth and increase dimensionality. Selenium has a larger d-orbital and is more polarisable than sulphur. Combining these properties, it was anticipated that selenium based electron donors would form charge transfer complexes and radical ion salts of higher conductivity than their sulphur based counterparts.

Tetraselenafulvalene (TSF) (58) was synthesised by phosphine or phosphite coupling of the appropriate selenone (59), scheme 17.

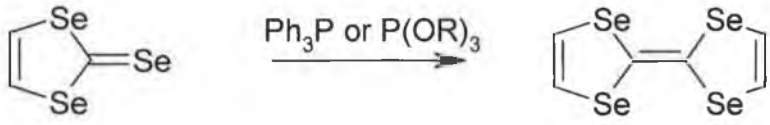

(59) (58)

Scheme 17

A large number of selenium based donors have been synthesised. The ideas that shaped the trends in the syntheses of TTF based donors were applied to TSF based

systems. The synthesis of TSF derivatives have been extensively reviewed.[53, 63] The most interesting selenium based donor is tetramethylselenafulvalene (61).

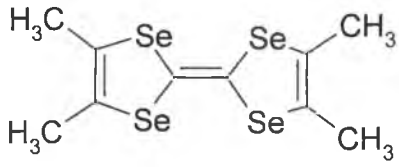

(61)

In order to avoid the very toxic H_2Se an alternative method was developed that used sodium hydrogen selenide as the source of elemental selenium and dimethylphosgene iminium chloride (60) to generate the required selenone, scheme 18.[64]

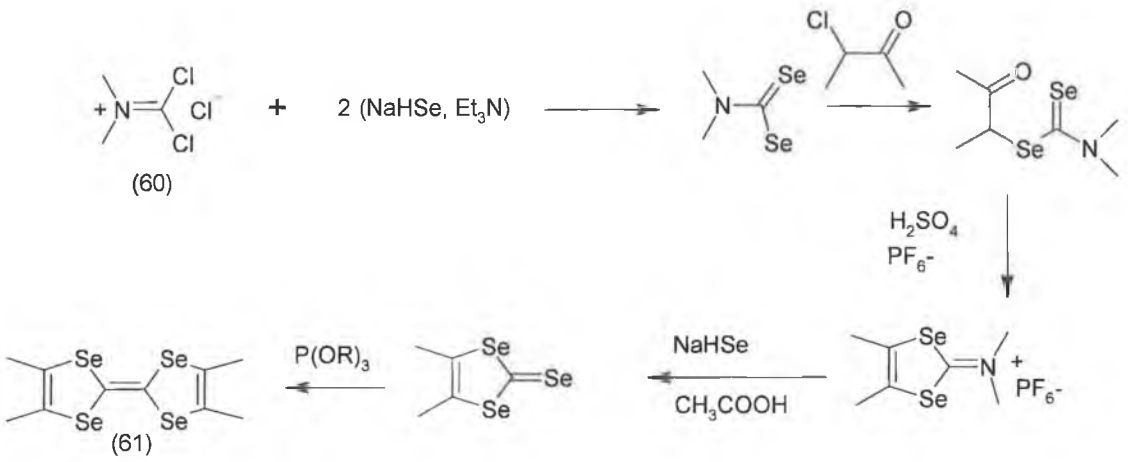

Scheme 18

In 1979[65] it was discovered that when the charge transfer complex formed between TMTSF and DMTCNQ (dimethyl-TCNQ) was subjected to a pressure of 10 kbar and then cooled an extremely high conductivity was achieved. The conductivity stabilized at 2 x 10^5(ohmcm)$^{-1}$.

Superconductivity was attained by radical cation salts of general formula $(TMTSF)_2X$, where X is a monovalent inorganic anion, collectively known as the Bechgaard salts. They are synthesised electrochemically in an H-shaped cell. Superconductivity was first discovered in the salt $(TMTSF)_2PF_6$,[66] which has a T_c= 0.9K

at an applied pressure of 9kbar. At the moment the only ambient pressure superconductor in the Bechgaard salt series is $(TMTSF)_2ClO_4$,[67] with T_c= 1.2K. TMTSF has formed superconducting salts with both octahedral and tetrahedral anions, for example X= PF_6^-, AsF_6^-, SbF_6^- and X= ClO_4^-, ReO_4^-, BF_4^-, respectively.

All of the salts formed by the combination of TMTSF and either octahedral or tetrahedral anion have similar crystal packing patterns. The TMTSF molecules stack in a zig-zag pattern. There are short interstack Se-Se contacts which lead to the formation of the 2-D network which is essential for high conductivity. The anions play no direct role in the conductivity of the salts formed but their symmetry and ordering affect the cause of the M-I transition at low temperatures (at normal pressure) and the amount of pressure required to bring about the onset of a superconducting state. When pressure is applied to Bechgaard salts the rate of contraction of Se-Se contacts differs. It was discovered that the intrastack Se-Se distances contracted approximately twice as much as the interstack Se-Se contacts when the temperature was lowered.[68] This phenomenon leads to the formation of an infinite sheet network. The metallic properties and superconductivity of $(TMTSF)_2X$ salts are due to intermolecular selenium orbital overlap.

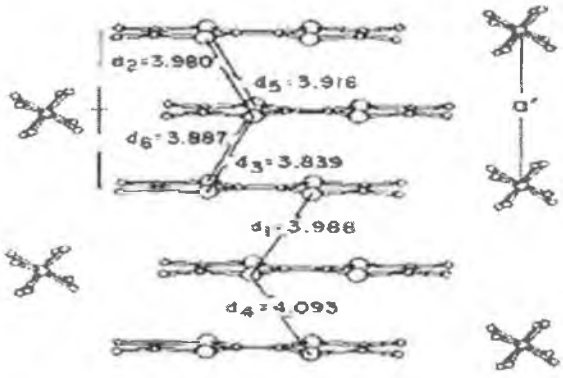

Figure 1.5. The stacking arrangement in $(TMTSF)_2ReO_4$

The TMTSF molecules cannot form a 3-D system due to the presence of a layer of anions, occupying the methyl group cavity of TMTSF molecule. Therefore the size of the counterion affects the size of the unit cell. As with BEDT-TTF based superconductors

less harsh conditions are required to achieve a superconducting state when the counter ion is small. This would partially explain why $(TMTSF)_2ClO_4$ is a superconductor at ambient pressure. However anion ordering and oxygen atom to methyl group hydogen atom (H_2C-H-----O-ClO_3^-) bonding interactions also play an important role.[69]

More recently superconducting complexes based on the hybrid donor bis-(ethylenedithio)tetraselenafulvalene (BETS) (62), a hybrid of BEDT-TTF and TSF have been developed. The first of these was λ-$(BETS)_2GaCl_4$, with T_c at 8K.[70]

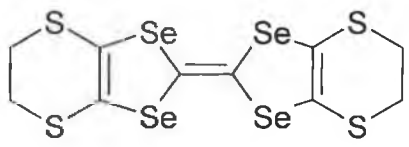

BETS (62)

A series of superconducting systems of general formula λ-$BETS_2GaX_zY_{4-z}$ have been produced where X, Y= halogen atom. When $0<z<1.0$ and X=Br and Y=Cl the superconducting transition occurs between 6 and 8K.[71] The $GaCl_3F$ salt undergoes a superconducting transition at 3.5K. Mixed metal derivatives have also been synthesised, for example λ-$BETS_2Fe_xGa_{1-x}Cl_4$.[72] When x= 0.43 the compound has T_c=4.2K at ambient pressure.

1.16 Tellurium compounds

The use of selenium atoms instead of sulphur in tetrachalcogenafulvalenes led to the formation of conductive complexes and ultimately superconductivity. The main advantage of using selenium instead of sulphur is that selenium introduces greater dimensionality that helps to develop 2-D conductivity. Similarly replacement of selenium with tellurium should yield further electron donors.

The first tellurium derivative of TTF, hexamethylenetetratellurafulvalene HMTTeF (63) was synthesised[73] in 1982 by the following route, scheme 19.

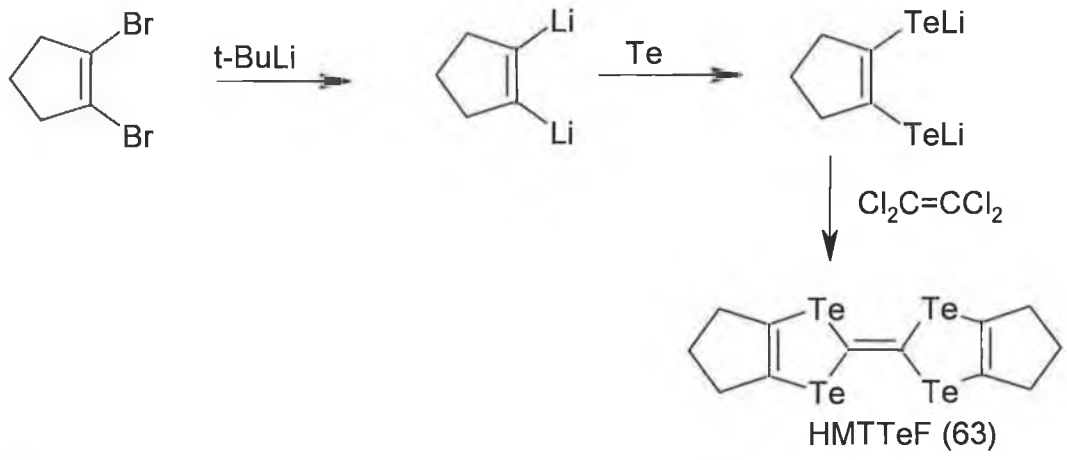

Scheme 19

HMTTeF underwent two reversible one-electron oxidations at 0.40V and 0.69V respectively. Since electron transfer is faster for HMTTeF than for TMTSF and TMTTF, ionization in this species occurs via the lone pairs on the tellurium atoms. In sulphur based tetrachalcogenafulvalenes ionization is thought to occur via the π-bonded network.

Tetratellurafulvalene (TTeF) (64) was finally synthesised in 1987[74] by a method similar to that described for HMTTeF, the starting material being 1,2-(trimethylstannyl) ethylene (65), scheme 20.

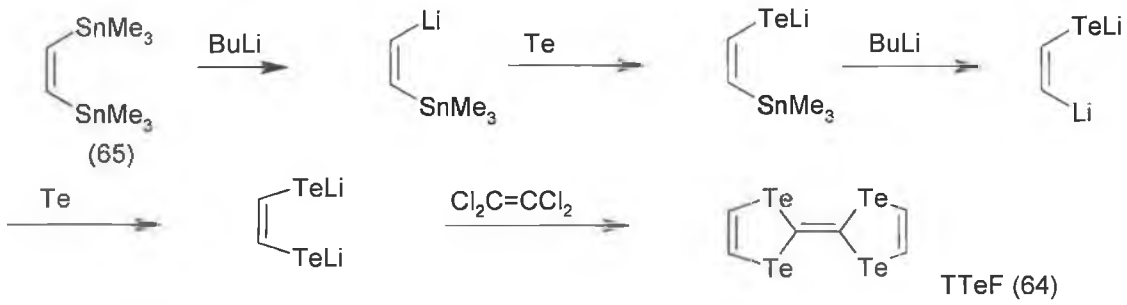

Scheme 20

TTeF shows two one-electron oxidations at 0.59V and 0.84V. The C-T complex formed between TTeF and TCNQ formed segregated stacks and has room temperature conductivity ≅ 1800Scm^{-1}.[75] Comparison of the electrochemical behaviour of TTF, TSF and TTeF can be seen below, table 1.1.

Donor	$E^1_{½}$ (V)	$E^2_{½}$ (V)	$\Delta E_{½}$ (V)
TTF	0.47	0.81	0.34
TSF	0.62	0.90	0.28
TTeF	0.59	0.84	0.25

Volts vs. SCE at Pt button electrode; 0.2M tetrabutylammonium tetrafluoroborate in DCM; 200 mV/s sweep rate.

Table 1.1

TTeF derivatives are very difficult to handle. In an effort to avoid this a number of mixed donors were developed. Compounds such as tetraalkyltellurium (66)[76] and ditelluride derivatives (67)[77] and (68)[78] have been synthesised.

Cyclic voltammetric analysis of (66) shows that both the first and second oxidation potentials are independent of alkyl chain length. Compound (68) shows two one-electron reversible oxidation waves at 0.48V and 0.83V. The fact that further oxidations are not observed in (68) means that the tellurium double bridge behaves as an electronic insulator, dividing the molecule into nearly independent TTF halves and preventing coulombic interactions between them.

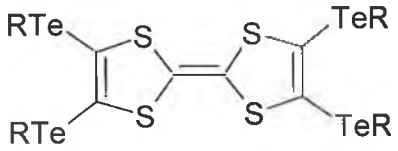

R= alkyl. (66)

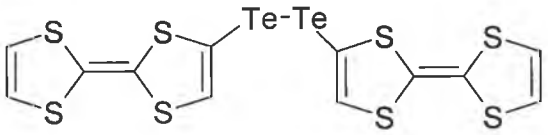

(67)

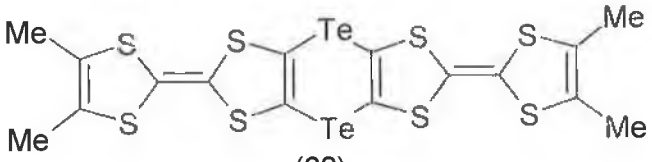

(68)

Electron Acceptors

1.17 Electron Acceptors

By definition electron acceptors are organic compounds with high electron affinity. This high electron affinity enables these compounds to form stable radical anions and dianions. Efforts to improve and tailor electron accepting ability effectively mirror the trends that shaped the research into electron donors. TCNQ displays a number of important properties that need to be replicated in order to synthesise other electron acceptors that will ultimately form C-T complexes with various electron donors. TCNQ is flat, highly symmetrical, possesses a conjugated π-system, has electron-withdrawing groups at disparate ends of the molecule and most importantly has high electron affinity. A number of well-defined synthetic strategies have been explored in an effort to modify the properties of TCNQ.

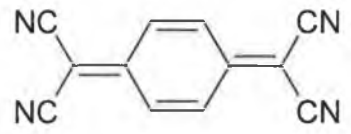

TCNQ

The synthetic trends can be summarised below.

1. Extension of the π-electron system. Achieving this should decrease the on-site coulombic repulsion experienced by both radical anions and in particular dianions. The stability of these species should consequently be increased.
2. Introduction of peripheral substituents. By adding either electron donating or electron withdrawing groups the effective strength of the parent acceptor can be modified.
3. Introduction of a heteroatom into the π-electron system. Heteroatoms alleviate steric strain and also increase dimensionality through better intermolecular contacts. This property improves the likelihood of segregated stacks being formed in a charge transfer complex.

1.18 Synthesis of TCNQ

TCNQ was first synthesised in 1962.[79] The synthesis involved the condensation of 1,4-cyclohexanedione with malononitrile and subsequent bromination and dehydrobromination to yield TCNQ, scheme 21.

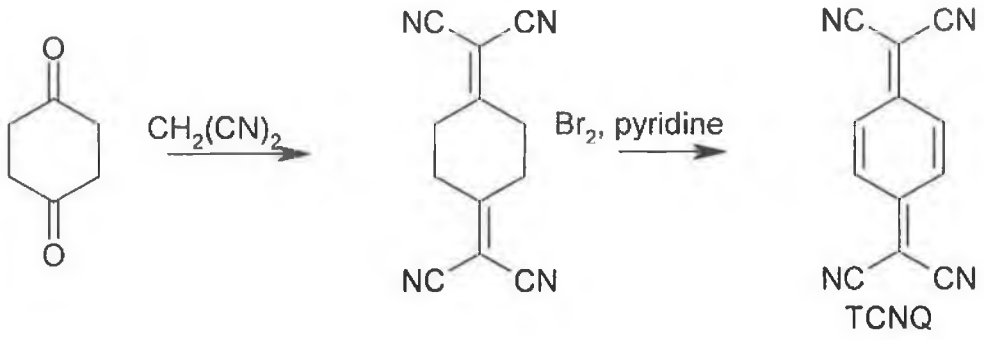

Scheme 21

Another synthesis involves phenylenedimalononitrile (69) as a key intermediate. Compound (69) can be prepared by the Pd catalysed reaction of diiodoarenes with malononitrile, scheme 22.[80] Oxidation of (69) yields TCNQ.

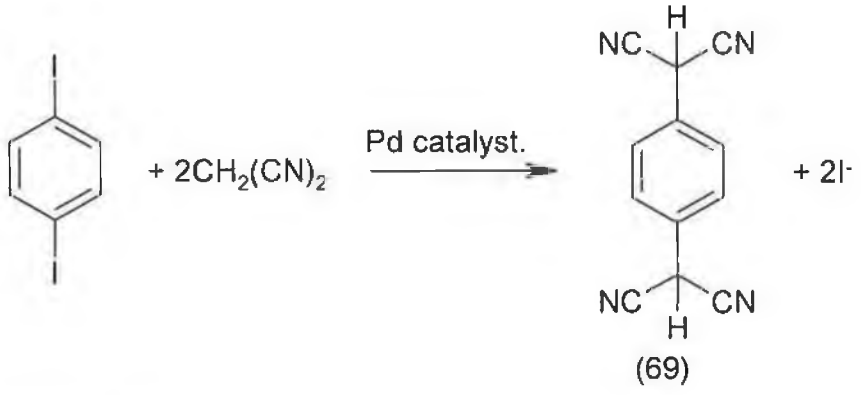

Scheme 22

The most versatile synthesis of TCNQ derivatives is the reaction of a suitable quinone malononitrile with titanium tetrachloride and pyridine (Lehnerts conditions), scheme 23.[81]

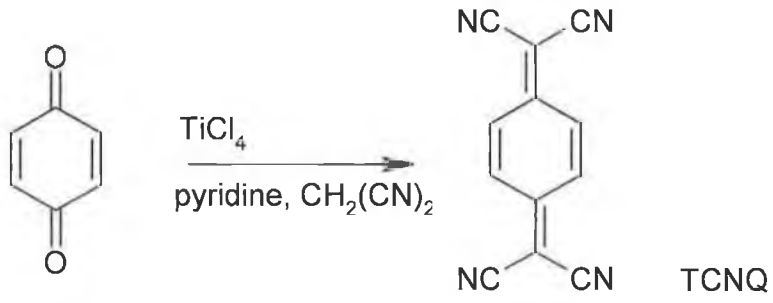

(70)

Scheme 23

The reaction involves a Lewis acid promoted condensation at the oxygen of the corresponding quinone (70). TCNQ undergoes two reversible reductions at $E^1_{1/2}$= 0.08V and $E^2_{1/2}$=-0.48V.[82] The most significant charge transfer complex formed by TCNQ was TCNQ-TTF.[2] This complex provided the benchmark with which other C-T complexes can be compared. TCNQ-TTF was found to crystallise in segregated columnar stacks of donors and acceptors. The intermolecular distances were found to be less than the van der Waal's radii for the neutral species. The complex showed metallic behaviour between 293K and 53K, the conductivity reaching a maximum value at 59K ($\sigma=10^4 Scm^{-1}$).[83]

1.19 Substituted TCNQ derivatives

Addition of various substituents onto the quinoid ring of TCNQ can affect the electron accepting ability of the parent compound quite dramatically. Alkyl derivatives, 2-methyl, 2-propyl and 2,5-dimethyl TCNQ were synthesised by a similar method to that of TCNQ itself.[84] Wheland and Martin described the synthesis of numerous substituted TCNQ derivatives.[85] The multi-step synthesis generally began with the appropriate substituted p-xylene dihalide, scheme 24. 2-Chlorobenzylthiocyanate can be used instead of the highly toxic CNCl.[86]

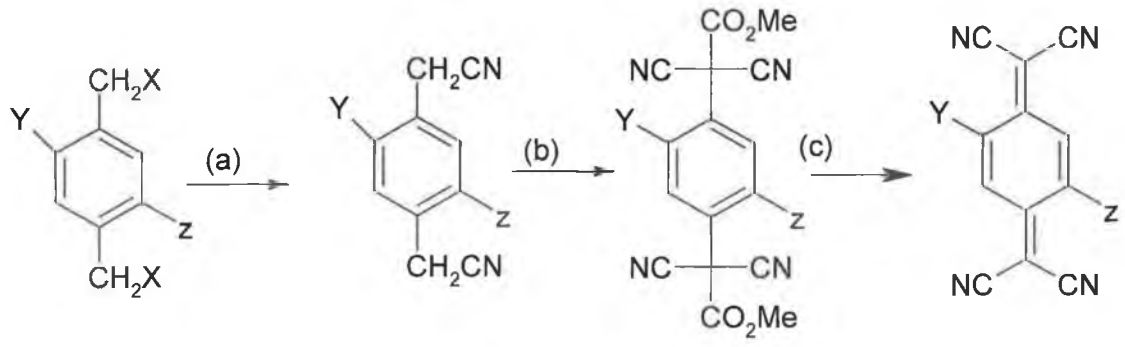

(a) NaCN, (b) (i) NaOMe, $(MeO)_2CO$, (ii) ClCN, (c) (i) KOH, (ii) HCl, (iii) pyr. Br_2.

Scheme 24

2,5-Dimethyl-TCNQ has also been synthesised by the reaction of terephthaloyl chloride (71) and excess cyanotrimethylsilane. The intermediate product 1,4-bis(dicyanotrimethylsiloxymethyl)benzene (72) can then be converted to the desired substituted TCNQ, scheme 25.[87]

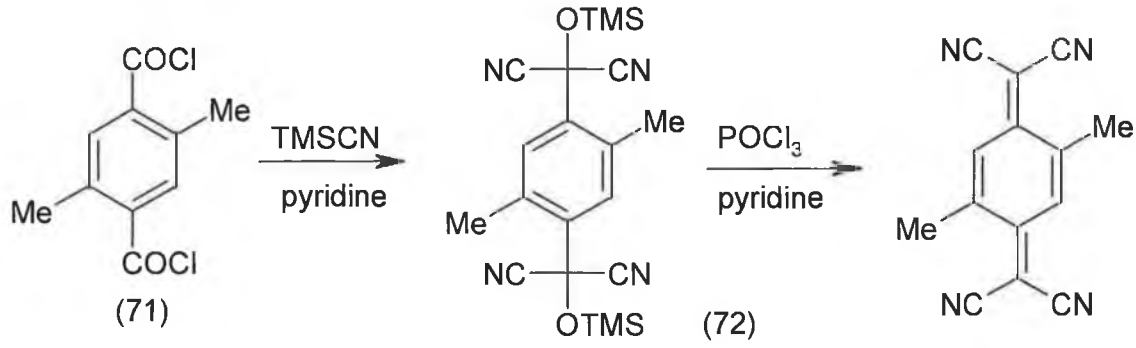

Scheme 25

Long chain diesters of succinic acid (73) were obtained from the reaction of succinic anhydride and various alcohols. These esters gave 2,5-disubstituted cyclohexane-1,4-dione (74) in good yields on treatment with ultrasonically dispersed potassium in toluene, scheme 26.[88] This reaction is a Dieckmann cyclisation. The TCNQ derivatives are again synthesised by the Knovenagel condensation of the dioxo esters with malononitrile, followed by oxidation with N-bromosuccinimide and pyridine.

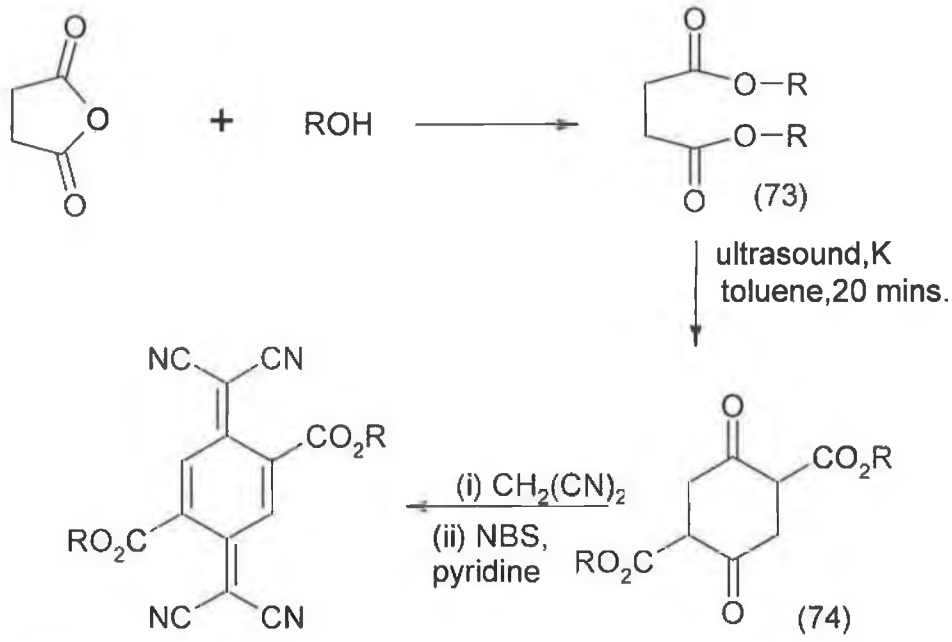

Scheme 26

The introduction of alkyl groups to the TCNQ molecule progressively lowers the reduction potential for radical anion formation. This observation agrees with the expectation of decreased π-acid character for alkyl substituted TCNQ derivatives.[89] Conversely the addition of electron withdrawing substituents raises the reduction potentials of potential acceptors, table 1.2.[90]

Compound	$E^1_{½}$ / V	$E^2_{½}$ / V
TCNQ	0.08	-0.48
Methyl-TCNQ	-0.17	-0.68
2,5-dimethyl-TCNQ	-0.23	-0.71
$TCNQF_4$	0.53	0.02

Table 1.2

1.20 π-Extended TCNQ derivatives

Extending the π-conjugation of the TCNQ unit both linearly and annullarly can reduce the onsite coulomb repulsion. The increased orbital overlap also increases the bandwidth. TNAP (11,11,12,12-tetracyanonaphtho-2,6-quinodimethane) (76) was synthesised from the corresponding dialkyl-halide (75) in a method reminiscent of the synthesis of substituted TCNQ's.[91] TNAP formed a 1:1 C-T complex with TTF.

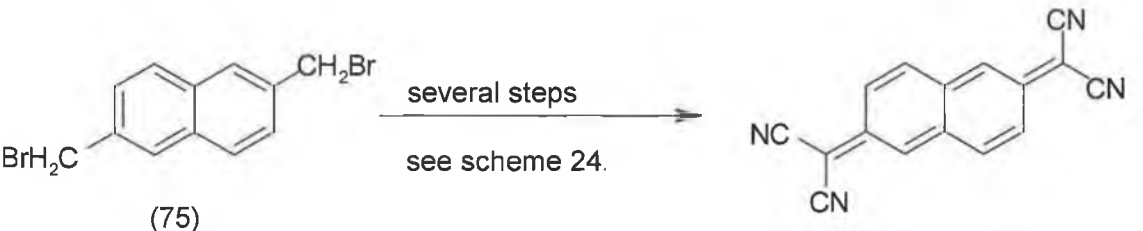

(75) (76)

TCNQ analogues fused laterally with aromatic rings provided the largest number of stable neutral π-extended derivatives of TCNQ. Benzo-TCNQ (77),[92] dibenzo-TCNQ (78) and naphtho-TCNQ (79a)[93] were all synthesised from the corresponding quinone derivatives under Lehnerts conditions.

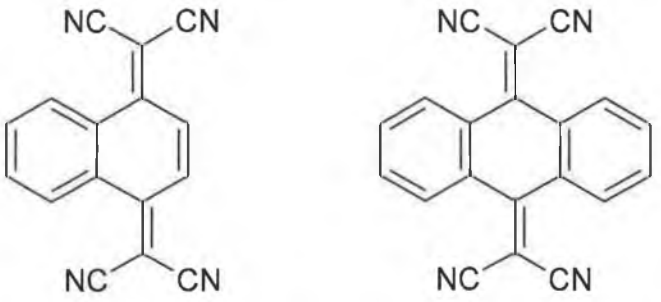

(77) (78)

Substituted naphtho-TCNQs (79a)-(79e) were synthesised from the corresponding diketones using Lehnerts reagent, malononitrile and pyridine.[94]

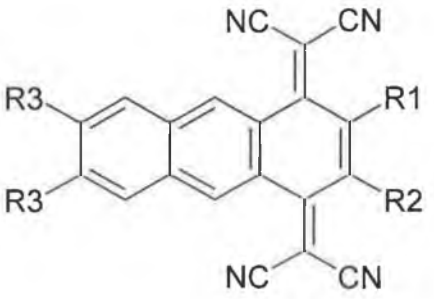

naphtho-TCNQ (79)

(79a): R1=R2=R3=H.
(79b): R1=MeO, R2=R3=H.
(79c): R1=MeO, R2=H, R3=MeO.
(79d): R1=R2=Me, R3=H.
(79e): R1=R2=Cl, R3=H.

Electrochemical data obtained for (77), (78) and (79a) showed a reduction in the value of ΔE (the difference between the first and second reduction potentials). The smallest ΔE value was 0.19V obtained for (78). Despite significant reduction of the onsite coulombic repulsion experienced by the charged species, no C-T complexes were isolated. The initial reduction potential for each compound has been shifted to a more negative value compared with TCNQ. In fact acceptor strength appears to decrease with increasing number of fused rings, i.e., TCNQ> (77)> (78). Electron accepting ability is weakened by naphtho annelation to a greater extent than benzo annelation, i.e., TCNQ> (77)> (79a).

For the naphtho-TCNQ series compounds (79a), (79b) and (79c) all display two reversible one-electron reductions, whereas (79d) and (79e) possess a single reversible two-electron reduction wave. This is due to the poor thermodynamic stability of the radical anion in each the latter cases. The low stability is probably due to the lack of planarity of the radical anions. Compound (79e) is the easiest to reduce.

11,11,12,12-Tetracyano-2,6-anthraquinodimethane (TANT) (80) was synthesised from 2,6-diaminoanthraquinone (81), scheme 27.[95]

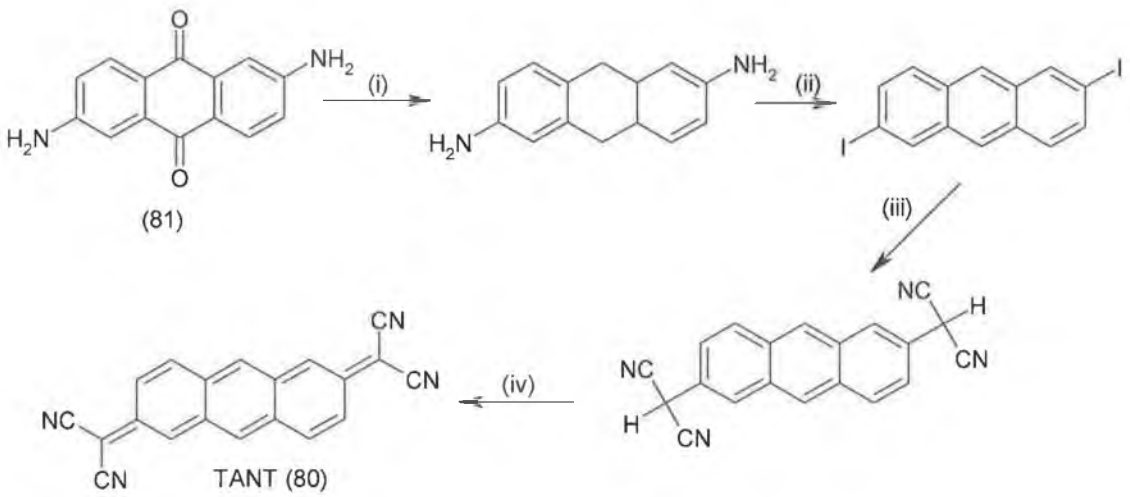

(i): Zn, aq. NH_4OH. (ii): $NaNO_2$, conc. HCl then KI. (iii): $Pd(PPh_3)_4$ NaH, $CH_2(CN)_2$, THF. (iv): DDQ, MeCN.

Scheme 27

TANT has two one-electron reversible redox waves at $E^1_{1/2}$= 0.20V and $E^2_{1/2}$= -0.12V, showing that it is a strong electron acceptor. TANT forms a 1:1 C-T complex with hexamethylenetetratellurafulvalene (HMTTeF) and this complex has high conductivity $\sigma = 11.5 Scm^{-1}$.

Compounds (82)-(84) were synthesised by the reaction of the corresponding quinones with malononitrile in the presence of titanium tetrachloride and pyridine.[96]

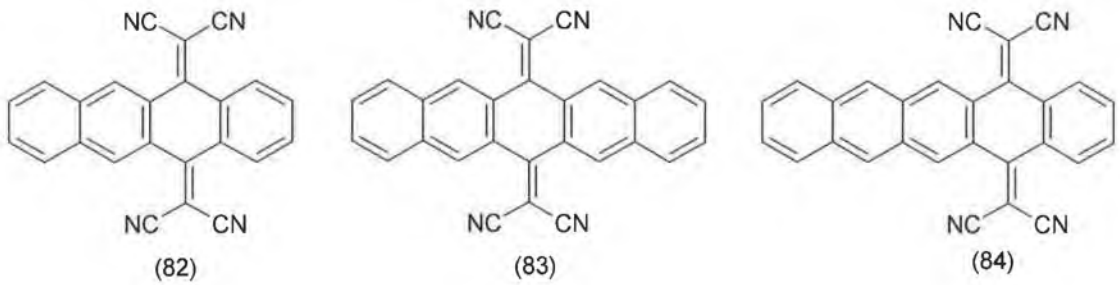

All three compounds undergo two one-electron reversible reduction waves, (83) being the worst acceptor and (82) being the best. However these both undergo a further reduction to a radical trianion, the additional electron is located in the aromatic skeleton. Compound (82) has $E^3_{1/2}$= -1.85V, compound (83) has $E^3_{1/2}$= -1.61V and compound (84) has $E^3_{1/2}$= -1.54V. The neutral compounds (82)-(84) are non-planar, the distortion being

due to the interaction between the dicyanomethylene groups and the peri-hydrogens of the aromatic skeleton. This deviation from planarity severely inhibits the ability of π-extended TCNQ derivatives from forming highly conductive complexes with organic electron donors.

The synthesis of various π-extended TCNQ derivatives has in fact reduced the onsite coulombic repulsion experienced by the reduced species. However extension of the π-system by fusing aromatic rings to the TCNQ skeleton decreases the electron acceptor ability. There is also a marked distortion from the ideal planar structure caused by the interaction of the peri-hydrogens and dicyanomethylene groups.

1.21 Heteroquinoid electron acceptors

Heteroquinoid systems based on thiophene, selenophene and furan have been used as building blocks for possible electron acceptors. Chalcogen-chalcogen interactions should increase dimensionality. Linearly conjugated systems containing heterocycles should suffer less from steric strain, because the heterocyclic rings should arrange themselves trans to one another.

The first hetero-TCNQ was 2,5-bis(dicyanomethylene)-2,5-dihydrothiophene (85), scheme 28.[97]

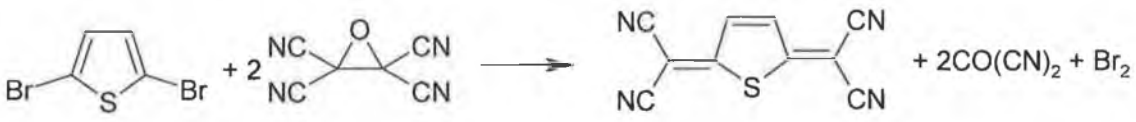

(85)

Scheme 28

Compound (85) is isoelectronic to TCNQ and undergoes two reversible single electron redox waves at 0.07V and –0.54V. It is a weaker electron acceptor than TCNQ, mainly due to the lower aromaticity of the central heterocyclic ring formed upon the reduction process. Selenoquinoid (86) and furanoquinoid (87)[98] derivatives both have the same reduction potential at 0.03V.

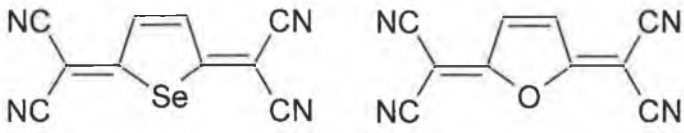

(86) (87)

Considering the order of aromaticity, thiophene> selenophene> furan, this means that the inductive effects of the introduced heteroatoms contribute to the enhancement of the electron accepting abilities of hetero-TCNQs.

A biheteroquinoid system is a suitable building block for extensive polyconjugation. These systems should remain planar because, by taking a trans configuration, hydrogen repulsion can be eliminated. The extended π-system should reduce the coulombic repulsion.

Hetero-TCNQ electron acceptors based on thiophenes (88) and (89), selenophenes (90) and (91) and furans (92) and (93) have been synthesised.[99,100]

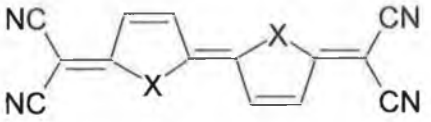

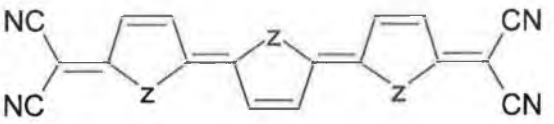

(88) X= S
(90) X= Se
(92) X= O

(89) Z= S
(91) Z= Se
(93) Z= O

The electron acceptors containing two heterocyclic moieties all display two one-electron reversible reduction waves. The compounds that contain three heterocyclic moieties undergo one two-electron reduction. This behaviour is not wholly unexpected, as it is quite common for electron acceptors with large π-extended systems to be easily reduced to dianions. It is possible to increase the electron accepting ability of all the compounds (88)-(93) by the introduction of electron withdrawing substituents. In these cases bromine substitution directly onto the heterocycle can dramatically increase the accepting ability and consequently enhance the conductivity of any C-T complexes formed.

Compound (90) has $E^1_{1/2}$= -0.03V and $E^2_{1/2}$= -0.25V. The introduction of bromo functions at 3,3'-positions improves the reduction potentials to $E^1_{1/2}$= 0.15V and $E^2_{1/2}$= -0.08V. The dibromo derivative (94) forms a highly conductive 1:1 C-T complex with HMTTeF (σ= 86.0Scm^{-1}).

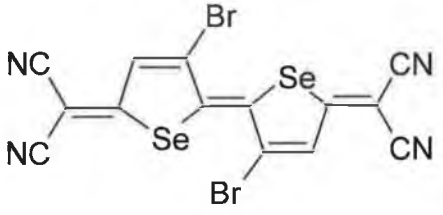

(94)

Hetero-TCNQs can also be synthesised by nucleophilic substitution of the respective dibromides using sodium dicyanomethanide and a catalytic amount of tetrakis(triphenylphosphine)palladium(0). The final oxidation can be accomplished using saturated bromine water, DDQ or lead acetate, scheme 29.

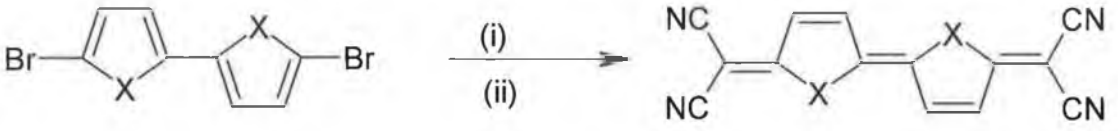

X= S, O, Se. (i): $NaCH(CN)_2$, $Pd(PPh_3)_4$. (ii): Br_2 aq.

Scheme 29

Application of this method led to the synthesis of novel acceptor (95) the bithiazole analogue of (88).[101] Compound (95a) displayed two reversible one-electron redox waves at 0.34V and 0.01V, indicating good accepting ability. Compound (95a) formed C-T complexes with TTF, TMTSF and BEDT-TTF. The (95a)-TTF complex has a conductivity of $2.1x10^{-3}Scm^{-1}$.

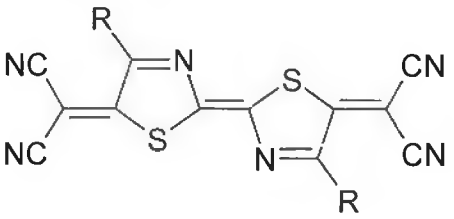

(95a) R=H
(95b) R=OMe

Vinylogous hetero-TCNQs (96)-(98) have been prepared from the corresponding dihalide (99), scheme 30.[102] The additional conjugation leads to coalescence of the first and second reduction waves. Poor solubility inhibited extensive complexation with electron donors.

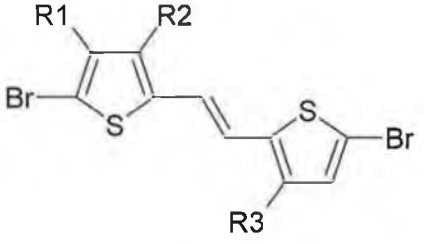

(99)

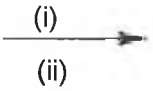

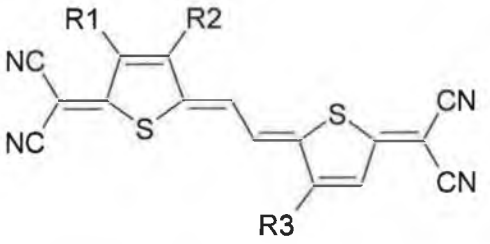

(96): R1=R2=R3=H.
(97): R1=H, R2=R3=Br.
(98): R1=R2=R3=Br.

(i): $NaCH(CN)_2$, $Pd(PPh_3)_4$. (ii): DDQ.

Scheme 30

Hetero-TCNQs containing fused heteroquinoid rings have been examined. Compounds (100) and (101) have been synthesised from dihalide precursors.[103] The syntheses can be carried out either using method A (TCNEO, reflux) or method B ($NaCH(CN)_2$, $Pd(PPh_3)_4$ and Br_2). Addition of bromine increased the acceptor ability of fused hetero-TCNQs.

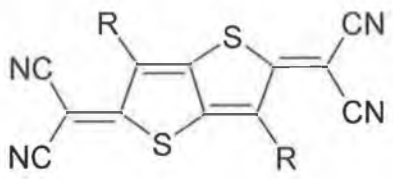

(100a): R=H
(100b): R=Br

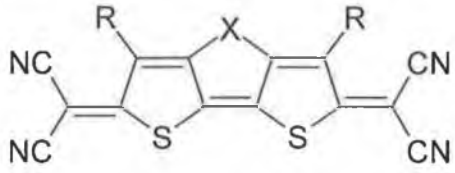

(101a): X=S, R=H
(101b): X=S, R=Br

Compounds (100) and (101) formed highly conductive 1:1 C-T complexes with numerous donors. Exceptionally high conductivity at room temperature was achieved by the 1:1 complex formed between (100b) and HMTTeF (σ= 140Scm^{-1}).

Although bromo-substitution can increase acceptor ability, additional substituent groups may sterically interfere with the formation of conductive complexes. Therefore it would be desirable to have novel TCNQ derivatives with inherently high electron affinity. Introduction of heteroquinoid rings that induce high aromaticity would improve the acceptor ability of hetero-TCNQs. This reasoning led to the synthesis of compounds (102) and (103).[104]

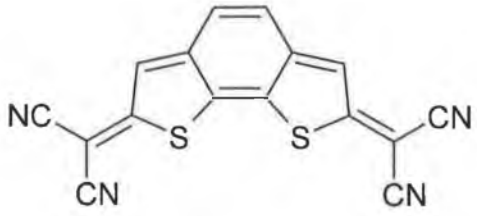

(102)

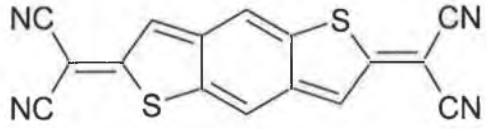

(103)

Compounds (102) and (103) have similar electron accepting strength when compared with TCNQ and both formed conductive complexes with various donors. Compound (102) formed a 1:1 C-T complex with TTF (σ= 1.0Scm^{-1}). The complex with the highest conductivity was the 1:1 complex formed by (103) with HMTTeF (σ= 25.0Scm^{-1}).

Takahashi and Tarutani recently synthesised the novel acceptor CPDT (104) that contains three terminal electron-withdrawing groups attached to a fused heteroquinoid structure similar to compound (101a).[105]

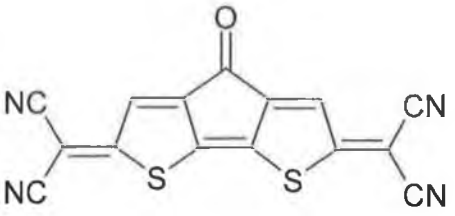

CPDT (104)

Compound (104) displays three reversible one-electron redox waves at 0.04V, -0.27V and –1.43V. It forms radical ion salts that demonstrate metallic behaviour with cations (Me_4N and Et_4N). The acceptor molecules form two-dimensional networks through which conduction takes place. This was the first time that an electron acceptor had provided the conduction pathway in a radical ion salt with metallic properties.

In order to reduce the interaction between the dicyanomethylene group and peri-hydrogens in π-extended TCNQ, compounds (105),[106] (106)[107] and (107) were synthesised.[108] These compounds have a heterocyclic ring fused to the π-extended system.

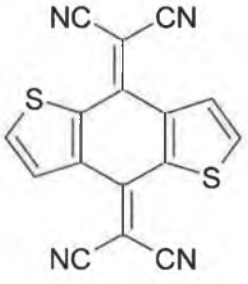

(105)

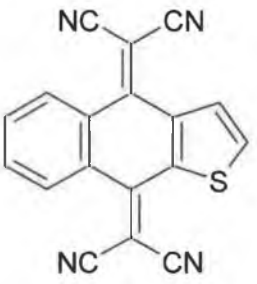

(106)

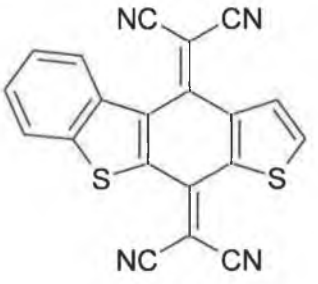

(107)

Both (105) and (106) are iso-electronic with dibenzo-TCNQ. Both adopt a butterfly shape but deviate from planarity to a lesser extent than dibenzo-TCNQ. Compound (105) underwent two one-electron reductions at 0.03V and –0.24V while (106) displayed a two-electron reduction directly to the dianion at –0.18V. Compound (105) formed a conductive 1:1 C-T complex with TTF (σ= 4.8Scm^{-1}).[109] Compound (107) undergoes two one-electron reversible reductions at 0.11V and –0.03V.

The preparation of hetero-TCNQs fused with 1,2,5-thiadiazole provided a way of increasing intermolecular contacts. Bis-1,2,5-thiadiazolo-TCNQ (BTDA) (108a)[110] and 1,2,5-thiadiazolo-TCNQ (TDA) (109)[111] both undergo two one-electron reductions. TDA is a stronger electron acceptor than BTDA. TDA $E^1_{1/2}$= 0.12V and $E^2_{1/2}$= -0.38V, BTDA $E^1_{1/2}$= -0.02V and $E^2_{1/2}$= -0.49V.

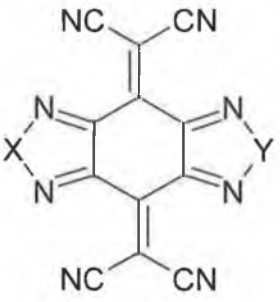

BTDA (108a): X=Y=S
TSDA (108b): X=S, Y=Se
BSDA (108c): X=Se, Y=Se

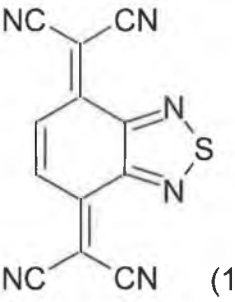

(109)

Selenium analogues of BTDA have also been synthesised.[112] However C-T complexes with strong donors and radical cation salts formed using (108b) and (108c) as electron acceptors had similar conductivities to their BTDA counterparts. Radical ion salts of BTDA exhibit two-dimensional electrical conductivity because of interheteroatom S---NC interactions.[113] However C-T complexes formed by BTDA and TTF and other organic donors are semi-conductors owing to mixed stack formation. The formation of mixed stacks is facilitated by the inclusion behaviour of BTDA and by interactions between the heteroatoms.[114] Removal of one heterocyclic component should eliminate the inclusion behaviour. This was proved by TDA (109). Intermolecular hydrogen bonding between cyano-N(6)----H(5) lead to the formation of a coplanar dyad. This dyad formation leads to reduction of coulombic repulsion. TDA forms highly conductive complexes with TTF and its derivatives.

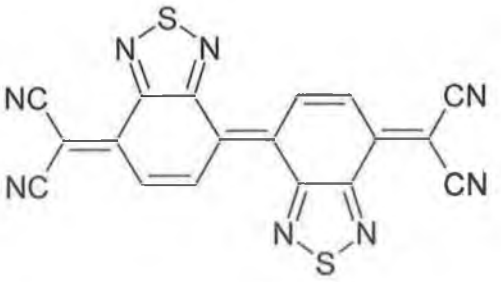

(110)

More recently bis-1,2,5-thiadiazolo-TCNDQ (110) has been synthesised.[115] It undergoes two reversible one-electron reductions at 0.33V and 0.12V, suggesting that (110) is a very strong electron acceptor. A crystal of neutral (110) exhibits extensive intermolecular contacts, C-H---N hydrogen bonding as in TDA and two types of N---S contacts. It forms conducting radical ion salts and C-T complexes. The complex with the highest conductivity is the 1:1 complex formed with HMTSF ($18Scm^{-1}$).

1.22 Electron Acceptors based on DCNQI derivatives

An alternative to TCNQ acceptors are compounds based on N,N'-dicyano-p-quinodiimine (DCNQI) (111).

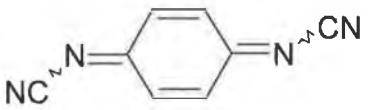

(111)

These compounds were discovered by Hunig and co-workers.[116] Their main advantage is that they do not suffer from the same extreme steric problems as experienced by TCNQ derivatives. The =N-CN group is smaller than $=C(CN)_2$. It can also arrange itself away from either hydrogen atoms or bulkier substituents and hence preserve the desired planar structure. The synthesis involves titanium tetrachloride ($TiCl_4$) and bis(trimethylsilyl)carbodiimide (BTC), scheme 31.

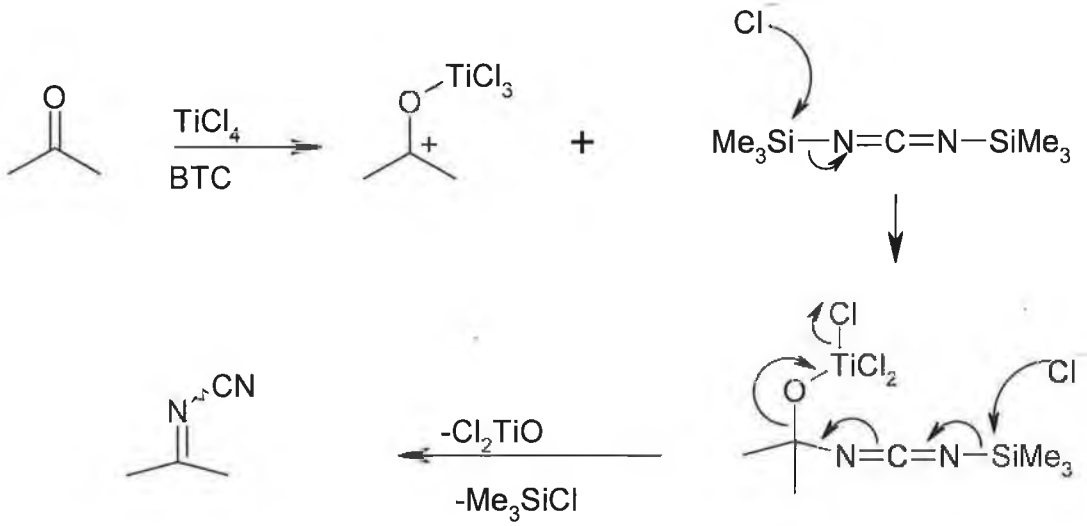

Scheme 31

This reaction is unusual as it involves condensation at the carbonyl group of a quinone. DCNQI displays very similar electrochemical behaviour to TCNQ. DCNQI has $E^1_{½}$= 0.39V and $E^1_{½}$= -0.25V[117] compared to TCNQ with $E^1_{½}$=0.39V and $E^1_{½}$=-0.28V. DCNQI forms a conductive C-T complex with TTF (TTF-DCNQI.$2H_2O$).[118] Exclusion of the water molecules prevents crystal formation.

The acceptor ability of DCNQI can be modified by the addition of either electron donating or electron withdrawing groups. Extending the π-system reduces the coulombic repulsion experienced by the charged species. However due to the small size of the =N-

CN group the peri-hydrogens of large benzannulated systems do not cause a large distortion away from the ideal planar structure. This property means that there has been no widespread synthetic research into heterocyclic-DCNQI derivatives.

A range of substituted p-benzoquinones was successfully converted into DCNQI derivatives (112), scheme 32.[119]

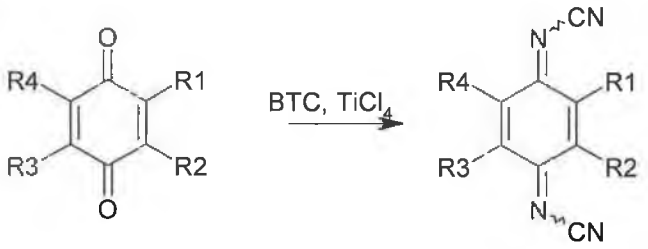

(112)

(112a) R1=Me, R2=R3=R4=H
(112b) R1=R3=Me, R2=R4=H
(112c) R1=R2=R3=R4=Me

Scheme 32

A series of fused aromatic DCNQI derivatives (113-116) has been synthesised.[120]

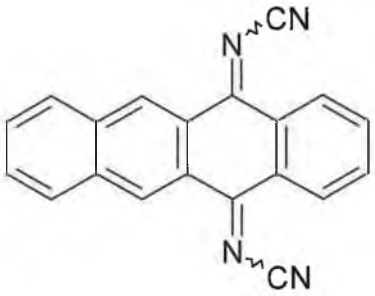

(113)

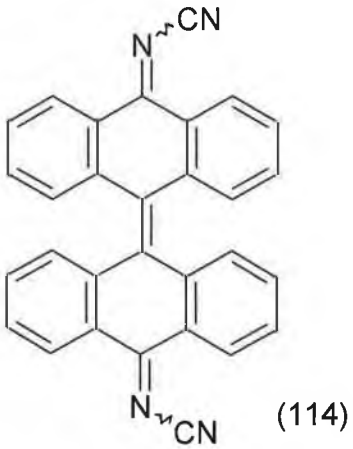

(114)

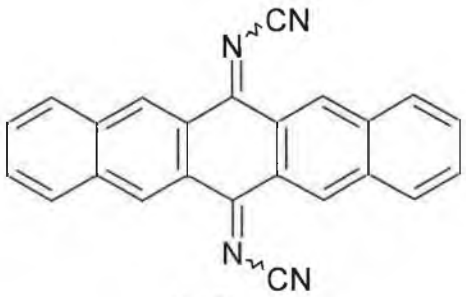

(115)

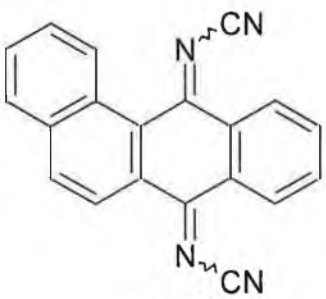

(116)

Extension of the π-system decreases the acceptor ability but reduces the onsite coulombic repulsion experienced by the charged species generated upon electrochemical reduction.

Compound (116) was the best acceptor with two reversible one-electron redox waves at -0.21V and -0.48V. Compounds (113) and (114) displayed two single-electron reductions at -0.32V and -0.62V and -0.43V and -0.67V respectively. The extended DCNQI derivatives do not suffer from the same steric problems as their TCNQ counterparts.

Another interesting development has been the synthesis of hybrid electron acceptors. These compounds contain both =NCN and $=C(CN)_2$ functional groups. These hybrid acceptors are generated by the treatment of suitable quinones with malononitrile, pyridine and titanium tetrachloride. The mono(dicyanomethylene) product is then treated with BTC and titanium tetrachloride to yield the desired hybrid structure (117), scheme 33.[121]

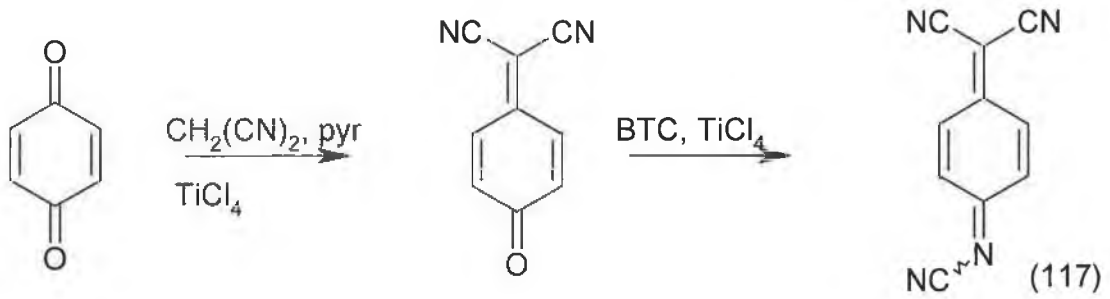

Scheme 33

The =N-CN group in DCNQI type compounds can occupy either syn or anti positions with respect to ring substituents. The =NCN groups generally arrange themselves in such a way as to minimise steric congestion. The DCNQI derivative of 1,4-dibromoanthracenedione (118) can have a number of configurations.

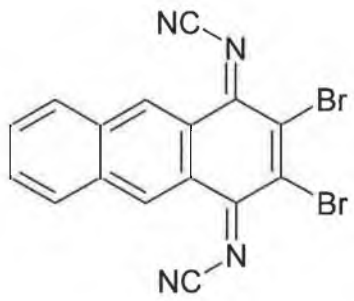

anti/anti (118)

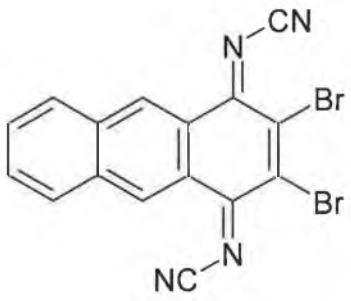

syn/anti (118)

The lowest energy isomer is the anti/anti isomer (333.6KJmol^{-1}). The syn/anti isomer (338.6KJmol^{-1}) has only slightly higher energy.[122] The small difference in energy

between these two isomers suggests fast isomerism of both =N-CN groups. This is supported by the fact that isolation of individual isomers is impossible.

The presence of a thiophene unit mitigates the steric hindrance and the presence of electronegative atoms leads to better accepting ability. This led to the synthesis of thiophene fused DCNQI derivatives (119) and (120).[123] Compound (119) underwent two one-electron reductions at 0.00V and –0.46V while (120) was reduced at –0.04V and –0.50V.

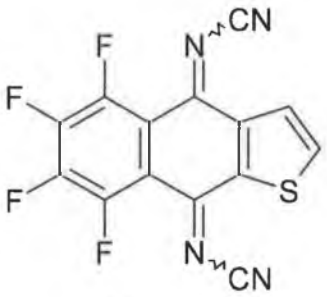

(119)

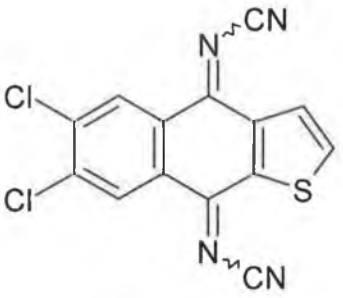

(120)

As well as forming C-T complexes DCNQI derivatives form radical ion salts with metals. The most important radical ion salts formed are those formed between 2,5-disubstituted DCNQIs and copper. These salts have high conductivity and have a 2:1 ratio with respect to the metal ion present. Other metals used to form these salts include the alkalis, thallium, rubidium and silver.[124]

2,5-Disubstituted DCNQI copper salts can be classified into two different groups according to the temperature dependence of their conductivity.

1. Group A (121a-i) show metallic behaviour down to very low temperatures.
2. Group B (121j-o) tend to undergo metal to insulator transitions between 160-230K.[125]

It would seem that the combination of two large substituents gives a stable metallic state. Conversely smaller substituents lead to phase transitions, the exception being (2,5-dimethyl-DCNQI)$_2$Cu.

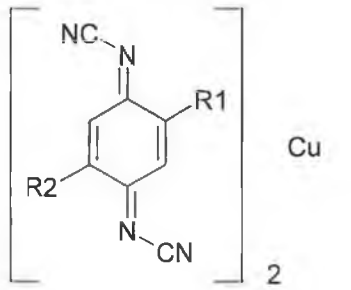

(121)

Group A
(a):R1=R2=Me, (b): R1=Me, R2=Cl, (c): R1=Cl, R2=I
(d): R1=Br, R2=I, (e): R1=Me, R2=OMe, (f): R1=Br, R2=OMe
(g): R1=R2=I, (h): R1=R2=OMe, (i): R1=R2=I

Group B
(j): R1=R2=Cl, (k): R1=Cl, R2=Me, (l):R1=Cl, R2=Br
(m): R1=Br, R2=Me, (n): R1=R2=Br, (o): R1=Cl, R2=OMe

Conduction occurs along the acceptor stacks. Conductivity associated with the cations can be ruled out due to the large intermolecular distances, the Cu-Cu distances being larger than the corresponding distances in Cu metal. A conductivity of 500,000 Scm^{-1} can be obtained at 3.5K for very pure crystals of (2,5-dimethyl-DCNQI)$_2$Cu,[126] in which the copper atoms are co-ordinated in a slightly distorted tetrahedral fashion to the cyano (=N-C**N**) N-atoms of four different acceptor molecules, with all the Cu-N distances being very similar.

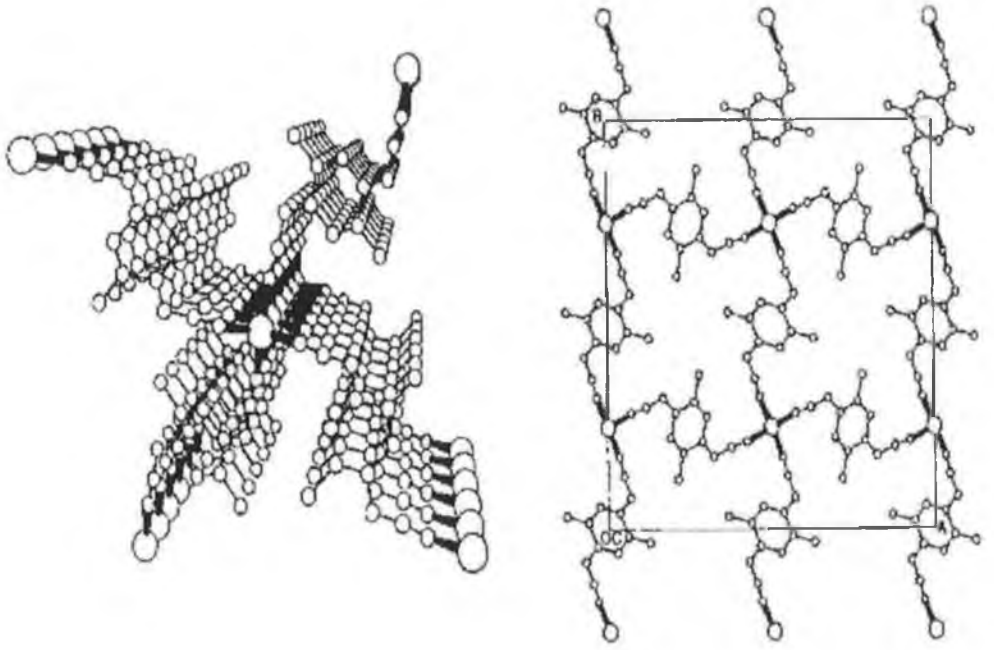

Figure 1.6. Crystal structure of (R,R'-disubstituted-DCNQI)$_2$Cu

If the Cu cation is a closed shell species, there seems to be almost no possibility of obtaining multi-dimensional electronic structure. However these radical ion salts possess a stable metallic state. X-ray diffraction experiments revealed the development of a three-fold superstructure below the metal-insulator transition temperature. The stacking structure of DCNQIs suggests the existence of a planar Fermi surface in the metallic state. However this planar situation must be removed by the development of a three-fold superlattice. This means that Cu is in a mixed valence state ($Cu^{+1\,3}$). This mixed valency means that the highest occupied 3d orbitals of the metal will be partially occupied and located near the Fermi level of the π-metallic band of DCNQI.[127] Therefore there is interaction between the metal d-orbitals and the π-orbitals of the acceptors. These interactions create a multi-Fermi surface. This means that no single modulation wave vector can produce a gap over all the Fermi surfaces. The metal-insulator transition is a co-operative structural-phase transition induced by the deformation of the co-ordination tetrahedron around Cu and the CDW formation in the DCNQI column.[128]

1.23 Other materials

The literature review has been confined to the synthesis and properties of organic compounds that are suitable candidates for the formation of C-T complexes. Although strictly speaking beyond the scope of this particular review there are a number of areas of research that deserve a mention.

Superconductivity has also been observed in salts containing the metal(dmit)$_2$ acceptor.[129]

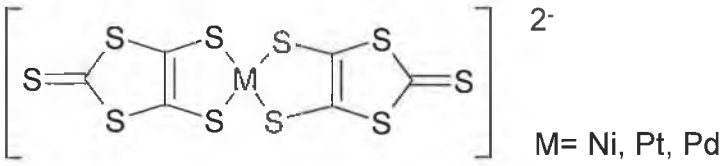

The complexation of this ligand with TTF and tetraalkylammonium cations has led to the formation of superconducting salts. The synthesis and behaviour of these molecular metals and superconductors has been extensively reviewed.[130]

Another noteworthy area is the synthesis of compounds that contain both donor and acceptor moieties. It is hoped that the synthesis of this type of compound will lead to single component conductivity. The first of these type of compounds to be investigated were D-σ-A systems like (122)[131] and (123).[132]

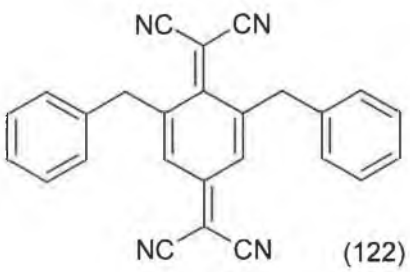

(122)

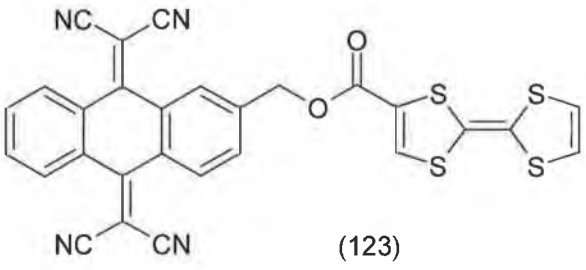

(123)

The peripheral benzene rings of compound (122) are orthogonal to the TCNQ unit thus preventing the desired stacking arrangement. Compound (123) displays both electrochemical oxidation (of donor unit) and reduction (of acceptor unit).

Alternatively D-π-A systems have been developed. Compound (124) displays an intramolecular CT band at 644nm.[133] D-π-A systems of type (125) possess non-linear optical properties.[134]

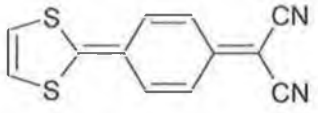

(124)

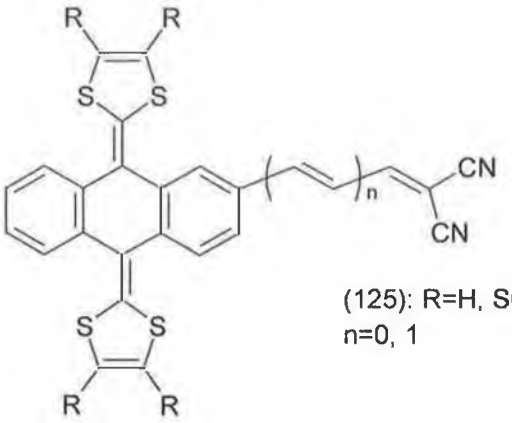

(125): R=H, SCH_2, $(SCH_2)_2$
n=0, 1

Compound (126) has been synthesised and used for electrical rectification.[135]

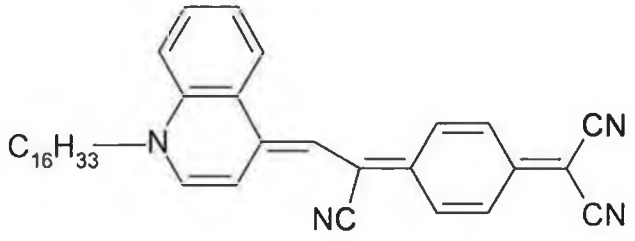

(126)

A similar situation has developed in the synthesis of TTF-like electron donors. TTF systems are no longer developed exclusively to make CT complexes but are now used to make cation sensors, supramolecular switches and devices and other complex systems.[136]

Chapter 2
Results and Discussion

2.1 Reactions of phthalonitrile with various amines

Numerous hetero-TCNQs have been developed. The vast majority of those synthesised to date contain thiophene and selenophene rings. Very little is known about compounds containing a pyrrole ring. Isoindoline derivative (127) is iso-π-electronic with benzo-TCNQ, which has poorer acceptor ability than TCNQ (mainly due to lack of planarity) but shows reduced on-site coulombic repulsion. Incorporation of a heterocyclic ring should ease steric problems.

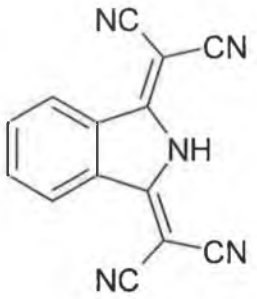

(127)

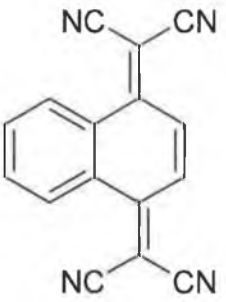

benzo-TCNQ

The aromaticity of pyrrole is intermediate between that of thiophene and furan. Therefore the electron accepting ability of compounds containing pyrrole should be between hetero-TCNQs containing oxygen and hetero-TCNQs containing sulphur. The acceptor ability of compound (127) can be modified by the addition of substituents onto the benzene ring or by substitution at the pyrrole nitrogen.

The N-methyl (128) and N-phenyl (129) derivatives of compound (127) were mentioned in a German patent by BASF in 1982.[137] However no synthetic details were given.

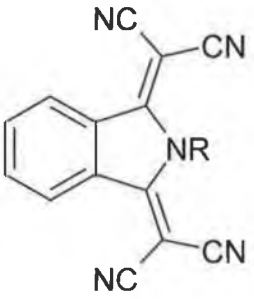

(128) R=Me
(129) R=Ph

The N-methyl derivative (128) has been synthesised in these laboratories by S. P. Conway, using the approaches outlined in scheme 34[138] though the desired product was only obtained in very low yields

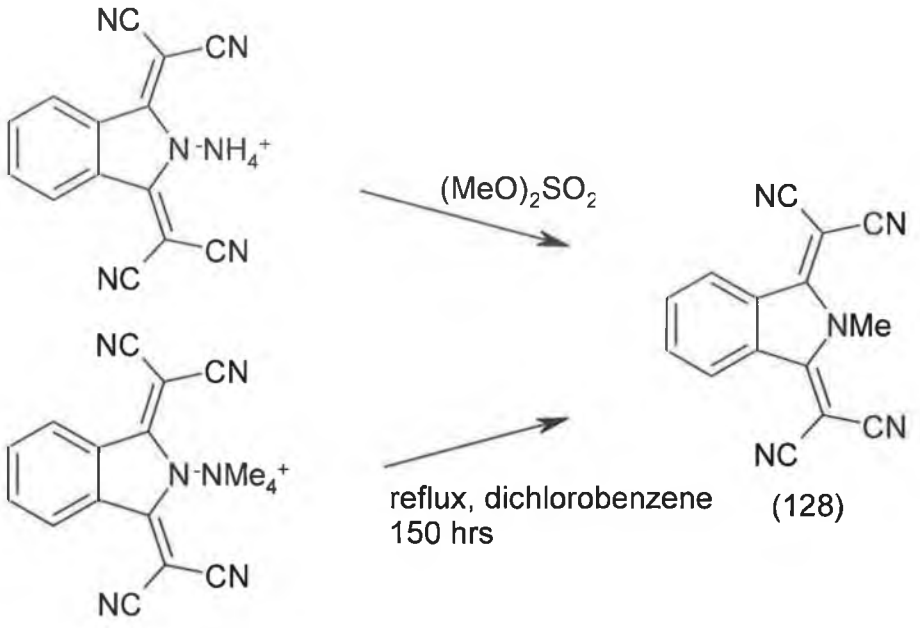

Scheme 34

All attempts to synthesise (128) from N-methylphthalimide by Conway proved unsuccessful. A more efficient method of N-substitution was required.

Linstead and Rowe had reported that the exocyclic imino group of compound (130) reacted with diethyl malonate to yield compound (131).[139] Diiminoisoindoline (132) underwent a bis-condensation reaction with ethyl cyanoacetate to yield compound (133)[140] and the tetra-cyano compound (127) could be similarly synthesised from di-imino derivative (132) according to a French patent, scheme 35.[141]

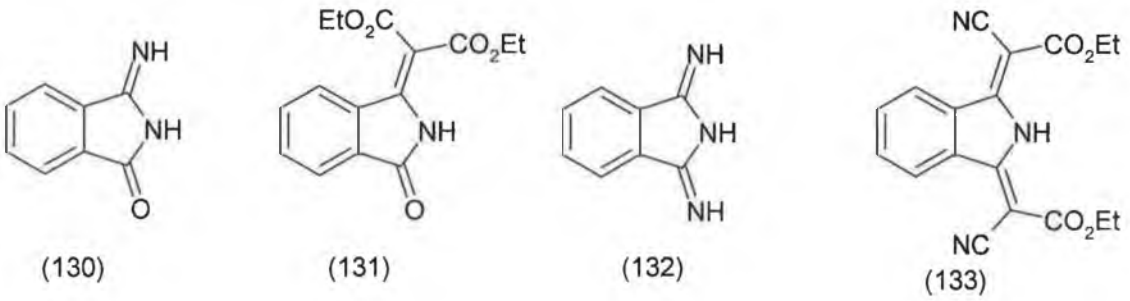

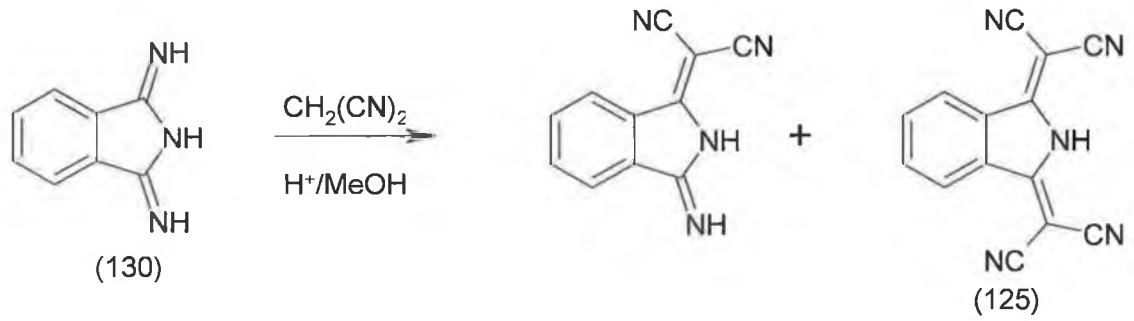

Scheme 35

Compound (127) has also been synthesised in these laboratories via salt (135), which was obtained from reaction of malononitrile with N-phenylimino compound (134) by Conway, scheme 36.[138] This synthetic route is much better because the N-phenylimino compound (134) is much easier to make than its di-imino analogue (132).

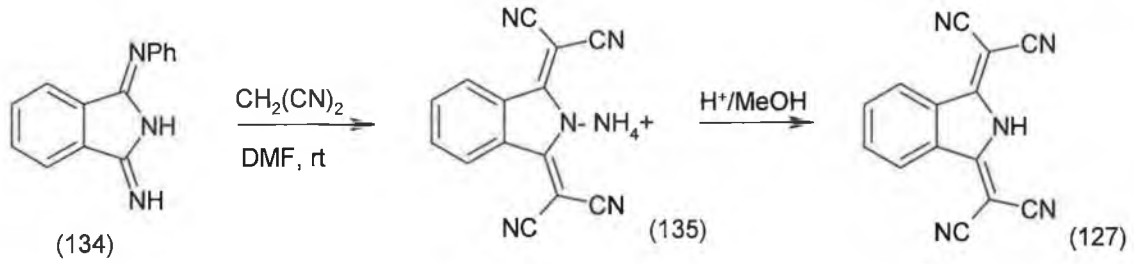

Scheme 36

Clark, Elvidge and Golden reported that 1,3-dimethylimino compound (136) rearranged to the tri-substituted compound (137) during reaction with aniline, scheme 37.[142] Subsequent reaction between (137) and malononitrile was thought to be a feasible alternative to the procedures depicted in scheme 34 for the synthesis of N-methyl derivative (128).

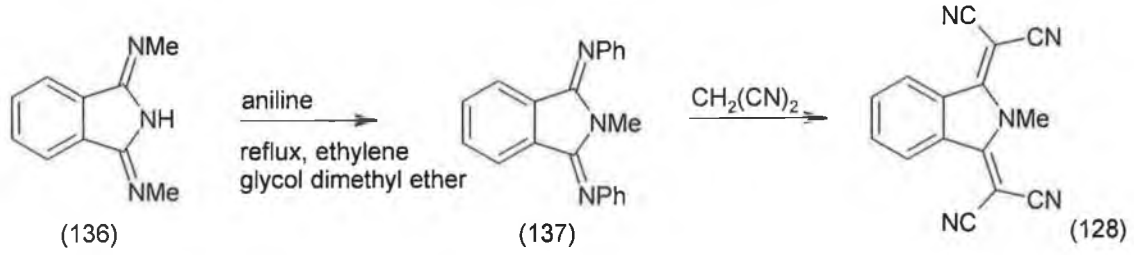

Scheme 37

It was also anticipated that 1,3-diethylimino (138), 1,3-dibenzylimino (139) and other dialkyl analogues would behave in a similar fashion and ultimately yield tetra-cyano compounds such as (140) and (141).

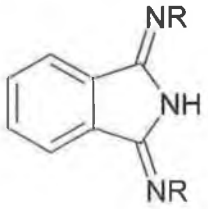

(138): R=Et
(139): R=Bz

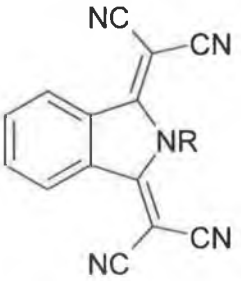

(140): R=Et
(141): R=Bz

2.2 Reactions involving Methylamine

Elvidge reported the synthesis of 1,3-dimethyliminoisoindoline. The synthesis involved the heating under reflux of an ethanolic solution of phthalonitrile and methylamine. The reaction of phthalonitrile with aqueous methylamine following the same procedure as described by Elvidge yielded a cream coloured solid, having a melting point (136-138°C) which was markedly different from reported value for the dimethylimino compound (136) (168-169°C). The presence of an IR peak at 1720cm^{-1} indicated the presence of a carbonyl group. The ^{1}H-NMR spectrum displayed three aromatic signals at 7.96, 7.87 and 7.64-7.60ppm with integration of 1:1:2 respectively. Two further signals were present at 3.69 and 3.15ppm, each corresponding to three hydrogens each. The ^{13}C-NMR spectrum displayed 10 signals. Six distinct aromatic signals at 133.0, 132.6, 131.4, 129.8, 125.6and 123.4ppm suggest an unsymmetrical product. Hydrolysis of the compound yielded N-methylphthalimide, confirming that substitution had occurred at the imide nitrogen. On the basis of this evidence the compound was thought to be the oxo-derivative (142) (61% yield), and the elemental microanalysis was consistent with this.

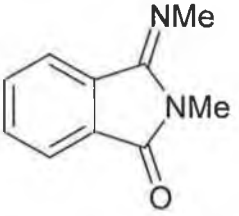

(142)

Independent spectral data for compound (142) was found in the literature.[143] The synthesis of the oxo-derivative (142) was achieved by the reaction of iminoisoindolinone and 33% aqueous methylamine solution. A possible mechanism for the formation of (142) is outlined in, scheme 38. Nucleophilic attack by methylamine leads to the

formation of an amidine intermediate (143). In this amidine the alkyl group can be accommodated either on the imino or the amino nitrogen. The tautomeric equilibrium favours the tautomer with the alkyl group attached to the amino nitrogen.[144] The lone pair of the imino nitrogen can then cause ring closure. The reaction was carried out in aqueous ethanol heated to reflux. Therefore the frequency of 'flipping' between tautomers is increased. It would appear that intermediate (143b) predominantly causes ring closure. The water in the reaction mixture then hydrolyses the exocyclic imino group.

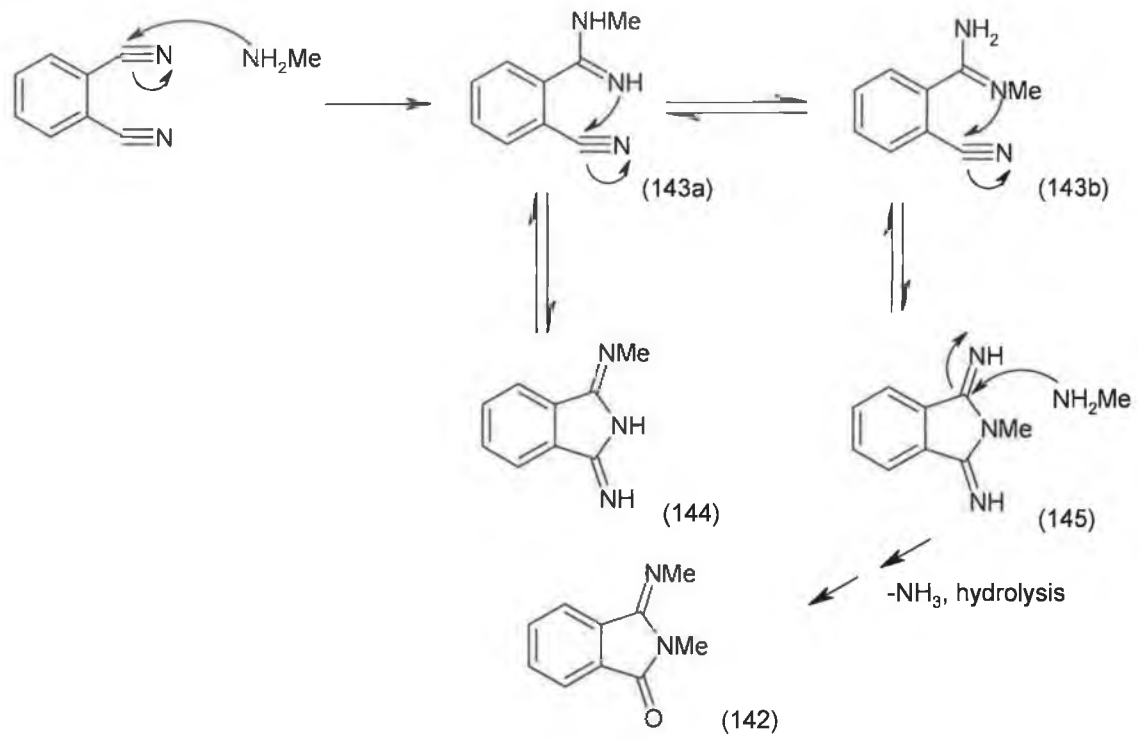

Scheme 38

During the course of their work Spiessens and Anteunis attempted to synthesise monomethylimino (146) compound from iminoisoindolinone (130). However treatment of (130) with aqueous methylamine solution only produced dimethyl compound (142) and the 2-methyl compound (147), scheme 39. In a separate experiment Spiessens and Anteunis obtained (147) by heating (146) in methanol in the presence of base. They concluded that (146) is formed first and then undergoes a rearrangement to (147). Application of this logic would suggest that (144) could rearrange to form (145). The reaction would then proceed as depicted in scheme 38.

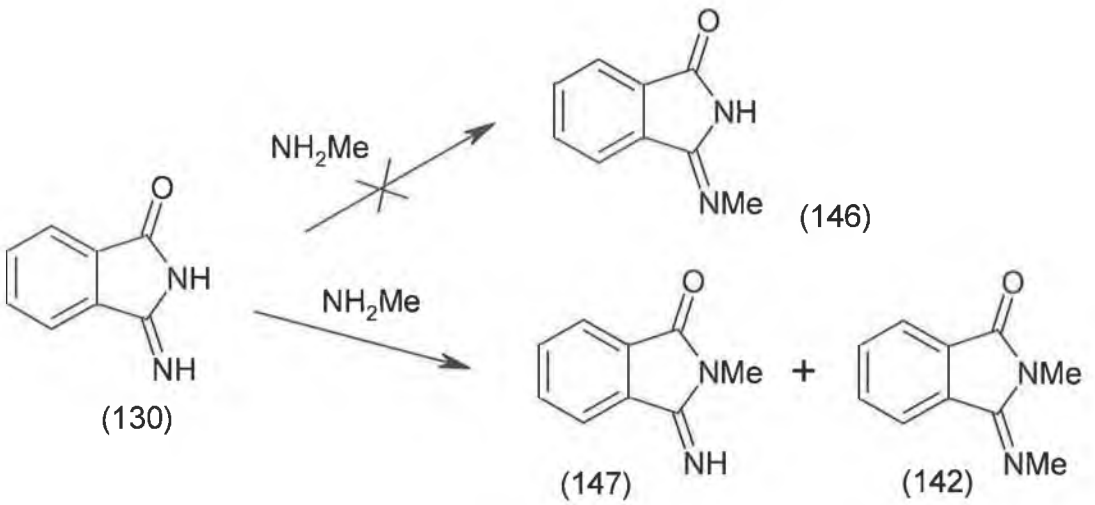

Scheme 39

When 1,3-diiminoisoindoline (132) was heated under reflux with aqueous methylamine in ethanol the same white solid (142) mp 136-138°C was formed. The mechanism for this reaction being analogous to the reaction described in scheme 38.

2.3 Reactions involving Ethylamine and Benzylamine

From the previous section it would appear that the reaction of aqueous primary amine solutions with phthalonitrile might provide a possible route to N-substituted compounds analogous to (142). However when phthalonitrile was heated under reflux with aqueous solutions of ethylamine and benzylamine in ethanol, TLC analysis showed a complex mixture of products.

When phthalonitrile was heated under reflux with liquid ethylamine in ethanol a cream coloured solid mp 158-160°C was isolated. The ^{1}H-NMR spectrum of this solid displayed multiplets at 7.70 and 7.33ppm each due to two aromatic hydrogens, a quartet at 3.84 (J=7.0Hz) corresponding to four hydrogens and a triplet at 1.32ppm (J=7.0Hz) due to six hydrogens. The ^{13}C-NMR spectrum displayed 6 peaks, indicating a symmetrical structure. Hydrolysis of (138) yielded phthalimide. On the basis of the

evidence this solid was identified as the 1,3-diethylimino compound (138) (36% yield) mp lit.[143] 158°C.

The reaction of benzylamine with phthalonitrile in methanol containing a catalytic amount of sodium methoxide yielded a white solid mp 160-162°C. The ^{1}H-NMR spectrum displayed two two-hydrogen multiplets at 7.68 and 7.49ppm. The aromatic region of the spectrum also contained further multiplets at 7.42, 7.32 and 7.24ppm corresponding to four, four and two hydrogens respectively. The final signal was a singlet at 4.92ppm due to four hydrogens. Hydrolysis of this solid yielded phthalimide this and spectral evidence, confirmed that the product was the dibenzylimino compound (139) (66% yield) lit.[143] 160°C.

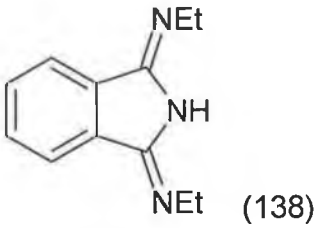

(138)

(139)

A probable mechanism for the formation of (138) and (139) is shown in scheme 40.

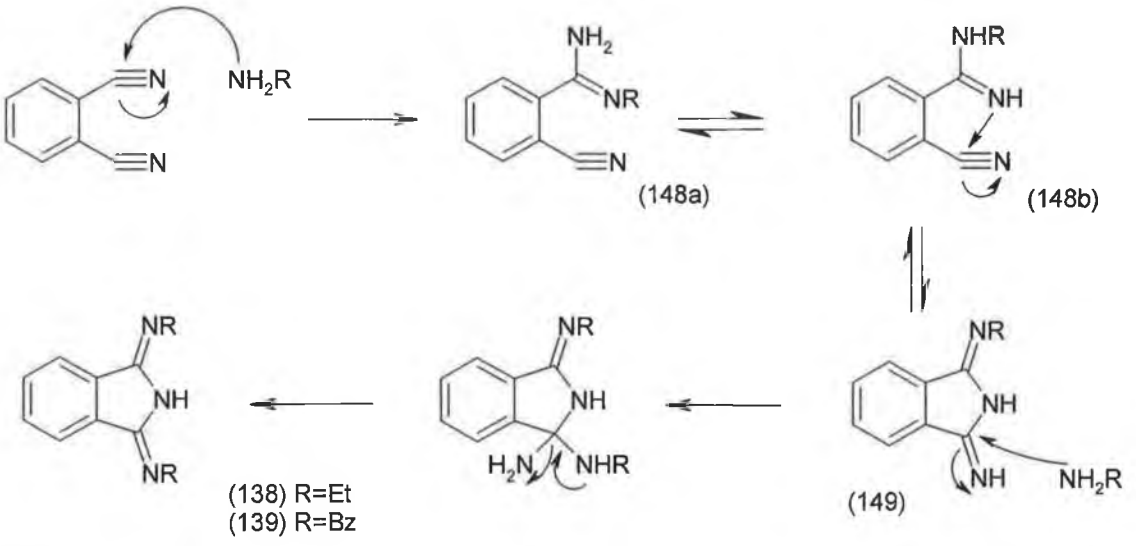

Scheme 40

Initial nucleophilic attack by an amine on phthalonitrile produced an amidine intermediate (148). This amidine can exist in two tautomeric forms (148a) and (148b). The larger ethyl and benzyl groups would appear to prefer tautomeric form (148b). Therefore it is more likely that cyclisation occurs via this intermediate to produce (149) and subsequently the symmetrical products (138) and (139). The absence of water means that there is no hydrolysis of any exocyclic imino groups.

2.4 Reactions involving aniline

The symmetrical compounds (138) and (139) were reacted with aniline in attempts to synthesise tri-substituted compounds (150) and (151). However both reactions failed to yield the desired products.

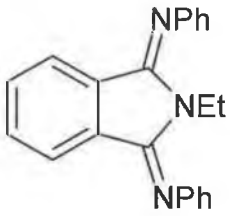

(150)

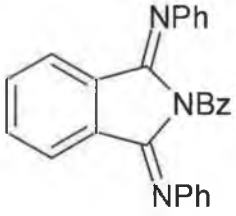

(151)

The reaction of the unsymmetrical dimethyl carbonyl compound (142) with aniline yielded a cream coloured solid mp 144-146°C. The IR spectrum showed a stretch at 1737cm^{-1} characteristic of a carbonyl group. The ^{1}H-NMR spectrum displayed 7 distinct aromatic signals. A 1H doublet at 7.84 (J=7.8Hz), a 1H multiplet at 7.52, a 2H multiplet at 7.39, two 1H triplets 7.28 (J=7.9Hz) and 7.20 (J=7.9Hz), a 2H doublet at 6.98 (J=7.8Hz) and 1H doublet 6.60ppm (J=7.9Hz). There was a further singlet at 3.36ppm corresponding to three hydrogens. The ^{13}C-NMR spectrum suggested an unsymmetrical compound. Hydrolysis of the compound yielded N-methylphthalimide. Microanalysis supported a formula of $C_{15}H_{12}N_2O$ and taken in conjunction with the spectral data assigned the phenylimino structure (152) (32% yield).

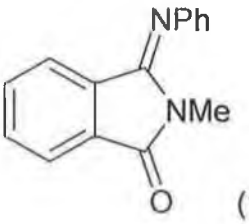

(152)

2.5 Conclusion

It would appear that there are two pathways available for the formation of products. The size of the alkyl group R attached to amine RNH_2 dictates the pathway taken by the various reactions. The equilibria experienced by many of the intermediates make exact mechanisms difficult to predict.

2.6 Reactions involving Malononitrile

Having established the structure of (142) its reaction with malononitrile was investigated to see whether a mono-condensation product (153) or bis-condensation product (128) could be isolated.

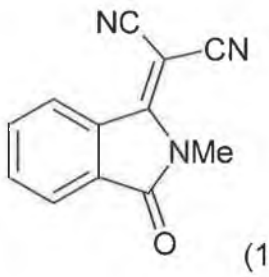

(153)

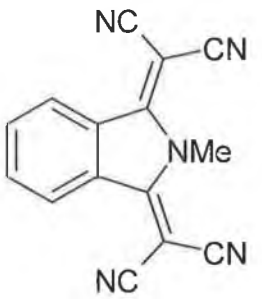

(128)

The reaction of compound (142) with malononitrile in DMF at room temperature yielded a fine white powder mp 178-180°C. When (142) and malononitrile were heated under reflux in ethanol an off-white crystalline solid mp 178-180°C, was isolated from the reaction mixture. Comparison of their respective IR spectra confirmed that these compounds were identical. The IR spectrum has characteristic stretches of an amide at 3315 (NH), of a carbonyl group at 1650 and of a cyano group at 2190cm^{-1}.

The ^{13}C-NMR spectrum shows 13 signals. Six signals correspond to an aromatic ring, two are attributed to methyl groups, two to cyano carbons, one to a carbonyl carbon and two to the vinylic carbons of a dicyanomethylene group. A DEPT-135 experiment confirmed these assignments.

The ^{1}H-NMR spectrum displays a quartet at 8.30ppm (J=4.4Hz) corresponding to one hydrogen. This signal has an accompanying doublet at 2.72ppm (J=4.4Hz) possibly due to a methyl group. A three-hydrogen singlet at 2.33ppm suggests another methyl group. There are three further multiplets at 7.58, 7.48 and 7.21ppm with integrations of 1:5:1. Those at 7.58 and 7.21ppm correspond to one aromatic hydrogen each. Addition of D_2O to ^{1}H-NMR sample results in the removal of signals due to exchangeable protons and any coupling associated with these protons. The ^{1}H-NMR spectrum obtained for the sample containing D_2O showed the removal of the NH signal at 8.30ppm with the doublet at 2.72ppm collapsing to a singlet consistent with the presence of a methyl amide

group. The region between 8.00 and 7.00ppm now showed three multiplets with integrations of 1:2:1, corresponding to four aromatic protons. The loss of signal due to three hydrogens in this area is consistent with the exchange of three alkylammonium protons.

The compound analysed for $C_{16}H_{14}N_6O$ and taken in conjuction with the spectral data and mechanistic considerations is consistent with the salt structure (154) (43% yield).

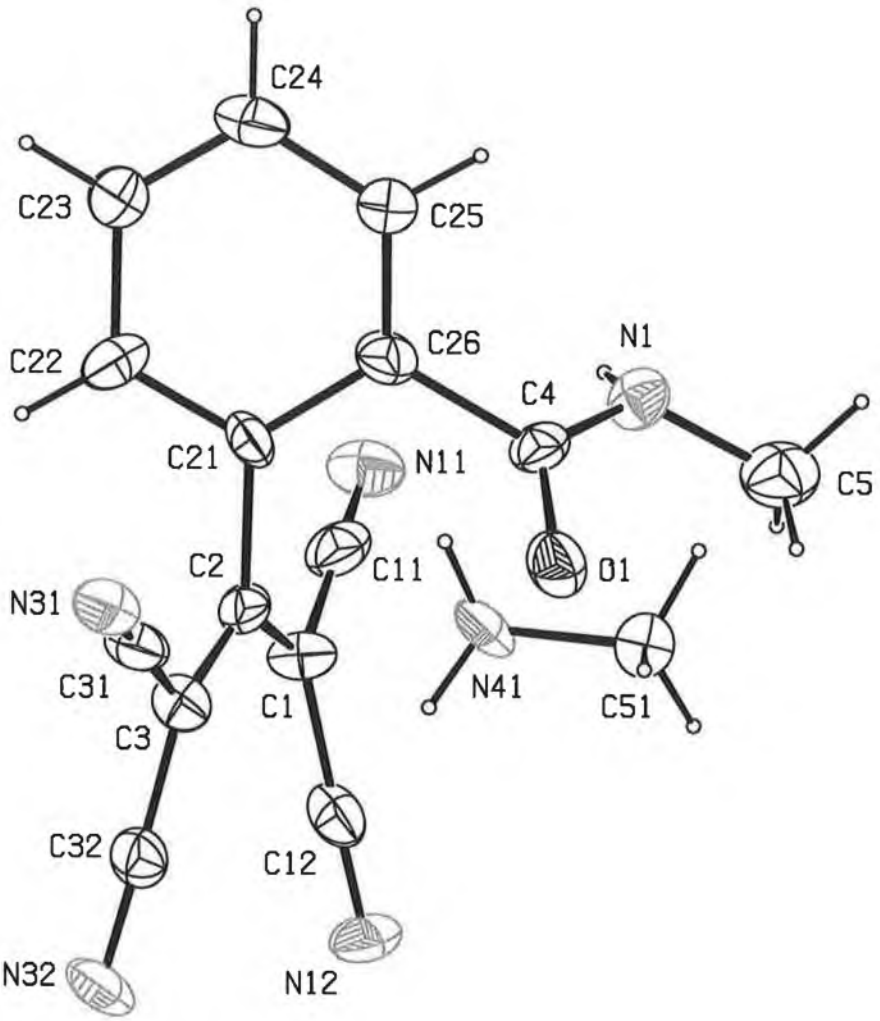

Figure 2.1

The X-ray crystal structure in figure 2.1 confirmed the methylammonium salt structure (154), probably formed by the reaction sequence shown in scheme 41. The standard uncertainties for the bond lengths and angles are high but the molecular structure was established. The bond lengths between C(1)-C(2) and C(2)-C(3) are 1.382 and 1.375Å respectively. Although they are not exactly equal they are very similar. This observation supported the idea that the negative charge was delocalised through carbons C(1), C(2) and C(3). The NH_3 is involved in strong hydrogen bonds with two cyano group nitrogens N(12) and N(32) as well as oxygen O(1). The data obtained for the crystal is in Appendix 1.

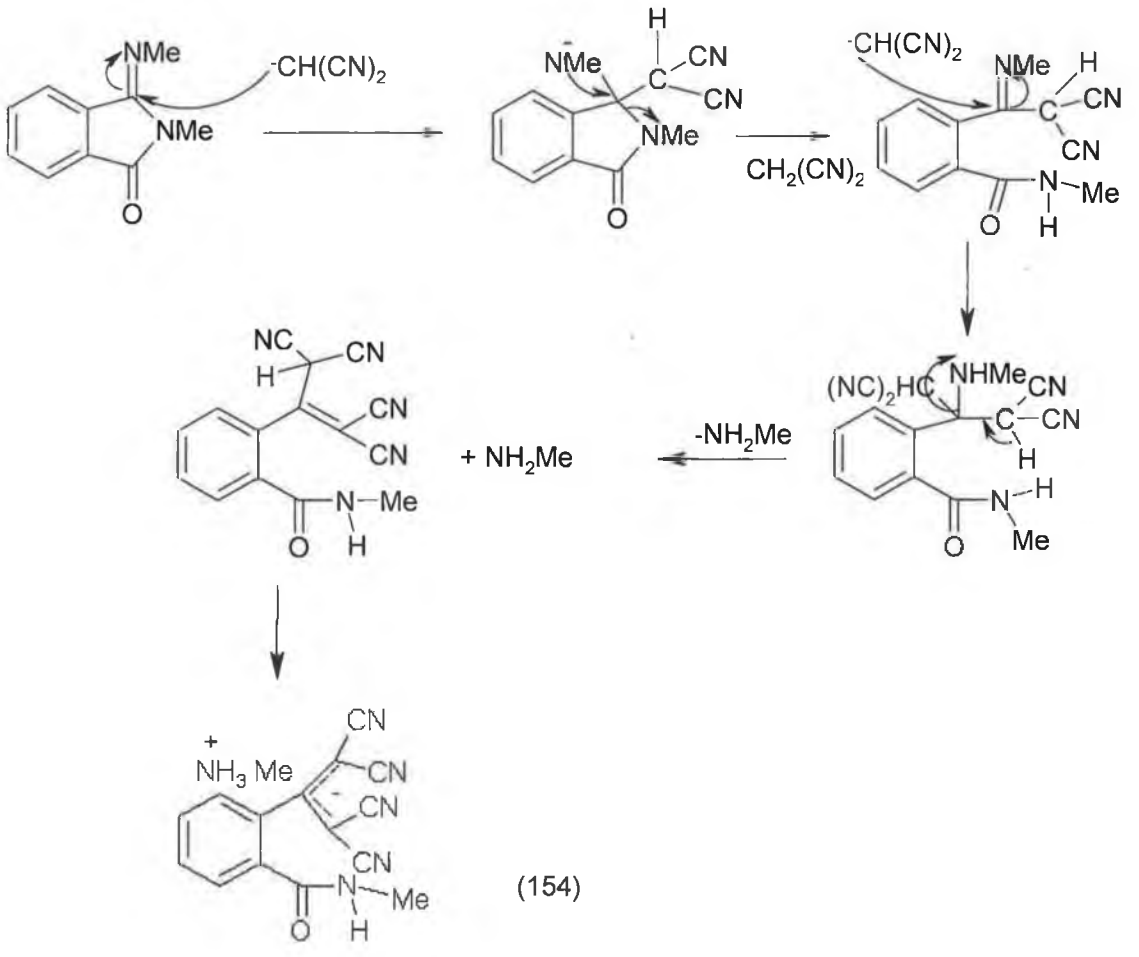

Scheme 41

The delocalised tetracyanopropenyl anion unit in (154) is symmetrical and results in the presence of two different types of cyano group and a single type of cyanosubstituted carbon in the ^{13}C-NMR spectrum.

Heating salt (154) under reflux in acetic acid yielded a red microcrystalline solid on cooling. The IR spectrum showed cyano peaks at 2228 and 2222cm^{-1} and a carbonyl peak at 1746cm^{-1}. The ^{1}H-NMR spectrum showed 4 non-equivalent aromatic hydrogens and an N-methyl group. The ^{13}C-NMR spectrum showed 12 signals, of which six are assigned as aromatic carbons suggesting an unsymmetrical compound. Microanalytical data was consistent with an empirical formula of $C_{12}H_7N_3O$. The compound was therefore the mono-condensation product (153). Ring closure, accompanied by the elimination of methylamine and malononitrile, possibly occurred by the mechanism shown in scheme 42.

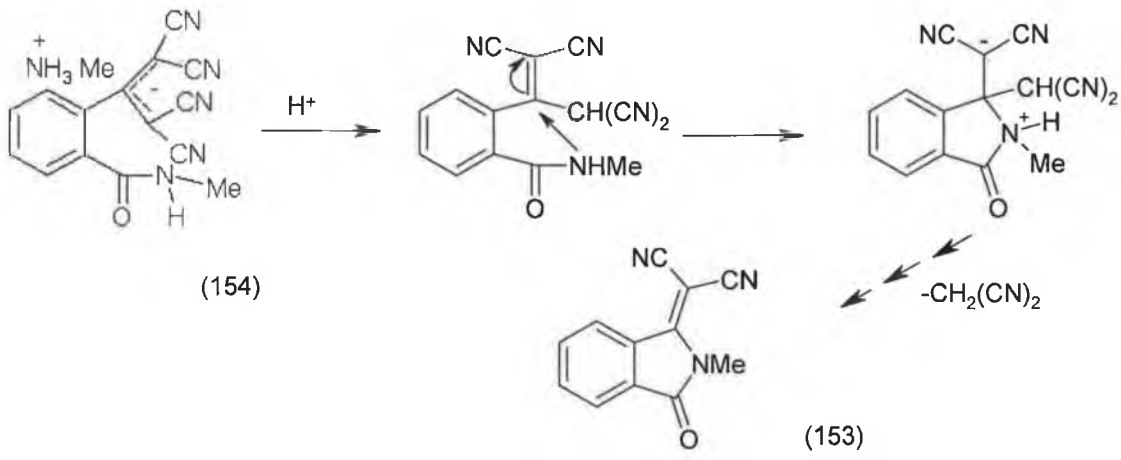

Scheme 42

When compound (142) was heated under reflux with excess malononitrile in acetic acid a pale gold crystalline compound mp 200-202°C was isolated both from hot and cold solutions. The gold compound had exactly the same spectral (IR, ^{1}H and ^{13}C-NMR) characteristics as (153) and also analysed for $C_{12}H_7N_3O$. On the basis of the spectral evidence the reaction product was identified as compound (153). The yield for the reaction was 47%. A probable mechanism is depicted in scheme 43.

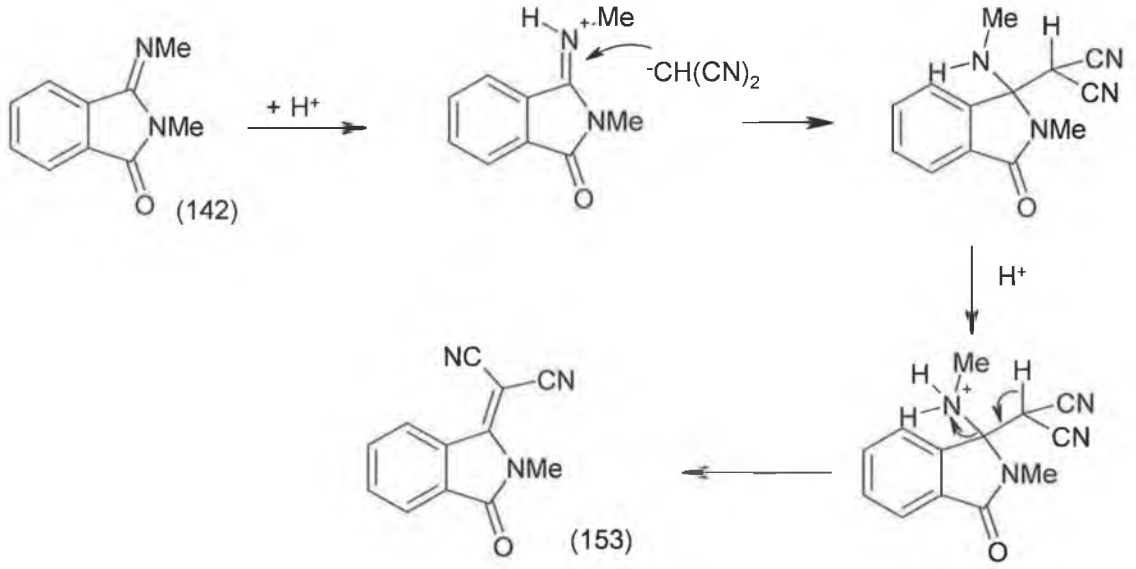

Scheme 43

The symmetrical diethyl derivative (138) was heated under reflux with malononitrile in acetic acid. A pale green solid mp 172-174°C was isolated. Peaks at 2220cm^{-1} and 1752cm^{-1} in the IR spectrum confirmed the presence of a cyano group and carbonyl group. The ^{1}H-NMR spectrum had an aromatic region analogous to that of (153), a two-hydrogen quartet at 4.10 (J=7.2Hz) and a three-hydrogen triplet at 1.25ppm (J=7.2Hz) confirmed the presence of an ethyl group. The ^{13}C-NMR spectrum had 13 separate signals consistent with structure (155) (32% yield) and supported by microanalytical data. A mechanism for the reaction is proposed in scheme 44.

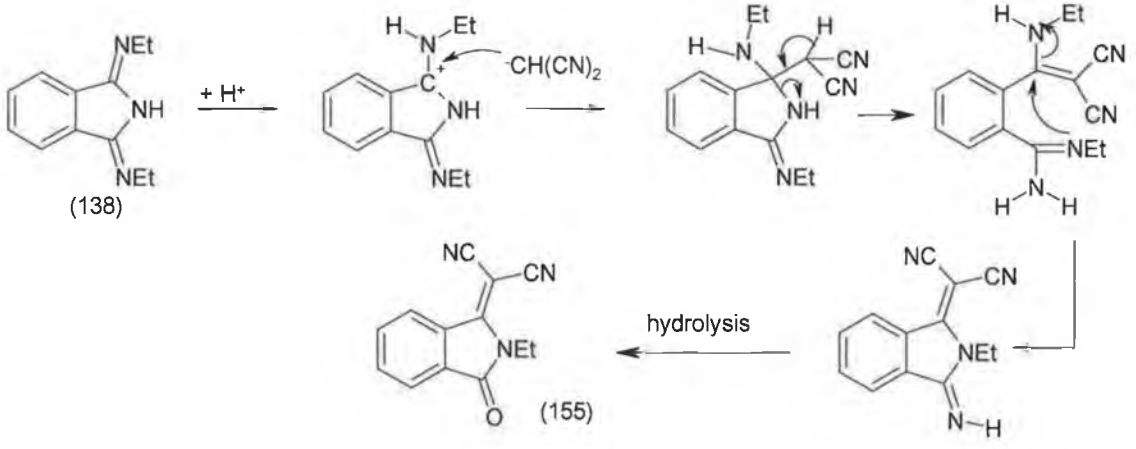

Scheme 44

Attempts to treat 1,3-dibenzyliminoisoindoline (139) in a similar fashion failed to yield an analogous product, TLC analysis of the reaction mixture showing a complex mixture with no apparent major new product being formed.

When compound (139) was treated with excess malononitrile in ethanol at room temperature a bright yellow solid, mp 250-252°C (62% yield), was isolated as the sole product. The IR spectrum shows a cyano peak at 2221cm^{-1} but no signal for carbonyl group. The ^{1}H-NMR spectrum had an aromatic region containing 4 sets of multiplets, with integration ratios of 2:2:4:1. There was also a two-hydrogen singlet at 4.94ppm. The ^{13}C-NMR spectrum contained 16 signals, 10 of which are due to aromatic carbons. A probable mechanism for the reaction can be seen in scheme 45. Hydrolysis of (156) in aqueous HCl produced a white crystalline solid mp 249-251°C. The IR spectrum of the isolated solid showed characteristic peaks due to a carbonyl group at 1765 and cyano group at 2214cm^{-1}. The ^{1}H-NMR spectrum showed multiplets at 8.26 and 7.94-7.84ppm corresponding to one and three hydrogens respectively. On the basis of this evidence the hyrolysis product was given the structure (170). Further confirmation of purported structure was obtained from the agreement of the melting point and the spectral data obtained here and the data obtained from the synthesis of (170) (described later).

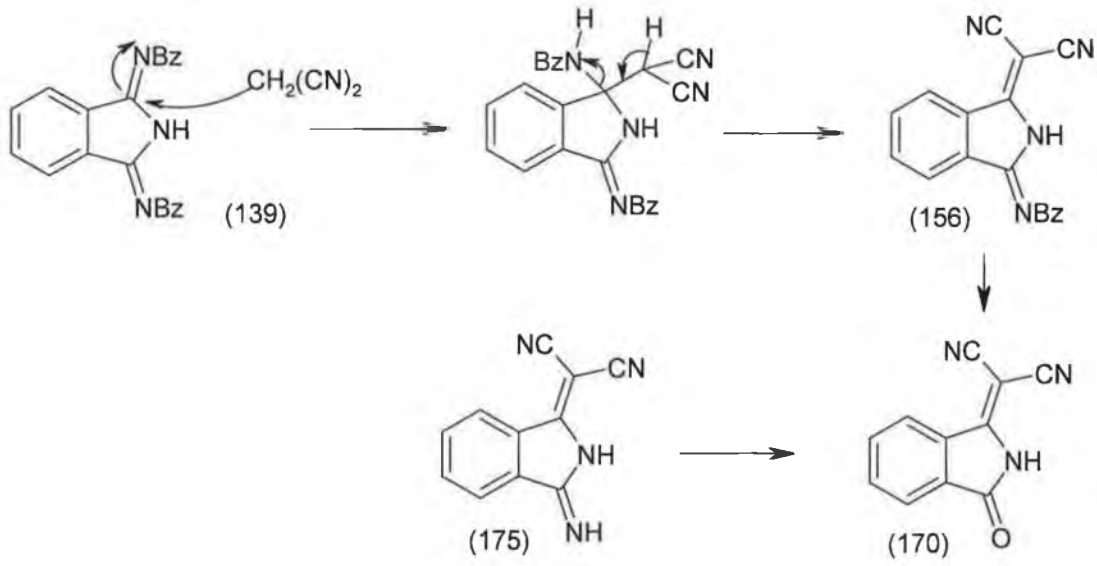

Scheme 45

2.7 Conclusion

Although the desired bis-condensation product (128) was not synthesised, compounds (153), (155) and (156) were. These compounds may behave as electron acceptors albeit with poorer accepting ability than tetra-cyano compounds.

2.8 Application of the Mitsunobu reaction to 2-(3-dicyanomethylene-2,3-dihydro-isoindol-1-ylidene)-malononitrile

N-Alkyl derivatives of tetra-cyano compound (127) were not obtained from condensation reactions of either N-alkyl phthalimides or N-alkyl iminoisoindolines with malononitrile. Alkylation of (127) by traditional methods (alkyl halides, dimethyl sulphate) proved unsuccessful partly due to the poor nucleophilicity of the ring nitrogen. Conversely the stability of the anion that is formed when compound (127) dissociates means that (127) can be considered to be slightly acidic. Compounds that possess an acidic proton have been alkylated using the Mitsunobu reaction. At first the Mitsunobu reaction used a carboxylic acid, an alcohol, triphenylphosphine and an azodicarboxylate to produce an ester.[146] If the Mitsunobu reaction could be applied to compound (127) and an alcohol, the product would be an N-alkylated derivative of the tetra-cyano compound (127).

In 1967 Mitsunobu and Yamada reported that carboxylic acids could be esterified with primary and secondary alcohols using the redox system of diethyl azodicarboxylate (DEAD) and triphenylphosphine.[147] Later, Mitsunobu and Eguchi showed that the reaction with optically pure secondary alcohols proceeded with complete inversion of stereochemistry.[148] This means that the stereochemistry of a particular alcohol can be inverted by an esterification/hydrolysis procedure, scheme 46.

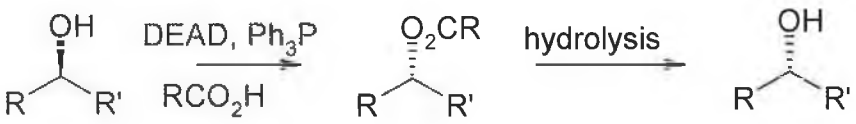

R, R'= alkyl

Scheme 46

The overall reaction can be summarised in scheme 47. The alcohol (R-OH) and acidic compound (H-Nu) are condensed to form product (R-Nu), while triphenylphosphine is oxidised to triphenylphosphine oxide and the azodicarboxylate is reduced to the corresponding hydrazine.

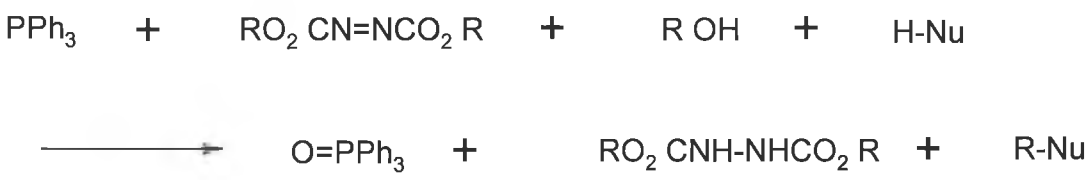

Scheme 47

DEAD and triphenylphosphine are the most commonly applied redox system. The reaction is generally limited to primary and secondary alcohols. The reaction of secondary alcohols generally proceeds with complete stereochemical inversion. This application of the Mitsunobu reaction is easily the most popular. The acidic component (H-Nu) can be oxygen, nitrogen, carbon or sulphur nucleophiles.

In 1981 Mitsunobu proposed that the reactions of alcohols using DEAD and triphenylphosphine proceeded in three steps.[149]

1. Reaction of DEAD with PPh_3 in the presence of the acid component to form a salt wherein a phosphorous-nitrogen bond is formed.
2. Reaction of the DEAD-PPh_3 adduct with the alcohol to form an activated oxyphosphonium ion intermediate.
3. Displacement by a S_N2 process to form the inverted product and the phosphine oxide.

The reaction can be shown schematically below, scheme 48.

STEP 1: ADDUCT FORMATION.

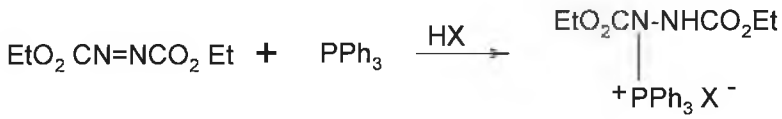

STEP 2: ALCOHOL ACTIVATION.

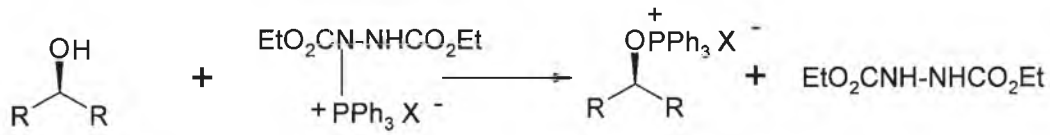

STEP 3: S_N2 REACTION.

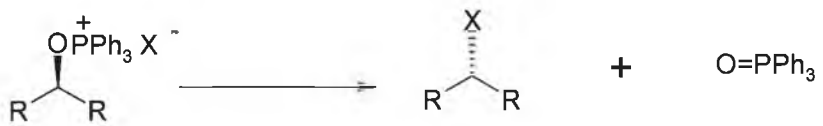

Scheme 48

Stages 1 and 3 of the reaction are adequately depicted in scheme 48. The alcohol activation step is not explained fully. Independent NMR studies carried out by Grochowski[150] and von Itzstein and Jenkins[151] clarified the situation. Both these groups concluded on the basis of ^{31}P NMR studies that the true intermediate was in fact a dialkoxyphosphorane $Ph_3P(OR)_2$ (158), which decomposes to products, scheme 49.

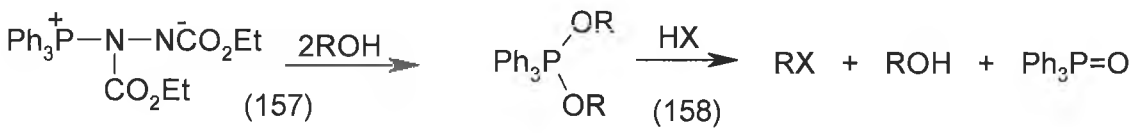

Scheme 49

Both these groups failed to account for an (unobserved) intermediate between the dialkoxyphosphorane and products. It was considered to be an alkoxyphosphonium salt (159) by Jenkins, scheme 50.

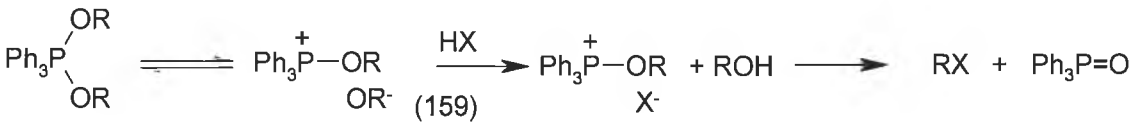

Scheme 50

However Walker and co-workers showed that the mechanism of the Mitsunobu reaction is dependent on the order of addition of reactants.[152] If the betaine is formed in the presence of the acidic component, the conjugate acid of the betaine then reacts with the alcohol to form the oxyphosphonium salt. This species decomposes to form the alkylated product and triphenylphosphine oxide. When the betaine (157) first reacts with the alcohol a dialkoxyphosphorane (158) is formed. The phosphorane then reacts with the acidic component to form the oxyphosphonium salt (161). The half equivalence of alcohol from dialkoxyphosphorane (158) is recycled through conjugate acid (160). This is due to the fact that the remaining betaine (157) is protonated by the acid present.
Their findings can be shown schematically in scheme 51.

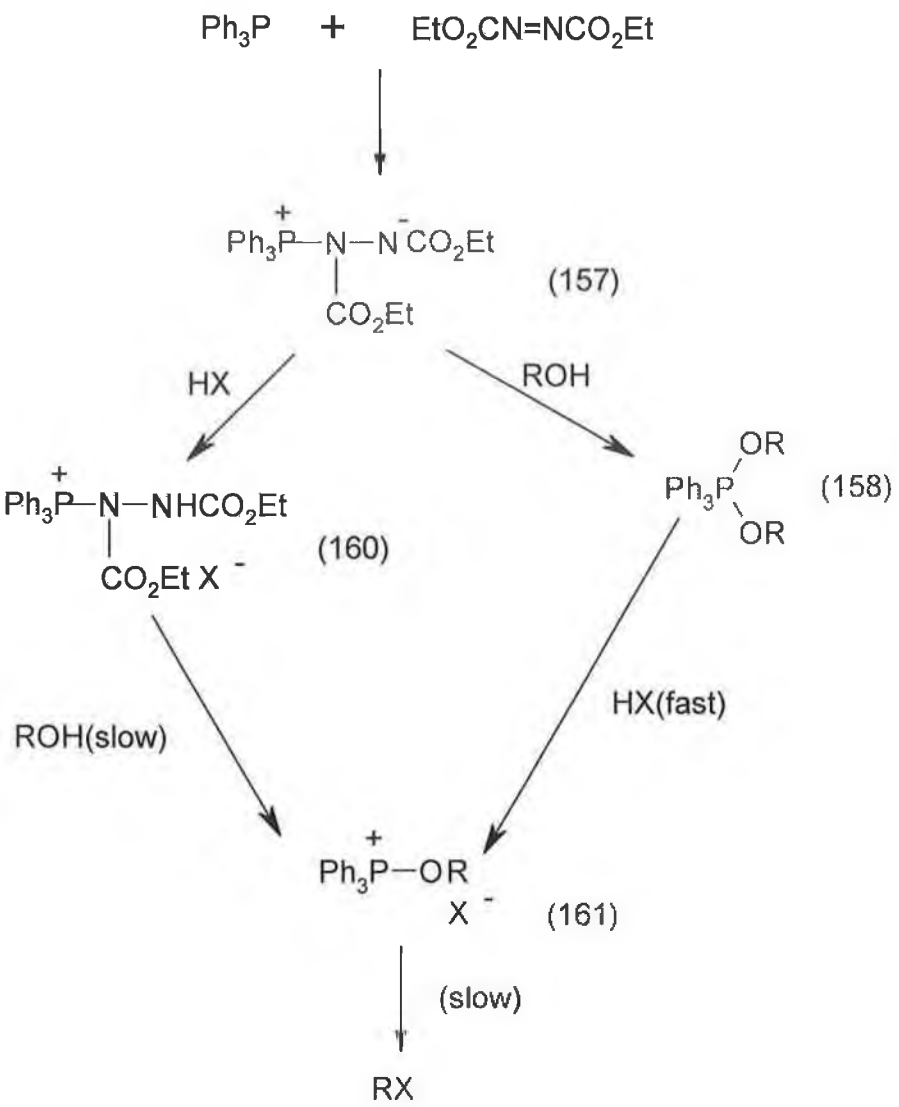

Scheme 51

Camp and Jenkins showed that when alcohol ROH is added to the protonated betaine (160) the dialkoxyphosphorane (158) and the oxyphosphonium salt (161) are formed. [153] The pKa of the acid and the polarity of the solvent govern the ratio of dialkoxyphosphorane to oxyphosphonium salt.

With acids of low pKa only the oxyphosphonium salt (161) is the only species observed. The use of polar solvents also favours this species, the one main exception being THF (ε=7.6) which favours the phosphorane intermediate because THF is a basic solvent. In THF any protons are effectively tied up by hydrogen bonding to the solvent and are therefore less available to solvate the X^- of the oxyphosphonium species.[154]

Hughes, Reamer and co-workers[155] stated that the main factors governing the rate of transfer of the $P^{+}Ph_3$ group from the azodicarboxylate-triphenylphosphine adduct to the alcohol are:

1. the basicity of the counterion generated in formation of the dialkylazodicarboxylate-triphenylphosphine adduct,
2. the extent of hydrogen bonding to this counterion,
3. substituent effects in the triarylphosphine.

The Mitsunobu reaction is generally useful only when the pKa of the acidic component is below 10. In an effort to improve this situation a number of new compounds have been developed. Improvements in the redox system used in the Mitsunobu reaction need to:

1. increase the nucleophilicity of the phosphine in the formation of the intermediate betaine,
2. localize the positive charge on phosphorus in the betaine and in the alkoxyphosphonium salt. This localization of charge facilitates nucleophilic attack by RO^{-} on the betaine and X^{-} on the alkoxyphoshonium salt,
3. localize the negative charge at the azo-nitrogen in order to increase its basicity in the azodicarboxylate anion.

The first two considerations lead to the use of tributylphosphine. The third consideration leads to the use 1,1′-(azodicarbonyl)dipiperidine (ADDP) (162)[156], N,N,N′,N′-tetramethylazodicarboxamide (TMAD) (163)[157] and 4,7-dimethyl-3,5,7-hexahydro-1,2,4,7-tetrazocin-3,8–dione (DHTD) (164).[158]

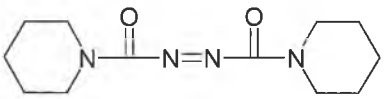

ADDP (162)

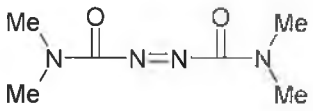

TMAD (163)

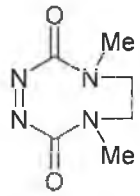

DHTD (164)

All three compounds when used with tributylphosphine alkylated acidic components with pKa values as high as 13. TMAD proved to be the most versatile compound as it produced the best results with sterically hindered reactants.[159] These reactants were generally used with benzene as solvent. Although the ADDP-TBP system is more reactive towards primary alcohols it is less reactive towards secondary alcohols when compared with the DEAD-TPP system. This difference in reactivity can be utilized for regioselective reactions of diols.

Phthalimides were first alkylated using the Mitsunobu protocol in 1971.[160] Other long chain N-alkylated phthalimides were obtained from gerianol, citronellol and 10-undecen-1-ol.[161] Similar N-alkylated succinimide derivatives were synthesised in a similar fashion by the same group.[162]

The syntheses described above all follow the standard Mitsunobu protocol. That is, the reactants are added in the following order: acid (HX), alcohol (ROH), triphenylphosphine and finally azodicarboxylate. Alternatively a series of N-alkyl derivatives of maleimide (165) were made using a different order of addition of the reactants: triphenylphosphine, azodicarboxylate, alcohol and acid.[163]

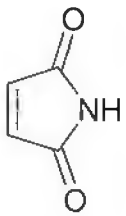

(165)

This order of addition pre-forms the reactive betaine and thus eliminates free triphenylphosphine and free azodicarboxylate from the reaction mixture.

Application of the Mitsunobu reaction to the problem of creating N-alkyl derivatives of (127) proved relatively successful and a number of N-alkyl-derivatives have been synthesised.

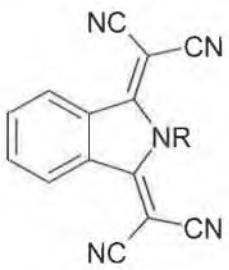

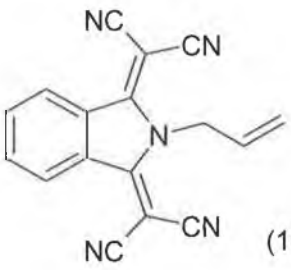

(168)

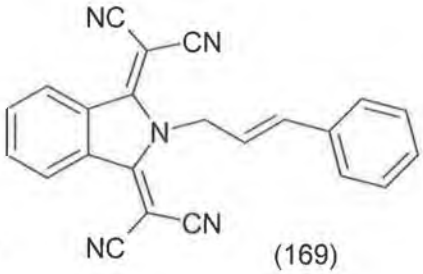

(169)

R= Methyl (128), Ethyl (140), Propyl (166), Butyl (167), Benzyl (141).

Applying the Mitsunobu protocol to compound (127) and methanol produced a yellowish/green crystalline solid mp 263-264°C. The IR spectrum showed the presence of a cyano group at 2212 cm^{-1}. The ^{1}H-NMR spectrum showed 2 aromatic multiplets that corresponded to two hydrogens each and a singlet at 4.14ppm which was attributed to an N-methyl group. The ^{13}C-NMR spectrum displayed 8 signals. On the basis of the spectral data achieved and its agreement with the data presented by Conway[138] the N-methyl structure (128) was assigned. The yield of the reaction was 47%.

The reaction was carried out a number of times. In the course of these trials a number of conditions were varied:

(i) replacement of DEAD with DIAD,

(ii) changing the order of addition of reactants,

(iii) varying the stoichiometric ratios of reactants,

(iv) increasing the time allowed for reaction to occur,

(v) changing the temperature at which reaction took place.

Using the guidelines listed above the optimum reaction conditions were established. Using DIAD instead of DEAD increased the yield of product. The order of addition of reactants that produced the most repeatable results involved pre-forming the azodicarboxylate-triphenylphosphine adduct in the absence of the acidic component, then adding the alcohol so as to form a pentavalent dialkoxy phosphorane intermediate. The acidic component (127) was added last. Increasing the amount of azodicarboxylate-

triphenylphosphine adduct and alcohol relative to (127) did improve the yield slightly. The best ratio was found to be DIAD (1.5): PPh_3 (1.5): ROH (1.5): HX (127) (1.0). The optimum reaction was found to be between 2-3 days, however longer reaction times were used during subsequent reactions. Room temperature proved to be an adequate reaction temperature. A reasonable mechanism is shown in scheme 52

The same reaction procedure with ethanol, propanol and butanol was subsequently investigated. The N-alkylated products were isolated in each case. However the yield of product from the reactions with propanol and butanol were very small. Coupled with the small yields the reactions exhibited poor reproducibility.

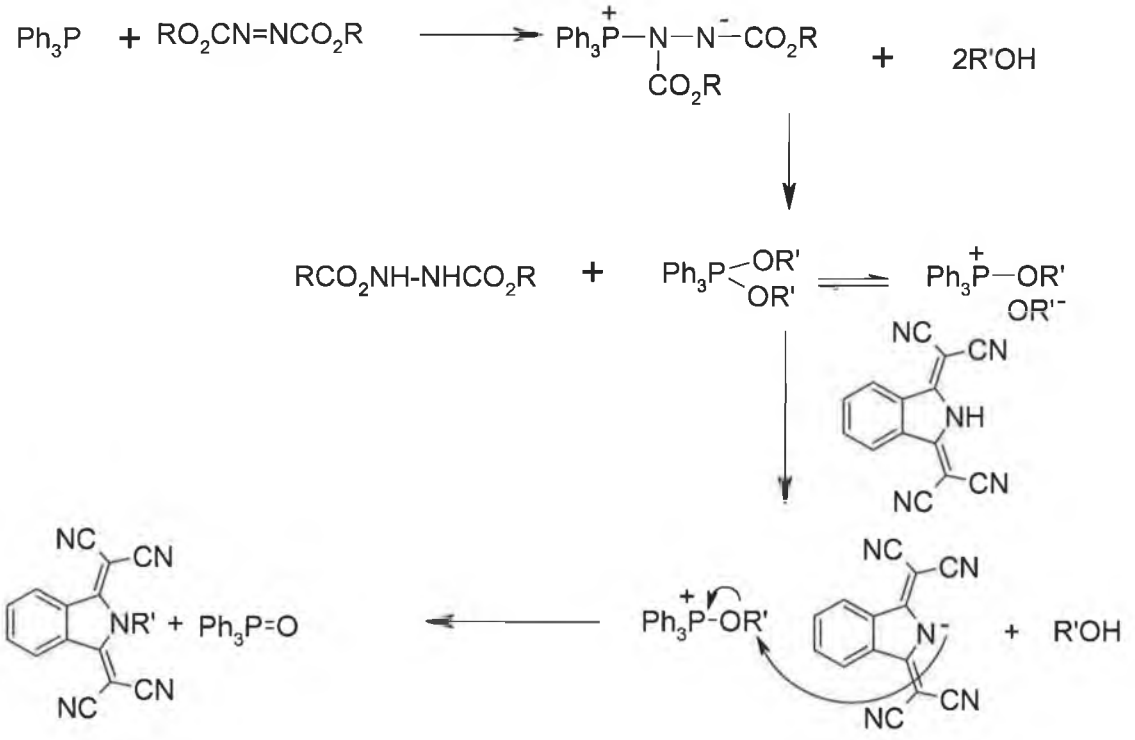

Scheme 52

The ethyl derivative (140) was isolated in 41% yield after one-week reaction time. ^{1}H-NMR spectrum showed 2 multiplets at 8.72 and 7.82ppm corresponding to four aromatic protons with a quartet at 4.72ppm and triplet at 1.64ppm corresponding to the CH_2 and the CH_3 of the N-ethyl group, both with J=6.9Hz. The ^{13}C-NMR spectrum showed a peak at 156.6 due to (**C**=C(CN)$_2$), three aromatic signals at 134.7, 130.9, 125.6,

two cyano peaks at 113.2 and 112.3, a peak at 61.3 due to ($\mathbf{C}(CN)_2$) and the N-ethyl group was depicted by two signals at 41.8 and 16.4ppm.

The propyl derivative (166) and the butyl derivative (167) were both synthesised in a similar fashion albeit in very poor yields. The ^{1}H-NMR spectrum of (166) had multiplets at 8.67 and 7.78ppm corresponding to 2 aromatic hydrogens each, 2 further multiplets at 4.50 and 1.95ppm corresponding to two CH_2 groups in the N-propyl group and a triplet at 1.06ppm (J= 8.0Hz) corresponding to the terminal CH_3 of the N-propyl group. The ^{13}C-NMR spectrum displayed 10 distinct signals as expected.

The ^{1}H-NMR spectrum of the N-butyl derivative (167) showed 2 multiplets at 8.67 and 7.78ppm corresponding to two aromatic hydrogens each, a triplet at 4.55ppm (J=8.4Hz), two multiplet at 1.92 and 1.48ppm each corresponding to CH_2 and a triplet at 0.98ppm (J=8.0Hz) corresponding to CH_3. The ^{13}C-NMR spectrum displayed 11 peaks as anticipated.

Not surprisingly the yield of N-alkylated products decreased as the alkyl chain attached to a hydroxyl group of an alcohol increased. Considering the results achieved from the previous trials it was obvious that more reactive alcohols were needed. It was felt that benzyl alcohol, allyl alcohol and cinnamyl alcohol would provide better results. These three alcohols should be considerably more reactive than either propanol or butanol.

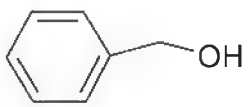

benzyl alcohol

allyl alcohol

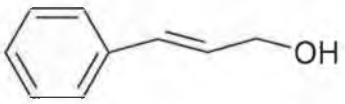

cinnamyl alcohol

The reaction involving benzyl alcohol yielded a yellow crystalline powder in 30% yield mp 232-234°C after one-week reaction time. The IR spectrum showed a cyano peak at 2220cm^{-1}. The ^{1}H-NMR spectrum had 2 multiplets at 8.76 and 7.87ppm, both corresponding to two aromatic hydrogens, two further multiplets at 7.39 and 7.05ppm, integration 3:2 respectively, corresponding to aromatic hydrogens and a singlet at 6.00ppm corresponding to the CH_2 of the benzyl group. The ^{13}C-NMR spectrum displayed twelve distinct signals, five signals due to the N-benzyl group and the

remainder were due to the tetra-cyano isoindoline unit. Microanalysis confirmed the reaction product as the N-benzyl derivative (141).

When allyl alcohol was used a green crystalline solid mp 240-242°C was isolated. The cyano peak in the IR spectrum was located at 2219cm^{-1}. The ^{1}H-NMR spectrum displayed the following peaks: 2 multiplets at 8.74 and 7.85ppm corresponding to four aromatic hydrogens, a multiplet at 6.05 due to one hydrogen, a doublet at 5.50 (J=10.4Hz) corresponding to one hydrogen, a two-hydrogen multiplet at 5.35 and a one-hydrogen doublet at 5.05ppm (J=17.2Hz). The two doublets are due to the two terminal methylene hydogens. Both of these hydrogens are coupled with the hydrogen atom attached to the adjacent carbon atom. However the presence of a double bond prevents free rotation. Therefore the coupling constant between the two cis hydrogen atoms will be different from the hydrogens that are trans to each other.

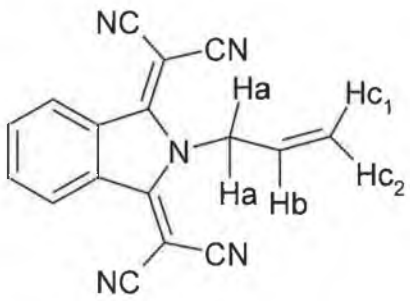

(168)

2Ha: 5.35ppm, m.
Hb: 6.05ppm, m.
Hc_1: 5.05ppm, d, J=17.2Hz.
Hc_2: 5.50ppm, d, J=10.4Hz.

The ^{13}C-NMR spectrum showed the 11 signals, the peaks at 131.3, 116.7 and 48.8ppm were due to the allyl group. The remaining signals at 157.8, 135.0, 132.6, 125.3, 114.5, 113.3 and 60.6ppm were attributed to the tetra-cyano isoindoline skeleton. Microanalysis and the spectral data confirmed the identity of the product as the N-allyl derivative (168) (46% yield).

The reaction of (127) and cinnamyl alcohol produced orange crystals mp 196-198°C. A cyano peak was observed at 2224cm^{-1}. The ^{1}H-NMR spectrum consisted of multiplets at 8.75, 7.85, 7.37 and 7.30ppm (ratio of 2:2:2:3) corresponding to aromatic hydrogens. The multiplets at 8.75 and 7.85ppm correspond to the four aromatic hydrogens attached to the aromatic moiety of the isoindoline skeleton. The multiplets at

7.37 and 7.30ppm correspond to the aromatic protons associated with the phenyl ring of the cinnamyl group. The alkyl chain of the cinnamyl group was represented by a one-hydrogen doublet at 6.48 (J=16.0Hz), a one-hydrogen double triplet at 6.25 (J_d=16.0Hz, J_t=4.8Hz) and a two-hydrogen doublet at 5.50ppm(J=4.8Hz).

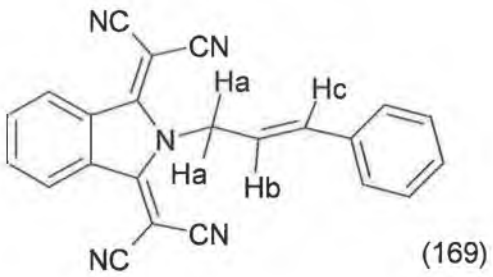

(169)

2Ha: 5.50ppm, d, J=4.8Hz.
Hb: 6.25ppm, dt, J_d=16.0Hz, J_t=4.8Hz.
Hc: 6.48ppm, d, J=16.0Hz.

The ^{13}C-NMR spectrum had 14 distinct signals, which was consistent with the proposed structure (169). Microanalysis confirmed the structure of (169) (45% yield).

Good quality crystals of the cinnamyl derivative (169) were obtained and one was used for the collection of x-ray crystal data. In the crystal the phenyl ring of the cinnamyl group is oriented at an angle of 77.17(6)° to the isoindoline skeleton. The dicyanomethylene groups display a small twist from planarity, making angles of 7.01(10)° (C6A) and 2.33(10)° (C6B) with the C_4N ring. There are intramolecular C-H···N contacts at C12-H12···N2A and C15-H15···N2B. There are also intermolecular interactions between the phenyl ring of the cinnamyl group and C14, which influence the crystal structure packing. Further details including all relevant data regarding bond angles and bond lengths are in Appendix 2.

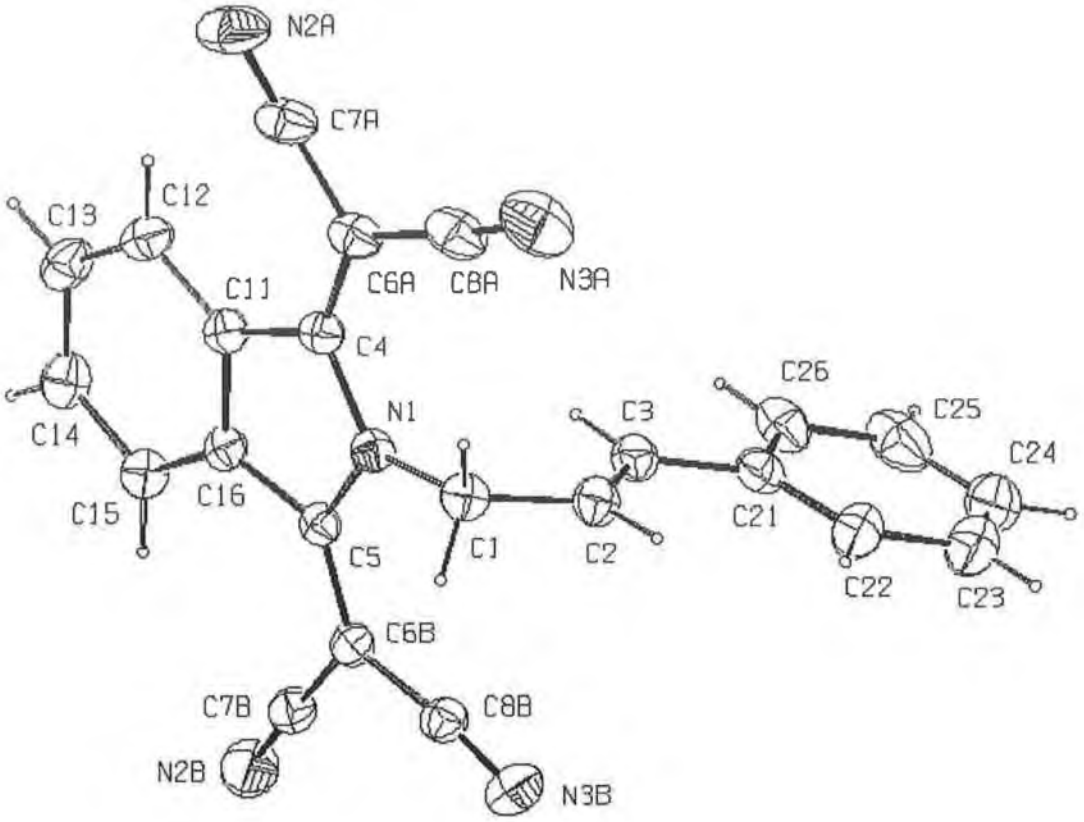

Figure 2.2 X-ray crystal structure of N-cinnamyl compound (169)

2.9 Conclusion

The Mitsunobu reaction has been used successfully to synthesise some N-alkyl derivatives of (127). However the reaction proved to be limited. Very poor yields were obtained from the reactions using propanol and butanol when compared with the reactions involving either methanol or ethanol. This trend is not wholly unexpected, as alcohols generally become less reactive as the alkyl group gets larger.

The successful procedures suffered from long reaction times and average yields. However the reactions to synthesise (128), (141), (168) and (169) were reproducible. The Mitsunobu reaction with this system has limitations. The bulky dicyanomethylene groups may sterically hinder the reaction. The negative charge on the nitrogen in the anion can be extensively delocalised throughout the molecule.

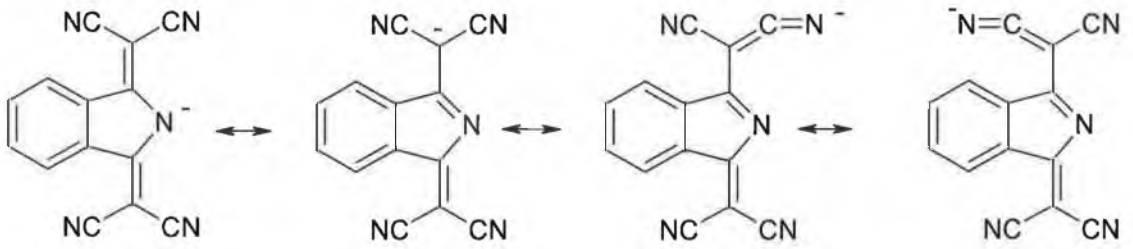

This delocalisation of charge means that the anion developed during the course of the reaction is unusually stable and consequently poorly nucleophilic.

2.10 The synthesis of N-alkylated 3-(dicyanomethylene)isoindolinone derivatives

N-Alkylated derivatives of the tetracyano compound (127) have been synthesised by applying the Mitsunobu reaction. However the reaction did not prove to be universally applicable. An alternative approach utilising carbonyl compound (170) was investigated. Successful alkylation via the Mitsunobu reaction would yield (171), scheme 53.

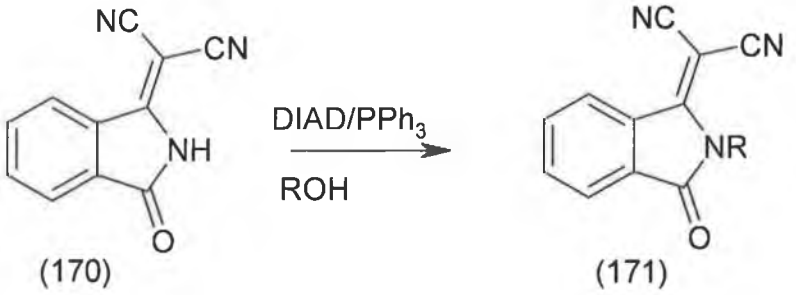

Scheme 53

The carbonyl group in compound (171) might be susceptible to further reaction, in particular with malononitrile under Lehnert's conditions to yield tetracyano compounds (173) analogous to the ones described in the previous section and with BTC and titanium tetrachloride to yield hybrid electron acceptors (172) that possess both dicyanomethylene and cyanoimino functionalities, scheme 54.

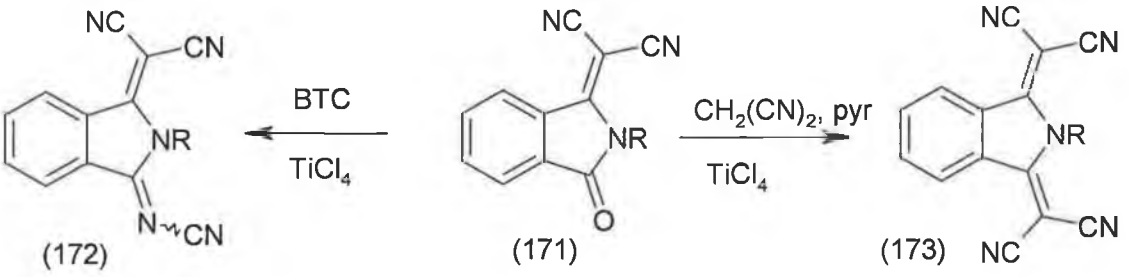

Scheme 54

Compound (170) has previously been synthesised[164] using a method that involves heating (174) with malononitrile at 150°C until no more ammonia is evolved.

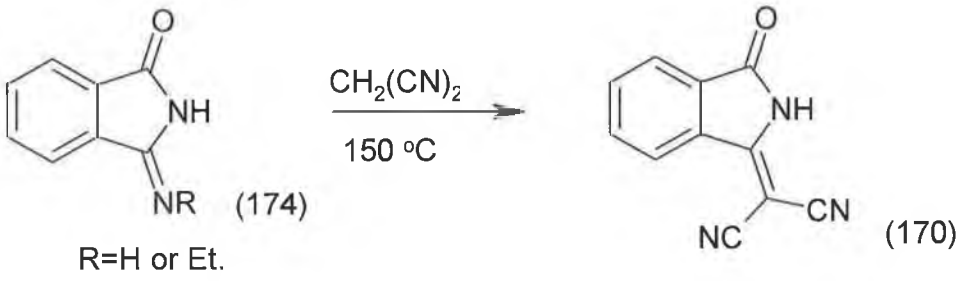

However it is much more conveniently accessible by hydrolysis of (175), obtainable from 1,2-dicyanobenzene as starting material using the method of Conway, scheme 55.[138]

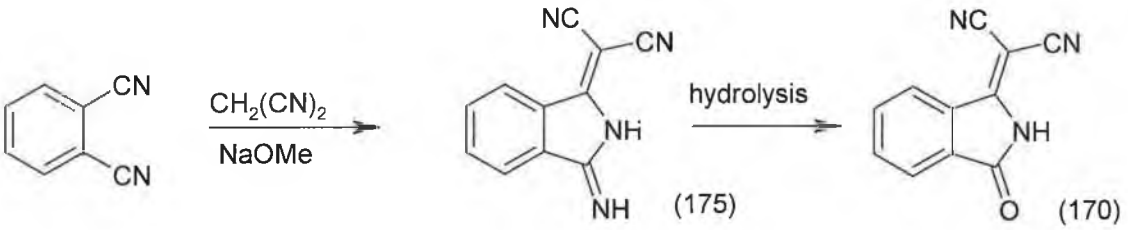

Scheme 55

Reflux of (175) in aqueous acetic acid gave compound (170), as a very pale yellow powder mp 249-251°C, on cooling. The IR spectrum showed both cyano and carbonyl peaks at 2214 and 1765cm^{-1} respectively. The ^{1}H-NMR spectrum showed three multiplets at 7.95, 7.77 and 7.48ppm corresponding to four aromatic hydrogens in a ratio of 1:1:2. The ^{13}C-NMR spectrum showed 11 distinct signals: a carbonyl peak at 167.9, a peak at 161.2 corresponding to (**C**=C(CN)$_2$), 6 aromatic signals at 135.0, 134.8, 133.3, 129.6, 124.9 and 124.7, two cyano peaks at 114.2 and 112.6, and a signal at 58.0ppm due to (**C**(CN)$_2$). On the basis of this data the structure (170) (57% yield) was confirmed. Compound (175) was also successfully hydrolysed in aqueous HCl, however it was easier to isolate the product when aqueous acetic acid was used.

The Mitsunobu reaction was then investigated as a means of alkylating compound (170). The order of addition of reactants was triphenylphosphine, DIAD, alcohol and acidic component (170). The solvent was THF and the reactions were carried out at room temperature.

The reaction of compound (170) with methanol yielded an off-white powder, mp 200-202°C, after three days reaction time. The ^{1}H-NMR spectrum showed three multiplets in the aromatic region, 8.50, 7.80 and 7.72ppm with integration of 1:1:2 and a singlet at 3.62ppm corresponding to the N-methyl group. The ^{13}C-NMR spectrum displayed 12 signals as expected. This spectral data confirmed the structure as the desired N-methyl derivative (153) (34% yield). This compound had the same IR spectrum as the compounds synthesised from the unsymmetrical dimethyl compound (142) and methylammonium salt (154).

Reaction of (170) with ethanol under Mitsunobu conditions yielded an off-white powder mp 172-174°C after three days reaction time. The ^{1}H-NMR spectrum showed three aromatic mulitplets at 8.84, 7.87 and 7.70ppm with integration of 1:1:2. The presence of the N-ethyl group was confirmed by the presence of a two-hydrogen quartet (J=7.2Hz) at 4.20ppm and a three-hydrogen triplet (J=7.2Hz) at 1.34ppm. The ^{13}C-NMR spectrum displayed 13 signals. On the basis of this evidence the compound was confirmed as the N-ethyl compound (155) (41% yield).

N-Alkylation was also successfully achieved using the Mitsunobu reaction with 1-butanol, 1-pentanol and 1-decanol as the sources of the required alkyl group, yielding compounds (176), (177) and (178) respectively. The yields of the reactions were 37, 35 and 51% respectively.

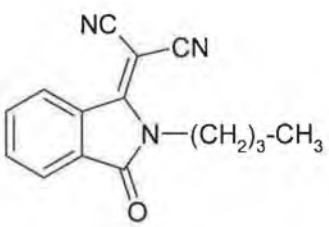

(176)

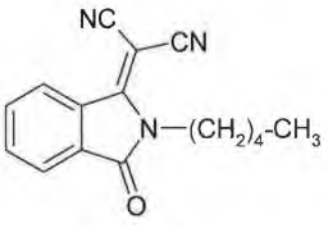

(177)

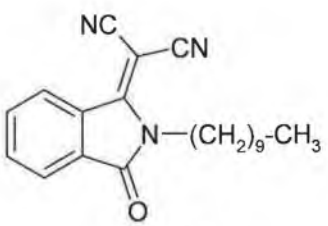

(178)

The ^{1}H-NMR spectrum for all three compounds, in addition to the expected patterns for the N-alkyl groups, displayed the trademark pattern of peaks in the aromatic region, 3 multiplets corresponding to 4 aromatic hydrogens with integration ratio of 1:1:2. The ^{13}C-NMR spectrum of the N-butyl compound (176) displayed 15 distinct signals, 11 of which corresponded to the isoindoline skeleton and the rest to the N-alkyl

group. Similarly the N-pentyl derivative (177) displayed 16 distinct signals and the N-decyl derivative (178) showed 21 distinct signals. These results show that the carbonyl compound (170) more reactive towards the Mitsunobu reaction than the tetra-cyano compound (127).

Benzyl, cinnamyl and allyl alcohols were also used as the sources of alkyl group each reaction giving products in 29, 22 and 36% yields respectively. In each case the spectral data obtained confirmed that the required N-alkylation had taken place, the ^{1}H-NMR spectrum of each compound displaying 3 multiplets for the 4 aromatic hydrogens of the isoindoline unit.

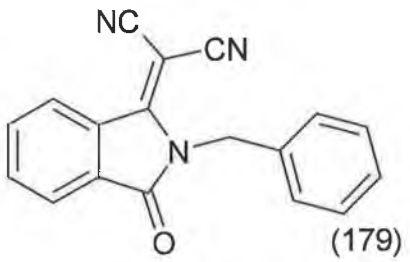

(179)

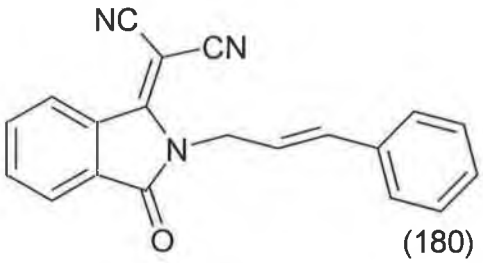

(180)

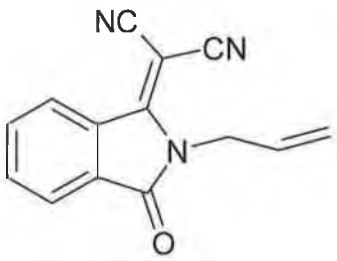

(181)

The N-benzyl derivative (179) also showed 2 further multiplets at 7.27 and 7.18ppm with integrations of 3:2 respectively corresponding to the aromatic ring of the benzyl group and a two-hydrogen singlet at 5.40ppm. The ^{13}C-NMR spectrum displayed 16 signals 11 corresponding to the isoindoline unit and 5 pertaining to the N-benzyl group.

The alkyl group in the N-cinnamyl derivative (180) displayed a similar pattern to its tetracyano analogue (170). The exocyclic phenyl ring was depicted by a two-hydrogen multiplet at 7.30 and a three-hydrogen multiplet at 7.21ppm. The remaining signals were

two doublets at 6.60 (J=16.0Hz) and 4.93 (J=6.0Hz) each due to one hydrogen and a double triplet at 6.20ppm (J_d=16.0Hz, J_t=6.0Hz) corresponding to one hydrogen.

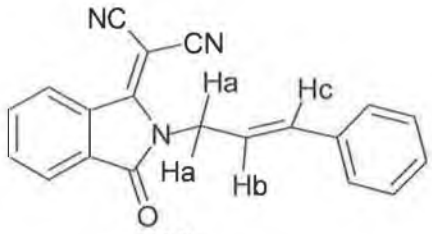

(180)

2Ha: 4.93ppm, J=6.0Hz.
Hb: 6.20ppm, J_d=16.0Hz, J_t=6.0Hz.
Hc: 6.60ppm, J=16.0Hz.

The ^{13}C-NMR spectrum showed 18 signals with 7 being attributed to the N-cinnamyl group, as anticipated.

The ^{1}H-NMR spectrum of the allyl derivative (181) is shown schematically below. The ^{13}C-NMR spectrum displayed 14 signals, 11 belonging to the isoindoline unit and 3 to the N-allyl group.

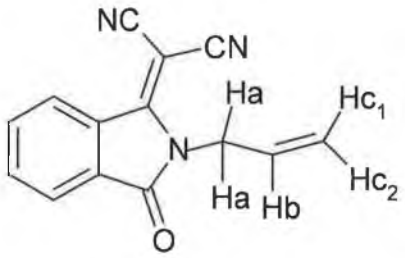

(181)

2Ha: 4.85ppm, m.
Hb: 5.95ppm, m.
Hc_1:5.15ppm, d, J=17.1Hz.
Hc_2: 5.34ppm, d, J=10.3Hz.

The results achieved have shown that compound (170) can be alkylated by a larger number of alcohols than its tetracyano analogue (127). This is probably due to the anion generated in the Mitsunobu reaction being more nucleophilic. This is supported by the observation that compound (170) could be alkylated by iso-propyl alcohol whereas all attempts to alkylate (127) with secondary alcohols failed.

The Mitsunobu reaction of (170) and iso-propyl alcohol produced pale needles mp 167-169°C. The ^{1}H-NMR spectrum displayed the usual aromatic pattern, 3 multiplets at 8.52, 7.81 and 7.69ppm, a one-hydogen multiplet at 5.03 and a doublet at 1.58ppm (J=6.8Hz) corresponding to two methyl groups. The ^{13}C-NMR spectrum displayed 13

signals, 11 due to the dicyanomethylene isoindolinone skeleton and 2 attributed to an iso-propyl group. A combination of the spectral data and satisfactory microanalysis confirmed structure (182) (27% yield).

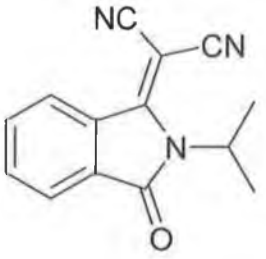

(182)

2.11 Conclusion

From the experimental results achieved it is clear that compound (170) is more reactive than (127) towards the Mitsunobu reaction. No new products were isolated from reactions with tetracyano derivative (127) and primary alcohols that contained more than 4 carbons. Similarly no product was isolated when secondary alcohols were used. However compound (170) proved to be more tolerant. The largest primary alcohol used was 1-decanol and reaction with iso-propyl alcohol was also successful.

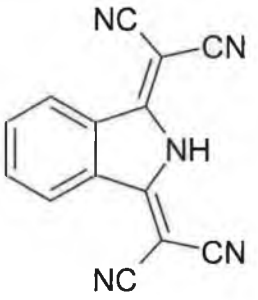

(127)

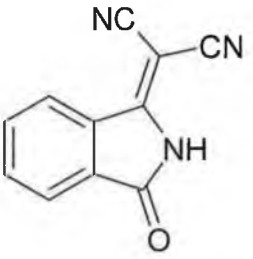

(170)

An obvious reason for this is the presence of the carbonyl group in (170) which may result in a lessening of the degree of delocalisation of the negative charge in the resonance structures of the anion of (170), thereby rendering it more reactive. The less bulky carbonyl group should also alleviate any steric hinderance associated with the reaction.

The Mitsunobu reaction proved to a reliable synthetic route to N-alkylated-3-(dicyanomethylene)isoindolinones. These compounds could be potential electron acceptors for CT complexes themselves or could be used as precursors to another series of potential electron acceptors.

2.12 The reaction of N-alkyl-(dicyanomethylene)isoindolinones with BTC and $TiCl_4$

Hybrid electron acceptors based on TCNQ and DCNQI have been synthesised by treating the carbonyl oxygen of compounds such as (183) with titanium tetrachloride and bis(trimethylsilyl)carbodiimide (BTC). Hunig and co-workers first developed the synthesis in 1984.

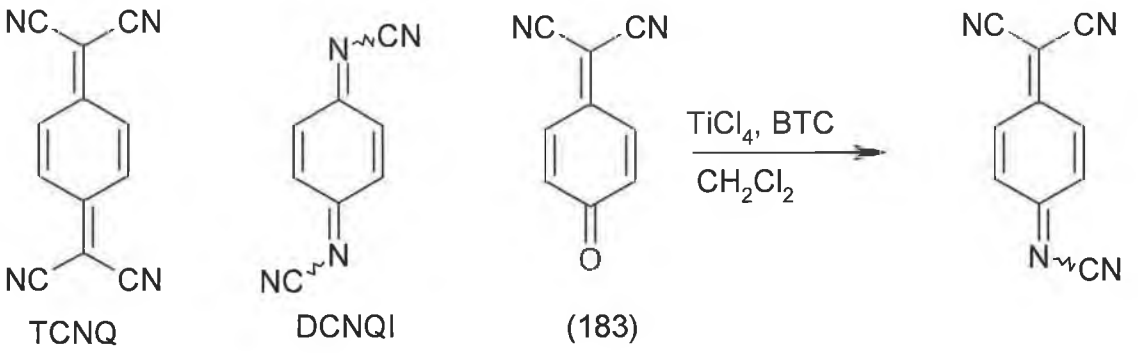

Heterocyclic derivatives of DCNQI have not been as extensively researched as their TCNQ counterparts. The smaller =NCN group suffers less steric problems when compared with the more bulky dicyanomethylene group. This means that the electron accepting ability of a DCNQI type molecule can be easily improved by the addition of electron withdrawing substituents directly on to the molecule. The =NCN group can arrange itself in a manner that will minimise any deviation from planarity.

It was anticipated that if N-alkyl-3-(dicyanomethylene)isoindolinones (171) were to be treated with $TiCl_4$ and BTC a novel series of electron acceptors (184) might be synthesised, scheme 55.

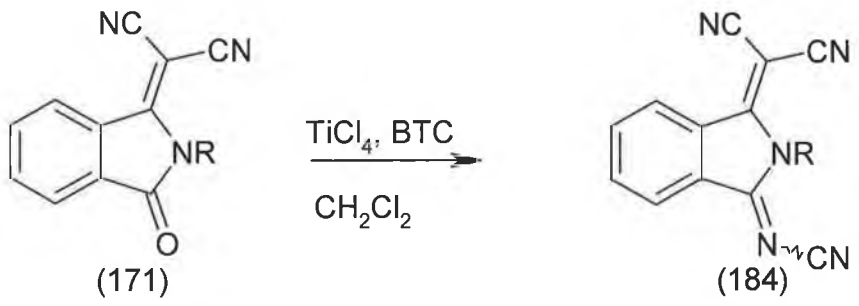

Scheme 55

The reaction was carried out with N-substituted (dicyanomethylene)isoindolinone (171) derivatives with straight chain saturated aliphatic alkyl groups (n-pentyl and n-decyl) attached to the nitrogen atom.

Firstly the N-pentyl compound (177) was used. TLC analysis of the reaction mixture showed the formation of a new product, which was isolated as a pale yellow powder, mp 155-157°C. The IR spectrum obtained showed that the carbonyl peak of the parent compound at 1744cm^{-1} had disappeared. The ^{1}H-NMR spectrum has 3 multiplets at 8.74, 8.58, and 7.79ppm corresponding to four aromatic protons. These signals integrated with a ratio of 1:1:2 respectively. The N-pentyl group was represented by four signals, a two-hydrogen triplet at 4.23 (J=8.0Hz), a two-hydrogen multiplet at 1.73, a multiplet at 1.35 due to four hydrogens and a triplet at 0.87ppm (J=6.8Hz) corresponding to three hydrogens. The ^{13}C-NMR spectrum showed a total of seventeen signals, of which 6 were attributed to the aromatic ring and 5 belonged to the N-pentyl group. More importantly there were 3 cyano peaks at 113.5, 113.1 and 112.5ppm. Good microanalysis confirmed that the desired product (185) (64% yield) had been formed.

The reaction of N-decyl-3-(dicyanomethylene)isoindolinone (178) with BTC and $TiCl_4$ yielded a pale yellow powder, mp 94-96°C. The ^{1}H-NMR spectrum showed three multiplets at 8.73, 8.58 and 7.79ppm due to four aromatic hydrogens, a two-hydrogen triplet at 4.22 (J=8.0Hz), a two-hydrogen mulitplet at 1.71, a multiplet at 1.30 [-$(CH_2)_7$-] and a triplet (J=6.8Hz) at 0.81ppm corresponding to three hydrogens. The ^{13}C-NMR spectrum displayed 22 distinct signals as expected. Again good microanalysis confirmed the structure of (186) (55% yield).

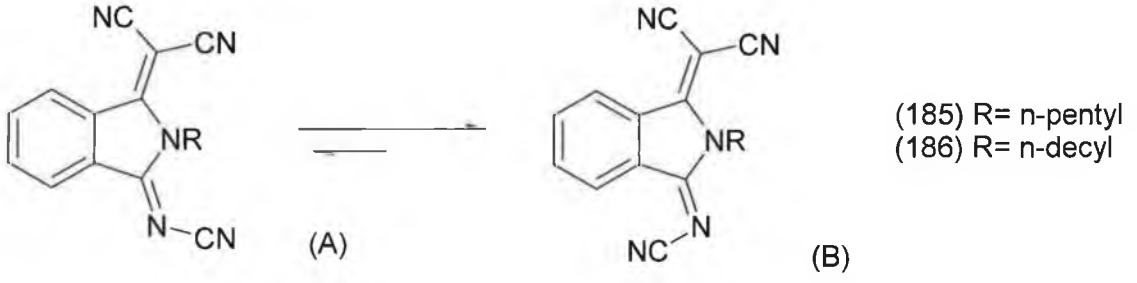

Both products can exist in either two different geometrical isomeric forms (A) and (B). But at any one time it is probable that the compounds find themselves adopting the second configuration, form (B). By adopting this configuration the cyano nitrogen in the cyanoimino group will maximise the distance between itself and its nearest neighbour and thus relieve steric strain, scheme 56

Scheme 56

The structures above represent the possible isomers of N-pentyl compound (185). The distance between the cyano nitrogen in the cyanoimino group and its nearest neighbour (hydrogen attached to second carbon in alkyl chain) in form (A) is 1.99Å. The distance between the corresponding nitrogen in form (B) and its nearest neighbour (aromatic hydrogen) is 2.37Å. The NMR spectrum recorded at room temperature for each compound shows the presence of only a single isomer in each case.

N-Phenylphthalimide (187) was also subjected to reaction with titanium tetrachloride and BTC. TLC analysis of the reaction mixture showed three major spots and the mixture was resolved by column chromatography. The fastest moving spot was recovered starting material, N-phenylphthalimide. The second eluting fraction was a very pale yellowish/green solid, mp 167-169°C (25% yield). The IR spectrum displayed cyano stretches at 2204 and 2174cm^{-1} and a carbonyl stretch at 1757cm^{-1}. The ^{1}H-NMR spectrum displayed three multiplets at 8.75, 7.95 and 7.81ppm with integration ratio of 1:1:2, a pattern similar to that obtained for the unsymmetrical N-alkyl-3-(dicyanomethylene)isoindolinone derivatives. Two further aromatic multiplets were found at 7.48 due to 3 hydrogens and 7.32ppm due to 2 hydrogens, corresponding to the N-phenyl group. The ^{13}C-NMR spectrum had 13 signals, a carbonyl peak at 168.2, a peak at 166.5 due to (**C**=N-CN), aromatic signals at 135.6, 131.4, 130.6, 130.0, 129.8, 129.7,

128.0, 127.0, 126.4, and 125.2 and a cyano peak at 113.9ppm. On the basis of this spectral data the structure was confirmed as (188).

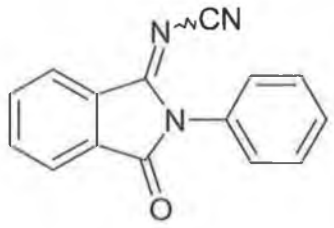

(188)

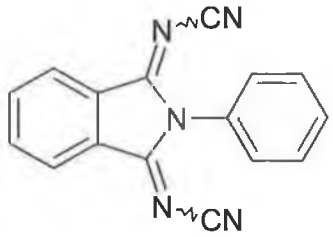

(189)

The slowest moving spot yielded pale yellow powder mp 278-280°C (31% yield). The IR spectrum showed that the carbonyl stretch had been removed. There was a single cyano peak at 2191cm^{-1}. The ^{1}H-NMR spectrum confirmed that the compound was symmetrical. Two multiplets at 8.80 and 7.91ppm were attributed to the four aromatic hydrogens of the aromatic moiety of the isoindoline skeleton. The N-phenyl group was depicted as expected by two multiplets at 7.51 and 7.27ppm due to three hydrogens and two hydrogens respectively. The ^{13}C-NMR spectrum showed a smaller number of peaks than were present in the spectrum obtained for (188), again implying that this product symmetrical, with peaks at, 167.5 due to (**C**=N-CN), aromatic peaks at 136.3, 130.9, 130.7, 130.0, 128.7, 128.5 and 127.0 and a cyano peak at 113.0ppm. The spectral data and microanalysis confirmed the compound as the di-cyanoimino derivative (189). The overall reaction is shown in scheme 57.

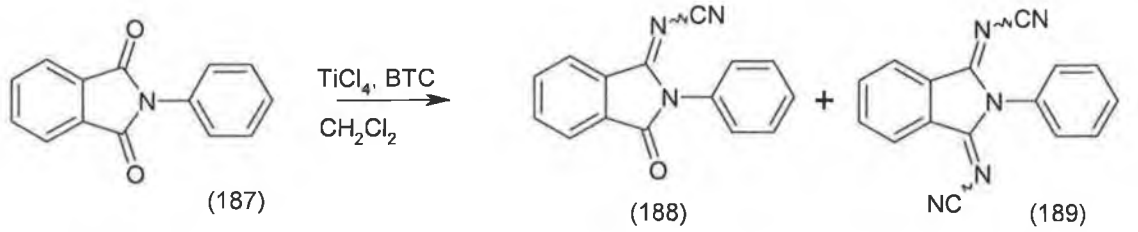

(187) (188) (189)

Scheme 57

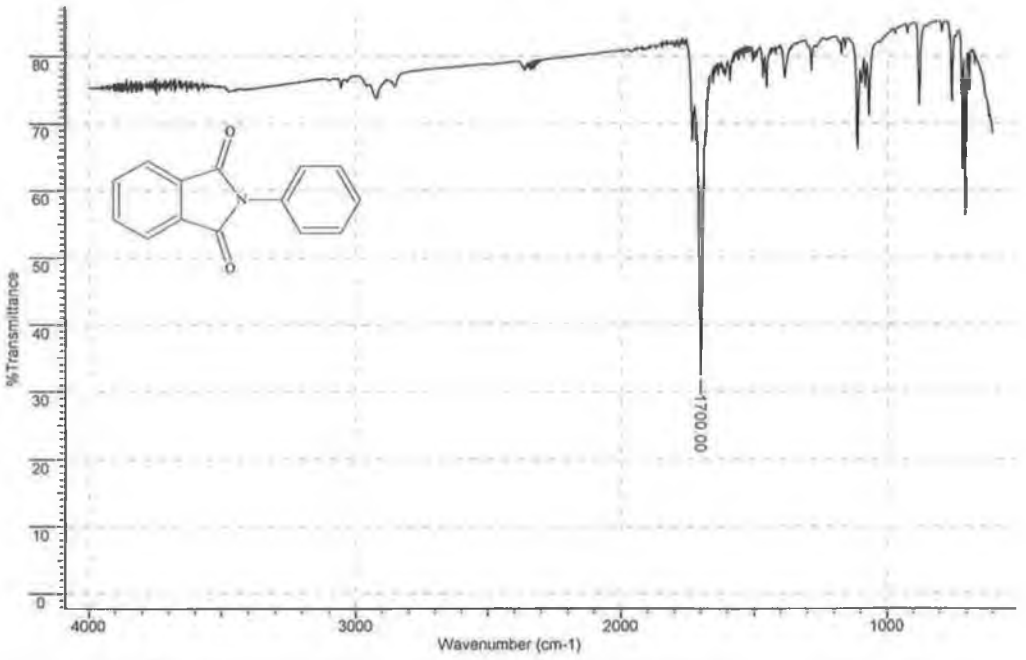

Figure 2.3 IR spectrum of N-phenylphthalimide highlighting C=O stretches.

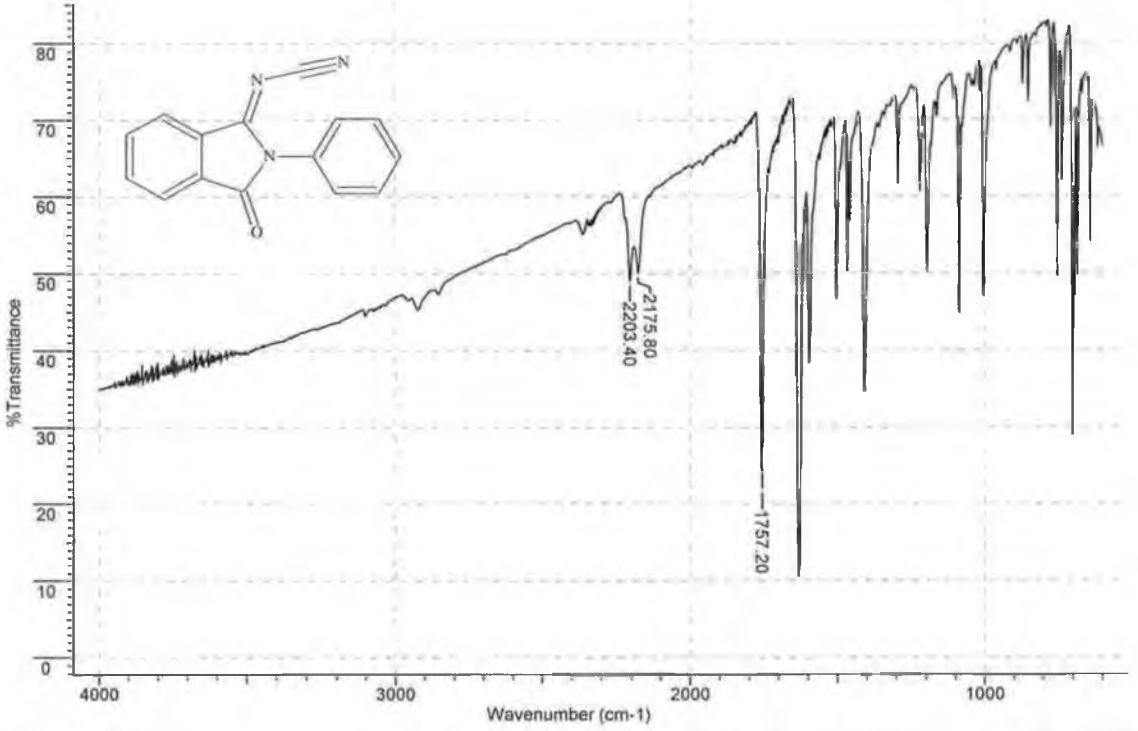

Figure 2.4 IR spectrum of mono-condensation product highlighting CN and C=O stretches.

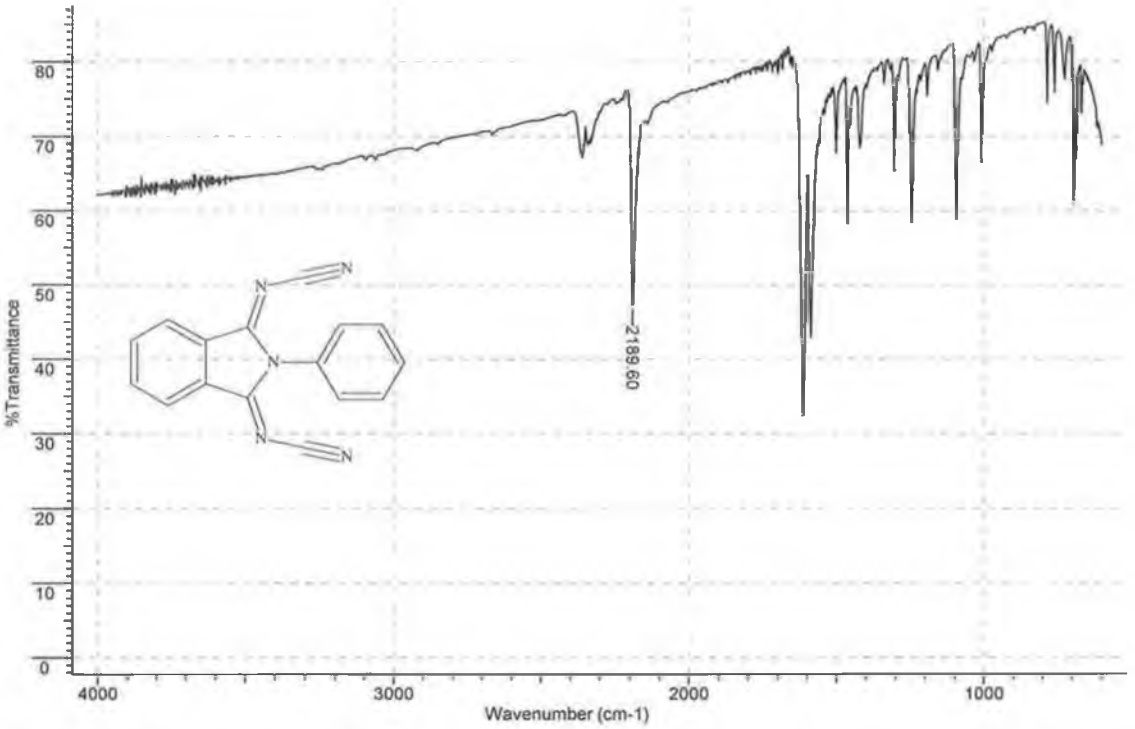

Figure 2.5 IR spectrum of bis-condensation product highlighting absence of C=O stretch.

2.13 Conclusion

The combination of BTC and $TiCl_4$ effected condensation at the carbonyl oxygen of N-alkyl-(dicyanomethylene)isoindolinones where the alkyl groups were straight chain alkyl groups. The reaction proved to be reliable and the isolation of products was relatively straightforward. The Mitsunobu reaction can provide a wide range of starting materials for this process. Therefore a possible synthetic route to a novel series of compounds has been developed.

Chapter 3
Cyclic Voltammetry

3.1 Cyclic Voltammetric analysis

Cyclic voltammetry (CV) and linear sweep voltammetry (LSV) involve a large periodic potential change imposed on a system. In LSV the potential is ramped between two chosen limits at a steady scan rate (v) and the current monitored. Cyclic voltammetry is the same as LSV except that the potential is swept back and forth between the two chosen limits one or more times and the current is monitored continuously. Sweeping the potential in a negative direction can provide information about the reduction of a neutral species to a radical anion, dianion and possibly trianion. When the negative limit is reached a positive potential sweep will provide information about the various oxidative processes that should ultimately lead back to the neutral species.

$$A + e^- \rightleftharpoons A^{\cdot-}$$

$$A^{\cdot-} + e^- \rightleftharpoons A^{2-}$$

When cyclic voltammetry is applied to potential electron acceptors a number of key questions can be answered. First is whether the compound is electrochemically reducible, then whether any reduction processes are part of reversible redox couples and finally the potentials at which the electrochemical phenomena become known.

The standard cell consists of three electrodes immersed in a non-agitated electrolyte. The electrodes are the working electrode (WE), counter electrode (CE) and reference electrode (RE). The potential at the WE is monitored and controlled precisely with respect to the RE via a potentiostat. A typical response curve (cyclic voltammogram) for the reversible reduction of a species A is shown below.

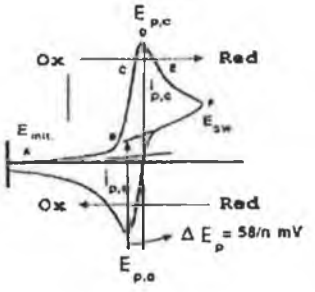

In order to explain the shape of the graph obtained the diagram can be considered to be the amalgamation of two scans, the cathodic scan (reductive process) and anodic scan (oxidative process). Considering the cathodic scan, the sweep is started at a suitably positive potential and at this potential no faradaic current flows as the only species present is A. When the potential approaches $E^{o'}$ (formal potential of couple) the current begins to rise sharply as the amount of A^- at the electrode surface increases. A maximum current value is achieved when there is no neutral A present at the surface of the electrode. The current then diminishes as the concentration of A in the solution surrounding the electrode decreases. When the negative limit is reached the anodic scan commences. Initially the potential is still negative enough to reduce A even though the potential is scanning in a positive direction. The increasingly positive electrode attracts A^- and the anodic current is generated by its oxidation to neutral A. The current then decays as the solution around the electrode is depleted of A^-.

The system described above is an electrochemically reversible system. This means that the redox couple adheres to the Nernst equation,

$$E = E^{o'} + RT/nF \ln([A]/[A^-])$$

where E= potential, $E^{o'}$ = formal potential, R= gas constant, T= temperature (K), F= Faraday constant, n= number of electrons per molecule of oxidised or reduced species, [A] is the concentration of neutral (oxidised) species and $[A^-]$ is the concentration of reduced species.

For a system to be considered electrochemically reversible the difference between the cathodic and anodic peak potentials should be 0.059/n Volts, where n= the number of electrons involved in the electrochemical process (for example one electron is exchanged in going from A to A^- and back again, therefore n= 1). The ratio of the cathodic and anodic peak currents should also be one.

In summary a system is electrochemically reversible when the forward and backward sweeps are exact mirror images of each other and their peak potentials are within 0.059/n V of each other.

3.2 Electrochemical Studies of potential electron acceptors

The electrochemical properties of a large number of the compounds synthesised were investigated,, scheme 58.

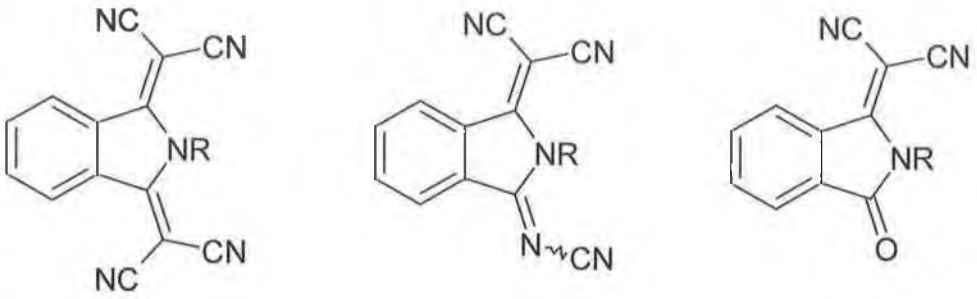

Scheme 58

The experimental set-up was as follows; WE = 3mm Pt disc shrouded in teflon, RE = Ag/Ag^{+} non-aqueous reference electrode, CE = $1cm^{3}$ Pt flag. solvent = acetonitrile, electrolyte = 0.1M tetrabutyl-ammonium tetrafluoroborate.

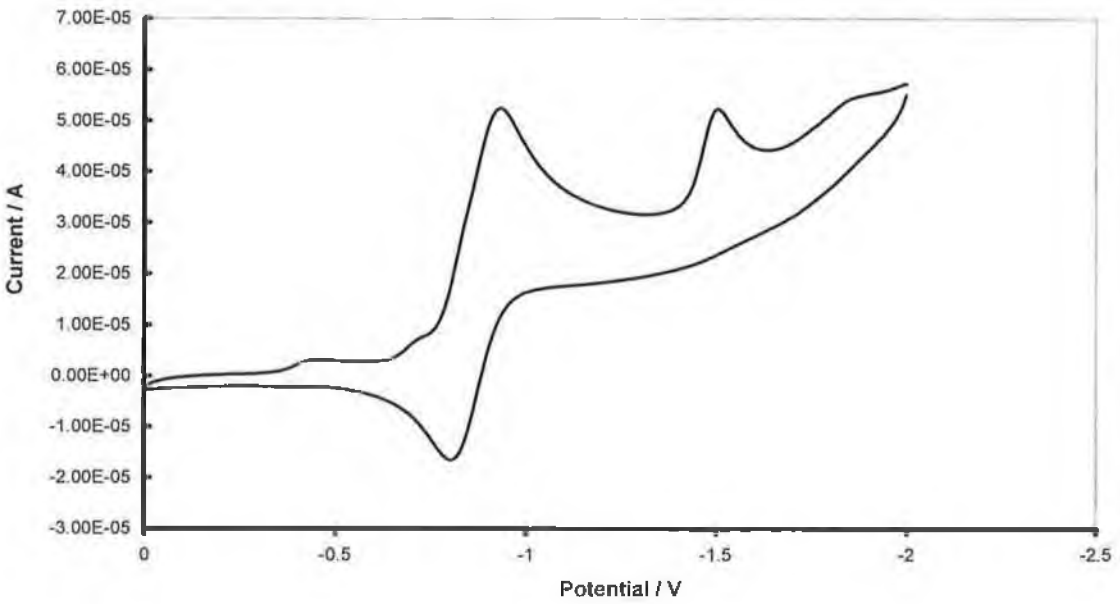

Figure 3.1. Cyclic voltammogram of tetra-cyano N-ethyl derivative (140) in 0.1M electrolyte in acetonitrile at scan rate (v) = 0.1 V/s.

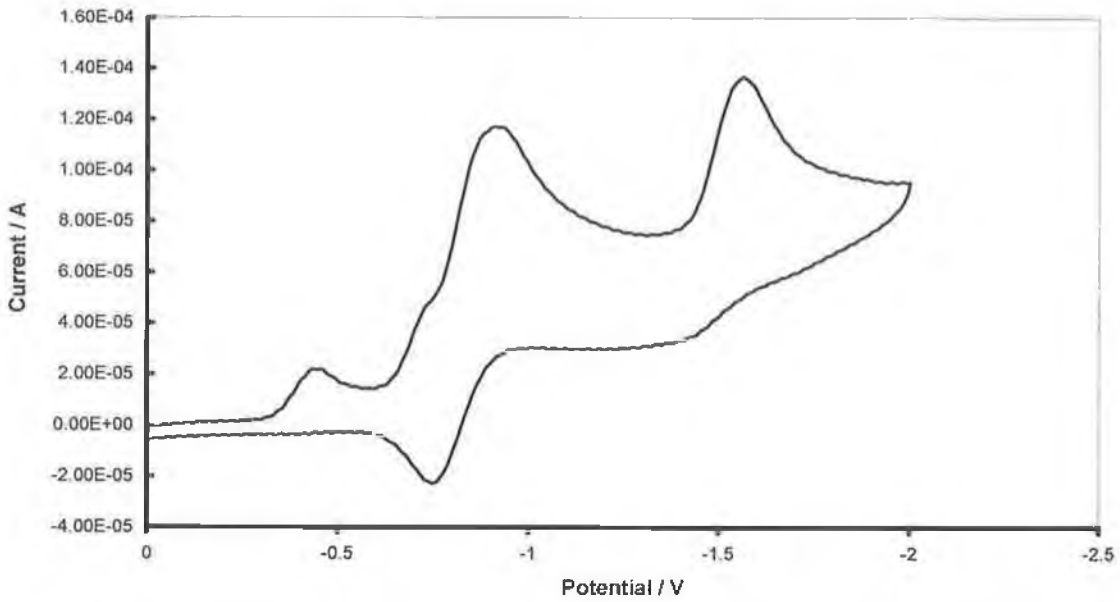

Figure 3.2. Cyclic voltammogram of tetra-cyano N-allyl derivative (168), $\nu = 0.5$V/s.

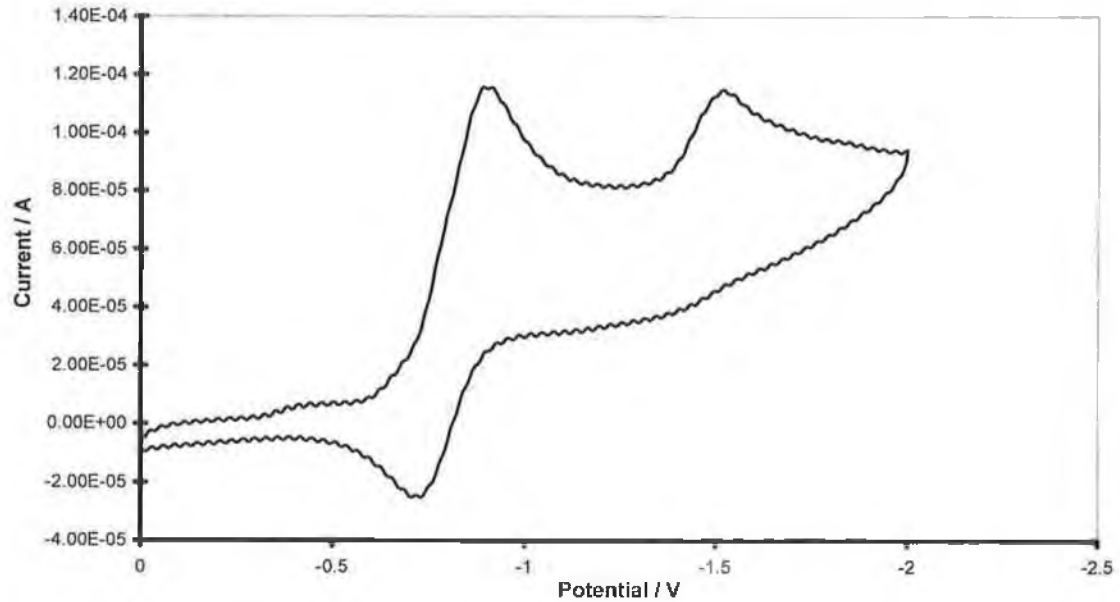

Figure 3.3. Cyclic voltammogram of tetra-cyano N-benzyl derivative (141), $\nu = 0.5$V/s.

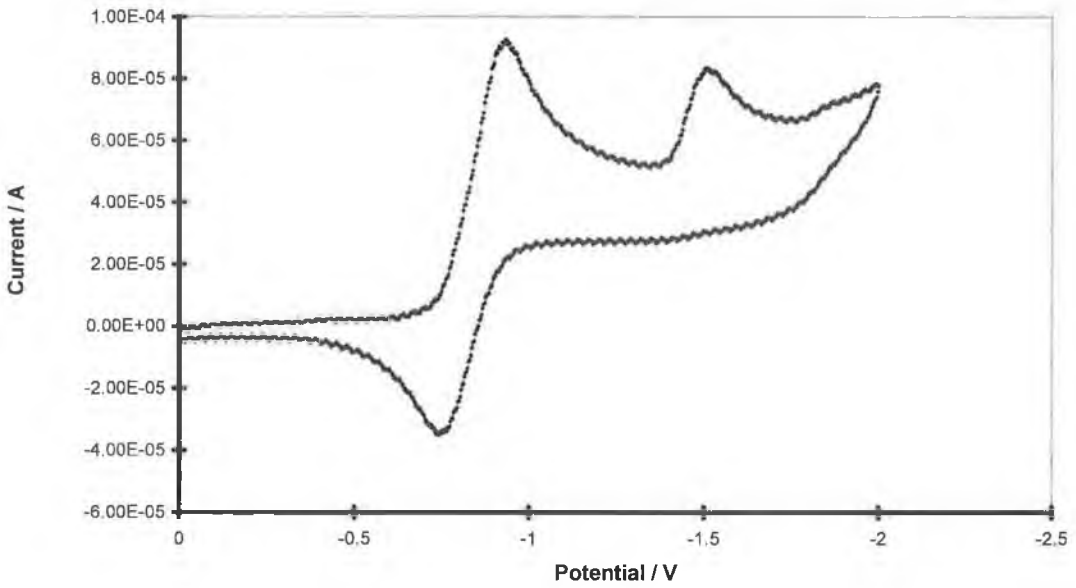

Figure 3.4. Cyclic voltammogram of tetra-cyano N-cinnamyl derivative (169), v = 0.5V/s.

Two clear reduction peaks can be seen in the cyclic voltammograms. However only the first reduction seems to have a noticeable reciprocal oxidative process. In fact the redox couple between the first reduction and the corresponding oxidation form a quasi-reversible couple. This means essentially that the rate constants for reduction and oxidation are the same order of magnitude over most of the potential range. In each case the second reduction is irreversible, as no noticeable anodic peak is visible.

The data obtained can be summarized in table 3.1.

Compound	Ep_c / V	Ep_{c2} / V	Ep_{a1} / V	Ep_{a2} / V	Ep_c-Ep_{a1} / V
NET (140)	-0.95	-1.52	-0.79	N/A	0.16
NAL (169)	-0.93	-1.58	-0.73	N/A	0.20
NBZ (141)	-0.92	-1.54	-0.71	N/A	0.21
NCIN (169)	-0.95	-1.53	-0.74	N/A	0.20

Table 3.1.

For the redox couple corresponding to reduction of neutral acceptor (A) to radical anion (A^-) to be considered reversible the difference between the peak potentials associated with the cathodic and anodic sweeps should be 0.059/n V, where n= the number of electrons involved in the electrochemical couple (in this case n= 1). In the experiments depicted above the values vary from 0.16 to 0.21V. Therefore the redox couple in question is quasi-reversible. The second reduction peaks depict an irreversible process. The irreversibility of the second reduction effectively means that the species generated by the second reduction (A^{2-}) is not re-oxidized by the electrode. A possible explanation for this is that the dianion reacts chemically with an unknown species (X) in solution.

CV analysis of hybrid compounds (185) and (186) was carried out using the same experimental set-up.

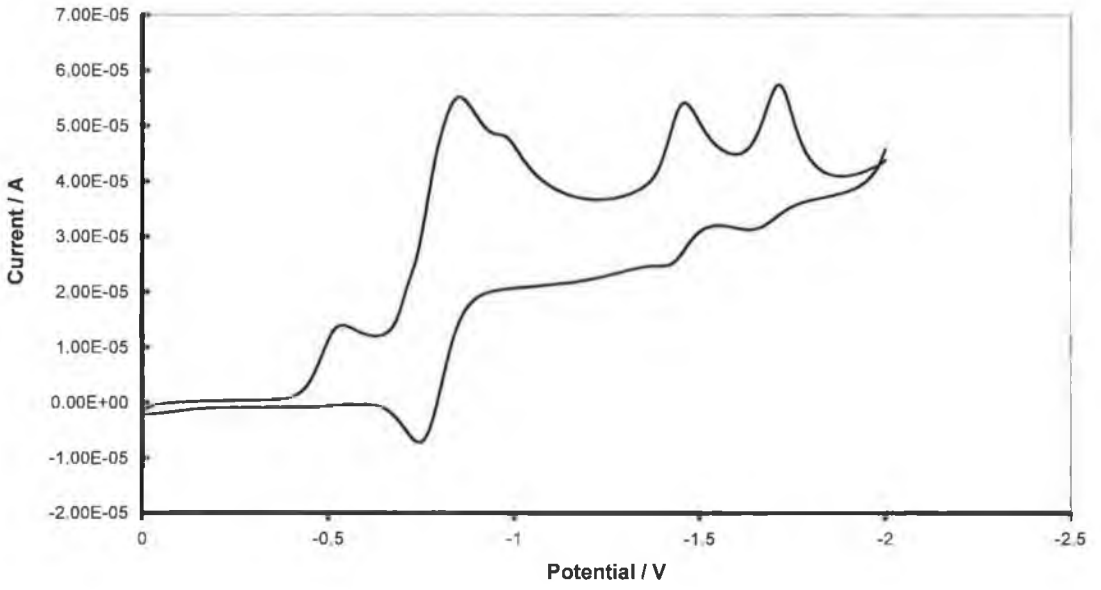

Figure 3.5. Cyclic voltammogram of (185), v = 0.1V/s.

Five reduction peaks are visible. Three appear to have an associated oxidation peak. The first one of these three was part of quasi-reversible couple and next two were irreversible. The analysis was then carried out at increasingly fast scan rates. At fast scan rates the extra electron is quickly added to the system and promptly removed. This

lessens the likelihood that the reduced species will undergo a chemical reaction to another unknown species. The electrochemical process can outrun a chemical reaction.

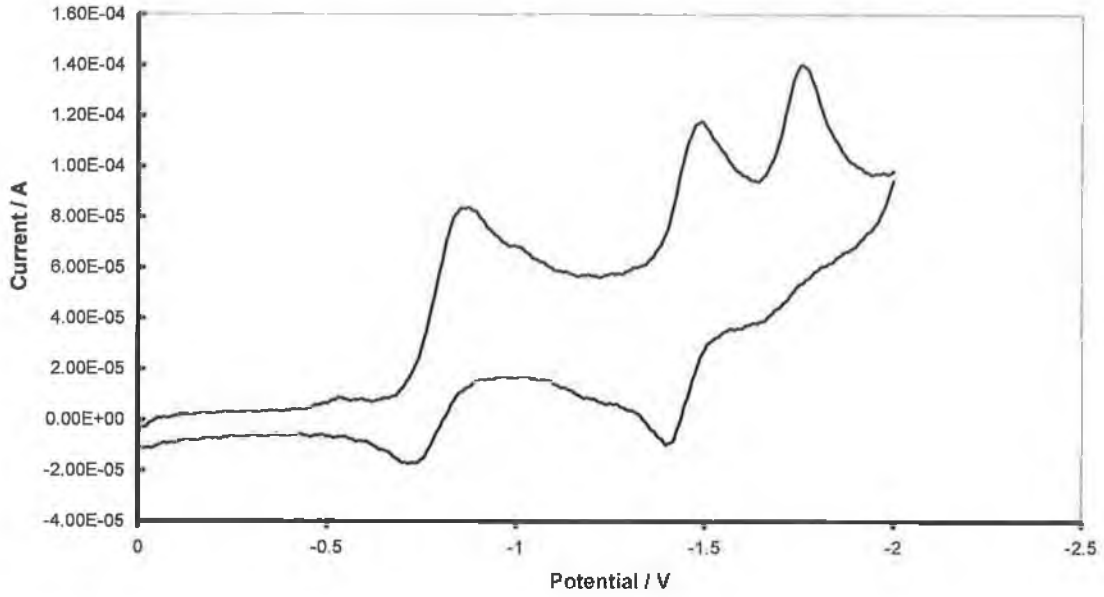

Figure 3.6. Cyclic voltammogram of (185), $v = 1.0$V/s.

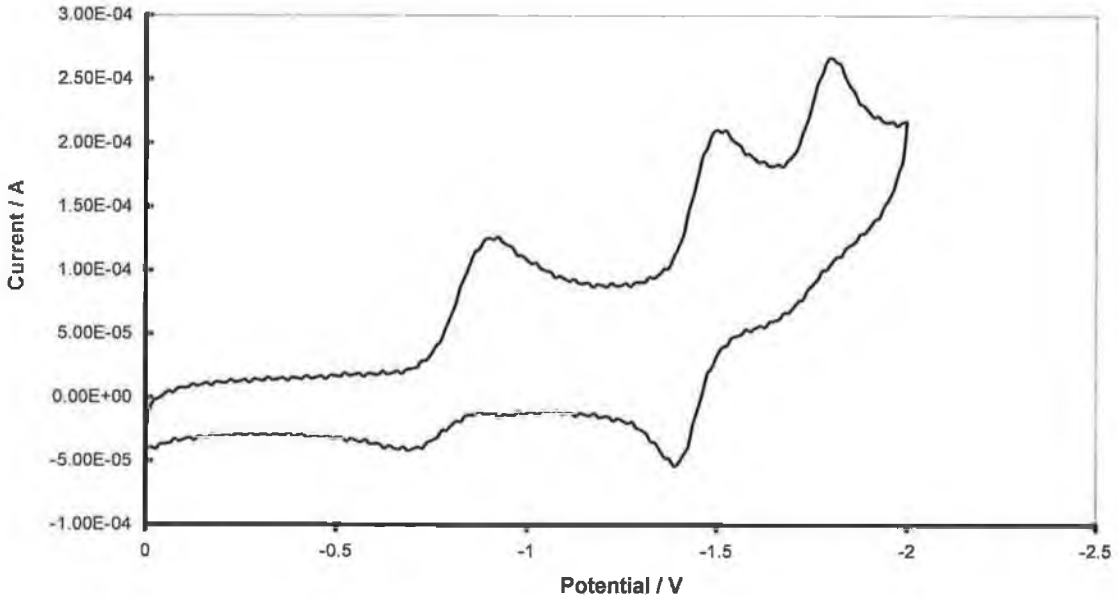

Figure 3.7. Cyclic voltammogram of (185), $v = 5.0$V/s.

When the scan rate was increased an oxidation peak associated with the second reduction peak appeared. The third reduction remained completely irreversible. Similar results were obtained with the N-decyl derivative (186). The data is reviewed in table 3.2.

Compound	Scan rate (V/s)	Ep_{a1} / V	Ep_{a2} / V	Ep_{a3} / V	Ep_{c1} / V	Ep_{c2} / V	ΔE_1 / V	ΔE_2 / V
(TRCNPT) (185)	0.1	-0.87	-1.50	-1.70	-0.73	N/A	0.14	N/A
(TRCNPT) (185)	1.0	-0.88	-1.50	-1.80	-0.71	-1.40	0.17	0.10
(TRCNPT) (185)	5.0	-0.93	-1.52	-1.82	-0.69	-1.38	0.21	0.14
(TRCNDC) (186)	0.1	-0.85	-1.46	-1.69	-0.72	N/A	0.13	N/A
(TRCNDC) (186)	1.0	-0.86	-1.47	-1.74	-0.71	N/A	0.15	N/A
(TRCNDC) (186)	10.0	-0.92	-1.48	-1.79	-0.67	-1.35	0.25	0.13

Table 3.2. $\Delta E_1 = Ep_{a1} - Ep_{c1}$ and $\Delta E_2 = Ep_{a2} - Ep_{c2}$

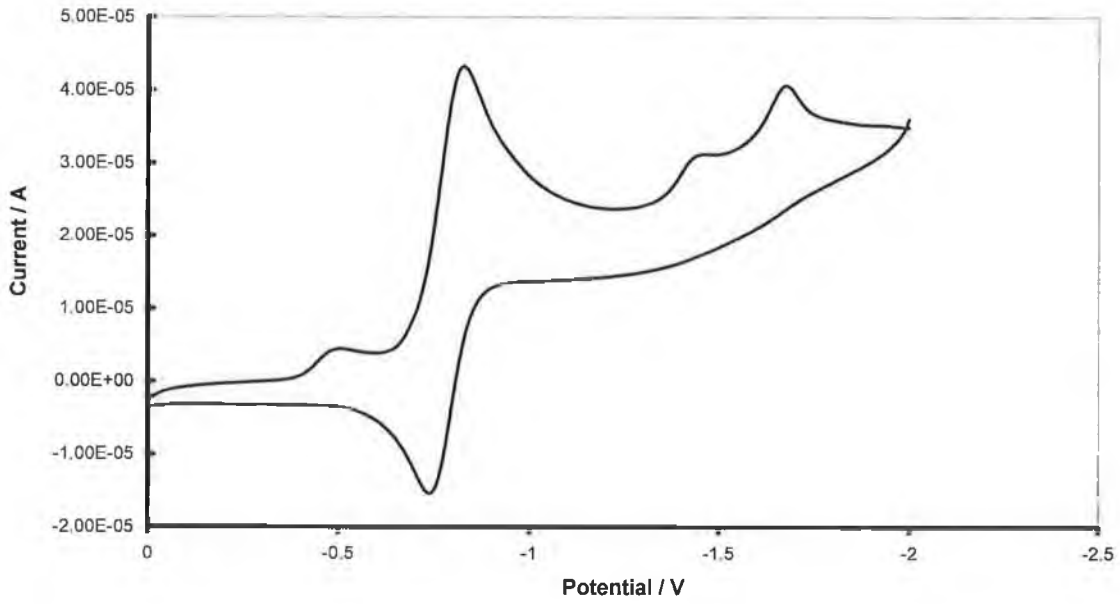

Figure 3.8. Cyclic voltammogram of (186), $v = 0.1$V/s.

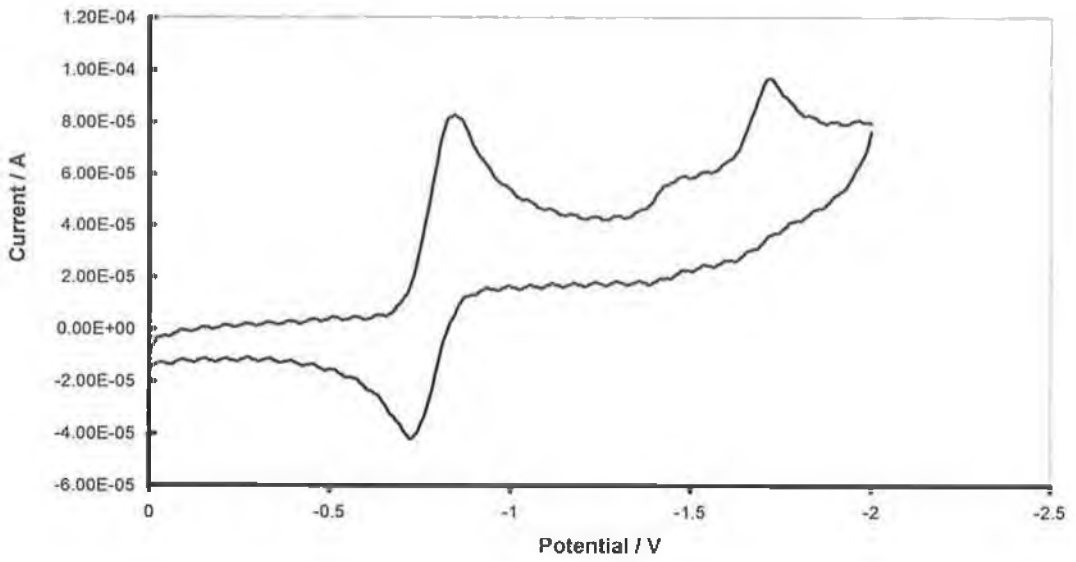

Figure 3.9. Cyclic voltammogram of (186), $v = 1.0$V/s.

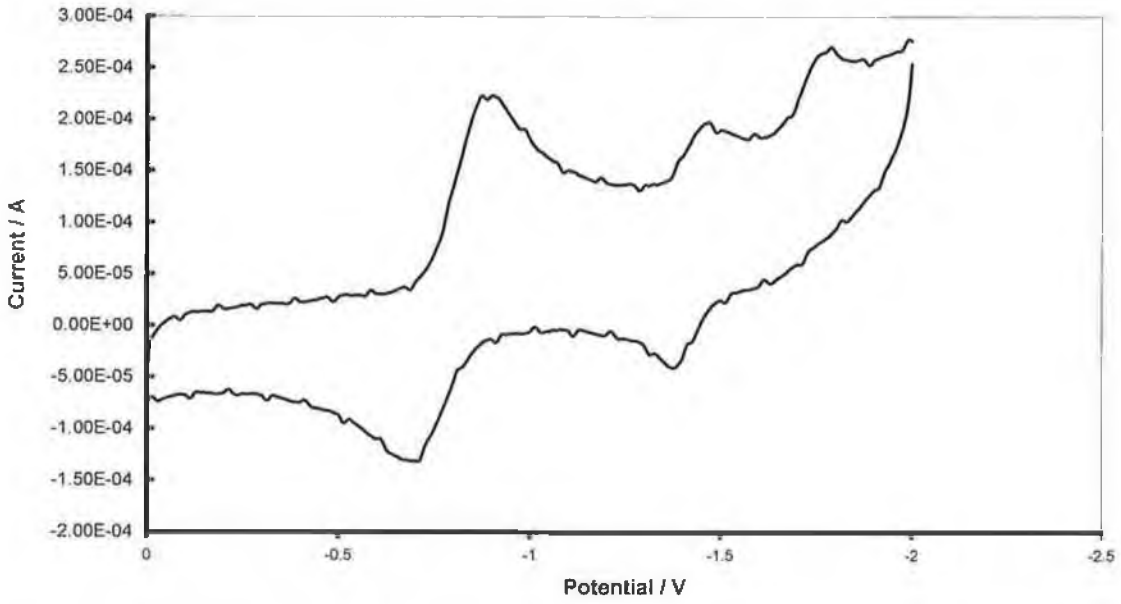

Figure 3.10. Cyclic voltammogram of (186), $v = 10.0$V/s.

As the scan rate was increased the value of ΔE for the first redox couple increased. This is due to the presence of a finite solution resistance between the reference and working electrode.[165] The true potential can be expressed as the sum of the applied potential and [I_p (peak current).R_s (solution resistance)]. The IR term is negative for anodic peak current and positive for cathodic peak current. Since the peak current is proportional to $v^{1/2}$, this means that the 'IR drop' increases with scan rate and therefore the peak potentials move apart.

At higher scan rates a quasi-reversible redox couple corresponding to the reduction of radical anion to dianion and oxidation back to the radical anion becomes visible. This means that the chemical reaction that oxidizes the dianion of both (185) and (186) at lower scan rates has been outrun.

Irrespective of scan rate the third reduction process remains irreversible. This behaviour suggests that the species generated is very unstable and undergoes chemical reaction extremely quickly. It is possible this wave originates from the reduction of some unplanned species resulting from the evolution of the unstable dianion.

Cyclic voltammograms were also obtained for some of the compounds that contained a dicyanomethylene and carbonyl moiety. The compounds used were (155), (180), (177) and (178). The first two were included because the CVs obtained for these compounds can be directly compared to analogous tetra-cyano derivatives.

The most significant aspect of the CVs obtained for the isoindolinone compounds is that the most reversible redox couple is the one that corresponds to the reduction of radical anion to dianion and subsequent oxidation back to radical anion. The presence of a carbonyl group in the place of a dicyanomethylene group seems to the reason for this change in electrochemical properties. Compounds (155) and (180) can be compared directly with their tetra-cyano counter-parts (140) and (169) respectively. Compounds (177) and (178) were chosen arbitrarily.

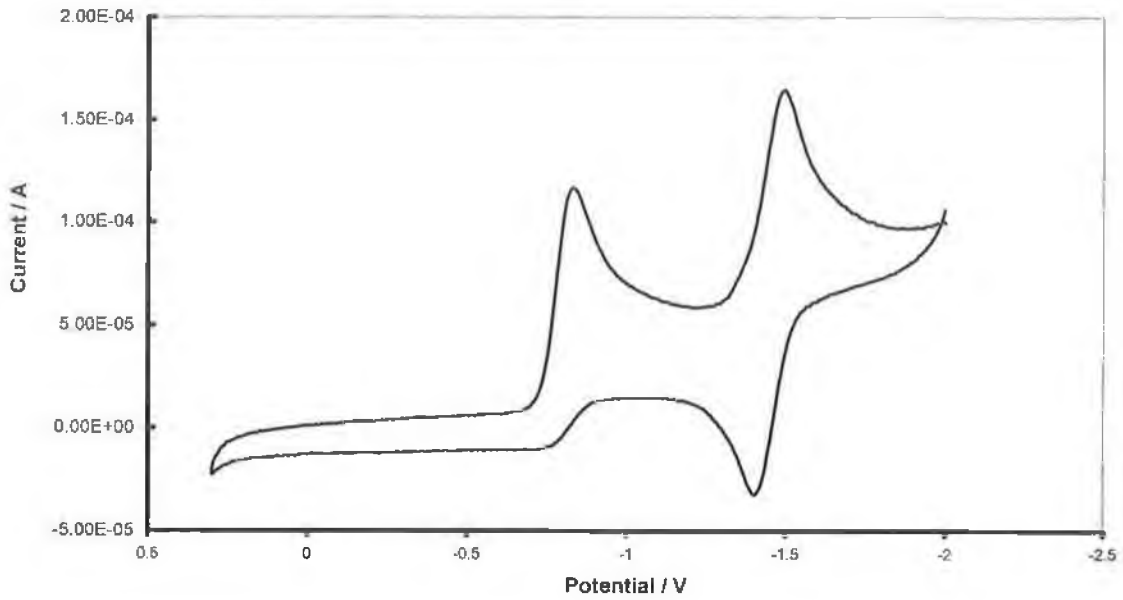

Figure 3.11. Cyclic voltammogram of (155), $v = 1.0$V/s.

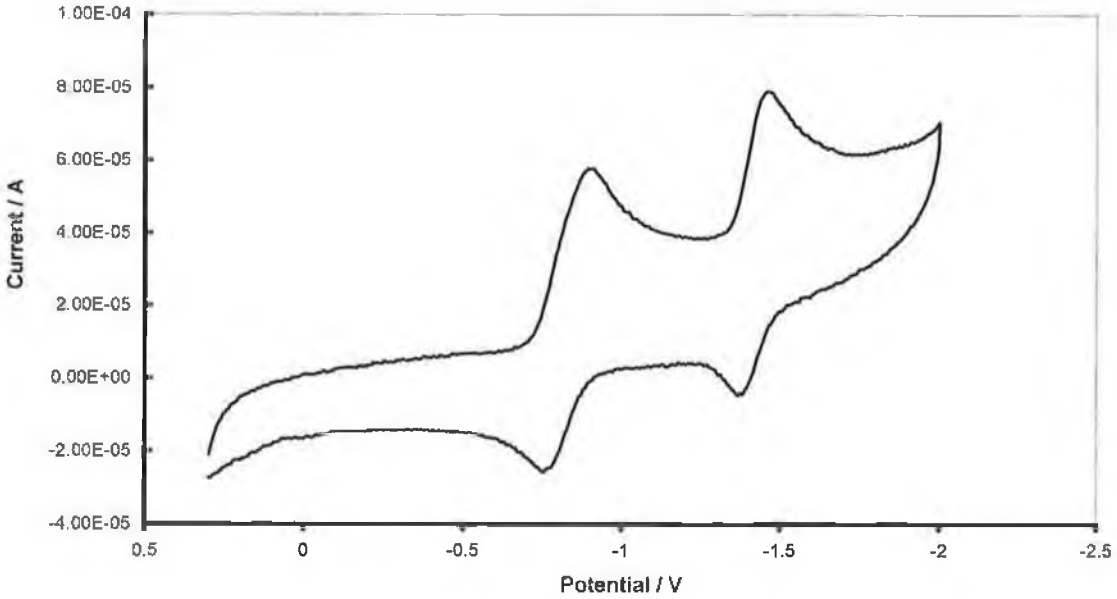

Figure 3.12. Cyclic voltammogram of (180), $v = 1.0$V/s.

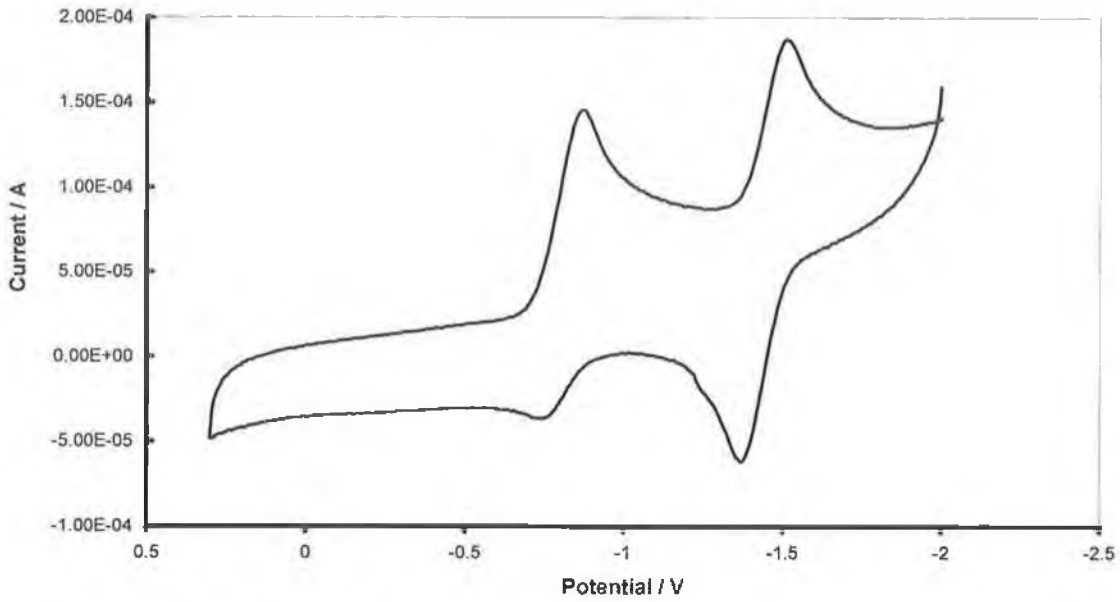

Figure 3.13. Cyclic voltammogram of (177), $v = 5.0$V/s.

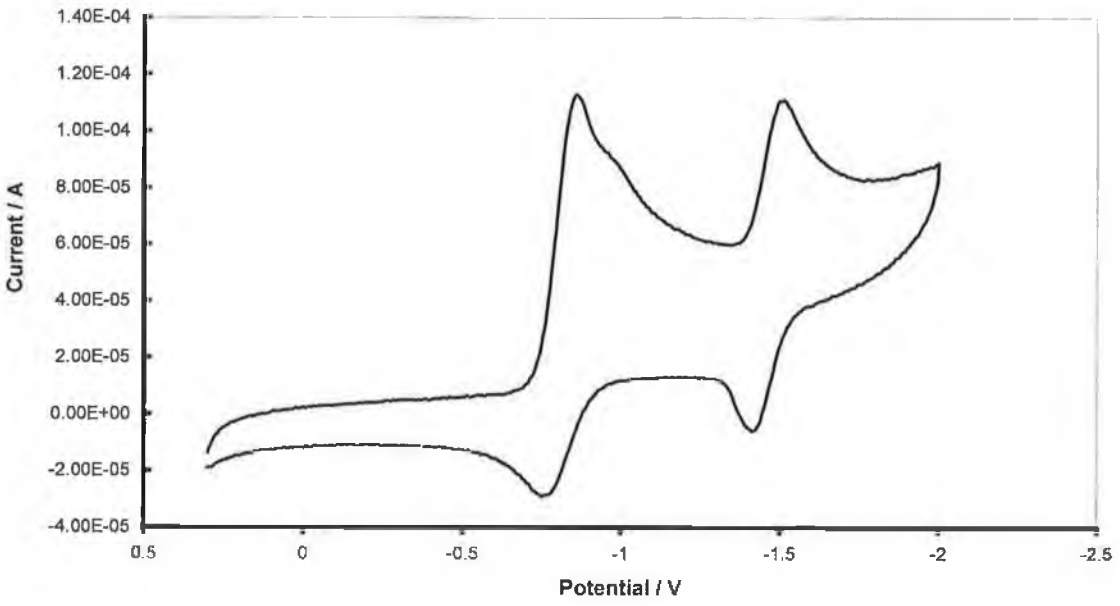

Figure 3.14. Cyclic voltammogram of (178), $v = 1.0$V/s.

Compound (155) underwent two reduction processes. The first reduction occurred at –0.85V and was irreversible. The second reduction, corresponding to the formation of the dianion occurred at –1.51V and was part of a quasi-reversible redox couple. The N-cinnamyl derivative (180) has two quasi-reversible redox couples at –0.92 and –1.48V respectively. Both (177) and (178) have two quasi-reversible one-electron redox couples at –0.89V and –1.54V for (177) and –0.88V and –1.52V for (178). The data is summarized in table 3.3.

Compound	Scan rate V/s	Ep_{a1} / V	Ep_{a2} / V	Ep_{c1} / V	Ep_{c2} / V	ΔE_1 / V	ΔE_2 / V
(NETO) (155)	1.0	-0.85	-1.51	-0.74	-1.39	0.11	0.12
(NCINO) (180)	1.0	-0.92	-1.48	-0.74	-1.35	0.18	0.13
(NPTO) (177)	5.0	-0.89	-1.54	-0.73	-1.35	0.16	0.19
(NDCO) (178)	1.0	-0.88	-1.52	-0.74	-1.39	0.14	0.13

Table 3.3 $\Delta E_1 = Ep_{a1} - Ep_{c1}$ and $\Delta E_2 = Ep_{a2} - Ep_{c2}$.

Replacement of a dicyanomethylene group with a carbonyl group appears to make the electrochemically generated dianion less reactive towards chemical reaction. Conversely the radical anion seems to be more susceptible to chemical reaction. Cyclic voltammetric analysis of the related compound (190) was carried out with slightly different results.[166]

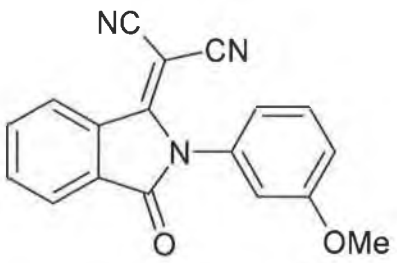

(190)

The reduction peak potentials for (190) were –0.92V and –1.43V, similar to the values obtained in this work. However the redox couple corresponding to the reduction of (190) to its radical anion and oxidation back to the neutral species was fully reversible while the reduction of the radical anion to the dianion had no significant oxidation peak.

3.3 Conclusion

Cyclic voltammetric analysis showed that all the compounds are reducible electrochemically. However none of the redox couples observed for any particular family of compounds were reversible. At best the neutral/radical anion couples for the N-alkyl derivatives of compound (127) and compounds (185) and (186) were quasi-reversible. The dianion of N-alkylated derivatives of compound (127) were unstable and could have reacted chemically with a species in solution to yield the radical anion. At faster scan rates a second quasi-reversible couple corresponding to radical anion/dianion was observed for (185) and (186).

Compounds (155) and (177) both had quasi-reversible redox couples corresponding to the radical anion/dianion couple. The reduction of the neutral compound to radical anion was 'more irreversible than quasi-reversible' for both compounds. (180) and (178) have two quasi-reversible redox couples.

Since no fully reversible couples were observed meant that calculation of the half wave potentials was impossible. However the observed reduction peak potentials show that all compounds analyzed are relatively poor electron acceptors. Benzo-TCNQ underwent two fully reversible reductions with half wave potentials of $E_{½}$ (1)= -0.30V and $E_{½}$(2)= -0.73V.

Chapter 4

Charge Transfer studies

4.1 Synthesis of Charge-Transfer Complexes

Compound (127) and its N-methyl derivative (128) have previously been shown[138] by Conway in these laboratories to form 1:1 C-T complexes with both TTF and TMDA.

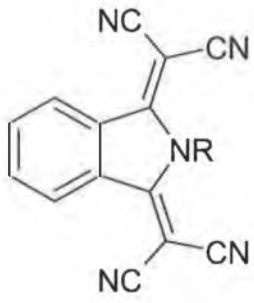

(127): R=H, (128): R=Me.

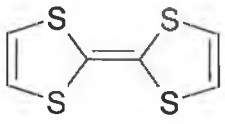

TTF

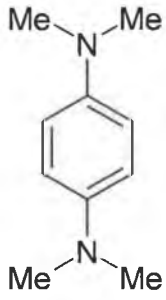

TMDA

X-ray crystallographic data obtained for the 1:1 C-T complex formed between (127) and TMDA showed a mixed stack arrangement. This means that at best the complex may be semi-conducting.

Synthetic trials were carried out first to see if solid complexes could be isolated from compounds synthesised as a result of the synthetic work reported in this thesis. If a solid complex was isolated further analysis was then carried out. The most informative analytical techniques are uv-vis and IR spectroscopy and X-ray diffractometry. The uv-vis spectrum of a particular complex can show new charge transfer bands that cannot be attributed to either parent compound. The cyano stretching frequency in the IR spectrum of a neutral acceptor is susceptible to movement towards a lower wavenumber when a C-T complex is formed with an electron donor. This is due to the coupling of conduction electrons and intramolecular phonons in the complex.[167] A large shift in frequency indicates large charge transfer. X-ray diffractometry provides information about the stacking pattern of the complex and ratio of components within the complex. ^{1}H-NMR spectroscopy can also give information about the ratio of donor to acceptor.

Synthesis of C-T complexes with TTF as donor

Solid C-T complexes were isolated when concentrated solutions of (140), (141), (168) and (169) were mixed with concentrated solutions of TTF.

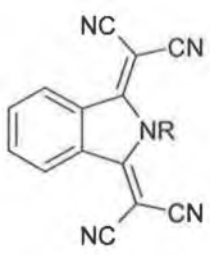

(140): R=Et, (141): R=benzyl

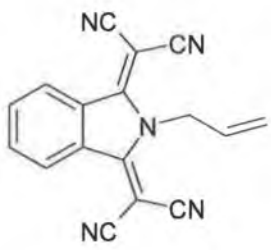

(168)

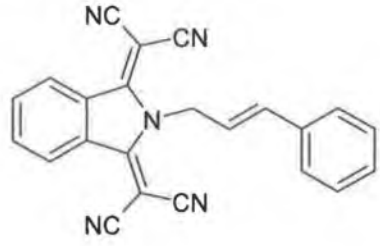

(169)

Mixing equimolar amounts of (140) and TTF in acetonitrile led to the immediate formation of a green solution. Removal of the solvent yielded a blackish/green solid which was recrystallised from acetonitrile to yield dark green needles, mp 177-179°C. TLC analysis of this solid showed two spots, corresponding to the individual components. The cyano IR peak was observed at 2217cm^{-1} compared with 2219cm^{-1} for compound (140) on its own.

A slightly different procedure was employed when (141) or (168) were mixed with TTF, solid electron acceptor being added to a concentrated solution of TTF in acetonitrile. The mixture was heated under reflux until all of the solid had dissolved and on cooling green needles were deposited. The C-T complex formed by (141) and TTF had mp 207-210°C. The ^{1}H-NMR spectrum displayed a mixture of (141) and TTF (δH: $CDCl_3$, 6.28ppm, singlet) as expected and with integration of the signals showing that the ratio of donor to acceptor was 1:1. The cyano stretch in the IR spectrum was found at 2219cm^{-1} compared with 2221cm^{-1} for neutral (141). The C-T complex of (168)-TTF was isolated as dark green needles, mp 169-172°C. The ^{1}H-NMR spectrum confirmed a complex with 1:1 ratio. The cyano stretch appeared at 2218cm^{-1} compared to 2222cm^{-1} for compound (168). The crystals obtained were of sufficient quality to allow analysis by X-ray diffraction, see figure 4.1. The relevant bond lengths and bond angles are summarised in table 4.1.

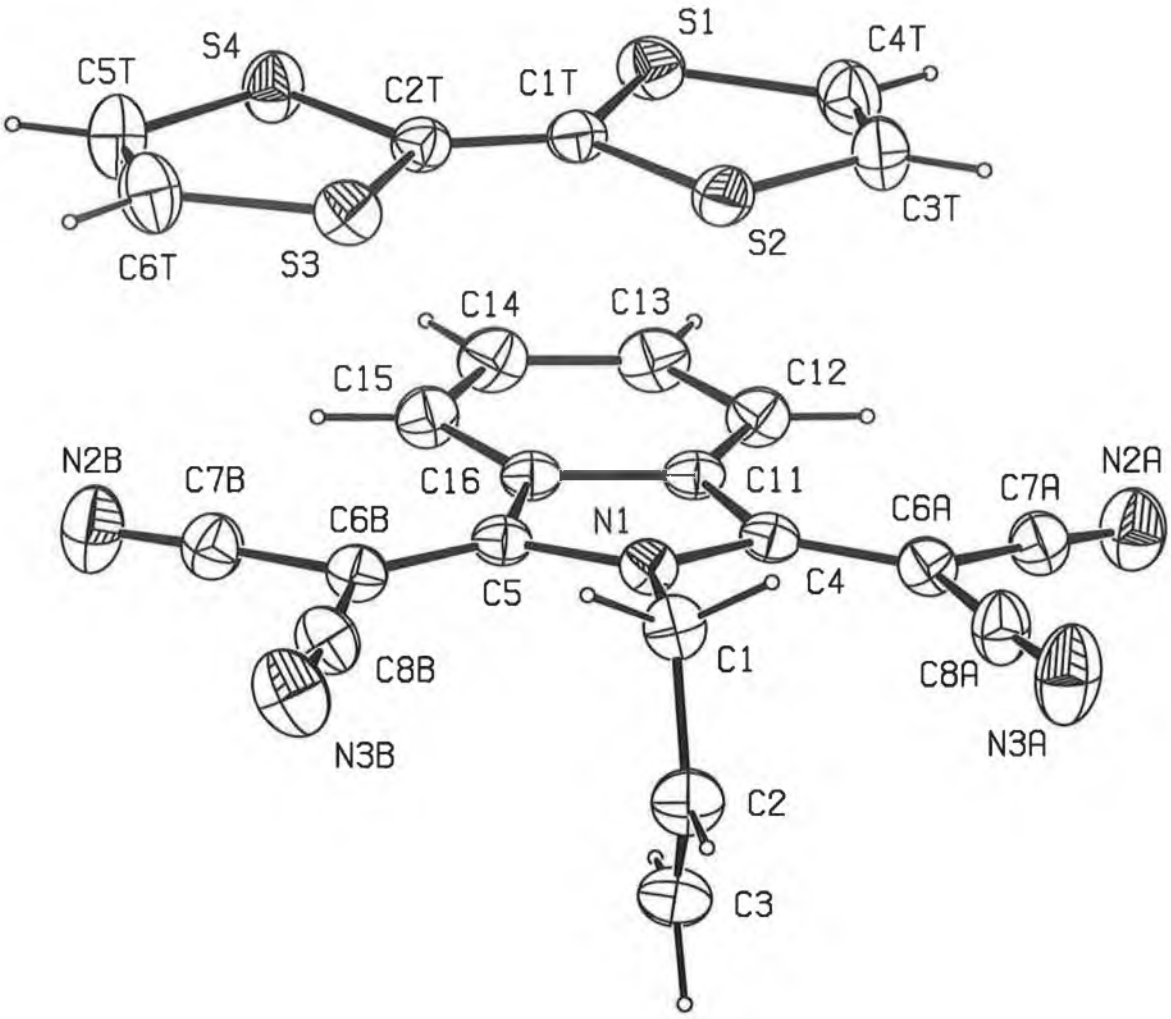

Figure 4.1 . X-ray crystal structure of C-T-complex formed between (168) and TTF.

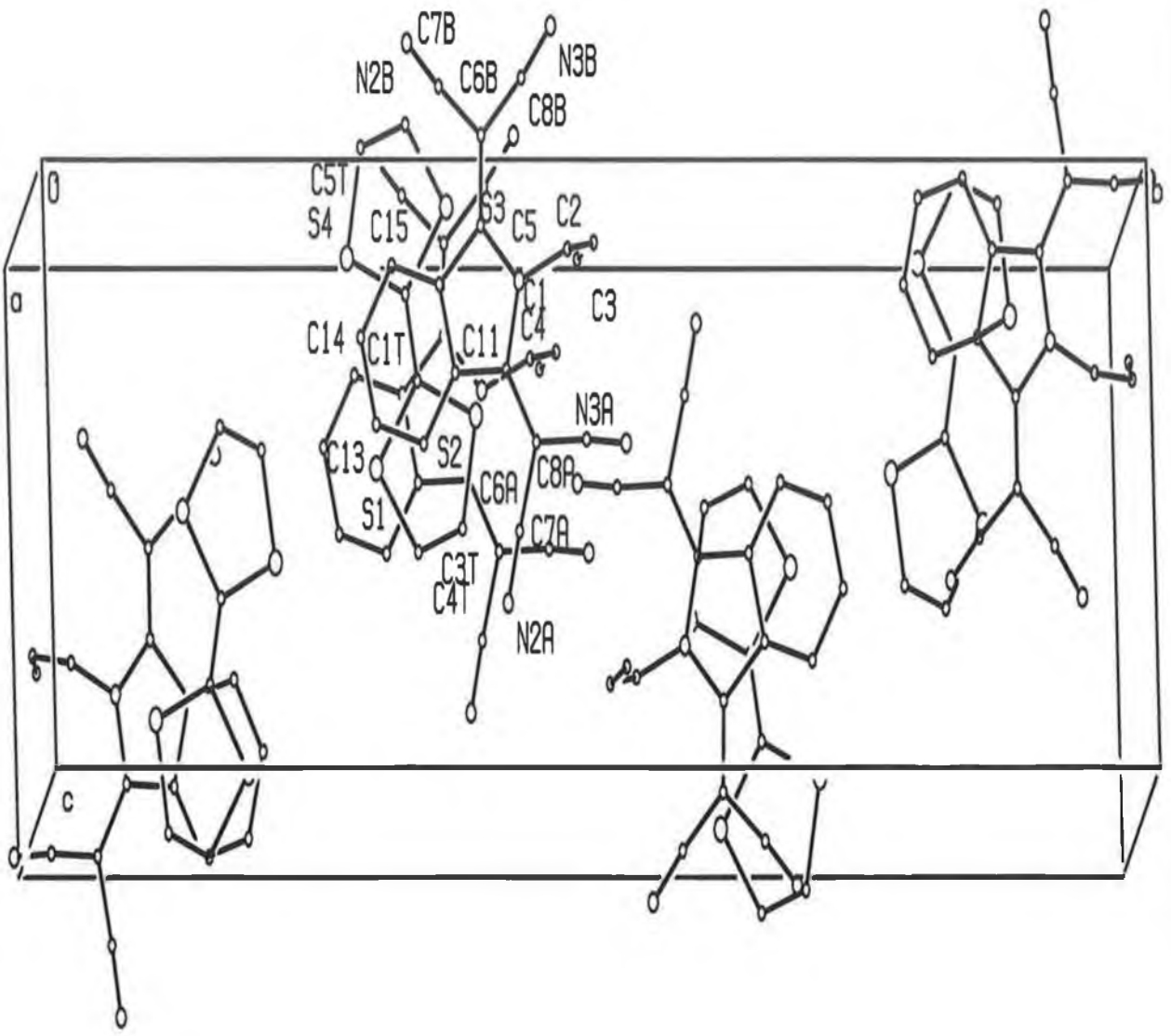

Figure 4.2. An alternative view of C-T-complex formed between (168) and TTF

The complex formed between (169) and TTF crystallised in mixed stacks. The stacks are linked by two weak hydrogen bonds formed between TTF hydrogens and nearest cyano nitrogens of (169), the crystal data is contained in Appendix 3.

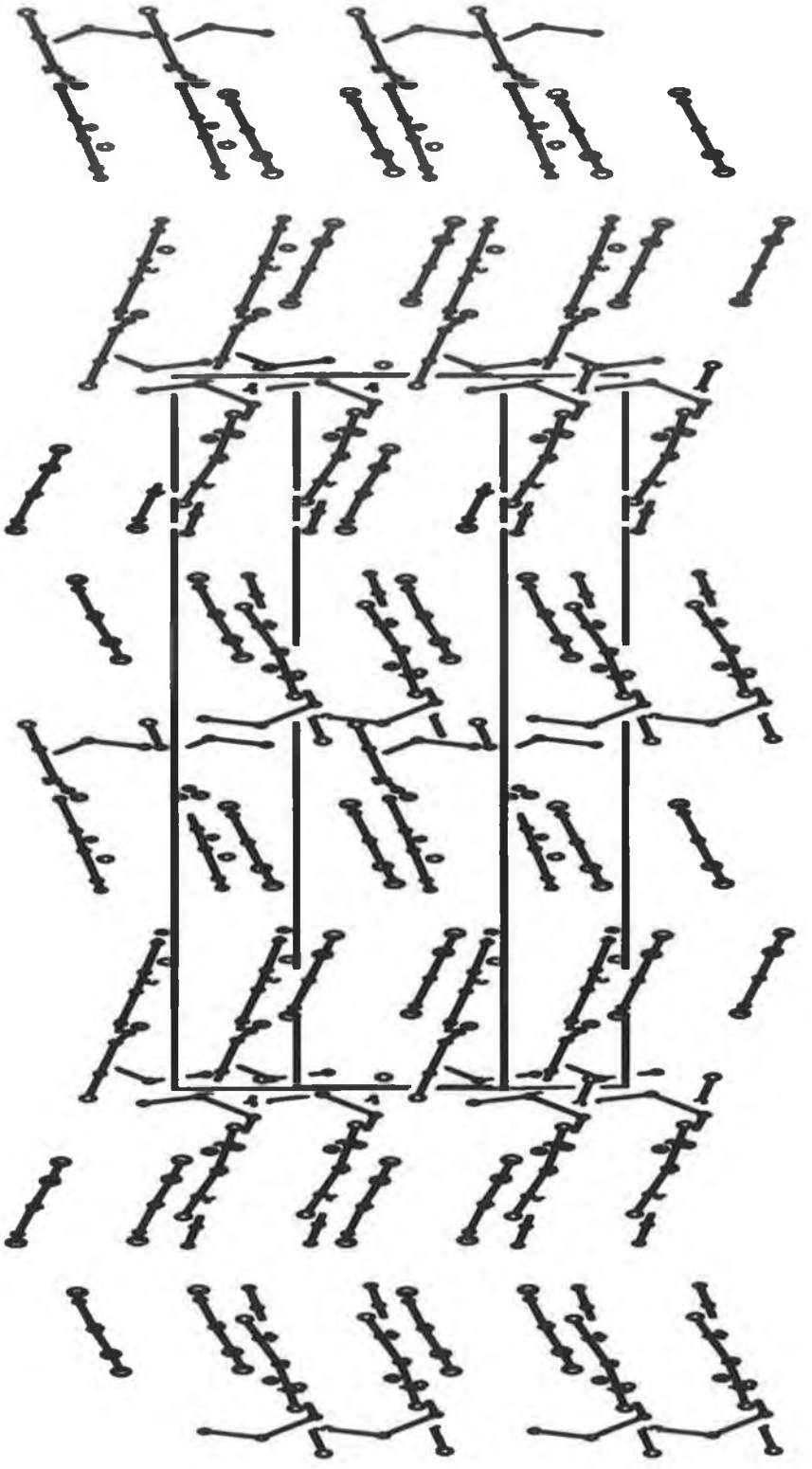

Figure 4.3. An alternative view of C-T-complex formed between (168) and TTF

Equimolar amounts of (169) and TTF were mixed in dichloromethane at room temperature. The solution was a green colour and removal of the solvent yielded a green solid. This solid was recrystallised from acetonitrile to give light green very fine needles, mp 146-148°C. The cyano stretch appeared at 2219cm^{-1} as opposed to 2221cm^{-1} for compound (169) on its own. The ^{1}H-NMR spectrum confirmed a 1:1 complex.

TTF also formed C-T complexes with both hybrid electron acceptors (185) and (186). The C-T complexes were synthesised when equimolar amounts of each electron acceptor were mixed in dichloromethane at room temperature. In both instances the solution was very dark green. Removal of the solvent yielded dark green shiny powders in both cases. Attempts to recrystallise these shiny powders from various solvent systems failed. The C-T complex between (185) and TTF had mp 105-107°C. From the ^{1}H-NMR spectrum the complex was found to be a 1:1 complex. Similarly a 1:1 complex formed by (186) and TTF was isolated as a dark green powder, mp 64-66°C.

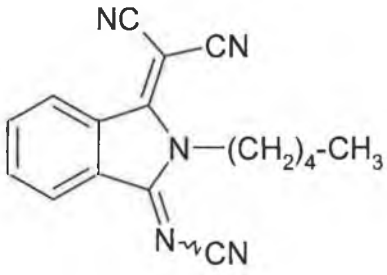

(185)

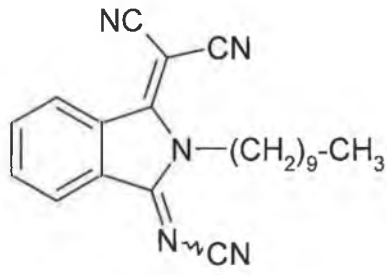

(186)

The cyano stretches in the IR spectrum of the complex (185)-TTF are 2222 and 2186cm^{-1} compared with 2224 and 2192cm^{-1} for (185) on its own. The cyano stretches in (186)-TTF are 2222 and 2192cm^{-1} as opposed to 2226 and 2193cm^{-1} for (186) alone.

Attempts were made to synthesise C-T complexes between TTF and numerous N-alkyl-3-(dicyanomethylene)-1-isoindolinone derivatives, however no C-T complexes were isolated. The solid material isolated after concentrated solutions of donor and acceptor had been mixed was simply a mixture of the two components. This can be determined by simple observation.

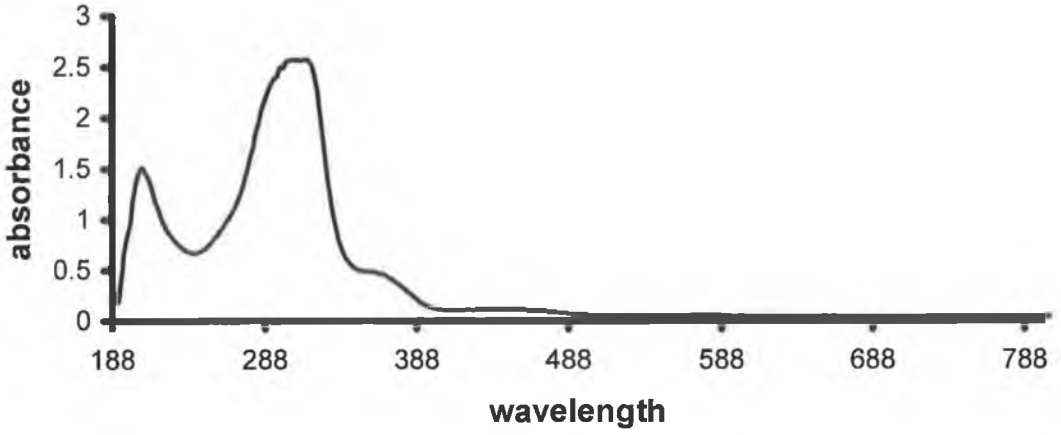

Figure 4.4. Uv-vis spectrum of TTF in acetonitrile.

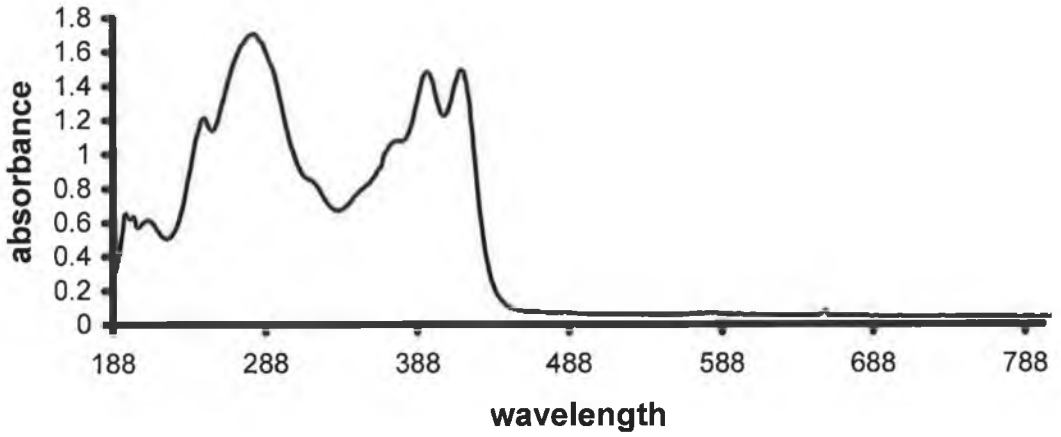

Figure 4.5. Uv-vis spectrum of (140)-(TTF) in acetonitrile.

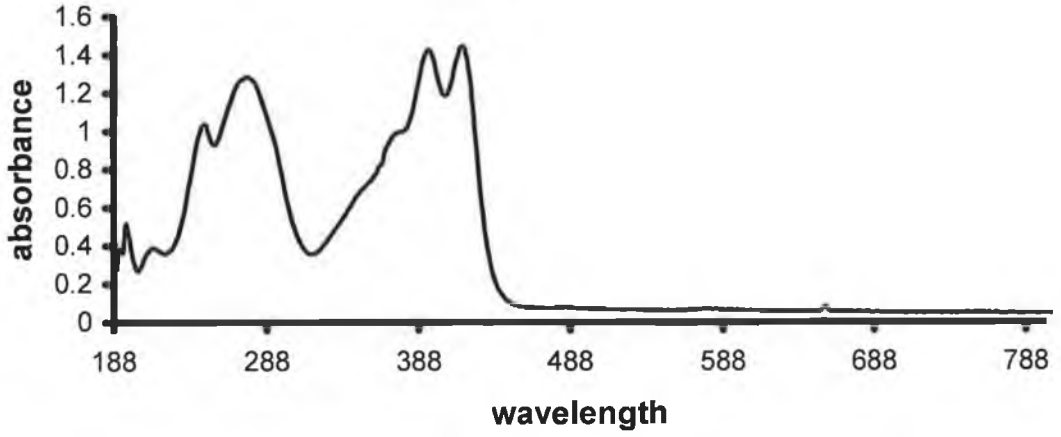

Figure 4.6. Uv-vis spectrum (140) in acetonitrile.

Whilst uv-vis spectroscopy can be very useful in the study of C-T phenomena, it is often very difficult to see a distinctive C-T band in solution. When a solid C-T complex is dissolved in a solvent the intensity of the absorption bands associated with the individual components commonly dwarf the C-T band absorption. The absorption spectra of TTF and (140) are shown in figure 4.4 and figure 4.5 respectively. Figure 4.6 shows the spectrum of an equimolar mixture of TTF and (140). No new C-T band is discernible though solutions of the individual components are orange/yellow whereas solutions containing both are green. Similar effects were observed for the other acceptor/TTF solutions.

Further uv-vis spectra were obtained for more concentrated solutions of the particular C-T complexes in question. Increasing the concentrations of both components should enhance the possibility of seeing any C-T band. However on doing so no obvious new bands were visible for the various acceptor/TTF pairs.

Since the absorption due to the electron acceptor dominates the long wavelength region of the spectrum addition of increasing amounts of donor should increase the likelihood of seeing the C-T band and avoid increasing the size of the absorption associated with the acceptor. The effect of adding increasing amounts of TTF to a solution of (140) in acetonitrile is shown in figure 4.7. Similar effects were seen for the other acceptor/TTF pairs.

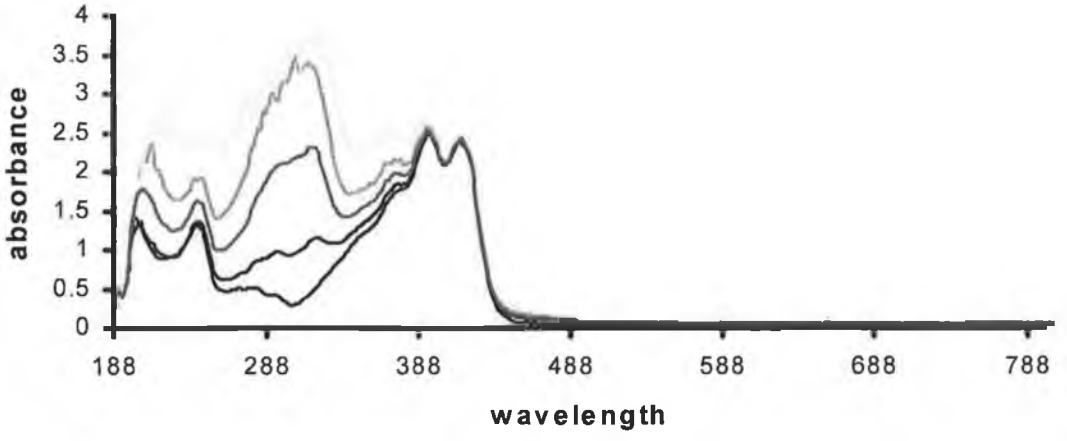

Figure 4.7. Uv-vis spectrum of (140) with increasing amounts of TTF.

From these experiments there appears to be a weak absorption band centred around 450-460nm. The fact that the absorption appears at almost identical wavelengths irrespective of which acceptor is used should not be too alarming since the solid C-T complexes are all very dark green in colour. However there is also a possibility that this absorption could be due to TTF itself. Uv-vis spectra were recorded for increasingly concentrated solutions of TTF, figure 4.8, in order to see whether the weak absorption band displayed in the previous experiments could be due to TTF itself and it would seem that a concentrated solution of TTF produces a band similar to the one depicted in figure 4.7. Therefore it would be inappropriate to assign this band as a charge transfer band.

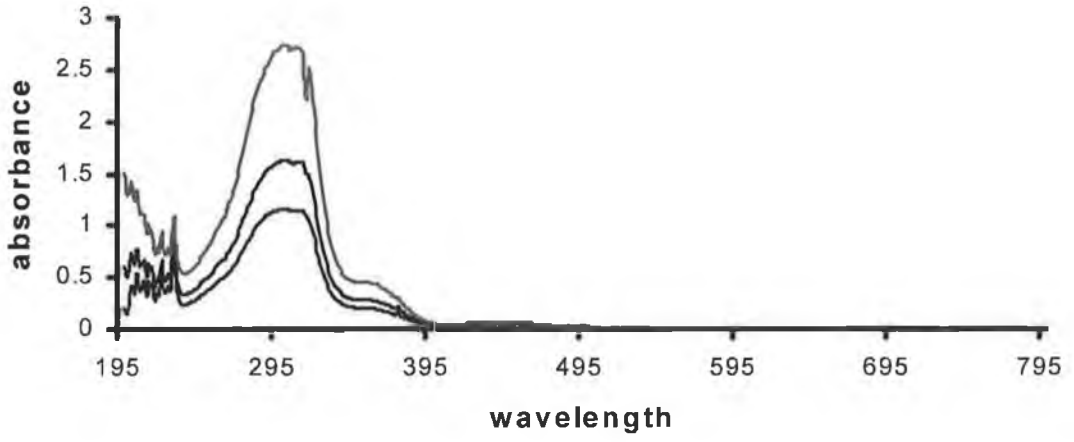

Figure 4.8. Uv-vis spectrum of increasingly concentrated TTF solutions.

Recording uv-vis spectra of C-T complexes in solution make observation of very weak absorptions due to partial charge transfer very difficult since in solution the absorption intensities due to both acceptor and donor are normally much larger than any C-T band. Recording uv-vis spectra of the solid complex should increase the likelihood of seeing any C-T band. However attempts to apply this technique to the C-T complexes isolated, resulted in poorly defined spectra which did not yield any useful information.

Attempts to synthesise solid C-T complexes with other donors, namely TMDA and BEDT-TTF, proved unsuccessful. Uv-vis analysis of various solutions containing

prospective acceptors and varying amounts of TMDA failed to display any obvious visible C-T absorption band.

4.2 Conclusion

The electrochemical data showed that a number of potential electron acceptors had been synthesised. Isolation of solid C-T complexes formed between TTF and various compounds (140), (141), (168), (169), (185) and (186) confirmed that some of these compounds behaved as the electron acceptor component for C-T complexes. The difficulty encountered trying to identify a C-T band in the uv spectrum of various complexes would seem to suggest that only a small amount of charge transfer actually took place. The small shift of the cyano stretch in the IR spectrum of neutral acceptor when compared to the cyano stretch in the respective C-T complexes again suggests small charge transfer.

Previously it was stated that the ground state of a C-T complex could be represented as the combination of a 'no-bond' structure and a 'dative bond' structure (see general introduction, p 4).

$$\Psi_N(D, A) = a\Psi_N(D, A) + b\Psi_N(D^+, A^-). \qquad \text{Equation 2.}$$

The 'no-bond' structure describes dipole-dipole interactions and other intermolecular interactions while the 'dative bond' structure is concerned with the degree of charge transfer. From the cyclic voltammetric data it is clear that the compounds synthesised are weak electron acceptors. The difference between the first oxidation potential of the donor TTF and the first reduction potential of any acceptor that formed a solid complex is large > 1.0V. This large discrepancy prohibits the formation of highly conductive complexes. Therefore the dominant structure in equation 2 for the complexes formed between acceptors in question and TTF is the 'no-bond' structure. This implies that the binding force holding these complexes together is due to dipole-dipole interactions.

Since a large amount of (but not total) charge transfer is a prerequisite for conductive materials to form, an improvement in the electron accepting ability of this family of compounds would be necessary. The poor accepting ability of the compounds in question is mainly due to the fused benzene ring in the isoindoline skeleton. When compounds of type (a) or type (b) have to accommodate an extra electron the aromaticity of the benzene ring is disrupted to make a less stabilised aromatic $4n+2\pi$ delocalised system.

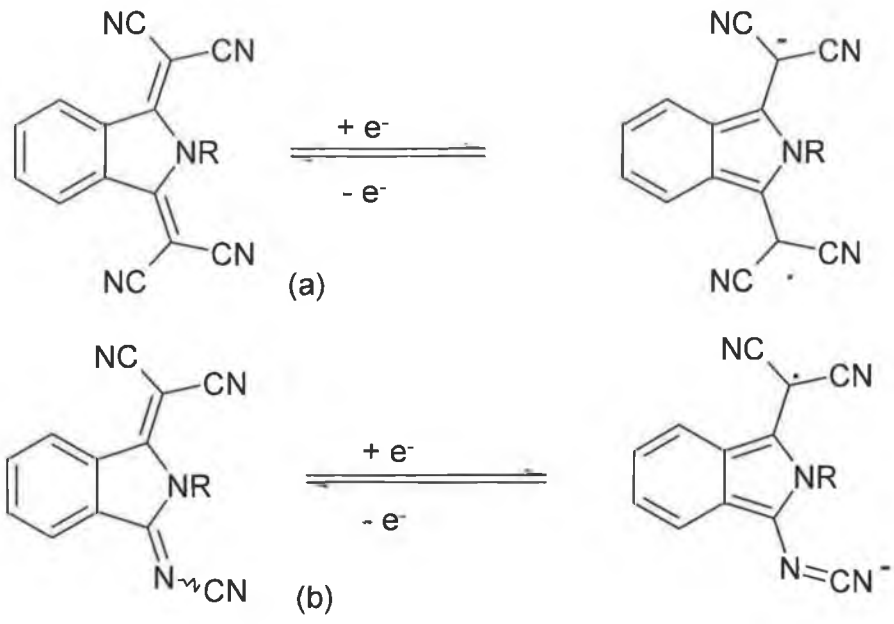

The presence of electron donating alkyl groups attached to the pyrrole nitrogen increase the electron density in the isoindoline skeleton and makes the accommodation of extra charge more difficult.

The electron accepting ability of these compounds could possibly be improved by the substitution of electron withdrawing groups such as halogens on the benzene ring. Using dichloro and tetrachloro dicyanobenzene as starting materials and applying similar procedures to those used during the course of this work could provide synthetic access to acceptors of the type shown.

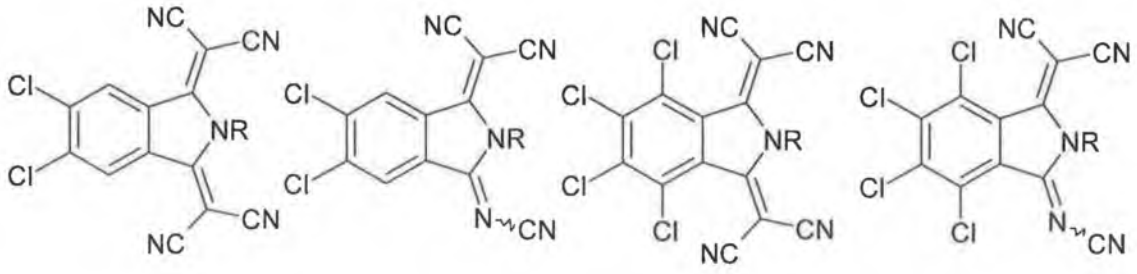

Compounds containing a pyrazine ring have been synthesised[168] and the presence of electronegative nitrogens made these compounds better acceptors than their isoindoline analogues.

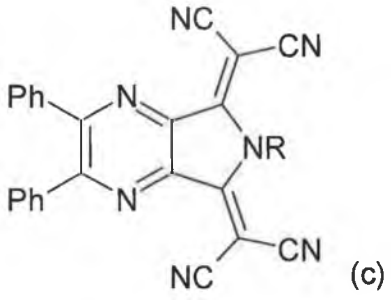

(c)

R=H
R=Me
R=Et
R=Bz

Electrochemical analysis of these compounds has shown first reduction waves at approximately –0.35V for the alkylated compounds. This is an improvement of about 0.50V from the values obtained for the compounds described in this work.

Further improvement would be necessary in order to make conductive C-T complexes with segregated stacks. The complex formed between TCNQ and TTF is highly conductive. TCNQ has a first reduction potential at 0.08V while TTF has a first oxidation potential at 0.32V under similar experimental conditions. The difference in potential is 0.24V, which is generally accepted as being ideal for partial electron transfer and segregrated stack formation.

Replacement of the peripheral phenyl groups with halogen atoms should further enhance the electron accepting ability of these compounds. Compound (d) has been synthesised via the method described in scheme 59.

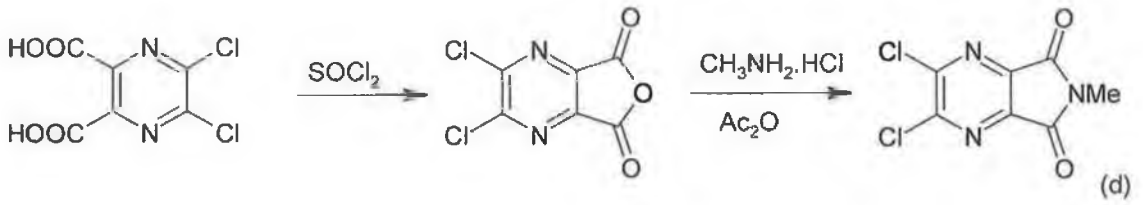

Scheme 59

Variation of the alkyl group in the second step should provide a range of N-alkylated derivatives. Attempts could then be made to effect condensation at the oxygen of the carbonyl group using $TiCl_4$/ $CH_2(CN)_2$/ pyridine to generate the tetra-cyano derivative or $TiCl_4$/ BTC to generate the di-cyanoimino derivative, scheme 60.

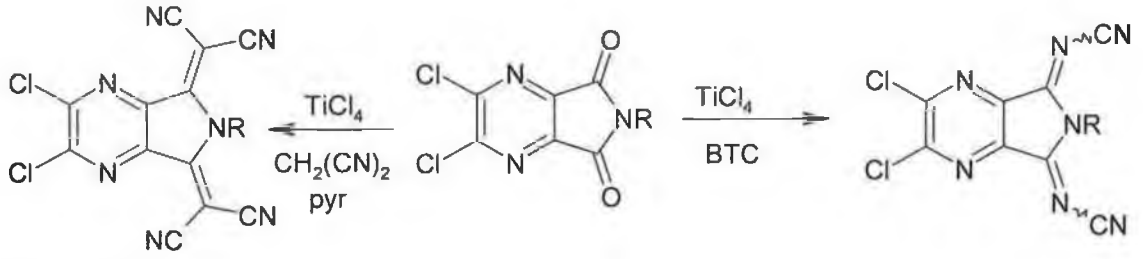

Scheme 60

Chapter 5
Experimental Section

NMR data was obtained using a Bruker Avance (400MHz) instrument. The chemical shifts were recorded relative to TMS. The spectra were converted from FID profiles using XWIN-NMR software. IR data was obtained using Nicolet Impact 410 FTIR Perkin-Elmer system 2000 FTIR. All spectra were recorded as KBr discs. Melting points were determined using a Griffin-Melting point apparatus and were uncorrected. UV-vis spectra were recorded with Hewlett-Packard 8452A photodiode array spectrometer using aquartz cell of 1cm path length. The X-ray data was collected using a kappa-CCD-diffractometer and a Bruker P4 diffractometer.

TLC plates were silica gel TLC cards 0.2mm layer thickness purchased from Sigma-Aldrich. All chromatography was carried out with silica gel 60 purchased from Sigma-Aldrich. THF was dried in a still containing sodium/benzophenone.

Synthesis of 2-methyl-3-methylimino-2,3-dihydroisoindol-1-one (142)

Phthalonitrile (20.00g, 156.0mmol), ethanol (80cm^3) and methylamine (40cm^3, 40% aqueous solution, 466.0mmol) were heated together under reflux for 24 hours. The resulting orange solution was evaporated to dryness under reduced pressure and the off-white solid was recrystallised from ethyl acetate to yield 2-methyl-3-methylimino-2,3-dihydroisoindol-1-one as fine white needles (142), (16.75g , 61%), mp 136-138°C (lit.[144] 138.5°C). $\nu_{max.}$: 3058, 2866, 1720, 1663, 1474, 1429, 1386, 1307, 1164, 1051, 1009, 784, 699 and 652cm^{-1}. $\lambda_{max.}$: CH_3CN: 554.5 (ε=2060), 530.0 (21464), 459.0 (2489), 360.5 (2919), 291.0 (7354.9), 249.0 (17228.3), 241.0 (16512.8) and 216.5nm (41153). δH: $CDCl_3$: 7.96 (m, 1H, aromatic), 7.87 (m, 1H, aromatic), 7.64-7.60 (m, 2H, aromatic), 3.69 (s, 3H) and 3.15ppm (s, 3H). δC: $CDCl_3$: 167.6 (**C**=O), 152.9 (**C**=N), 133.0, 132.6, 131.4, 129.8, 125.6, 123.4 (aromatic), 37.8 and 24.9ppm (N-methyl).

Found C: 68.59%, H: 5.88%, N: 15.91%. $C_{10}H_{10}N_2O$ requires C: 68.95%, H: 5.79%, N: 16.08% and O: 9.18%.

Hydrolysis of 2-methyl-3-methylimino-2,3-dihydroisoindol-1-one (142)

A mixture of 2-methyl-3-methylimino-2,3-dihydroisoindol-1-one (142) (0.30g, 1.7mmol) and 2M HCl (5cm^3) was heated to reflux for 5 minutes. On cooling a white solid precipitated. This compound was N-methylphthalimide (78), (0.20g, 72%) mp 130-132°C, (lit. 129-132°C). The IR spectrum obtained for this compound was identical to the IR spectrum of an authentic sample of N-methylphthalimide. δH: $CDCl_3$: 7.83-7.80 (m, 2H aromatic), 7.70-7.67 (m, 2H aromatic) and 3.19ppm (s, 3H). δC: $CDCl_3$: 168.5 (**C**=O), 133.8, 132.2, 123.1 (aromatic) and 23.9ppm (N-methyl).

Synthesis of 1,3-diethyliminoisoindoline (138)

Phthalonitrile (10.00g, 78.0mmol) in ethanol (40cm^3) containing ethylamine (20cm^3, 307.0mmol)* were heated under reflux for 36 hours. The solvent was then removed under reduced pressure. The residue was then placed in the freezer for 48

hours. The residue was washed with light petroleum (bp 60-80°C) (2 x 20cm^3). The residue was then washed with ethyl acetate (2 x 10cm^3) and filtered. The remaining cream coloured solid was washed again with ethyl acetate (15cm^3) and once with diethyl ether (15cm^3). The remaining off-white solid was 1,2-diethyliminoisoindoline (138), (5.64g, 36%) mp 158-160°C, (lit.[143] 158°C). λ_{max}: CH_3CN: 261.5 (ε=16610) and 223.0nm (33953). δH: $CDCl_3$: 7.70 (m, 2H aromatic), 7.34-7.32 (m, 2H aromatic), 3.84 (q, J=7.0Hz, 4H) and 1.32ppm (t, J=7.0Hz, 6H). δC: $CDCl_3$: 166.7 (**C**=N), 137.8, 129.9, 120.3 (aromatic), 41.5 and 15.4ppm (N-ethyl).

Found C: 70.73%, H: 7.43, N: 20.23%. $C_{12}H_{15}N_3$ requires C: 71.6%, H: 7.5% and N: 20.88%.

*NB: Ethylamine gas was distilled from 70% aqueous solution. The receiving vessel was cooled in order to condense gas to a liquid. The volume of liquid used was determined using a cooled graduated cylinder.

Hydrolysis of 1,3-diethyliminoisoindoline (138)

1,3-Diethyliminoisoindoline (138) (0.30g, 1.5mmol) was added to 2M HCl (5cm^3). The mixture was then heated to boiling point. On cooling a white solid was isolated. This solid was phthalimide (0.17g, 78%) mp 233-236°C, (lit. 233-235°C). The IR spectrum obtained for this compound was identical to the IR spectrum of an authentic sample of phthalimide δH: $CDCl_3$: 7.87-7.83 (m, 2H, aromatic) and 7.76-7.72ppm (m, 2H aromatic).

Synthesis of 1,3-dibenzyliminoisoindoline (139)

Sodium metal (0.01g) was carefully added to methanol (15cm^3). This solution was then slowly added to a solution of phthalonitrile (2.50g, 19.5mmol) and benzylamine (4.28g, 40.0mmol) in methanol (20cm^3). The reaction mixture was then heated under reflux for 5 hours. The solvent was evaporated off to yield a green oil. Addition of boiling toluene to this oil yielded a small amount of white solid, which was isolated by vacuum filtration. Further white solid was isolated from the cold

toluene filtrate. The batches were combined and washed with diethyl ether and recrystallised from toluene, yielding 1,3-dibenzyliminoisoindoline (139), (4.20g, 66%) mp 160-162°C, (lit.[143] 160°C). $\nu_{max.}$: 2933, 2854, 1651, 1545, 1210, 1132, 1033, 954, 869, 790 and 705cm^{-1}. $\lambda_{max.}$: CH_3CN: 265.5 (ε=18768) and 223.0nm (32256). δH: $CDCl_3$: 7.69-7.67 (m, 2H, aromatic), 7.50-7.47 (m, 2H, aromatic), 7.42 (m, 4H, aromatic), 7.34-7.30 (m, 4H, aromatic), 7.26-7.22 (m, aromatic) and 4.92ppm (s, 4H). δC: $CDCl_3$: 171.7 (**C**=N), 127.9, 127.6, 127.6, 127.3, 126.7, 125.6 and 120.5 (aromatic) and 53.4ppm ((N-**C**H_2-Ph).
Found C: 80.76%, H: 5.96%, N: 12.99%. $C_{24}H_{23}N_3$ requires C: 81.20%, H: 5.89% and N: 12.97%.

Hydrolysis 1,3-dibenzyliminoisoindoline (139)

1,3-Dibenzyliminoisoindoline (139) (0.30g, 0.9mmol) was heated under reflux with ethanol (2.5cm^3) and 50% aqueous HCl (2.5cm^3) for 30 minutes. Addition of a small amount of water and cooling in ice yielded phthalimide as a white solid, (0.10g, 74%) mp 234-236°C, (lit.[72] 233-235°C). The IR spectrum obtained for this compound was identical to the IR spectrum of an authentic sample of phthalimide.

Synthesis of 1,3-diiminoisoindoline (130)

Light petroleum (bp 40-60°C) (10cm^3) was added to sodium hydride (60% dispersion in oil, 0.72g). The suspension was swirled and the supernatant liquid removed with a Pasteur pipette. Methanol (10cm^3) was then added and the resultant sodium methoxide solution was added to phthalonitrile (5.00g, 39.0mmol) in methanol (110cm^3). Ammonia was bubbled through the stirred solution for one hour. The reaction was then heated under reflux for 3 hours. Removal of the solvent yielded a green oil. Scratching with a glass rod yielded 1,3-diiminoisoindoline (130) as a yellow solid, (1.70g, 30%) mp 194-196°C, (lit.[139] 194-195°C). Comparison of its IR spectrum with a known sample provided evidence for purported structure.

Synthesis of 2-methyl-3-methylimino-2,3-dihydroisoindol-1-one (142) from 1,3-diiminoisoindoline (130)

1,3-Diiminoisoindoline (130) (1.00g, 6.9mmol), 40% aqueous methylamine ($2cm^3$) in ethanol ($10cm^3$) were heated together under reflux for 16 hours. When the solvent was removed a greenish/white solid was isolated. This solid was recrystallised twice from ethyl acetate to yield (142) as white needles, (0.75g, 63%), mp 136-138°C, (lit.[69] 138.5°C). IR, ^1H and ^{13}C-NMR spectra were identical to those obtained in the initial synthesis of 2-methyl-3-methylimino-2,3-dihydroisoindol-1-one (142).

Hydrolysis of 2-methyl-3-methylimino-2,3-dihydroisoindol-1-one (142)

Using the same reaction conditions as described in the previous hydrolysis of compound (142) yielded N-methylphthalimide, identified by mp, IR and NMR.

Synthesis of 3-phenylimino-1-iminoisoindoline (134)

Phthalonitrile (20.00g, 156.0mmol) and aniline (14.60g, 180.0mmol) were added to methanol ($350cm^3$). Sodium metal (0.68g, 29.6mmol) was dissolved in methanol ($40cm^3$). This solution was then added to the phthalonitrile/aniline mixture and heated under reflux for 2.5 hours. The mixture was filtered hot. Removal of the solvent under reduced pressure yielded 3-phenylimino-1-iminoisoindoline (134) as yellow powder, (22.92g, 66%) mp 200-202°C, (lit.[138] 202°C). δH: DMSO: 8.55 (brs, 2NH), 7.87 (m, 1H, aromatic), 7.81 (m, 1H, aromatic), 7.57 (m, 2H, aromatic), 7.27 (m, 2H, aromatic), 7.20 (m, 2H, aromatic) and 7.01ppm (m, 1H, aromatic).

Synthesis of 2-methyl-3-phenylimino-2,3-dihydroisoindol-1-one (152)

2-Methyl-3-methylimino-2,3-dihydroisoindol-1-one (142) (3.00g, 17.2mmol), aniline ($12cm^3$, 150.0mmol) were added to diethylene glycol diethyl ether ($30cm^3$)

and heated under reflux for 5 hours. The solvent was then removed under reduced pressure. The residual solid was washed with light petroleum (bp 60-80°C) (2 x $10cm^3$). TLC analysis of this solid showed two spots. These two components were separated by column chromatography using ethyl acetate/light petroleum (bp 40-60°C)[20:80] mixture as mobile phase. When the faster moving yellow band had been isolated, the second slower band was flushed off the column with methanol. The slower moving fraction was found to be starting material. While the first eluting fraction was found to be 2-methyl-3-phenylimino-2,3-dihydroisoindol-1-one (152), (1.30g, 32%) mp 144-146°C. ν_{max}: 3068, 3011, 2961, 1737, 1680, 1594, 1445, 1388, 1310, 1196, 1082, 1040, 991 and $783cm^{-1}$. $\lambda_{max.}$: CH_3CN: 549.0 (ε=1652), 339.5 (3520), 250.5 (22341.3) and 213.5nm (38389). δH: $CDCl_3$: 7.84 (d, J=7.8Hz, 1H aromatic), 7.52 (m, 1H aromatic), 7.39 (m, 2H aromatic), 7.28 (t, J=7.9Hz, 1H aromatic), 7.20 (t, J=7.9Hz, 1H aromatic), 6.98 (d, J=7.8Hz, 2H aromatic), 6.60 (d, J=7.9Hz, 1H aromatic) and 3.36ppm (s, 3H). δC: $CDCl_3$: 167.8 (**C**=O), 151.4 (**C**=N), 148.7, 133.8, 132.7, 132.4, 131.7, 129.5, 129.3, 125.3, 124.1, 123.2 and 119.8 (aromatic) and 25.2ppm (N-methyl).

Found: C: 76.20%, H: 5.22%, N: 11.82%. $C_{15}H_{12}N_2O$ requires C: 76.25%, H: 5.12%, N: 11.86%.

Hydrolysis 2-methyl-3-phenylimino-2,3-dihydroisoindol-1-one (152)

2-Methyl-3-phenylimino-2,3-dihydroisoindol-1-one (152) (0.20g, 0.8mmol) in ethanol ($4cm^3$) was warmed on a steam bath with 2M HCl ($8cm^3$) for ten minutes. On cooling N-methylphthalimide isolated as colourless needles, identified by comparison (mp, IR, NMR) with an authentic sample.

Attempted synthesis of 2-ethyl-1,3-diphenyliminoisoindoline (150)

1,3-Diethyliminoisoindoline (138) (1.00g, 5.0mmol), aniline ($4cm^3$, 50.0mmol) were added to diethylene glycol diethyl ether ($10cm^3$). The reaction

mixture was then heated under reflux for 5 hours. The solvent was removed under vacuum. Residual gum was chromatographed using ethyl acetate/Light petroleum (bp 40-60°C) [20:80] mixture. Chromatography did not resolve the mixture.

Attempted synthesis of 2-benzyl-1,3-diphenyliminoisoindoline (151)

1,3-dibenzyliminoisoindoline (139) (0.50g, 2.1mmol), aniline (0.85g, 10.4mmol) were added to diethylene glycol diethyl ether (10cm^3). The reaction mixture was then refluxed for 5 hours. TLC analysis of the reaction showed a new complex mixture of products. The solvent was removed under vacuum. The residual gum was chromatographed. However, no new products were isolated.

Synthesis of methylammonium salt of 2-(2,2-dicyano-1-dicyanomethyl-vinyl)-N-methyl-benzamide (154)

2-methyl-3-methylimino-2,3-dihydroisoindol-1-one (142) (1.00g, 5.8mmol) was added to ethanol (10cm^3). Malononitrile (0.77g, 11.6mmol) was then added drop-wise to the ethanol solution. The resultant suspension was then heated under reflux for 4 hours. During the reflux a crystalline solid precipitated. The reaction mixture was filtered hot. On cooling further product was isolated. The batches were combined and washed 3 times with hot methanol. The methylammonium salt of 2-(2,2-dicyano-1-dicyanomethyl-vinyl)-N-methyl-benzamide (154) was isolated as an off-white solid, (0.75g, 43%) mp 178-180°C. $\lambda_{max.}$: CH_3CN: 486.5 (ε=2333), 457.0 (2361) and 359.5nm (26639). $\nu_{max.}$: 3304, 2481, 2437, 2223, 1685, 1323, 963, 763and 707cm^{-1}. δH: DMSO: 8.30 (q, J=4.4Hz, 1H), 7.58 (m, 1H), 7.48 (m, 5H), 7.21 (m, 1H), 2.79 (d, J=4.4Hz, 3H) and 2.42ppm (s, 3H). δC: DMSO: 168.7 (**C**=O), 166.6 (**C**=C(CN)$_2$), 136.4, 135.0, 130.3, 129.3, 129.3, 127.6 (aromatic), 118.9 and 116.6 (CN), 53.2 (**C**(CN)$_2$), 26.4 (methyl) and 24.6ppm (methyl).

Found C: 62.55%, H: 4.67%, N: 27.39%. $C_{16}H_{14}N_6O$ requires C: 62.73%, H: 4.61%, N: 27.44% and O: 5.22%.

The same product was isolated when the solvent used in the reflux set-up was (a) methanol, (b) THF.

Similarly the same product was isolated as a white powder when the reaction was carried out at room temperature using DMF as the solvent. The product salt was precipitated from the reaction mixture by the addition of chloroform. The isolated white powder had identical mp, IR and NMR as the compound isolated from the previous experiment.

Synthesis of 2-(2-methyl-3-oxo-2,3-dihydro-isoindol-1-ylidene)-malononitrile (153)

2-methyl-3-methylimino-2,3-dihydroisoindol-1-one (142) (1.00g, 5.8mmol), malononitrile (0.77g, 11.6mmol) were dissolved in acetic acid ($10cm^3$). The resultant mixture was heated under reflux for 4 hours. During the reflux the colour of the reaction mixture darkened considerably. Some solid material precipitated from the solution during the reflux. Further solid was isolated on cooling. The golden solid was washed twice with hot ethanol and recrystallised from methanol, to yield 2-(2-methyl-3-oxo-2,3-dihydro-isoindol-1-ylidene)-malononitrile (153) as golden crystals, (0.56g, 47%) mp 200-202°C. $\nu_{max.}$: 2226, 2222, 1746, 1685, 1600, 1296, 1260, 1205, 1048, 954, 916, 799, 782 and $704cm^{-1}$. δH: DMSO: 8.37 (d=7.9Hz, 1H aromatic), 7.97 (m, 1H, aromatic), 7.93 (m, 1H, aromatic), 7.86 (m, 1H, aromatic) and 3.35ppm (s, 3H) δC: $CDCl_3$: 166.1 (**C**=O), 158.6 (**C**=C$(CN)_2$), 134.7, 134.0, 132.8, 127.4, 125.2, 124.9 (aromatic), 114.0 and 113.1 (CN), 59.9 (**C**$(CN)_2$) and 28.5ppm (methyl).

Found C: 68.63%, H: 3.52%, N: 20.27%. $C_{12}H_7N_3O$ requires C: 68.89%, H: 3.37%, N: 20.09%, O: 7.65%.

Synthesis of 2-(2-methyl-3-oxo-2,3-dihydro-isoindol-1-ylidene)-malononitrile (153) from salt (154)

Methylammonium salt of 2-(2,2-dicyano-1-dicyanomethyl-vinyl)-N-methyl-benzamide (154) (0.50g, 1.6mmol) was added to acetic acid ($10cm^3$). The resultant suspension was then heated under reflux for 8 hours. By this time the solid material

had dissolved and the reaction mixture had turned a red colour. When the mixture was cold a red microcrystalline solid was isolated by vacuum filtration. This red solid had identical mp, IR and NMR spectra to compound (153).

Synthesis of 2-(2-ethyl-3-oxo-2,3-dihydro-isoindol-1-ylidene)-malononitrile (155)

1,3-Diethyliminoisoindoline (138) (1.00g, 5mmol), malononitrile (0.66g, 11.6mmol) were added to acetic acid ($10cm^3$). The mixture was then heated under reflux for 5 hours. The solution was allowed to stand overnight. The reaction mixture was then filtered, isolating a pale green solid. This solid was then added to hot methanol and boiled for 2 minutes. The hot mixture was then vacuum filtered. The residual insoluble solid was washed twice with small volumes of boiling methanol. This solid was 2-(2-ethyl-3-oxo-2,3-dihydro-isoindol-1-ylidene)-malononitrile (155), (0.36g, 32%) mp 172-174°C. ν_{max}: 3113, 2991, 2220, 1752, 1602, 1405, 1325, 1214, 1058, 919, 792, 777 and $709cm^{-1}$. δH: DMSO: 8.40 (d, J=7.9Hz, 1H aromatic), 8.00-7.85 (m, 3H aromatic), 4.10 (q, J=7.2Hz, 2H) and 1.26ppm (t, J=7.2Hz, 3H). δC: DMSO: 166.1 (**C**=O), 158.0 (**C**=$C(CN)_2$), 135.0, 134.3, 133.1, 127.2, 124.7 and 124.3 (aromatic), 114.5, 113.3 (CN), 60.1 (**C**$(CN)_2$), 35.6 and 14.4ppm (N-ethyl).
Found: C: 69.67%, H: 4.22%, N: 18.84%. $C_{13}H_9N_3O$ requires C: 69.94%, H: 4.22%, N: 18.83%, O: 7.17%.

Synthesis of 2-(3-benzylimino-2,3-dihydro-isoindol-1-ylidene)-malononitrile (156)

1,3-Dibenzyliminoisoindoline (139) (0.50g, 1.5mmol) was dissolved in ethanol ($20cm^3$). Malononitrile (0.20g, 3.0mmol) was added drop-wise to this solution. The solution immediately darkened to a yellow colour. After a few minutes a yellow precipitate formed. This precipitate was isolated by vacuum filtration. The resultant yellow solid was recrystallised from methanol to yield 2-(3-benzylimino-2,3-

dihydro-isoindol-1-ylidene)-malononitrile (156), (0.27g, 62%) mp 250-252°C. ν_{max}: 3302, 3267, 3025, 2221, 1659, 1552, 1452, 1295, 1239, 1089, 1025, 790, 748 and 698cm^{-1}. δH: DMSO: 10.87 (s, NH), 8.10 (m, 2H aromatic), 7.71 (m, 2H aromatic), 7.40 (m, 5H, aromatic) and 4.95ppm (s, CH_2). δC: DMSO: 175.2 (**C**=N), 170.0 (**C**=C(CN)$_2$), 137.4, 137.0, 134.4, 132.9, 132.4, 129.0, 128.5, 128.1, 123.8 and 123.0 (aromatic), 115.9 and 115.1 (CN), 60.4 (**C**(CN)$_2$) and 47.2ppm (N-**C**H$_2$-Ph).

Attempted synthesis of 2-(2-benzyl-3-oxo-2,3-dihydro-isoindol-1-ylidene)-malononitrile (179)

1,3-Dibenzyliminoisoindoline (139) (0.50g, 1.5mmol) was dissolved in acetic acid (12cm^3). Malononitrile (0.22g, 3.3mmol) was then added drop-wise. The resultant mixture was then heated in a reflux set-up for 3 hours. An orange suspension was observed in the solution. TLC analysis of both liquid phase and solid showed a complex mixture. No other data was obtained.

Synthesis of ammonium salt of 2-(3-dicyanomethylene-2,3-dihydro-isoindol-1-ylidene)-malononitrile (135)

3-Phenylimino-1-iminoisoindoline (134) (15.00g, 76.0mmol) was dissolved in DMF (130cm^3). Malononitrile (9.42g, 143.0mmol) was then added dropwise with stirring to the above solution. The solution immediately became red in colour. There was also a distinct smell of ammonia. Addition of chloroform causes a red precipitate to form. This precipitate was separated by vacuum filtration. This solid was washed with ethanol. This yielded the ammonium salt of 2-(3-dicyanomethylene-2,3-dihydro-isoindol-1-ylidene)-malononitrile (135), (13.50g, 77%) mp >300°C. δH: DMSO: 8.09 (m, 2H aromatic), 7.63 (m, 2H aromatic) and 7.19-6.94ppm (1:1:1 t 4H NH).

Synthesis of 2-(3-dicyanomethylene-2,3-dihydro-isoindol-1-ylidene)-malononitrile (127)

The ammonium salt of 2-(3-dicyanomethylene-2,3-dihydro-isoindol-1-ylidene)-malononitrile (135) (11.42g, 50.9mmol) was dissolved in warm methanol (350cm^3). 10% ^{v}/v HCl was added causing a yeliow precipitate. This was filtered and the solid washed twice with water and ethanol and dried, yielding 2-(3-dicyanomethylene-2,3-dihydro-isoindol-1-ylidene)-malononitrile (127), (8.42g, 79%) mp >300°C. δH: DMSO: 8.19 (m, 2H aromatic), 7.79 (m, 2H aromatic) and 5.31ppm (s, NH).

Synthesis of 2-(3-dicyanomethylene-2-methyl-2,3-dihydro-isoindol-1-ylidene)-malononitrile (128)

2-(3-Dicyanomethylene-2,3-dihydro-isoindol-1-ylidene)-malononitrile (127) (0.50g, 2.1mmol) was added to THF (40cm^3) which contained diisopropylazodicarboxylate (DIAD) (0.63g, 3.1mmol), methanol (0.20g, 6.2mmol) and triphenylphosphine (0.81g, 3.1mmol). The solution immediately darkened to a red-orange colour. Argon was bubbled through the reaction mixture for 1 minute. The flask was then sealed and placed in the freezer for 2 days. TLC analysis showed formation of a fast moving highly coloured product. The solvent was removed. The solid residue was then dissolved in the minimum volume of dichloromethane and chromatographed using the same solvent. Isolation of the fast eluting yellow/green band and removal of solvent gave 2-(3-dicyanomethylene-2-methyl-2,3-dihydro-isoindol-1-ylidene)-malononitrile (128), (0.25g, 47%) mp 263-264°C. $\nu_{max.}$: 3120, 2962, 2911, 2846, 2212, 1556, 1440, 1318, 1109, 777 and 677cm^{-1}. $\lambda_{max.}$: CH_3CN: 416.5 (ε=32759), 395.0 (32552), 273.5 (16409), 244.0nm (21691). δH: $CDCl_3$: 8.60 (m, 2H aromatic), 7.80 (m, 2H aromatic) and 4.14ppm (s, 3H). δC: $CDCl_3$: 159.4 (**C**=C(CN)$_2$), 134.8, 130.7, 125.6 (aromatic), 112.8 and 112.2 (CN), 62.2 (**C**(CN)$_2$) and 37.2ppm (N-methyl).

Synthesis of 2-(3-dicyanomethylene-2-ethyl-2,3-dihydro-isoindol-1-ylidene)-malononitrile (140)

Triphenylphosphine (0.81g, 3.1mmol) was dissolved in THF (40cm^3). DIAD (0.62g, 3.1mmol) was then added dropwise. The mixture was then shaken for 30 seconds. Ethanol (0.20g, 4.3mmol) was then added. The mixture was then allowed to stand for 1-2 minutes. 2-(3-Dicyanomethylene-2,3-dihydro-isoindol-1-ylidene)-malononitrile (127) (0.50g, 2.1mmol) was then added. Argon was then bubbled through the reaction mixture. The flask was stoppered and sealed. After 1 week the solvent was removed and the solid residue was chromatographed using dichloromethane as mobile phase giving crude 2-(3-dicyanomethylene-2-ethyl-2,3-dihydro-isoindol-1-ylidene)-malononitrile (140) as yellow/orange crystalline solid, (0.23g, 41%) mp 223-225°C. ν_{max}: 3120, 2930, 2218, 1550, 1338, 1225, 1095, 784, 743 and 694cm^{-1}. λ_{max}: 245.0 (ε=22535), 281.0 (11448), 393.0 (42349) and 413.0nm (41793). δH: $CDCl_3$: 8.72 (m, 2H aromatic), 7.82 (m, 2H aromatic), 4.72 (q, J=6.9Hz, 2H) and 1.64ppm (t, J=6.9Hz, 3H). δC: $CDCl_3$: 156.6 (**C**=C(CN)$_2$), 134.7, 130.9, 125.9 (aromatic), 113.2 and 112.3 (CN), 61.3 (**C**(CN)$_2$), 41.8 and 16.4ppm (N-ethyl). Found C: 70.55%, H: 3.77%, N: 24.77%. $C_{16}H_9N_5$ requires C: 70.84%, H: 3.34%, N: 25.82%.

Synthesis of 2-(3-dicyanomethylene-2-benzyl-2,3-dihydro-isoindol-1-ylidene)-malononitrile (141)

DIAD (0.37g, 1.9mmol) was added to a solution of triphenylphosphine (0.49g, 1.9mmol) in THF (40cm^3). Benzyl alcohol (0.20g, 1.9mmol) was also added. 2-(3-Dicyanomethylene-2,3-dihydro-isoindol-1-ylidene)-malononitrile (127) (0.30g, 1.2mmol) was then added to the mixture, which was then sealed under an argon atmosphere for 1 week. The solvent was removed under reduced pressure. The fast moving yellow/green fraction was isolated by column chromatography using dichloromethane as mobile phase, yielding 2-(3-dicyanomethylene-2-benzyl-2,3-dihydro-isoindol-1-ylidene)-malononitrile (141) (0.12g, 30%) mp 232-234°C. ν_{max}: 2931, 2221, 1560, 1470, 1456, 1244, 1165, 1107, 777, 739 and 687cm^{-1}. $\lambda_{max.}$: CH_3CN: 413.5 (ε=33038), 390.5 (32873), 279.5 (12652), 270.0 (12486), 245.0nm

(19945) .δH: $CDCl_3$: 8.76 (m, 2H aromatic), 7.87 (m, 2H aromatic), 7.39 (m, 3H aromatic), 7.05 (m, 2H aromatic) and 6.00ppm (s, 2H). δC: $CDCl_3$: 157.9 (**C**=C(CN)$_2$), 135.3, 133.3, 131.3, 130.0, 129.3, 126.4 and 125.5 (aromatic), 113.4 and 112.3 (CN), 62.9 (**C**(CN)$_2$) and 50.1ppm (N-**C**H$_2$-)

Found C: 75.49%, H: 3.61%, N: 20.50%. $C_{22}H_{11}N_5$ requires C: 75.67%, H: 3.35%, N: 21%.

Synthesis of 2-(2-allyl-3-dicyanomethylene-2,3-dihydro-isoindol-1-ylidene)-malononitrile (168)

DIAD (0.37g, 1.9mmol), triphenylphosphine (0.49g, 1.9mmol), 2-(3-dicyanomethylene-2,3-dihydro-isoindol-1-ylidene)-malononitrile (127) (0.30g, 1.2mmol), allyl alcohol (0.20g, 3.4mmol) were mixed in THF following the procedure used in the synthesis of 2-(3-dicyanomethylene-2-ethyl-2,3-dihydro-isoindol-1-ylidene)-malononitrile (140). The reaction mixture was sealed under argon and allowed stand at room temperature for 1 week. The solvent was then removed. The residue was chromatographed using dichloromethane as mobile phase. 2-(2-Allyl-3-dicyanomethylene-2,3-dihydro-isoindol-1-ylidene)-malononitrile (168) (0.16g, 46%) was isolated as a green solid, mp 240-242°C. $\nu_{max.}$: 3106, 2222, 1560, 1459, 1332, 1222, 1162, 1111 and 783cm^{-1}. $\lambda_{max.}$: CH_3CN: 414.0 (ε=35589), 391.0 (35522), 291.0 (9394), 279.0 (10303), 269.0 (10202), 243.0nm (19966). δH: $CDCl_3$: 8.74 (m, 2H aromatic), 7.85 (m, 2H aromatic), 6.05 (m, 1H), 5.50 (d, J=10.4Hz, 1H), 5.35 (s, 2H) and 5.05ppm (d, J=17.2Hz, 1H). δC: DMSO: 157.8 (**C**=C(CN)$_2$), 135.0, 132.6 and 1125.3 (aromatic), 114.5, 113.3 (CN), 60.6 (**C**(CN)$_2$), 131.3, 116.7 and 48.8ppm (N-allyl).

Found C: 71.83%, H: 3.28%, N: 24.60%. $C_{17}H_9N_5$ requires C: 72.08%, H: 3.20%, N: 24.72%.

Synthesis of 2-(3-dicyanomethylene-2-(3-phenyl-allyl)-2,3-dihydro-isoindol-1-ylidene)-malononitrile (169)

DIAD (0.37g, 1.9mmol), triphenylphosphine (0.49g, 1.9mmol), 2-(3-dicyanomethylene-2,3-dihydro-isoindol-1-ylidene)-malononitrile (127) (0.30g, 1.2mmol), cinnamyl alcohol (0.25g, 1.9mmol) were mixed together in THF ($40cm^3$) using the procedure outlined in the synthesis of 2-(3-dicyanomethylene-2-ethyl-2,3-dihydro-isoindol-1-ylidene)-malononitrile (140). The reaction mixture was sealed under argon for 5 days. 2-(3-dicyanomethylene-2-(phenyl-3-allyl)-2,3-dihydro-isoindol-1-ylidene)-malononitrile (169) (0.22g, 45%) was isolated as orange crystals by column chromatography, mp 196-198°C. $\nu_{max.}$: 3049, 2372, 2335, 2221, 1559, 1464, 1405, 1327, 123 and 1157cm^{-1}. $\lambda_{max.}$:CH_3CN: 551.5 (ε=5250), 458.5 (6667), 414.0 (38333), 391.5 (39167) and 249.0nm (47083). δH: $CDCl_3$: 8.75 (m, 2H aromatic), 7.85 (m, 2H aromatic), 7.37 (m, 2H aromatic), 7.30 (m, 3H aromatic), 6.48 (d, J=16.0Hz, 1H), 6.25 (dt, J_d=16.0Hz, J_t=4.8Hz, 1H) and 5.50ppm (d, J=4.8Hz, 2H). δC: $CDCl_3$: 156.8 (**C**=C$(CN)_2$), 135.0, 134.8, 134.0, 130.9, 128.8, 128.8, 126.9 (aromatic), 126.0 (**C**H=CH), 120.5 (CH=**C**H), 113.1 and 112.3ppm (CN), 62.1ppm (**C**$(CN)_2$) and 47.6ppm (N-**C**H_2)

Found: C: 76.58%, H: 3.72%, N: 19.51%. $C_{23}H_{13}N_5$ requires C: 76.87%, H: 3.64%, N: 19.49%.

Synthesis of 2-(3-imino-2,3-dihydro-isoindol-1-ylidene)-malononitrile (175)

Phthalonitrile (9.15g, 71.5mmol) was added to methanol ($180cm^3$). Sodium metal (4.14g, 180.0mmol) was added with extreme caution to methanol ($100cm^3$). When the sodium was dissolved and the solution had cooled to room temperature, it was then added slowly to the phthalonitrile/methanol mixture. The resultant brownish solution was stirred continuously. Malononitrile (5.94g, 90.0mmol) was then added dropwise. The solution became a brighter brown/orange colour. The reaction mixture was then stirred at 30°C for 3 hours. 2-(3-Imino-2,3-dihydro-isoindol-1-ylidene)-malononitrile (175) was then isolated by vacuum filtration, as a yellow/orange powder, (10.13g, 73%), mp 209-211°C (d); δH: DMSO: 8.26 (m, 1H, aromatic) and 7.94-7.84 (m, 3H, aromatic). δC: DMSO: 173.1 (**C**=N), 172.5 (**C**=C$(CN)_2$), 139.7,

138.6, 130.4, 130.0, 121.9 and 121.6 (aromatic), 121.4 and 119.8 (CN) and 40.9ppm (**C**$(CN)_2$).

Synthesis of 2-(3-oxo-2,3-dihydro-isoindol-1-ylidene)-malononitrile (170)

2-(3-Imino-2,3-dihydro-isoindol-1-ylidene)-malononitrile (175) (1.70g, 8.8mmol) was added to an aqueous solution of acetic acid (50cm^3). The solution contained acetic acid (40cm^3) and water (10cm^3). The solution was heated under reflux for 2 hours. By this time there was no solid observed in the round-bottomed flask. TLC analysis of the reaction mixture showed the formation of a new spot that travelled slightly further up the TLC plate than the starting material. The reaction mixture was then cooled in the freezer overnight. 2-(3-Oxo-2,3-dihydro-isoindol-1-ylidene)-malononitrile (170) was isolated by vacuum filtration as a very pale yellow solid, (0.98g, 57%); mp 249-251°C; $\nu_{max.}$: 3281, 2214, 1765, 1616, 1394, 1189 and 790cm^{-1}. δH: DMSO: 7.95 (m, 1H, aromatic), 7.77 (m, 1H, aromatic) and 7.48 (2H, aromatic). δC: DMSO: 167.9 (**C**=O), 161.2 (**C**=C$(CN)_2$), 135.0, 134.8, 133.2, 129.6, 124.9 and 124.7 (aromatic), 114.2 and 112.6 (CN), 58.0ppm (**C**$(CN)_2$).

Synthesis of 2-(2-methyl-3-oxo-2,3-dihydro-isoindol-1-ylidene)-malononitrile (153)

Triphenylphosphine (0.60g, 2.3mmol) was dissolved in THF (20cm^3). DIAD (0.47g, 2.3mmol) was then added dropwise. Methanol (0.1g, 3.1mmol) was then added and the mixture was allowed stand for 1-2 minutes. 2-(3-Oxo-2,3-dihydro-isoindol-1-ylidene)-malononitrile (170) (0.30g, 1.5mmol) was then added. The mixture was then sealed under an argon atmosphere. After 24 hours TLC analysis showed the formation of a new compound, which travelled slightly faster then the starting material. The solvent was removed under reduced pressure after 3 days. The residual gum was chromatographed using dichloromethane as mobile phase. 2-(2-Methyl-3-oxo-2,3-dihydro-isoindol-1-ylidene)-malononitrile (153) was isolated as a pale yellow solid, (0.11g, 34%); mp 200-202°C. The IR spectrum obtained here was

identical to the IR spectrum of the compound synthesised by the reaction of malononitrile and 2-methyl-3-methylimino-2,3-dihydroisoindol-1-one (142). δH: $CDCl_3$: 8.50 (m, 1H, aromatic), 7.80 (m, 1H, aromatic), 7.72 (m, 2H, aromatic) and 3.62ppm (s, 3H). δC: $CDCl_3$: 166.6 (**C**=O), 159.0 (**C**=C(CN)$_2$), 135.1, 134.4, 133.2, 127.8, 125.6, 125.4 (aromatic), 114.0 and 113.0 (CN), 60.3 (**C**(CN)$_2$) and 28.9ppm (N-methyl).

Synthesis of 2-(2-ethyl-3-oxo-2,3-dihydro-isoindol-1-ylidene)-malononitrile (155)

Triphenylphosphine (0.61g, 2.3mmol) was dissolved in THF (20cm^3). DIAD (0.47g, 2.3mmol) was then added. The solution was then allowed to stand for 1-2 minutes. Ethanol (0.11g, 2.4mmol) was then added and the resultant solution was allowed stand for 1-2 minutes. 2-(3-Oxo-2,3-dihydro-isoindol-1-ylidene)-malononitrile (170) (0.30g, 1.5mmol) was then added. The reaction mixture was then sealed under argon. TLC analysis after 24 hours showed the formation of a new product of slightly larger rf than the starting material. The solvent was removed after 3 days. 2-(2-Ethyl-3-oxo-2,3-dihydro-isoindol-1-ylidene)-malononitrile (155) was isolated after column chromatography using dichloromethane as solvent, as an off-white solid, (0.14g, 41%); mp 172-174°C. The IR spectrum obtained here was identical to the IR spectrum of the compound synthesised by the reaction of malononitrile and 1,3-diethyliminoisoindoline (138). δH: $CDCl_3$: 8.53 (m, 1H aromatic), 7.88 (m, 1H aromatic), 7.72 (m, 2H aromatic), 4.20 (q, J=7.2Hz, 2H) and 1.34ppm (t, J=7.2Hz, 3H). δC: $CDCl_3$: 166.7 (**C**=O), 158.3 (**C**=C(CN)$_2$), 135.4, 134.6, 133.9, 128.0, 126.0 and 125.5 (aromatic), 114.4 and 113.3 (CN), 59.9 (**C**(CN)$_2$), 37.0 and 15.6ppm (N-ethyl).

Synthesis of 2-(2-butyl-3-oxo-2,3-dihydro-isoindol-1-ylidene)-malononitrile (176)

Triphenylphosphine (2.02g, 7.70mmol) was dissolved in THF (40cm^3). DIAD (1.55g, 7.70mmol) was then added. The mixture was allowed stand for about 1 minute. Butanol (0.57g, 7.70mmol) was then added. 2-(3-Oxo-2,3-dihydro-isoindol-1-

ylidene)-malononitrile (170) (1.00g, 5.13mmol) was finally added. The reaction mixture was then sealed under argon. The solvent was removed after 5 days. 2-(2-butyl-3-oxo-2,3-dihydro-isoindol-1-ylidene)-malononitrile (176) was isolated by column chromatography using dichloromethane as solvent, as an off white solid (0.48g, 37%), mp 97-99°C. ν_{max}: 3039, 2229, 2217, 1751, 1576, 1497, 1450, 1304, 1121, 954, 744cm^{-1}.λ_{max}: CH_3CN: 235.0 (ε=22800) and 277.5nm (41840). δH: $CDCl_3$: 8.60 (m, 1H aromatic), 7.97 (m, 1H aromatic), 7.79 (m, 2H aromatic), 4.20 (t, J=8.0Hz, 2H), 1.75 (m, 2H) and 1.46 (m, 2H) and 1.00ppm (t, J=8.0Hz, 3H). δC: $CDCl_3$: 166.8 (**C**=O), 158.1 (**C**=C(CN)$_2$), 135.1, 134.3, 133.6, 127.7, 125.7, 125.3 (aromatic), 114.2 and 113.0 (CN), 59.9 (**C**(CN)$_2$), 41.5, 32.0, 19.9 and 14.1ppm (N-butyl).

Found: C: 71.53%, H: 5.21%, N: 16.72%. $C_{15}H_{13}N_3O$ requires C: 71.70%, H: 5.25%, N: 16.72%, O: 6.37%.

Synthesis of 2-(2-benzyl-3-oxo-2,3-dihydro-isoindol-1-ylidene)-malononitrile (179)

Triphenylphosphine (2.02g, 7.70mmol) was dissolved in THF (35cm^3). DIAD (1.55g, 7.70mmol) was added drop-wise to the solution. The solution was allowed stand for about a minute. Benzyl alcohol (0.83g, 7.70mmol) was also added. 2-(3-Oxo-2,3-dihydro-isoindol-1-ylidene)-malononitrile (170) (1.00g, 5.13mmol) was then added to the reaction mixture. The flask was then sealed under an argon atmosphere. The solvent was removed after 5 days. The residue was chromatographed using dichloromethane as the solvent. 2-(2-Benzyl-3-oxo-2,3-dihydro-isoindol-1-ylidene)-malononitrile (179) was isolated as an off-white solid (0.42g, 29%), mp 160-162°C. ν_{max}: 3109, 2939, 2883, 2224, 2210, 1751, 1571, 1460, 1406, 1330, 1183, 951 and 707cm^{-1}. δH: $CDCl_3$: 8.54 (m, 1H aromatic), 7.96 (m, 1H aromatic), 7.75 (m, 2H aromatic), 7.27 (m, 3H aromatic), 7.18 (m, 2H aromatic) and 5.40ppm (s, 2H). δC: $CDCl_3$: 167.1 (**C**=O), 157.8 (**C**=C(CN)$_2$), 135.4, 134.9, 134.5, 133.7, 129.5, 128.6, 127.5, 127.1, 125.9 and 125.7 (aromatic), 114.0 and 112.9 (CN), 61.9 (**C**(CN)$_2$) and 44.4ppm (N-**C**H$_2$-).

Found: C: 74.15%, H: 3.94%, N: 14.36%. $C_{18}H_{11}N_3O$ requires C: 75.78%, H: 3.89%, N: 14.73%, O: 5.61%.

Synthesis of 2-(2-allyl-3-oxo-2,3-dihydro-isoindol-1-ylidene)-malononitrile (181)

Triphenylphosphine (0.61g, 2.3mmol) was dissolved in THF (50cm^3). DIAD (0.47g, 2.3mmol) was then added. Allyl alcohol (0.20g, 2.1mmol) was subsequently added. 2-(3-Oxo-2,3-dihydro-isoindol-1-ylidene)-malononitrile (170) (0.30g, 1.5mmol) was finally added. The reaction was sealed under argon. The solvent was removed under reduced pressure after 4 days. Column chromatography with dichloromethane as solvent, yielded 2-(2-allyl-3-oxo-2,3-dihydro-isoindol-1-ylidene)-malononitrile (181) as a cream coloured solid. Recrystallisation from methanol afforded a white solid (0.12g, 36%), mp 154-156°C. ν_{max}: 3094, 2226, 2218, 1751, 1575, 1442, 1401, 1314, 1130, 955 and 715cm^{-1}. δH: $CDCl_3$: 8.60 (m, 1H aromatic), 8.00 (m, 1H aromatic), 7.80 (m, 2H aromatic), 5.95 (m, 1H), 4.85 (m, 2H), 5.34 (d, J=10.3Hz, 1H) and 5.15ppm (d, J=17.1Hz, 1H). δC: 166.5 (**C**=O), 157.6 (**C**=C(CN)$_2$), 135.3, 134.5, 133.5, 127.6, 125.8, 125.5 (aromatic), 114.0, 113.0 (CN), 60.7 (**C**(CN)$_2$), 131.1, 118.4 and 43.0ppm (N-allyl).

Found: C: 71.36%, H: 3.96%, N: 17.67%. $C_{14}H_9N_3O$ requires C: 71.48%, H: 3.86%, N: 17.86%, O: 6.80%.

Synthesis of 2-(3-oxo-2-(3-phenyl-allyl)-2,3-dihydro-isoindol-1-ylidene)-malononitrile (180)

Triphenylphosphine (2.02g, 7.7mmol) was dissolved in THF (70cm^3). DIAD (1.55g, 7.7mmol) and cinnamyl alcohol (1.03g, 7.7mmol) were subsequently added. 2-(3-Oxo-2,3-dihydro-isoindol-1-ylidene)-malononitrile (170) (1.00g, 5.1mmol) was then added. The reaction mixture was sealed under argon and stored at room temperature. The solvent was removed after 1 week. Column chromatography using dichloromethane as solvent yielded a cream coloured solid, which was recrystallised from methanol to yield, 2-(3-oxo-2-(3-phenyl-allyl)-2,3-dihydro-isoindol-1-ylidene)-

malononitrile (180) as a fine off-white powder (0.35g, 22%); mp 156-158°C. ν_{max}: 3028, 2227, 2216, 1744, 1574, 1400, 1206, 1129, 1091, 971 and 710 cm^{-1}. λ_{max}: CH_3CN: 268.0nm (ε=64481). δH: 8.55 (m, 1H aromatic), 7.92 (m, 1H aromatic), 7.73 (m, 2H aromatic), 7.30 (m, 2H aromatic), 7.21 (m, 3H aromatic), 6.60 (d, J=16.0Hz, 1H), 6.20 (dt, J_d=16.0Hz, J_t=6.0Hz, 1H) and 4.93ppm (d, J=6.0Hz, 2H). δC: 166.9 (**C**=O), 158.0 (**C**=C(CN)$_2$), 136.3, 135.5, 135.2, 134.7, 133.9, 129.3, 129.0, 127.9, 127.3 and 125.8 (aromatic), 126.1 (**C**H=CH), 122.3 (CH=**C**H), 114.3 and 113.4 (CN), 60.9 (**C**(CN)$_2$) and 43.0ppm (N-**C**H$_2$).

Found: C: 76.90%, H: 4.27%, N: 13.28%. $C_{20}H_{13}N_3O$ requires C: 77.16%, H: 4.21%, N: 13.50%, O: 5.14%.

Synthesis of 2-(3-oxo-2-pentyl-2,3-dihydro-isoindol-1-ylidene)-malononitrile (177)

Triphenylphosphine (2.02g, 7.7mmol), DIAD (1.55g, 7.7mmol) and pentanol (0.68g, 7.7mmol) were all dissolved in THF (70cm^3) using protocol developed for the synthesis of N-alkyl derivatives of 2-(3-oxo-2,3-dihydro-isoindol-1-ylidene)-malononitrile. 2-(3-Oxo-2,3-dihydro-isoindol-1-ylidene)-malononitrile (170) (1.00g, 5.1mmol) was then added. The reaction mixture was sealed under argon. The solvent was removed under reduced pressure after 1 week. Column chromatography using dichloromethane as mobile phase afforded viscous oil. The oil solidified on cooling. Recrystallisation from methanol yielded 2-(3-oxo-2-pentyl-2,3-dihydro-isoindol-1-ylidene)-malononitrile (177) as colourless needles (0.47g, 35%); mp 90-92°C. ν_{max}: 3115, 2916, 2858, 2225, 2215, 1744, 1583, 1456, 1398, 1203, 1086, 921, 770 and 701cm^{-1}. λ_{max}: CH_3CN: 235.0 (ε=21132) and 276.0nm (43316). δH: $CDCl_3$: 8.53 (m, 1H aromatic), 7.88 (m, 1H aromatic), 7.72 (m, 2H aromatic), 4.10 (t, J=7.2Hz, 2H), 1.67 (m, 2H), 1.33 (m, 4H) and 0.85ppm (t, J=7.2Hz, 3H). δC: $CDCl_3$: 166.8 (**C**=O), 158.0 (**C**=C(CN)$_2$), 135.1, 134.3, 133.6, 127.7, 125.7 and 125.3 (aromatic), 59.8 (**C**(CN)$_2$), 41.6, 29.7, 28.6, 22.7 and 14.3ppm (N-pentyl).

Found: C: 72.13%, H: 5.74%, N: 15.71%. $C_{16}H_{15}N_3O$ requires C: 72.43%, H: 5.70%, N: 15.84%, O: 6.03%.

Synthesis of 2-(2-decyl-3-oxo-2,3-dihydro-isoindol-1-ylidene)-malononitrile (178)

Triphenylphosphine (2.02g, 7.7mmol), DIAD (1.55g, 7.7mmol) and decanol (1.22g, 7.7mmol) were dissolved in THF (70cm^3). 2-(3-Oxo-2,3-dihydro-isoindol-1-ylidene)-malononitrile (170) (1.00g, 5.1mmol) was then added. The reaction mixture was sealed under an argon atmosphere. The solvent was removed after 1 week. Column chromatography using dichloromethane as solvent yielded off-white oil, which solidified on cooling. Recrystallisation from methanol yielded 2-(2-decyl-3-oxo-2,3-dihydro-isoindol-1-ylidene)-malononitrile (178) as a fine white powder (0.88g, 51%), mp 49-51°C. ν_{max}: 2922, 2853, 2222, 2213, 1752, 1570, 1465, 1406, 1335, 1205, 1073, 915, 779 and 707cm^{-1}. λ_{max}: CH_3CN: 235.0 (ε=27182) and 266.5nm (75697). δH: $CDCl_3$: 8.52 (m, 1H aromatic), 7.88 (m, 1H aromatic), 7.71 (m, 2H aromatic), 4.10 (t, J=7.8Hz, 2H), 1.66 (m, 2H), 1.29 (m, $(CH_2)_7$) and 0.80ppm (t, J=7.2Hz, 3H). δC: $CDCl_3$: 166.4 (**C**=O), 157.7 (**C**=C$(CN)_2$), 134.7, 133.9, 133.2, 127.4, 125.3, 124.9 (aromatic), 113.8 and 112.7ppm (CN), 59.5 (**C**$(CN)_2$), 41.3, 31.9, 29.6, 29.5, 29.4, 29.3, 29.2, 26.2, 22.7 and 14.1ppm (N-decyl).

Synthesis of 2-(2-isopropyl-3-oxo-2,3-dihydro-isoindol-1-ylidene)-malononitrile (182)

Triphenylphosphine (2.02g, 7.7mmol), DIAD (1.55g, 7.7mmol) and iso-propyl alcohol (0.47g, 7.7mmol) were dissolved in THF (70cm^3). 2-(3-Oxo-2,3-dihydro-isoindol-1-ylidene)-malononitrile (170) (1.00g, 5.1mmol) was then added. TLC analysis of the reaction mixture after 24 hours showed the formation of a new product. The solvent was removed after 3 days. The solid residue was chromatographed using dichloromethane as solvent. Recrystallisation of the isolated solid from methanol produced 2-(2-isopropyl-3-oxo-2,3-dihydro-isoindol-1-ylidene)-malononitrile (182) as colourless crystals (0.33g, 27%), mp 167-169°C. ν_{max}: 2234, 2217, 1750, 1702, 1589, 1281, 1194, 1099 and 1074cm^{-1}. λ_{max}: CH_3CN: 235.5 (ε=17536) and 276.5nm (42036). δH: $CDCl_3$: 8.52 (m, 1H aromatic), 7.81 (m, 1H aromatic), 7.69 (m, 2H aromatic), 5.03 (m, 1H) and 1.58ppm (s, 6H ($2CH_3$)). δC:

$CDCl_3$: 167.4 (**C**=O), 159.0 (**C**=C(CN)$_2$), 134.9, 134.3, 133.7, 128.2, 125.6, 124.8 (aromatic), 114.5, 113.1 (CN), 59.6 (**C**(CN)$_2$), 49.4 and 21.0ppm (N-iso-propyl).
Found: C: 70.99%, H: 4.73%, N: 17.85%. $C_{14}H_{11}N_3O$ requires C: 70.87%, H: 4.67%, N: 17.71%, O: 6.74%.

Synthesis of 3-dicyanomethylene-2-pentyl-2,3-dihydro-isoindol-1-ylidene-cyanamide (185)

2-(3-Oxo-2-pentyl-2,3-dihydro-isoindol-1-ylidene)-malononitrile(177) (0.30g, 1.1mmol) was dissolved in dichloromethane (25cm^3). The flask was then stoppered and sealed under an argon atmosphere. Titanium(IV) chloride (0.33g,1.7mmol) was added to the stirred dichloromethane solution using a syringe. The reaction mixture became a very dark red colour. Bis(trimethylsilyl)carbodiimide(BTC) (1cm^3, 4.4mmol) was subsequently added using a syringe. The colour of the reaction mixture darkened further. The mixture was stirred at room temperature for 3 days. The mixture was then poured into an iced water/dichloromethane mix (50:50, 400cm^3). The organic layer was separated from the aqueous layer and dried over magnesium sulphate. The drying agent was removed by vacuum filtration. A greenish solid was isolated when the solvent was removed. TLC analysis of this solid showed the formation of a new product. The new spot had a smaller rf value compared to the starting material. Column chromotography with dichloromethane as solvent yielded a pale yellow powder. Recrystallisation from methanol afforded 3-dicyanomethylene-2-pentyl-2,3-dihydro-isoindol-1-ylidene-cyanamide (185) as a very pale yellow solid (0.21g, 64%), mp 155-157°C. ν_{max}: 2962, 2926, 2224, 2192, 1638, 1573, 1472, 1407, 1213, 1103, 786 and 689cm^{-1}. λ_{max}: CH_3CN: 240.0 (ε=18127), 377.0 (21914) and 396.0nm (18468). δH: $CDCl_3$: 8.74 (m, 1H aromatic), 8.58 (m, 1H aromatic), 7.79 (m, 2H aromatic), 4.23 (t, J=8.0Hz, 2H), 1.73 (m, 2H), 1.35 (m, 4H (-CH_2-CH_2-)) and 0.87ppm (t, J=6.8Hz, 3H). δC: 166.4 (**C**=N(CN)), 156.9 (**C**=C(CN)$_2$), 135.8, 135.1, 132.3, 127.2, 126.8, 126.1 (aromatic), 113.5, 113.2, 112.5 (CN), 63.0 (**C**(CN)$_2$), 43.9, 29.2, 28.4, 22.6 and 14.3ppm (N-pentyl).
Found: C: 70.36%, H: 5.28%, N: 24.24%. $C_{17}H_{15}N_5$ requires C: 70.57%, H: 5.23%, N: 24.21%.

Synthesis of 3-dicyanomethylene-2-decyl-2,3-dihydro-isoindol-1-ylidene-cyanamide (186)

Following the procedure described for the synthesis of 3-dicyanomethylene-2-pentyl-2,3-dihydro-isoindol-1-ylidene-cyanamide (185). 2-(2-Decyl-3-oxo-2,3-dihydro-isoindol-1-ylidene)-malononitrile (178) (0.54g, 1.6mmol), titanium(IV) chloride(0.46g, 2.4mmol) and BTC (1cm^3, 4.4mmol) were added to dichloromethane (30cm^3). The resultant very dark red solution was stirred at room temperature for 3 days. The reaction mixture was added to a mixture of iced water (200cm^3) and dichloromethane (200cm^3). The organic layer was then separated from the aqueous layer and dried over magnesium sulphate. The drying agent was removed by vacuum filtration. The solvent was removed and a pale yellow oil was isolated. This oil solidified after a couple of minutes. TLC analysis of this solid showed 2 spots corresponding to some remaining starting material and a new product. The new product did not travel as far up the TLC plate as the starting material. The new product was isolated using column chromatography with dichloromethane as solvent. Recrystallisation of the isolated off white solid from methanol yielded 3-dicyanomethylene-2-decyl-2,3-dihydro-isoindol-1-ylidene-cyanamide (186) as a very pale yellow powder (0.32g, 55%), mp 94-96°C. ν_{max}: 2960, 2923, 2226, 2193, 1646, 1575, 1471, 1409, 1216, 1103, 783 and 697cm^{-1}. λ_{max}: CH_3CN: 240.0 (ε=22444), 349.0 (24166), 377.0 (27194) and 369.0nm (22917). δH: $CDCl_3$: 8.73 (1H, aromatic), 8.58 (1H, aromatic), 7.79 (2H, aromatic), 4.22 (t J=8.0Hz, 2H), 1.71 (m, 2H), 1.30 (m, 14H, $(CH_2)_7$) and 0.81ppm (t, J=6.8Hz, 3H). δC: $CDCl_3$: 166.4 (**C**=N(CN)), 156.9 (**C**=C$(CN)_2$), 135.8, 135.1, 132.3, 127.2, 126.8, 126.1 (aromatic), 113.5, 113.1, 112.5 (CN), 63.0 (**C**$(CN)_2$), 43.9, 32.2, 29.8, 29.8, 29.7, 29.5, 29.5, 26.4, 23.1 and 14.5ppm (N-decyl).

Found: C: 73.47%, H: 7.03%, N: 19.57%. $C_{22}H_{25}N_5$ requires C: 73.51%, H: 7.01%, N: 19.48%.

Synthesis of 3-(cyanoimino)-2-phenyl-2,3-dihydro-isoindol-1-ylidenecyanamide (189)

N-Phenylphthalimide (2.00g, 9.0mmol) was dissolved in dichloromethane ($100cm^3$). The reaction mixture was sealed under argon. $TiCl_4$ (2.55g, 13.4mmol) was then added. BTC (2.5g, 13.4mmol) was added. The resultant dark solution was stirred at room temperature over the weekend. The reaction mixture was then added to a mixture of dichloromethane ($100cm^3$) and iced water ($100cm^3$). The organic phase was separated and dried over magnesium sulphate. The solution was then filtered and the solvent removed under reduced pressure. TLC analysis of the solid isolated showed 3 major products. The mixture was chromatographed using dichloromethane as the solvent. The fastest moving spot appeared to be the starting material, N-phenylphthalimide. The white solid isolated when the solvent was removed had the same mp and IR spectrum as the starting material. The second isolated fraction was an off white/yellow solid. The IR spectrum of this solid showed both carbonyl and cyano stretches. This compound was 3-oxo-2-phenyl-2,3-dihydro-isoindol-1-ylidenecyanaminde (188) (0.54g, 25%) mp 167-169°C. $\nu_{max.}$: 2204, 2174, 1758, 1633, 1409, 1188, 1083, 1000 and $702cm^{-1}$. δH: $CDCl_3$: 8.75 (m, 1H aromatic), 7.95 (m, 1H aromatic), 7.81 (m, 2H aromatic), 7.48 (m, 3H aromatic) and 7.32ppm (m, 2H aromatic). δC: $CDCl_3$: 168.2 (**C**=O), 166.4 (**C**=N-CN), 135.6, 131.4, 130.6, 130.0, 129.8, 129.7, 128.0, 127.0, 126.4 and 125.2 (aromatic) and 113.9ppm (CN).

Found: C: 75.48%, H: 3.31%, N: 15.53%. $C_{17}H_9N_3O$ requires C: 75.27%, H: 3.34%, N: 15.49%, O: 5.90%.

The final fraction was 3-(cyanoimino)-2-phenyl-2,3-dihydro-isoindol-1-ylidenecyanamide (189), (0.69g, 31%) mp 278-280°C. ν_{max}: 2191, 1614, 1419, 1302, 1246, 1096 and $1000cm^{-1}$. $\lambda_{max.}$: CH_3CN: 275.5nm (ε=75238). δH: $CDCl_3$: 8.80 (m, 2H aromatic), 7.91 (m, 2H aromatic), 7.51 (m, 3H aromatic) and 7.27 (m, 2H aromatic). δC: $CDCl_3$: 167.5 (**C**=N-CN), 136.3, 130.9, 130.7, 130.1, 128.7, 128.5 and 127.0 (aromatic) and 113.0ppm (CN).

Found: C: 70.54%, H: 3.32%, N: 25.62%. $C_{16}H_9N_5$ requires C: 70.84%, H: 3.34%, N: 25.62%.

5.2 Synthesis of Charge-Transfer complexes

2-(3-dicyanomethylene-2-(3-phenyl-allyl)-2,3-dihydro-isoindol-1-ylidene)-malononitrile (169)-TTF complex

2-(3-Dicyanomethylene-2-(3-phenyl-allyl)-2,3-dihydro-isoindol-1-ylidene)-malononitrile (169) (0.05g, 0.1mmol) was dissolved in dichloromethane (25cm^3). TTF (0.06g, 0.3mmol) was then added to the solution. The reaction mixture immediately became a green colour. The mixture was sealed under argon and stored at room temperature overnight. The solvent was then evaporated off to yield a green solid. TLC analysis of this green solid showed 2 spots, each corresponding to one of the starting materials. This solid was recrystallised from acetonitrile to give 2-(3-dicyanomethylene-2-(3-phenyl-allyl)-2,3-dihydro-isoindol-1-ylidene)-malononitrile (169)-TTF complex as very fine green needles, (0.03, 53%), mp 146-148°C. ν_{max}: 3065, 2219, 1557, 1455, 1401, 1331, 1227, 1135 and 1112cm^{-1}.
Found C: 62.07%, H: 3.10%, N: 12.45%, S: 22.38%. $C_{29}H_{17}N_5S_4$ requires C: 61.79%, H: 3.04%, N: 12.42%, S: 22.75%.

2-(2-Allyl-3-dicyanomethylene-2,3-dihydro-isoindol-1-ylidene)-malononitrile (168)-TTF complex

2-(2-Allyl-3-dicyanomethylene-2,3-dihydro-isoindol-1-ylidene)-malononitrile (168) (0.05g, 0.2mmol) and TTF (0.04g, 0.2mmol) were added to acetonitrile (15cm^3). The mixture was heated under reflux until all the solid material had dissolved. The resultant solution was now green in colour. Heating was terminated and the solution was allowed to cool to room temperature. 2-(2-Allyl-3-dicyanomethylene-2,3-dihydro-isoindol-1-ylidene)-malononitrile (168)-TTF complex precipitated from the solution as dark green needles. These crystals were isolated by filtration and recrystallised from acetonitrile to give blackish/green needles, (0.04g, 41%), mp 169-172°C. ν_{max}: 2218, 1551, 1472, 1327, 1145, 975 and 651cm^{-1}.

Found C: 56.61%, H: 2.62%, N: 14.24%, S: 25.11%. $C_{23}H_{13}N_5S_4$ requires C: 56.65%, H: 2.69%, N: 14.36%, S: 26.30%.

2-(2-Benzyl-3-dicyanomethylene-2,3-dihydro-isoindol-1-ylidene)-malononitrile (141)-TTF complex

2-(2-Benzyl-3-dicyanomethylene-2,3-dihydro-isoindol-1-ylidene)-malononitrile (141) (0.05g, 0.15mmol) and TTF (0.03g, 0.15mmol) were added to acetonitrile (15cm^3). The resultant mixture was heated under reflux until all the solid material was dissolved. An oil bath was used in order to facilitate slower cooling. The reaction mixture was allowed to cool to room temperature overnight. 2-(2-Benzyl-3-dicyanomethylene-2,3-dihydro-isoindol-1-ylidene)-malononitrile (141)-TTF complex was isolated as dark green needles. The complex was recrystallised from acetonitrile, to yield the 2-(2-benzyl-3-dicyanomethylene-2,3-dihydro-isoindol-1-ylidene)-malononitrile (141)-TTF complex, (0.05g, 62%), mp 207-210°C. ν_{max}: 2924, 2219, 1558, 1480, 1331, 1223, 147, 1113, 978, 779, 732 and 654cm^{-1}.
Found C: 60.24%, H: 2.78%, N: 13.00%, S: 23.44%. $C_{27}H_{15}N_5S_4$ requires C: 60.31%, H: 2.81%, N: 13.02%, S: 23.85%.

2-(2-Ethyl-3-dicyanomethylene-2,3-dihydro-isoindol-1-ylidene)-malononitrile (140)-TTF complex

2-(2-Ethyl-3-dicyanomethylene-2,3-dihydro-isoindol-1-ylidene)-malononitrile (140) (0.02g, 0.07mmol) was dissolved in dichloromethane (20cm^3). TTF (0.015g, 0.07mmol) was then added. The solution immediately became green in colour. The reaction mixture was sealed under argon and allowed stand overnight. The solvent was evaporated off to yield a green solid. This solid was recrystallised from acetonitrile to give 2-(2-ethyl-3-dicyanomethylene-2,3-dihydro-isoindol-1-ylidene)-malononitrile (140)-TTF complex as dark green needles, (0.02g, 60%), mp 177-179°C. ν_{max}: 2217, 1547, 1397, 1338, 1226, 1088, 759 and 688cm^{-1}.

3-Dicyanomethylene-2-pentyl-2,3-dihydro-isoindol-1-ylidene-cyanamide (185)-TTF complex

3-Dicyanomethylene-2-pentyl-2,3-dihydro-isoindol-1-ylidene-cyanamide (185) (0.03g, 0.1mmol) was dissolved in dichloromethane (15cm^3). TTF (0.02g, 0.1mmol) was then added. The solution immediately changed colour, to dark green. The mixture was sealed under argon and stored at room temperature for 24 hours. The solvent was then removed under reduced pressure. A very dark green viscous oil was subsequently isolated. On cooling this oil solidified, to yield 3-dicyanomethylene-2-pentyl-2,3-dihydro-isoindol-1-ylidene-cyanamide (185)-TTF complex as a green powder, (0.04g, 81%), mp 105-107°C. ν_{max}: 3068, 2930, 2222, 2186, 1633, 1570, 1405, 1215, 1102, 795 and 657cm^{-1}.

Found C: 55.79%, H: 3.87%, N: 13.98%, S: 24.87%. $C_{23}H_{19}N_5S_4$ requires C: 55.95%, H: 3.88%, N: 14.19%, S: 25.98%.

3-Dicyanomethylene-2-decyl-2,3-dihydro-isoindol-1-ylidene-cyanamide (186)-TTF complex

3-Dicyanomethylene-2-decyl-2,3-dihydro-isoindol-1-ylidene-cyanamide (186) (0.03g, 0.08mmol) was dissolved in dichloromethane (15cm^3). TTF (0.02g, 0.08mmol) was then added. The solution turned a green colour. After 24 hours the solvent was evaporated off to yield a dark green oil. This oil was placed in the freezer overnight. 3-Dicyanomethylene-2-decyl-2,3-dihydro-isoindol-1-ylidene-cyanamide (186)-TTF complex was isolated as a dark green powder, (0.03g, 67%), mp 64-66°C. ν_{max}: 3069, 2923, 2222, 2191, 1637, 1570, 1472, 1408, 1214, 1100, 794 and 687cm^{-1}.

Found C: 60.50%, H: 5.28%, N: 12.53%, S: 21.69%. $C_{28}H_{29}N_5S_4$ requires C: 59.65%, H: 5.18%, N: 12.42%, S: 22.75%.

Chapter 6
References

1. H. Amamatu, H. Inokuchi and Y. Matsunaga, *Nature*, 1954, **173**, 168.
2. T.E. Philips, T.J. Kistenmacher, J.P. Ferraris and D.O. Cowan, *J. Chem. Soc. Chem. Commun.*, 1973, 471.
3. L.R. Melby, R.J. Harder, W.R. Hartler, W, Mahler, R.E Benson and W.E. Mochel, *J. Am. Chem. Soc.*, 1962, **84**, 3374.
4. F. Wudl, G.M. Smith and E.F. Hufnagel, *J. Chem. Soc. Chem. Commun.*, 1970, 1453.
5. (a)J. Jerome, A Mazand, M. Ribault and K. Bechgaard, *J. Phys. Lett.,* 1980, **41**, 495. (b) K. Bechgaard, C.S. Jacobsen, K. Mortonsen, H.J. Pedersen and N. Thorup, *Solid State Commun.*, 1980, **33**, 1119.
6. H.W. Kroto, J.R. Heath, C.O' Brien, R.F. Curl and R.E. Smalley, *Nature*, 1985, **318**, 162. (b) W. Krattscher, L.D. Lamb, K. Fostirpoulos and D.R. Huffman, *Nature*, 1990, **347**, 354.
7. A.F. Hebard, M.J. Rosseinsky, D.W. Murphy, S.H. Glarum, T.T.M. Palstra, A.P. Ramirez and A.R. Kortan, *Nature,* 1991, **350**, 600.
8. R.S. Mulliken, *J. Am. Chem. Soc.*, 1952, **74**, 811. (b) R.S. Mulliken and W.B. Person, *J. Am. Chem. Soc.*, 1969, **91**, 3409.
9. J.B. Torrance, *Mol. Cryst. Liq. Cryst.*, 1985, **126**, 55.
10. A.W. Hanson, *Acta. Cryst.*, 1968, **B24**, 768.
11. R.E. Periels, *Quantum Theory of Solids*, Oxford University Press, Oxford, 1972.
12. J.K. Burdett, *Chem. Soc. Rev.*, 1994, 299.
13. S.S.P. Parkin, F. Creuzet, M.Ribault, D. Jerome, K. Bechgaard and J.M. Fabre, *Mol. Cryst. Liq. Cryst.*, 1982, **79**, 249.
14. J. Bardeen, L.N Cooper and J.R. Schrieffer, *Phys. Rev.*, 1957, **108**, 1175.
15. W.A. Little, *Scientific American,* 1965, **212**, 21.
16. F. Wudl, G.M. Smith and E.J. Hufnagel, *J. Chem. Soc., Chem. Commun.,* 1970,1453.
17. F.D. Seava, B.P. Morgan, M.W. Fichner and N.F. Haley, *J. Org. Chem.,* 1984, **49**, 390.
18. G. Scherowsky and J. Weiland, *Chem. Ber.,* 1974, **107**, 3155.
19. P. Blanchard, M. Salle, G. Duguay, M. Jubault and A. Gorgues, *Tetrahedron Lett.,* 1992, **33**, 2685.
20. T. Kawase, H. Awaji, S. Yoneda and Z. Yosida, *Heterocycles,* 1982, **18**, 123.

21. Z. Yoshida, T. Kawase H. Awaji and S.Yoneda, *Tetrahedron Lett.,* 1983, **24**, 3469.
22. Z. Yoshida, T. Kawase, H. Awaji and S. Yoneda, *ibid.,* 1983, **24**, 3473.
23. T.K. Hansen, M.V. Lakshmikantham, M.P. Cava R.M. Metzger and J. Becher, *J. Org. Chem.,* 1991, **56**, 2720.
24. A. Moore, M. Bryce, *Tetrahedron Lett.,* 1993, **33**, 1373.
25. Y. Misaki, N. Higuchi, H. Fujiwara, T. Yamabe, T. Mori, H. Mori and S. Tanaka, *Angew. Chem. Int. Ed. Engl.,* 1995, **34**, 11, 1222.
26. S. Liu, M. Cariou and A. Gorgues, *Tetrahedron Lett.,* 1998, **39**, 8663.
27. A. Moore and M. Bryce, *J. Chem. Soc. Perkin Trans. 1*, 1991, 157.
28. (a) N. Martin, L. Sanchez, C. Seoane and, C. Fernandez, *Synth. Met.,* 1996, **78**, 137. (b) N. Martin, L. Sanchez, C. Seoane, E. Orti, P. M. Viruela and R. Viruela, *J. Org. Chem.,* 1998, **63**, 1268.
29. Y. Yamashita, M. Tomura, S. Tanaka and K. Imaeda, *ibid.,* 1997, **86**, 1795.
30. A. Faldt, M. Pedersen, T. Krogh, L. Hviid and J. Christensen, *ibid.,* 1998, **94**, 307.
31. K. Takashi, T. Nihira, M. Yoshifuji and K. Tomitani, *Bull. Chem. Soc. Jpn.,* 1993, **66**, 2330.
32. K. Takimiya, T. Otsubo, F. Ogura, H. Ashitaka, K. Morita and T. Suehiro, *ibid.,* 1994, **67**, 255.
33. K. Takahashi and K. Tomitani, *J. Chem. Soc., Chem. Commun.,* 1995, 821.
34. D. Green, *J. Chem. Soc., Chem. Co*mmun., 1977, 161.
35. D. Green, *J. Org. Chem.*, 1979, **44**, 9, 1476.
36. M Bryce, G. Cooke, A. Dhinsda, D. Lorcy, A. Moore, M. Petty, M. Hursthouse and A. Karaulov, *J. Chem. Soc., Chem. Commun.,* 1990, 816.
37. J-M. Febre, J. Garin, S. Uriel, *Tetrahedron Lett.*, 1991, **32**, 6407.
38. J Becker, J Bernstein, S. Bittner, L. Shahal and S. Shaik, *J. Chem. Soc.*, Chem. Commun., 1991, 93.
39. R. Andreu, J. Garin, J. Orduna, M. Saviron and S. Uriel, *Tetrahedron Lett.*, 1995, **36**, 4319.
40. S.-Y. Hsu and L. Chiang, *J. Org. Chem.*, 1987, **52**, 3444.
41. A. Moore, M. Bryce, G. Cooke, G. Marshallsay, P. Skabara, A. Batsanov, J. Howard and S. Daley, *J. Chem. Soc., Perkin Trans. 1*, 1993, 1403.

42. A. Moore, M. Bryce, A. Batsanov, J. Heaton, C. Lehmann, J. Howard, N. Robertson, A. Underhill and I. Perepichka, *J. Mater. Chem.*, 1998, **8**, 1541.
43. M. Iyoda, S. Sasski, M. Miura, M. Fukuda and J. Yamauchi, *Tetrahedron Lett.*, 1999, **40**, 2807.
44. K. Simonsen, N. Svenstrup, J. Lau, O. Simonsen, P. Mork, G. Kristensen and J. Becher, *Synthesis,* 1996, 407.
45. A. Batsanov, D. John, M. Bryce and J. Howard, *Adv. Mater.*, **10**, 16, 1360, 1998.
46. A. Krief, *Tetrahedron*, 1986, **42**, 1209.
47. G. Papavassiliou, A. Terzis and P. Delhaes, *Handbook of Organic Conductive Molecules and Polymers*, ed. H. Nalwa, Wiley, 1997, **1**.
48. T K. Hanson, I. Jenkins, K. S. Vaima, S. Edge, S. Larsen, J. Becher, A. E. Underhill, *J. Chem. Soc., Perkin Trans. 2*, 1991, 1963.
49. M. Mizuno, A. Garrito and M. P. Cava, *J. Chem. Soc., Chem. Commun.,* 1978,18.
50. S. Nakatsuji, Y. Amano, H. Kawamura and H. Anzai, *J. Chem. Soc., Chem. Commun.,* , 841.
51. R. L. Meline and R. L. Elsebaumer, *Synth. Met.,* 1997, **86**, 1845.
52. J. M. Williams, M. A. Beno, H. H. Wang, P. C. Leung, T. J. Enge and K. D. Carlson, *Acc. Chem. Res.,* 1985, **18**, 261.
53. J. M. Williams, T. J. Emge, H. H. Wang, M. A. Beno, P. T. Copps, L. N. Hall, K. D. Carlson and G. W. Crabtree, *Inorg. Chem.,* 1984, **23**, 2558.
54. J. M. Williams, H. H. Wang, M. A. Beno, T. J. Emge, L. M. Sowa, P. T. Copps, F. Behroozi, L. N. Hall, K. D. Carlson and G. W. Crabtree, *Inorg. Chem.,* 1984, **23**, 3839.
55. H. Urayama, H. Yamochi, G. Saito, K. Nozawa, T. Sugano, M. Kinoshita, S. Sato, K. Oshima, A. Kawamoto and J. Tanaka, *Chem. Lett.,* 1988, 55.
56. A. M. Kini, U. Geiser, H. H. Wang, K. D. Carlson, J. M. Williams, W. K. Kwok, K. G. Vandervoort, J. E. Thompson, D. L. Stupka, D. Lung and M-H. Whangbo, *Inorg. Chem.,* 1990, **29**, 2555.
57. J. M. Williams, A. M. Kini, H. H. Wang, K. D. Carlson, U. Geiser, L. K. Montgomery, G. J. Pyrka, D. M. Watkins, J. M. Kommers, S. J. Boryschuk, A. V.

Strieby Crouch, W. K. Kwok, J. E. Schirber, D. L. Overmyer, D. Jung and M-H. Whangbo, *Inorg. Chem.,* 1990, **29**, 3262.

58. U. Geiser, J. A. Schlueter, K. D. Carlson, J. M. Williams, H. H. Wang, W-K. Kwok, U. Welp, J. A. Fendrich, J. D. Dudek, C. A. Achenbach, A. S. Komosa, P. M. Keane, D. Naumann, T. Roy, J. E. Schirber, W. R. Bayless, J. Ren and M-H. Whangbo, *Synth. Met.,* 1995, **70**, 1105.
59. (a) T. Mochida, T. Hasegawa, S. Kagoshima, S. Sugiura and Y. Iwasa, *Synth. Met.,* 1997, **86**, 1797. (b) T. Hasegawa, K. Inukai, S. Kagoshima, T. Sugawara, T. Mochida, S. Sugiura and Y. Iwasa, *ibid.,* 1997, **86**, 1801.
60. T. Suzuki, H. Yamochi, G. Srdanov, K. Hinkelmann and F. Wudl, *J. Am. Chem. Soc.,* 1989, **111**, 3108.
61. M. A. Beno, H. H. Wang, A. M. Kini, K. D. Carlson, U. Geiser, W. K. Kwok, J. E. Thompson, J. M. Williams, J. Ren and M-H. Whangbo, *Inorg. Chem.,* 1990, **29**, 1601.
62. S. Kahlich, D. Scheitzer, I. Heinen, S. En Lan, B. Nuber, H. J. Keller, K. Winzer and H. W. Helberg, *Solid State Commun.,* 1991, **80**, 1991.
63. J. Garin, *Adv. in Heterocyclic Chem.,* 1995, **62**, 249.
64. A. Moradpour, V. Peryrussan, I. Johansen, K. Bechgaard, *J. Org. Chem.,* 1982, **48**, 388.
65. A. Andrieux, C. Duroure, D. Jerome and K. Bechgaard, *J. Phys. Lett.,* 1979, **40**, 381.
66. D. Jerome, A. Mazoud, M. Ribault and K. Bechgaard, *J. Phys.,* 1980, **41**, 95.
67. K. Bechgaard, K. Carneiro, F. B. Rasmussen and M. Olsen, *J. Am. Chem. Soc.,* 1981, **103,** 2440.
68. M-H. Whango, J. W. Williams, M. A. Beno and J. R. Dorfman, *J. Am. Chem. Soc.,* 1983, **105**, 645.
69. M. A. Beno, G. S. Blackman, P. C. W. Leung and J. M. Williams, *Solid State Commun.,* 1983, **48**, 99.
70. H. Kobayashi, T. Udagawa, H. Tomita, K. Bun, T. Naito and A. Kobayashi, *Chem. Lett.,* 1993, 1559.

71. (a) H. Kobayashi, T. Tomita, T. Naito, H. Tanaka, A. Kobayashi and T. Saito, *J. Chem. Soc. Chem. Commun.,* 1995, 1225. (b) Y. Misaki, H. Fujiwara, T. Yamabe, T. Mori, H. Mori and S. Tanaka, *Chem. Lett.,* 1994, 1653.
72. H. Kobayashi, A. Sato, H. Akutsu, E. Arai, H. Akutsu, A. Kobayashi and P. Cassoux, *J. Am. Chem. Soc.,* 1997, **119**, 12392.
73. F. Wudl and E. Aharon-Shalom, *J. Am. Chem. Soc.,* 1982, **104**, 1154.
74. R. D. McCullough, G. B. Kok, K. A. Lerstup and D. O. Cowan, *J. Am. Chem. Soc.,* 1987, **109**, 4115.
75. M. D. Mays, R. D. McCullough, D. O. Cowan, T. O. Poehler, W. A. Bryden and T. J. Kistenmacher, *Soild State Commun.,* 1988, **65**, 1089.
76. (a) E. Aharon-Shalom, J. Y. Becker, J. Bernstein, S. Bittner and S. Shaik, *Tetrahedron Lett.,* 1985, **26**, 23, 278. (b) N. Okada, H. Yamochi, F. Shinozaki, K. Oshima and G. Saito, *Chem. Lett.,* 1986, 1861.
77. J. Y. Becker, J. Bernstein, M. Dayan and L. Shalal, *J. Chem. Soc. Chem. Commun.,* 1992, 1048.
78. C. Wang, A. Ellern, J. Y. Becker and J. Bernstein, *Tetrahedron Lett.,* 1994, **35**, 45, 8489.
79. D. S. Ackler and W. R. Hertler, *J. Am. Chem. Soc.,* 1962, **84**, 3370.
80. M. Uno, K. Seto, M. Masuda, W. Ueda and S. Takahashi, *Tetrahedron Lett.,* 1985, **26**, 12, 1553.
81. W. Lehnert, *Tetrahedron Lett.,* 1970, 4723.
82. A. Aumuller, S. Hunig, *Liebegs Ann. Chem.,* 1984, 618.
83. L. B. Coleman, M. J. Cohen, D. J. Sandman, F. G. Yamagishi, A. F. Garito and A. J. Heeger, *Solid State Commun.,* 1973, **12**, 1125.
84. J. Diekmann, W.R. Hertler and R. E. Benson, *J. Org. Chem.,* 1963, **28**, 2719.
85. R. C. Wheland and E. L. Martin, *J. Org. Chem.,* 1975, **40**, 3101.
86. M. R. Bryce, A. M. Grainger, M. Hasan, G. J. Ashwell, P. A. Bates and M. B. Husrthouse, *J. Chem. Soc., Perkin Trans. 1,* 1992, 611.
87. S. Yamaguchi and T. Hanafusa, *Chem. Lett.,* 1985, 689.
88. S. L. Vorobeva and N. N. Korotkova, *J. Chem. Res.*, 1993, 34.
89. A. Kini, M. Mays and D. Cowan, *J. Chem. Soc., Chem. Commun.,* 1985, 286.

90. M. D. Ward, *Electroanal. Chem.,* 1989, **16**, 182.

91. D. J. Sandman and A. F. Garito, *J. Org. Chem.,* 1974, **39**, 1165.

92. S. Chaterjee, *J. Chem. Soc. B,* 1967, 1170.

93. S. Yamaguchi, H. Tatemitsu, Y. Sakata and S. Misumi, *Chem. Lett.,* 1983, 1229.

94. N. Martin, J. L. Segura, C. Seoane, P de la Cruz, F. Langa, E. Orti, P. M. Viruela and R. Viruela, *J. Org. Chem.,* 1995, **60**, 4077.

95. T. Yanagimoto, K. Takimiya, T. Otsubo and F. Ogura, *J. Chem. Soc., Chem. Commun.,* 1993, 519.

96. N. Martin, R. Behnisch and M. Hanack, *J. Org. Chem.,* 1989, **54**, 2563

97. S. Gronowitz and B. Uppstrom, *Acta Chemica Scand. B*, 1974, **28**, 981.

98. H. Ishida, K. Yui, Y. Aso, T. Otsubo and F. Ogura, *Bull. Chem. Soc. Jpn.*, 1990, **63**, 2828.

99. K. Yui, Y. Aso, T. Otsuba and F. Ogura, *J. Chem. Soc., Chem. Commun.,* 1987, 1816.

100. K. Yui, Y. Aso, T. Otsubo and F. Ogura, *Chem. Lett.*, 1988, 1179.

101. K. Suzuki, M. Tomura, S. Tanaka and Y. Yamashita, *Tetrahedron Lett.,* 2000, **41**, 8359.

102. M. Fuji, Y.Aso, T. Otsubo and F. Ogura, *Synth. Met.,* 1993, **55-57**, 2136.

103. K. Yui, H. Ishida, Y. Aso, T. Otsubo, F. Ogura, A. Kawamoto and J. Tanaka, 1989, **62**, 1547.

104. S. Yoshida, M. Fujii, Y. Aso, T. Otsubo and F. Ogura, *J. Org. Chem.,* 1994, **59**, 3077.

105. K. Takahashi and S. Tarutani, *J. Chem. Soc., Chem. Commun.,* 1998, 1233.

106. K. Kobayashi and C. L. Gajurel, *J. Chem. Soc., Chem. Commun.,* 1986, 1779.

107. P. de la Cruz, N. Martin, F. Miguel, C. Seoane, A. Albert, F. H. Cano, A. Gonzalez and J. M. Pingarron, *J. Org. Chem.,* 1992, **57**, 6192.

108. Y. Ohba, Y. Murakami, T. Sone and H. Awano, *J. Heterocyclic Chem.,* 1997, **34**, 781.

109. F. Iwasaki, S. Hironaka, N. Yamazaki and K. Kobayashi, *Bull. Chem. Soc. Jpn.,* 1992, **65**, 2187.

110. Y. Yamashita, T. Suzuki, T. Mukai and G. Saito, *J. Chem. Soc., Chem. Commun.*, 1985, 1044.

111. T. Suzuki, Y. Yamashita, C. Kabuto and T. Miyashi, *J. Chem. Soc., Chem. Commun.,* 1989, 1102.

112. T. Suzuki, H. Fujii, Y. Yamashita, C. Kabuto, S. Tanaka, M. Harasawa, T. Mukai and T. Miyashi, *J. Am. Chem. Soc.,* 1992, **114**, 3034.

113. T. Suzuki, C. Kabuto, Y. Yamashita, T. Mukai, T. Miyashi and G. Saito, *Bull. Chem. Soc. Jpn.,* 1988, **61**, 483.

114. T. Suzuki, C. Kabuto, Y. Yamashita and T. Mukai, *Bull. Chem. Soc. Jpn.,* 1987, **60**, 2111.

115. T. Fukushima, N. Okazeri, T. Miyashi, K. Suzuki, Y. Yamashita and T. Suzuki, *Tetrahedron Lett.,* 1999, **40**, 1175.

116. A. Aumuller and S. Hunig, Angew. *Chem. Int. Ed. Engl.,* 1984, **23**, 447.

117. H. Almen, T. Bauer, S. Hunig, V. Kupcik, U. Langohr, T. Metzenthin, K. Meyer, H. Rieder, J. U. von Schultz, E. Tillsmann and H. C. Wolff, *Angew. Chem. Int. Ed. Engl.,* 1991, **30**, 561.

118. A. Aumuller, P. Erk, S. Hunig, J. U. von Schultz, W. C. Wolf and G. Klebe, *Chem. Ber.,* 1991, **124**, 1445.

119. A. Aumuller and S. Hunig, *Liebigs Ann. Chem.,* 1986, 142.

120. N. Martin, J. A. Navarro, C. Seoane, A. Albert, F. H. Cano, J. Y. Becker, V. Khodorkovsky, E. Harlev and M. Hanack, *J. Org. Chem.,* 1992, **57**, 5726.

121. M. R. Bryce, S. R. Davies, A. M. Grainger, J. Hellberg, M. B. Hursthouse, M. Mazid, R. Bachmann and F. Gerson, *J. Org. Chem.,* 1992, **57**, 1690.

122. E. Barranco, N. Martin, J. L. Segura, C. Seoane, P. de la Cruz, F. Langa, A. Gonzalez and J. M. Pingarron, *Tetrahedron,* 1993, **49**, 22, 4881.

123. N. Martin, P. de Miguel, C. Seoane, A. Albert and F. H. Cano, *J. Mater. Chem.,* 1997, **7**, 25.

124. S. Hunig and P. Erk, *Adv. Mater.,* 1991, **3**, 225.

125. K. Sinzger, S. Hunig, M. Jopp, D. Bauer, W. Bietsch, J. U. von Schultz, H. C. Wolf, R. K. Kremer, T. Metzmann, R. Bau, S. I. Kahn, A. Lindbaum, C. L. Lengauer and E. Tillmans, *J. Am. Chem. Soc.,* 1993, **115**, 7696.

126. A. Aumuller, P. Erk, G. Klebe, S. Hunig, J. U. von Schultz and H-P. Werner, *Angew, Chem. Int, Ed, Engl.,* 1986, **25**, 740.

127. A. Kobayashi, R. Kato, H. Kobayashi, T. Mori and H. Inokuchi, *Solid State Commun.,* 1987, **64**, 45.

128. R. Kato, H. Kobayashi and A. Kobayashi, *J. Am. Chem. Soc.,* 1989, **111**, 5224.

129. C. Wang, A. S. Batsanov, M. R. Bryce and J. A. K. Howard, *Synthesis,* 1998, 1615.

130. (a) A. Kobayashi and H. Kobayashi, *Handbook of Conductive Molecules and Polymers,* **Vol 1**, ed. H. S. Nalwa, Wiley, 1997. (b) P. Cassoux, *Coordination Chem. Rev.,* 1999, **185-186**, 213.

131. J. Y. Becher, J. Bernstein, S. Bittner, N. Levi and S. Shaik, *J. Org. Chem.,* 1988, **53**, 1689.

132. J. L. Segura, N. Martin, C. Seoane and M. Hanack, *Tetrahedron Lett.,* 1996, **37**, 2503.

133. R. Gompper, H-U. Wagner and E. Kuttner, *Chem. Ber.,* 1968, **101**, 4123.

134. M. A. Herranz, N. Martin, L. Sanchez, J. Garin, J. Orduna, R. Alcala, B. Villacampa and C. Sanchez, *Tetrahedron,* 1998, **54**, 11651.

135. R. A. Metzger, B. Chen, U. Hopfer, M. V. Lakshmikantham, D. Vuillaume, T. Kawai, X. Wu, H. Tachibana, T. V. Hughes, H. Sakurai, J. W. Baldwin, C. Hosch, M. P. Cava, L. Brehmer and G. J. Ashwell, *J. Am. Chem. Soc.,* 1997, **119**, 10455.

136. M. R. Bryce, *J. Mater. Chem.,* 2000, **10**, 589.

137. A. Eckell, H. Eilingsfeld, A. Elzer, F. Feichmayr, G. Hoffmann, R. J. Leyrer and P. Neumann, DE 310953, BASF AG, 1982.

138. S. P. Conway, Ph. D. Thesis, DCU, 1996.

139. R. P. Linstead and Rowe, *J. Chem. Soc.*, 1940, 1070.

140. J. A. Elvidge, J. S. Fitt and R. P. Linstead, *J. Chem. Soc.*, 1956, 235.

141. Farbenfabriken Bayer Aktiongesellschaft, *French Patent No.* 1537299, 1968.

142. P. F. Clark, J. A. Elvidge and R. P. Linstead, *J. Chem. Soc.*, 1953, 3593.

143. P. F. Clark, J. A. Elvidge and J. H. Golden, *J. Chem. Soc.*, 1956, 4135.

144. L. I. Spiessens and M. J. O. Anteunis, Bull. *Soc. Chim. Belg.*, 1983, **92**, 965.

145. (a) D. R. Prevorsek, *J. Phys. Chem.* **66**, 769, 1962. (b) D. R. Prevorsek, *Bull. Chim. Fr.*, 1958, 788.

146. O. Mitsunobu, *Bull. Chem. Soc. Jpn.,* 1967, **40**, 935.

147. O. Mitsunobu and M. Yamada, *ibid.,* 1967, **40**, 2380.

148. O. Mitsunobu and M. Eguchi, *ibid.,* 1971, **44**, 3427.

149. O. Mitsunobu, *Synthesis,* 1981,1.

150. E. Grochowski, B. D. Hilton, R. J. Kupper and C. J. Michejda, *J. Am. Chem. Soc.,* 1982, **104**, 6876.

151. M. von Itzstein and I. D. Jenkins, *Aust. J. Chem.,* 1983, **36**, 557.

152. M. Varasi, K. A. M. Walker and M. L. Maddox, *J. Org. Chem.,* 1987, **52**, 4235.

153. D. Camp and I. D. Jenkins, *J. Org. Chem.,* 1989, **54**, 3045.

154. J. March, *Advanced Organic Chemistry*, 2nd ed., 232.

155. D. L. Hughes, R. A. Reamer, J. J. Bergan and E. Grabowski, *J. Am. Soc.*, 1988, **110**, 6487.

156. T. Tsunoda, Y. Yamamiya and S. Ito, *Tetrahedron Lett.*, 1993, **34**, 1639.

157. T. Tsunoda, J. Otsuka, Y. Yamamiya and S. Ito, *Chem. Lett.*, 1994, 539.

158. T. Tsunoda, M. Nagaku, C. Nagino, Y. Kawamura, F. Ozaki, H. Hioki and S. Ito, *Tetrahedron Lett.,* 1995, **36**, 2531.

159. T. Tsunoda, Y. Yamamiya, Y. Kawamura and S. Ito, *Tetrahedron Lett.,* 1995, **36**, 2529.

160. O. Mitsunobu, M. Wada and T. Sano, *J. Am. Chem. Soc.,* 1971, **94**, 679.

161. O. P. Vig, I. R. Trehan, G. L. Kad and J. Ghose, *Indian J. Chem.,* 1983, **22B**, 515.

162. O. P. Vig, I. R. Trehan, G. L. Kad, S. Kumari and A. L. Bedi, *Indian J. Chem.,* 1985, **62**, 238.

163. M. A. Walker, *J. Org. Chem.,* 1995, **60**, 5353.

164. A. D. Dunn, *J. Heterocyclic Chem.,* 1984, **21**, 965.

165. P. A. Christensen and A. Hamnet, *Techniques and Mechanisms in Electrochemistry*, Blackie Academic and Professional, 1994.

166. P. Carloni, L. Greci, P. Stipa, D. Dopp, A. El-Din, A. Hafeez Hassan and A. Alberti, *Tetrahedron,* 1995, **51**, 7451.

167. J. S. Chappell, A. N. Bloch, W. A. Bryden, M. Maxfield, T.O. Poehler and D. O. Cowan, *J. Am. Chem. Soc.*, 1981, **103**, 2442.

168. J. Delaney, Ph. D. Thesis DCU, 1997.

Appendices

Appendix 1

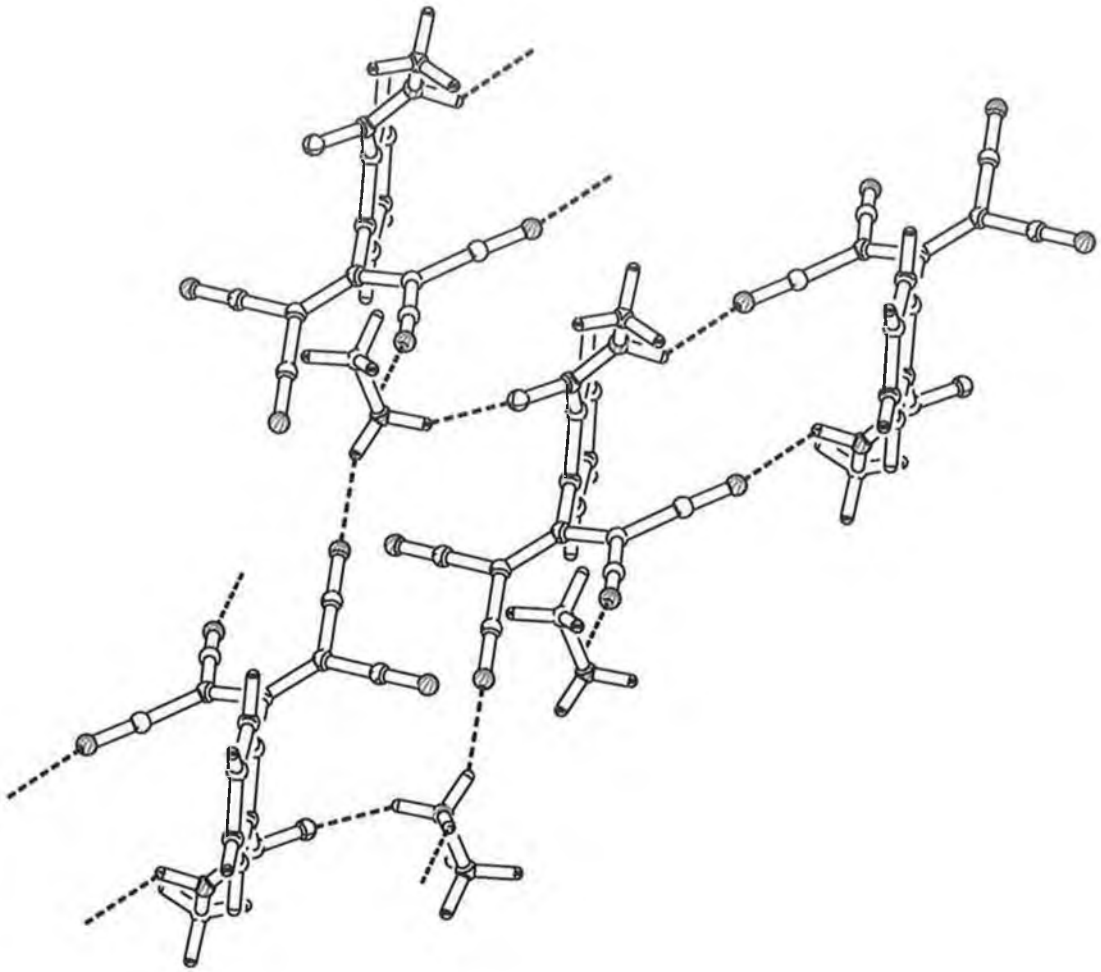

Hydrogen bonding in methylammonium salt (154)

The hydrogen bonding details are as follows and can be viewed in Figure 2:

Intra- and Intermolecular hydrogen bonds and contacts

N-H... N	code	D-H	H... D	D... A	Angle
N1-H1... N11	[2_567]	0.89	2.35	2.994(17)	129
N41-H41... N12	[1_655]	0.89	2.10	2.900(17)	150
N41-H42... N32	[2_556]	0.89	2.14	2.957(16)	152
N41-H43... O1	[1_555]	0.89	1.88	2.711(14)	155

Translation of ARU-code to Equivalent Position

[2_567] = -x,1-y,2-z

[2_556] = -x,-y,1-z

[1_655] = 1+x,y,z

Acknowledgements

Dr.Alan J. Lough (University of Toronto) should be thanked for the crystal selection and subsequent data collection on the kappa-CCD diffractometer and initial interpretation of the crystal structure.

Table 1. Crystal data and structure refinement for (154).

Identification code	ACP
Empirical formula	C16 H14 N5 O
Formula weight	292.32
Temperature	150(2) K
Wavelength	0.71073 A
Crystal system, space group	Triclinic, P-1 (No. 2)
Unit cell dimensions	a = 8.0328(16) A alpha = 77.72(3) deg
	b = 10.056(2) A beta = 86.86(3) deg
	c = 10.144(2) A gamma = 85.52(3) deg
Volume	797.5(3)
Z, Calculated density	2, 1.217 Mg/m^3
Absorption coefficient	0.081 mm^-1
F(000)	306
Crystal size	0.1 x 0.1 x 0.05 mm
Theta range for data collection	4.20 to 25.63 deg.
Index ranges	-9<=h<=0, -11<=k<=11, -12<=l<=11
Reflections collected / unique	2262 / 2262 [R(int) = 0.08]
Completeness to 2theta = 25.63	75.2%
Refinement method	Full-matrix least-squares on F^2
Data / restraints / parameters	2262 / 1 / 216
Goodness-of-fit on F^2	1.819
Final R indices [I>2sigma(I)]	R1 = 0.1922, wR2 = 0.4649
R indices (all data)	R1 = 0.2609, wR2 = 0.4852
Extinction coefficient	0.15(5)
Largest diff. peak and hole	0.439 and -0.567 e.A^-3

Table 2. Atomic coordinates (x 10^4) and equivalent isotropic displacement parameters (A^2 x 10^3) for (154).
U(eq) is defined as one third of the trace of the orthogonalized Uij tensor.

	x	y	z	U(eq)
O(1)	1855(11)	3894(8)	6086(9)	56(3)
N(1)	1513(13)	5379(11)	7470(11)	48(3)
C(1)	-1076(15)	2325(13)	8089(12)	49(3)
C(2)	408(14)	1562(12)	7958(12)	43(3)
C(3)	654(17)	564(13)	7214(13)	50(3)
N(11)	-1592(15)	3806(13)	9863(13)	64(4)
C(11)	-1326(15)	3155(15)	9078(14)	54(4)
N(12)	-3552(16)	2479(12)	6526(12)	65(4)
C(12)	-2493(17)	2405(12)	7223(15)	51(3)
N(31)	3556(16)	-593(11)	6819(11)	59(3)
C(31)	2278(17)	-90(13)	7035(13)	47(3)
N(32)	-1734(14)	-524(11)	6267(11)	60(3)
C(32)	-647(17)	-14(12)	6687(12)	47(3)
C(21)	1831(16)	1852(11)	8724(12)	44(3)
C(22)	2390(17)	872(15)	9775(12)	55(4)
C(23)	3712(16)	1156(13)	10564(14)	57(4)

C(24)	4427(16)	2360(14)	10248(14)	56(4)
C(25)	3804(15)	3344(13)	9161(12)	48(3)
C(26)	2568(14)	3106(12)	8436(13)	48(3)
C(4)	1940(15)	4213(13)	7230(13)	45(3)
C(5)	813(17)	6471(16)	6482(15)	70(4)
N(41)	3876(14)	2379(10)	4658(11)	58(3)
C(51)	4267(18)	3518(13)	3519(14)	62(4)

Table 3. Selected bond lengths [A] and angles [deg] for (154).

O(1)-C(4)	1.274(14)
N(1)-C(4)	1.266(15)
N(1)-C(5)	1.422(18)
N(1)-H(1)	0.89(3)
C(1)-C(2)	1.382(17)
C(1)-C(11)	1.43(2)
C(1)-C(12)	1.463(19)
C(2)-C(3)	1.375(17)
C(2)-C(21)	1.497(16)
C(3)-C(32)	1.416(18)
C(3)-C(31)	1.44(2)
N(11)-C(11)	1.137(16)
N(12)-C(12)	1.124(15)
N(31)-C(31)	1.139(15)
N(32)-C(32)	1.187(15)
C(21)-C(22)	1.358(17)
C(21)-C(26)	1.403(16)
C(22)-C(23)	1.444(17)
C(22)-H(22)	0.9300
C(23)-C(24)	1.350(18)
C(23)-H(23)	0.9300
C(24)-C(25)	1.401(18)
C(24)-H(24)	0.9300
C(25)-C(26)	1.332(16)
C(25)-H(25)	0.9300
C(26)-C(4)	1.546(17)
C(5)-H(5A)	0.9600
C(5)-H(5B)	0.9600
C(5)-H(5C)	0.9600
N(41)-C(51)	1.483(16)
N(41)-H(41)	0.8900
N(41)-H(42)	0.8900
N(41)-H(43)	0.8900
C(51)-H(51)	0.9600
C(51)-H(52)	0.9600
C(51)-H(53)	0.9600
C(4)-N(1)-C(5)	122.8(12)
C(4)-N(1)-H(1)	116(9)
C(5)-N(1)-H(1)	106(9)
C(2)-C(1)-C(11)	121.8(10)
C(2)-C(1)-C(12)	124.1(11)
C(11)-C(1)-C(12)	114.0(10)
C(3)-C(2)-C(1)	125.4(10)
C(3)-C(2)-C(21)	118.7(11)

C(1)-C(2)-C(21)	115.8(12)
C(2)-C(3)-C(32)	124.4(12)
C(2)-C(3)-C(31)	121.5(11)
C(32)-C(3)-C(31)	113.8(11)
N(11)-C(11)-C(1)	177.2(13)
N(12)-C(12)-C(1)	178.1(14)
N(31)-C(31)-C(3)	176.3(14)
N(32)-C(32)-C(3)	178.5(12)
C(22)-C(21)-C(26)	118.7(11)
C(22)-C(21)-C(2)	118.4(11)
C(26)-C(21)-C(2)	122.9(10)
C(21)-C(22)-C(23)	119.2(13)
C(21)-C(22)-H(22)	120.4
C(23)-C(22)-H(22)	120.4
C(24)-C(23)-C(22)	121.0(12)
C(24)-C(23)-H(23)	119.5
C(22)-C(23)-H(23)	119.5
C(23)-C(24)-C(25)	117.8(11)
C(23)-C(24)-H(24)	121.1
C(25)-C(24)-H(24)	121.1
C(26)-C(25)-C(24)	121.8(12)
C(26)-C(25)-H(25)	119.1
C(24)-C(25)-H(25)	119.1
C(25)-C(26)-C(21)	121.4(11)
C(25)-C(26)-C(4)	120.1(11)
C(21)-C(26)-C(4)	118.5(10)
N(1)-C(4)-O(1)	124.7(11)
N(1)-C(4)-C(26)	116.5(11)
O(1)-C(4)-C(26)	118.8(11)
N(1)-C(5)-H(5A)	109.5
N(1)-C(5)-H(5B)	109.5
H(5A)-C(5)-H(5B)	109.5
N(1)-C(5)-H(5C)	109.5
H(5A)-C(5)-H(5C)	109.5
H(5B)-C(5)-H(5C)	109.5
C(51)-N(41)-H(41)	109.5
C(51)-N(41)-H(42)	109.5
H(41)-N(41)-H(42)	109.5
C(51)-N(41)-H(43)	109.5
H(41)-N(41)-H(43)	109.5
H(42)-N(41)-H(43)	109.5
N(41)-C(51)-H(51)	109.5
N(41)-C(51)-H(52)	109.5
H(51)-C(51)-H(52)	109.5
N(41)-C(51)-H(53)	109.5
H(51)-C(51)-H(53)	109.5
H(52)-C(51)-H(53)	109.5

Symmetry transformations used to generate equivalent atoms:

Table 4. Torsion angles [deg] for (154).

C(11)-C(1)-C(2)-C(3)	167.8(12)
C(12)-C(1)-C(2)-C(3)	-14.6(19)

C(11)-C(1)-C(2)-C(21)	-10.8(17)
C(12)-C(1)-C(2)-C(21)	166.8(11)
C(1)-C(2)-C(3)-C(32)	-12.8(19)
C(21)-C(2)-C(3)-C(32)	165.8(11)
C(1)-C(2)-C(3)-C(31)	174.2(12)
C(21)-C(2)-C(3)-C(31)	-7.2(17)
C(2)-C(1)-C(11)-N(11)	-152(27)
C(12)-C(1)-C(11)-N(11)	30(27)
C(2)-C(1)-C(12)-N(12)	-55(39)
C(11)-C(1)-C(12)-N(12)	123(39)
C(2)-C(3)-C(31)-N(31)	-128(20)
C(32)-C(3)-C(31)-N(31)	58(20)
C(2)-C(3)-C(32)-N(32)	-101(55)
C(31)-C(3)-C(32)-N(32)	72(55)
C(3)-C(2)-C(21)-C(22)	-66.5(16)
C(1)-C(2)-C(21)-C(22)	112.2(14)
C(3)-C(2)-C(21)-C(26)	115.9(14)
C(1)-C(2)-C(21)-C(26)	-65.4(16)
C(26)-C(21)-C(22)-C(23)	0.4(19)
C(2)-C(21)-C(22)-C(23)	-177.2(12)
C(21)-C(22)-C(23)-C(24)	-2(2)
C(22)-C(23)-C(24)-C(25)	2(2)
C(23)-C(24)-C(25)-C(26)	-1(2)
C(24)-C(25)-C(26)-C(21)	-0.2(19)
C(24)-C(25)-C(26)-C(4)	-179.0(12)
C(22)-C(21)-C(26)-C(25)	0.6(19)
C(2)-C(21)-C(26)-C(25)	178.2(12)
C(22)-C(21)-C(26)-C(4)	179.4(12)
C(2)-C(21)-C(26)-C(4)	-3.0(18)
C(5)-N(1)-C(4)-O(1)	3(2)
C(5)-N(1)-C(4)-C(26)	-175.9(11)
C(25)-C(26)-C(4)-N(1)	-53.5(17)
C(21)-C(26)-C(4)-N(1)	127.7(13)
C(25)-C(26)-C(4)-O(1)	127.7(13)
C(21)-C(26)-C(4)-O(1)	-51.0(16)

Symmetry transformations used to generate equivalent atoms:

Table 5. Anisotropic displacement parameters (A^2 x 10^3) for (154).
The anisotropic displacement factor exponent takes the form:
-2 pi^2 [h^2 a*^2 U11 + ... + 2 h k a* b* U12]

	U11	U22	U33	U23	U13	U12
O(1)	63(6)	39(5)	67(6)	-14(5)	-5(5)	-3(4)
N(1)	45(7)	46(7)	51(7)	-12(6)	-5(6)	11(5)
C(1)	45(8)	61(8)	45(7)	-20(7)	-12(6)	-4(6)
C(2)	34(7)	45(7)	47(7)	6(6)	-15(6)	-9(6)
C(3)	59(9)	44(7)	50(8)	-12(7)	-8(7)	-9(6)
N(11)	66(8)	73(8)	61(8)	-31(7)	-12(6)	-7(6)
C(11)	40(8)	70(10)	49(8)	1(8)	-14(7)	-5(7)
N(12)	59(7)	67(8)	74(8)	-13(6)	-41(7)	1(6)

C(12)	50(8)	36(7)	68(9)	-15(6)	-1(8)	-7(6)
N(31)	63(8)	52(7)	67(8)	-18(6)	-17(7)	-11(6)
C(31)	39(8)	45(7)	64(9)	-21(7)	-13(7)	-5(6)
N(32)	64(7)	52(7)	72(8)	-25(6)	-6(6)	-27(6)
C(32)	62(9)	38(7)	43(7)	-13(6)	-1(6)	-5(6)
C(21)	63(8)	29(6)	44(7)	-8(6)	-2(6)	-19(6)
C(22)	57(8)	67(9)	40(7)	-5(7)	-18(7)	1(7)
C(23)	58(9)	47(8)	64(9)	-6(7)	-17(7)	-2(7)
C(24)	44(7)	64(9)	70(9)	-30(8)	-13(7)	-9(7)
C(25)	47(8)	48(8)	50(8)	-9(6)	-9(7)	-7(6)
C(26)	34(7)	49(8)	62(8)	-11(7)	-9(7)	-9(6)
C(4)	40(7)	46(8)	48(8)	-9(7)	-18(6)	6(6)
C(5)	48(8)	86(11)	78(10)	-17(9)	-8(8)	-8(8)
N(41)	63(7)	38(6)	79(8)	-16(6)	-13(6)	-24(5)
C(51)	73(10)	50(8)	61(9)	-2(7)	-16(8)	-8(7)

Table 6. Hydrogen coordinates (x 10^4) and isotropic displacement parameters (A^2 x 10^3) for (154).

	x	y	z	U(eq)
H(1)	910(14)	5400(14)	8230(8)	60(4)
H(22)	1928	30	9983	66
H(23)	4075	499	11301	68
H(24)	5305	2531	10736	68
H(25)	4267	4186	8940	58
H(5A)	-361	6610	6684	105
H(5B)	975	6251	5606	105
H(5C)	1352	7288	6489	105
H(41)	4775	2119	5147	87
H(42)	3574	1681	4335	87
H(43)	3043	2654	5173	87
H(51)	3252	3921	3101	93
H(52)	4998	3178	2867	93
H(53)	4805	4194	3851	93

Appendix 2

Supplementary data

The tables of data shown below are not normally printed in *Acta Cryst. Section C* but the data will be available electronically *via* the online contents pages at

http://journals.iucr.org/c/journalhomepage.html

Specific tables may be included in the printed manuscript at the discretion of the Co-editor. If you wish to include any of the following tables in your paper, please state which tables are required in the _publ_contact_letter field of the CIF. In the case of tables of atomic coordinates, please state whether you wish the coordinates of any H atoms to be included.

Table *S*1. *Fractional atomic coordinates and equivalent isotropic displacement parameters (Å²)*

$$U_{\rm eq} = (1/3)\Sigma_i\Sigma_j U^{ij} a^i a^j \mathbf{a}_i.\mathbf{a}_j.$$

	x	y	z	$U_{\rm eq}$
N1	−0.00647 (8)	0.87131 (15)	0.15563 (8)	0.0367 (3)
N2A	−0.11664 (14)	1.4060 (2)	0.04262 (12)	0.0788 (6)
N3A	−0.24231 (13)	1.0780 (3)	0.17486 (15)	0.0907 (6)
N2B	0.28853 (13)	0.5619 (2)	0.18438 (12)	0.0732 (5)
N3B	0.04444 (12)	0.42660 (19)	0.24932 (11)	0.0620 (4)
C1	−0.07949 (11)	0.7765 (2)	0.18104 (10)	0.0437 (4)
C2	−0.05987 (12)	0.7661 (2)	0.27751 (11)	0.0470 (4)
C3	0.00903 (12)	0.8440 (2)	0.33779 (11)	0.0458 (4)
C4	−0.01804 (11)	1.02862 (18)	0.12450 (9)	0.0380 (3)
C5	0.08302 (10)	0.80880 (18)	0.15561 (9)	0.0349 (3)
C11	0.06880 (11)	1.06855 (18)	0.10020 (9)	0.0380 (3)
C12	0.09685 (13)	1.2087 (2)	0.06691 (10)	0.0479 (4)
C13	0.18639 (13)	1.2119 (2)	0.05246 (11)	0.0539 (5)
C14	0.24716 (13)	1.0783 (2)	0.07089 (11)	0.0524 (4)
C15	0.22077 (11)	0.9379 (2)	0.10446 (10)	0.0443 (4)
C16	0.13076 (10)	0.93386 (18)	0.11947 (9)	0.0363 (3)
C6A	−0.09671 (11)	1.1275 (2)	0.11819 (10)	0.0465 (4)
C7A	−0.10479 (13)	1.2830 (2)	0.07685 (12)	0.0559 (5)
C8A	−0.17655 (13)	1.0939 (2)	0.14997 (13)	0.0598 (5)
C6B	0.11864 (11)	0.65823 (18)	0.18467 (9)	0.0390 (4)
C7B	0.21323 (13)	0.6091 (2)	0.18276 (11)	0.0483 (4)
C8B	0.07334 (12)	0.5348 (2)	0.22056 (10)	0.0441 (4)
C21	0.03457 (13)	0.8243 (2)	0.43290 (11)	0.0488 (4)
C22	−0.01487 (18)	0.7189 (2)	0.47126 (13)	0.0697 (6)
C23	0.0135 (2)	0.6989 (3)	0.56013 (15)	0.0909 (8)
C24	0.0913 (2)	0.7812 (3)	0.61307 (15)	0.0896 (8)
C25	0.14131 (17)	0.8881 (3)	0.57716 (14)	0.0791 (7)
C26	0.11258 (13)	0.9101 (3)	0.48711 (12)	0.0601 (5)
H1A	−0.0814	0.6679	0.1578	0.052
H1B	−0.1435	0.8246	0.1547	0.052
H2	−0.1002	0.6980	0.2969	0.056
H3	0.0453	0.9194	0.3181	0.055
H12	0.0560	1.2987	0.0546	0.057
H13	0.2060	1.3048	0.0301	0.065
H14	0.3071	1.0829	0.0605	0.063
H15	0.2621	0.8486	0.1167	0.053
H22	−0.0681	0.6608	0.4362	0.084
H23	−0.0210	0.6282	0.5844	0.109
H24	0.1107	0.7655	0.6731	0.108
H25	0.1943	0.9455	0.6131	0.095
H26	0.1462	0.9831	0.4632	0.072

Table *S*2. *Anisotropic displacement parameters* (Å²)

U_{11}	U_{22}	U_{33}	U_{12}	U_{13}	U_{23}

N1	0.0329 (6)	0.0395 (7)	0.0373 (6)	0.0023 (5)	0.0102 (5)	0.0005 (5)
N2A	0.0846 (13)	0.0526 (10)	0.0805 (12)	0.0195 (9)	−0.0009 (10)	0.0042 (9)
N3A	0.0570 (11)	0.1029 (16)	0.1203 (17)	0.0166 (11)	0.0396 (11)	−0.0124 (13)
N2B	0.0652 (11)	0.0815 (12)	0.0802 (12)	0.0323 (10)	0.0333 (9)	0.0223 (10)
N3B	0.0682 (10)	0.0506 (9)	0.0639 (10)	−0.0038 (8)	0.0162 (8)	0.0115 (8)
C1	0.0340 (8)	0.0465 (9)	0.0508 (9)	−0.0028 (7)	0.0133 (7)	−0.0014 (7)
C2	0.0429 (9)	0.0499 (10)	0.0543 (10)	−0.0040 (8)	0.0241 (8)	0.0002 (8)
C3	0.0461 (9)	0.0452 (9)	0.0516 (9)	−0.0007 (7)	0.0232 (8)	−0.0014 (8)
C4	0.0376 (8)	0.0377 (8)	0.0331 (7)	0.0013 (6)	0.0030 (6)	−0.0037 (6)
C5	0.0330 (7)	0.0390 (8)	0.0302 (7)	0.0013 (6)	0.0063 (6)	−0.0030 (6)
C11	0.0375 (8)	0.0391 (8)	0.0325 (7)	−0.0016 (6)	0.0042 (6)	−0.0024 (6)
C12	0.0539 (10)	0.0373 (9)	0.0462 (9)	−0.0018 (7)	0.0070 (7)	0.0019 (7)
C13	0.0580 (11)	0.0481 (10)	0.0537 (10)	−0.0152 (9)	0.0148 (8)	0.0051 (8)
C14	0.0446 (9)	0.0603 (11)	0.0528 (10)	−0.0107 (8)	0.0160 (8)	0.0012 (8)
C15	0.0381 (8)	0.0501 (9)	0.0439 (8)	−0.0003 (7)	0.0116 (7)	0.0009 (7)
C16	0.0351 (7)	0.0397 (8)	0.0305 (7)	−0.0014 (6)	0.0051 (6)	−0.0015 (6)
C6A	0.0405 (8)	0.0460 (9)	0.0460 (9)	0.0071 (7)	0.0035 (7)	−0.0070 (7)
C7A	0.0512 (10)	0.0479 (11)	0.0550 (10)	0.0125 (8)	−0.0028 (8)	−0.0075 (9)
C8A	0.0430 (10)	0.0642 (12)	0.0672 (12)	0.0152 (9)	0.0102 (9)	−0.0109 (9)
C6B	0.0393 (8)	0.0404 (8)	0.0358 (7)	0.0043 (7)	0.0097 (6)	0.0017 (6)
C7B	0.0517 (10)	0.0477 (9)	0.0469 (9)	0.0126 (8)	0.0173 (8)	0.0090 (8)
C8B	0.0469 (9)	0.0416 (9)	0.0400 (8)	0.0052 (7)	0.0080 (7)	0.0020 (7)
C21	0.0536 (10)	0.0469 (9)	0.0495 (9)	0.0109 (8)	0.0212 (8)	−0.0031 (8)
C22	0.0976 (16)	0.0588 (12)	0.0567 (11)	−0.0052 (11)	0.0299 (11)	0.0051 (9)
C23	0.148 (2)	0.0689 (15)	0.0624 (14)	−0.0006 (16)	0.0430 (16)	0.0082 (12)
C24	0.137 (2)	0.0792 (16)	0.0507 (12)	0.0340 (17)	0.0264 (14)	0.0085 (12)
C25	0.0769 (14)	0.0912 (17)	0.0586 (12)	0.0252 (13)	0.0061 (11)	−0.0192 (12)
C26	0.0550 (11)	0.0695 (13)	0.0572 (11)	0.0104 (10)	0.0197 (9)	−0.0117 (9)

Table *S3*. *Geometric parameters (Å, °)*

N1—C1	1.469 (2)	C11—C16	1.399 (2)
N1—C4	1.386 (2)	C12—C13	1.380 (2)
N1—C5	1.388 (2)	C13—C14	1.382 (3)
N2A—C7A	1.145 (2)	C14—C15	1.384 (2)
N3A—C8A	1.146 (2)	C15—C16	1.391 (2)
N2B—C7B	1.144 (2)	C6A—C8A	1.425 (3)
N3B—C8B	1.145 (2)	C6A—C7A	1.436 (3)
C1—C2	1.495 (2)	C6B—C8B	1.428 (2)
C2—C3	1.319 (2)	C6B—C7B	1.430 (2)
C3—C21	1.471 (2)	C21—C26	1.382 (3)
C4—C6A	1.374 (2)	C21—C22	1.388 (3)
C4—C11	1.460 (2)	C22—C23	1.373 (3)
C5—C6B	1.372 (2)	C23—C24	1.359 (4)
C5—C16	1.461 (2)	C24—C25	1.377 (4)
C11—C12	1.389 (2)	C25—C26	1.393 (3)

C1—N1—C4	125.99 (12)	C5—C16—C11	107.80 (13)
C1—N1—C5	123.11 (12)	C5—C16—C15	131.85 (14)
C4—N1—C5	110.82 (12)	C4—C6A—C7A	120.78 (16)
N1—C1—C2	113.84 (13)	C4—C6A—C8A	126.56 (16)
C1—C2—C3	126.34 (15)	C8A—C6A—C7A	112.66 (15)
C2—C3—C21	126.82 (16)	N2A—C7A—C6A	176.3 (2)
N1—C4—C6A	126.02 (15)	N3A—C8A—C6A	175.3 (2)
N1—C5—C6B	125.80 (14)	C5—C6B—C7B	120.42 (14)
N1—C4—C11	107.12 (12)	C5—C6B—C8B	128.19 (14)
C6A—C4—C11	126.86 (15)	C8B—C6B—C7B	111.37 (14)
C6B—C5—C16	127.39 (13)	N2B—C7B—C6B	175.81 (18)
N1—C5—C16	106.81 (12)	N3B—C8B—C6B	173.41 (18)
C4—C11—C12	132.04 (14)	C3—C21—C22	122.70 (17)
C4—C11—C16	107.42 (13)	C3—C21—C26	119.39 (17)
C12—C11—C16	120.50 (14)	C22—C21—C26	117.89 (18)
C11—C12—C13	118.79 (16)	C21—C22—C23	121.1 (2)
C12—C13—C14	120.64 (16)	C22—C23—C24	120.8 (2)
C13—C14—C15	121.46 (16)	C23—C24—C25	119.5 (2)
C14—C15—C16	118.26 (16)	C24—C25—C26	120.0 (2)
C11—C16—C15	120.35 (14)	C21—C26—C25	120.6 (2)
C4—N1—C1—C2	−102.16 (17)	C4—C11—C16—C5	0.19 (15)
C5—N1—C1—C2	81.50 (18)	C4—C11—C16—C15	−178.86 (13)
N1—C1—C2—C3	6.6 (2)	C6B—C5—C16—C11	−178.82 (14)
C1—C2—C3—C21	−174.28 (16)	C6B—C5—C16—C15	0.1 (3)
C1—N1—C4—C6A	5.3 (2)	N1—C5—C16—C11	0.90 (15)
C5—N1—C4—C6A	−178.02 (14)	N1—C5—C16—C15	179.80 (15)
C1—N1—C4—C11	−174.88 (13)	N1—C4—C6A—C7A	−173.84 (14)
C5—N1—C4—C11	1.84 (15)	N1—C4—C6A—C8A	6.6 (3)
C1—N1—C5—C6B	−5.2 (2)	C11—C4—C6A—C7A	6.3 (2)
C4—N1—C5—C6B	178.01 (13)	C11—C4—C6A—C8A	−173.25 (15)
C1—N1—C5—C16	175.11 (12)	N1—C5—C6B—C7B	−178.75 (14)
C4—N1—C5—C16	−1.72 (15)	N1—C5—C6B—C8B	0.0 (2)
N1—C4—C11—C12	−178.93 (15)	C16—C5—C6B—C7B	0.9 (2)
N1—C4—C11—C16	−1.22 (15)	C16—C5—C6B—C8B	179.65 (14)
C6A—C4—C11—C12	0.9 (3)	C2—C3—C21—C22	−1.5 (3)
C6A—C4—C11—C16	178.64 (14)	C2—C3—C21—C26	176.66 (17)
C4—C11—C12—C13	178.09 (15)	C26—C21—C22—C23	−0.8 (3)
C16—C11—C12—C13	0.6 (2)	C3—C21—C22—C23	177.4 (2)
C12—C11—C16—C5	178.22 (13)	C3—C21—C26—C25	−176.94 (17)
C12—C11—C16—C15	−0.8 (2)	C21—C22—C23—C24	−0.4 (4)
C11—C12—C13—C14	−0.1 (2)	C22—C23—C24—C25	1.1 (4)
C12—C13—C14—C15	−0.2 (3)	C23—C24—C25—C26	−0.6 (3)
C13—C14—C15—C16	0.0 (2)	C22—C21—C26—C25	1.3 (3)
C14—C15—C16—C11	0.5 (2)	C24—C25—C26—C21	−0.6 (3)
C14—C15—C16—C5	−178.28 (15)		

Appendix 3

Supplementary data

The tables of data shown below are not normally printed in *Acta Cryst. Section C* but the data will be available electronically *via* the online contents pages at

http://journals.iucr.org/c/journalhomepage.html

Specific tables may be included in the printed manuscript at the discretion of the Co-editor. If you wish to include any of the following tables in your paper, please state which tables are required in the _publ_contact_letter field of the CIF. In the case of tables of atomic coordinates, please state whether you wish the coordinates of any H atoms to be included.

Table *S*1. *Fractional atomic coordinates and equivalent isotropic displacement parameters (Å²)*

$$U_{eq} = (1/3)\Sigma_i\Sigma_j U^{ij} a^i a^j \mathbf{a}_i.\mathbf{a}_j.$$

	x	y	z	U_{eq}
S1	0.42240 (8)	**0.311005** (18)	0.43274 (6)	0.05158 (15)
S2	0.29873 (8)	**0.397780** (17)	0.36781 (6)	0.04844 (14)
S3	0.20999 (8)	**0.372260** (17)	0.04086 (6)	0.05053 (15)
S4	0.33541 (9)	**0.285452** (17)	0.10331 (6)	0.05370 (16)
C1T	0.3349 (3)	0.34667 (6)	0.3047 (2)	0.0406 (4)
C2T	0.2992 (3)	0.33626 (6)	0.1685 (2)	0.0412 (4)
C3T	0.3757 (4)	0.38603 (9)	0.5401 (2)	0.0626 (6)
C4T	0.4310 (4)	0.34756 (9)	0.5689 (2)	0.0634 (6)
C5T	0.2666 (4)	0.29802 (9)	−0.0692 (3)	0.0635 (6)
C6T	0.2110 (4)	0.33689 (9)	−0.0971 (2)	0.0625 (6)
N1	−0.2780 (2)	0.41884 (5)	0.25033 (16)	0.0370 (3)
N2A	−0.0196 (3)	0.41153 (7)	0.7339 (2)	0.0666 (6)
N3A	−0.2593 (4)	0.51313 (7)	0.5137 (3)	0.0823 (8)
N2B	−0.2645 (4)	0.32291 (7)	−0.1453 (2)	0.0711 (6)
N3B	−0.4189 (3)	0.44801 (8)	−0.1456 (2)	0.0729 (6)
C1	−0.3455 (3)	0.46094 (6)	0.2103 (2)	0.0440 (4)
C2	−0.1977 (3)	0.48993 (7)	0.1729 (2)	0.0552 (6)
C3	−0.0272 (4)	0.48082 (8)	0.1703 (3)	0.0601 (6)
C4	−0.2067 (2)	0.40810 (6)	0.38449 (19)	0.0361 (4)
C5	−0.2669 (2)	0.38570 (6)	0.15770 (19)	0.0359 (4)
C11	−0.1602 (2)	0.36343 (5)	0.3808 (2)	0.0359 (4)
C12	−0.0962 (3)	0.33577 (6)	0.4859 (2)	0.0446 (4)
C13	−0.0705 (3)	0.29412 (7)	0.4495 (2)	0.0512 (5)
C14	−0.1085 (3)	0.28042 (6)	0.3131 (2)	0.0513 (5)
C15	−0.1727 (3)	0.30756 (6)	0.2067 (2)	0.0460 (4)
C16	−0.1979 (2)	0.34963 (6)	0.24217 (19)	0.0360 (4)
C6A	−0.1806 (3)	0.43472 (6)	0.4976 (2)	0.0420 (4)
C7A	−0.0920 (3)	0.42079 (6)	0.6283 (2)	0.0480 (5)
C8A	−0.2266 (3)	0.47860 (7)	0.5015 (2)	0.0541 (5)
C6B	−0.3069 (3)	0.38675 (6)	0.0142 (2)	0.0419 (4)
C7B	−0.2814 (3)	0.35038 (7)	−0.0704 (2)	0.0494 (5)
C8B	−0.3692 (3)	0.42203 (7)	−0.0695 (2)	0.0505 (5)
H3T	0.3779	0.4064	0.6102	0.075
H4T	0.4737	0.3400	0.6600	0.076
H5T	0.2685	0.2781	−0.1405	0.076
H6T	0.1734	0.3450	−0.1887	0.075
H1A	−0.4053	0.4729	0.2881	0.053
H1B	−0.4348	0.4585	0.1303	0.053
H2	−0.2316	0.5173	0.1489	0.066
H3A	0.0136	0.4539	0.1934	0.072
H3B	0.0543	0.5012	0.1455	0.072
H12	−0.0712	0.3449	0.5783	0.054
H13	−0.0269	0.2752	0.5184	0.061
H14	−0.0907	0.2523	0.2919	0.062
H15	−0.1981	0.2981	0.1147	0.055

Table *S2. Anisotropic displacement parameters* (Å^2)

	U_{11}	U_{22}	U_{33}	U_{12}	U_{13}	U_{23}
S1	0.0551 (3)	0.0500 (3)	0.0493 (3)	0.0000 (2)	0.0016 (2)	0.0095 (2)
S2	0.0518 (3)	0.0415 (3)	0.0527 (3)	−0.0018 (2)	0.0085 (2)	−0.0052 (2)
S3	0.0547 (3)	0.0452 (3)	0.0513 (3)	0.0057 (2)	0.0021 (2)	0.0079 (2)
S4	0.0721 (4)	0.0400 (3)	0.0484 (3)	0.0047 (2)	0.0012 (3)	−0.0020 (2)
C1T	0.0390 (10)	0.0382 (9)	0.0450 (10)	−0.0031 (8)	0.0059 (8)	0.0006 (8)
C2T	0.0436 (10)	0.0367 (9)	0.0434 (10)	−0.0014 (8)	0.0044 (8)	0.0026 (8)
C3T	0.0694 (16)	0.0723 (16)	0.0463 (12)	−0.0032 (13)	0.0066 (11)	−0.0135 (11)
C4T	0.0669 (15)	0.0818 (18)	0.0405 (11)	−0.0003 (13)	−0.0004 (10)	0.0024 (11)
C5T	0.0734 (16)	0.0682 (15)	0.0469 (12)	0.0133 (13)	−0.0070 (11)	−0.0110 (11)
C6T	0.0700 (16)	0.0729 (16)	0.0431 (11)	0.0134 (13)	−0.0048 (11)	0.0012 (11)
N1	0.0401 (8)	0.0311 (7)	0.0397 (8)	0.0051 (6)	0.0037 (6)	0.0051 (6)
N2A	0.0947 (16)	0.0528 (11)	0.0506 (11)	0.0065 (11)	−0.0055 (11)	0.0038 (9)
N3A	0.130 (2)	0.0469 (12)	0.0673 (14)	0.0220 (13)	−0.0099 (14)	−0.0118 (10)
N2B	0.1015 (18)	0.0563 (12)	0.0536 (11)	0.0069 (12)	−0.0058 (11)	−0.0079 (10)
N3B	0.0888 (16)	0.0725 (14)	0.0569 (12)	0.0256 (12)	0.0023 (11)	0.0176 (11)
C1	0.0511 (11)	0.0344 (9)	0.0459 (10)	0.0114 (8)	0.0012 (8)	0.0056 (8)
C2	0.0728 (16)	0.0344 (10)	0.0583 (13)	0.0024 (10)	0.0037 (11)	0.0131 (9)
C3	0.0676 (15)	0.0532 (13)	0.0605 (14)	−0.0105 (12)	0.0118 (11)	0.0106 (11)
C4	0.0353 (9)	0.0334 (9)	0.0401 (9)	0.0011 (7)	0.0068 (7)	0.0066 (7)
C5	0.0315 (9)	0.0337 (8)	0.0429 (9)	0.0014 (7)	0.0056 (7)	0.0037 (7)
C11	0.0339 (9)	0.0301 (8)	0.0442 (9)	−0.0001 (7)	0.0058 (7)	0.0055 (7)
C12	0.0502 (11)	0.0375 (10)	0.0456 (10)	0.0014 (8)	0.0003 (9)	0.0073 (8)
C13	0.0572 (13)	0.0381 (10)	0.0574 (12)	0.0048 (9)	−0.0001 (10)	0.0140 (9)
C14	0.0610 (13)	0.0309 (9)	0.0623 (13)	0.0061 (9)	0.0068 (10)	0.0048 (9)
C15	0.0545 (12)	0.0340 (9)	0.0494 (11)	0.0030 (8)	0.0040 (9)	0.0021 (8)
C16	0.0340 (9)	0.0315 (8)	0.0427 (9)	−0.0001 (7)	0.0045 (7)	0.0052 (7)
C6A	0.0479 (11)	0.0362 (9)	0.0423 (9)	0.0039 (8)	0.0060 (8)	0.0034 (7)
C7A	0.0618 (13)	0.0379 (10)	0.0448 (10)	0.0017 (9)	0.0066 (9)	0.0009 (8)
C8A	0.0726 (15)	0.0431 (11)	0.0459 (11)	0.0082 (10)	0.0012 (10)	−0.0041 (9)
C6B	0.0412 (10)	0.0419 (10)	0.0424 (10)	0.0016 (8)	0.0029 (8)	0.0038 (8)
C7B	0.0552 (12)	0.0482 (11)	0.0437 (10)	0.0022 (9)	−0.0028 (9)	0.0032 (9)
C8B	0.0533 (12)	0.0543 (12)	0.0439 (10)	0.0095 (10)	0.0037 (9)	0.0059 (9)

Table *S3. Geometric parameters* (Å, °)

S1—C1T	1.751 (2)	C6A—C7A	1.430 (3)
S1—C4T	1.740 (3)	C6A—C8A	1.440 (3)
S2—C1T	1.763 (2)	C6B—C7B	1.432 (3)
S2—C3T	1.733 (3)	C6B—C8B	1.432 (3)
S3—C2T	1.760 (2)	C11—C12	1.387 (3)
S3—C6T	1.731 (3)	C11—C16	1.398 (3)
S4—C2T	1.761 (2)	C12—C13	1.388 (3)
S4—C5T	1.726 (3)	C13—C14	1.377 (3)
C1T—C2T	1.344 (3)	C14—C15	1.387 (3)
C3T—C4T	1.314 (4)	C15—C16	1.398 (3)
C5T—C6T	1.325 (4)	C3T—H3T	0.9300
N1—C1	1.471 (2)	C4T—H4T	0.9300
N1—C4	1.385 (2)	C5T—H5T	0.9300
N1—C5	1.382 (2)	C6T—H6T	0.9300
N2A—C7A	1.139 (3)	C1—H1A	0.9700
N3A—C8A	1.134 (3)	C1—H1B	0.9700
N2B—C7B	1.142 (3)	C2—H2	0.9300
N3B—C8B	1.141 (3)	C3—H3A	0.9300
C1—C2	1.496 (3)	C3—H3B	0.9300
C2—C3	1.296 (3)	C12—H12	0.9300
C4—C6A	1.372 (3)	C13—H13	0.9300
C4—C11	1.465 (2)	C14—H14	0.9300
C5—C6B	1.374 (3)	C15—H15	0.9300
C5—C16	1.470 (2)		

S1—C1T—S2	114.83 (11)
S3—C2T—S4	114.51 (11)
C1T—S1—C4T	94.21 (11)
C1T—S2—C3T	94.32 (11)
C2T—S3—C6T	94.30 (11)
C2T—S4—C5T	94.60 (11)
C2T—C1T—S1	122.97 (16)
C2T—C1T—S2	122.20 (16)
C1T—C2T—S3	122.61 (16)
C1T—C2T—S4	122.88 (15)
C3T—C4T—S1	118.46 (19)
C4T—C3T—S2	118.18 (19)
C5T—C6T—S3	118.47 (19)
C6T—C5T—S4	118.06 (19)
S1—C4T—H4T	120.8
S2—C3T—H3T	120.9
S3—C6T—H6T	120.8
S4—C5T—H5T	121.0
C3T—C4T—H4T	120.8
C4T—C3T—H3T	120.9
C5T—C6T—H6T	120.8
C6T—C5T—H5T	121.0
C1—N1—C4	124.08 (16)
C1—N1—C5	124.61 (16)
C4—N1—C5	111.20 (15)
N1—C1—C2	112.65 (17)
C1—C2—C3	126.6 (2)
C6A—C4—N1	126.14 (17)
C6A—C4—C11	126.93 (17)
N1—C4—C11	106.91 (16)
C6B—C5—N1	126.59 (17)
C6B—C5—C16	126.88 (17)
N1—C5—C16	106.51 (15)
C12—C11—C4	131.83 (18)
C16—C11—C4	107.37 (15)
C12—C11—C16	120.77 (17)

S1—C1T—C2T—S3	179.61 (11)
S2—C1T—C2T—S3	−1.0 (3)
S1—C1T—C2T—S4	0.3 (3)
S2—C1T—C2T—S4	179.70 (11)
S2—C3T—C4T—S1	−0.2 (3)
S4—C5T—C6T—S3	−0.3 (3)
C3T—S2—C1T—S1	0.27 (14)
C4T—S1—C1T—S2	−0.36 (14)
C5T—S4—C2T—S3	2.12 (15)
C6T—S3—C2T—S4	−2.24 (15)
C4T—S1—C1T—C2T	179.11 (19)
C3T—S2—C1T—C2T	−179.21 (19)
C6T—S3—C2T—C1T	178.37 (19)
C5T—S4—C2T—C1T	−178.5 (2)
C1T—S2—C3T—C4T	0.0 (2)
C1T—S1—C4T—C3T	0.4 (2)
C2T—S4—C5T—C6T	−1.1 (3)
C2T—S3—C6T—C5T	1.6 (3)
C4—N1—C1—C2	84.3 (2)
C5—N1—C1—C2	−91.4 (2)
N1—C1—C2—C3	1.6 (3)
C1—N1—C4—C6A	−3.0 (3)
C5—N1—C4—C6A	173.26 (18)
C1—N1—C4—C11	178.58 (16)
C5—N1—C4—C11	−5.2 (2)
C1—N1—C5—C6B	3.6 (3)
C4—N1—C5—C6B	−172.65 (18)
C1—N1—C5—C16	−178.33 (17)

C11—C12—C13	118.20 (19)
C12—C13—C14	121.12 (19)
C13—C14—C15	121.54 (19)
C14—C15—C16	117.8 (2)
C11—C16—C15	120.62 (17)
C11—C16—C5	107.74 (16)
C15—C16—C5	131.62 (18)
C4—C6A—C7A	121.10 (17)
C4—C6A—C8A	127.01 (18)
C5—C6B—C7B	120.75 (18)
C5—C6B—C8B	127.29 (19)
N2A—C7A—C6A	176.9 (2)
N3A—C8A—C6A	175.5 (3)
N2B—C7B—C6B	175.6 (2)
N3B—C8B—C6B	174.3 (3)
C7A—C6A—C8A	111.82 (18)
C7B—C6B—C8B	111.92 (18)
N1—C1—H1A	109.1
C2—C1—H1A	109.1
N1—C1—H1B	109.1
C2—C1—H1B	109.1
C3—C2—H2	116.7
C1—C2—H2	116.7
C2—C3—H3A	120.0
C2—C3—H3B	120.0
H3A—C3—H3B	120.0
H1A—C1—H1B	107.8
C11—C12—H12	120.9
C13—C12—H12	120.9
C14—C13—H13	119.4
C12—C13—H13	119.4
C13—C14—H14	119.2
C15—C14—H14	119.2
C14—C15—H15	121.1
C16—C15—H15	121.1

C4—N1—C5—C16	5.4 (2)
C6A—C4—C11—C12	6.5 (3)
N1—C4—C11—C12	−175.1 (2)
C6A—C4—C11—C16	−175.68 (18)
N1—C4—C11—C16	2.7 (2)
C16—C11—C12—C13	0.1 (3)
C4—C11—C12—C13	177.7 (2)
C11—C12—C13—C14	−0.4 (3)
C12—C13—C14—C15	0.4 (4)
C13—C14—C15—C16	0.0 (3)
C12—C11—C16—C15	0.3 (3)
C4—C11—C16—C15	−177.86 (17)
C12—C11—C16—C5	178.64 (17)
C4—C11—C16—C5	0.5 (2)
C14—C15—C16—C11	−0.3 (3)
C14—C15—C16—C5	−178.2 (2)
C6B—C5—C16—C11	174.54 (18)
N1—C5—C16—C11	−3.5 (2)
C6B—C5—C16—C15	−7.4 (3)
N1—C5—C16—C15	174.6 (2)
N1—C4—C6A—C7A	−174.86 (18)
C11—C4—C6A—C7A	3.3 (3)
N1—C4—C6A—C8A	2.0 (3)
C11—C4—C6A—C8A	−179.8 (2)
N1—C5—C6B—C7B	177.14 (19)
C16—C5—C6B—C7B	−0.6 (3)
N1—C5—C6B—C8B	−0.4 (3)
C16—C5—C6B—C8B	−178.1 (2)

Appendix 4

Acta Crystallographica Section E
Structure Reports Online
ISSN 1600-5368

2,2′-{2-[(*E*)-3-Phenylprop-2-enyl]-2,3-dihydro-1*H*-isoindol-1,3-diylidene}dimalononitrile, a π-deficient system for $\pi\cdots\pi$ (1:1) stacking investigations

Colm Crean, John F. Gallagher* and Albert C. Pratt

School of Chemical Sciences, Dublin City University, Dublin 9, Ireland

Correspondence e-mail: john.gallagher@dcu.ie

Key indicators

Single-crystal X-ray study
T = 296 K
Mean σ(C–C) = 0.003 Å
R factor = 0.042
wR factor = 0.112
Data-to-parameter ratio = 13.3

For details of how these key indicators were automatically derived from the article, see http://journals.iucr.org/e.

Received 31 January 2001
Accepted 5 February 2001
Online 13 February 2001

The title compound, $C_{23}H_{13}N_5$, derived from cinnamyl alcohol and 2,2′-(isoindolin-1,3-diylidene)bispropanedinitrile, is a heterocyclic TCNQ analogue of interest as an electron-deficient component in charge-transfer complexes. A small perturbation of the four C—C≡N angles from linearity is observed, which are in the range 173.41 (18)–176.3 (2)°; the C≡N bond lengths are in the range 1.144 (2)–1.146 (2) Å. The terminal phenyl group is oriented at an angle of 77.17 (6)° to the C_4N ring and the C=C bond is short, 1.319 (2) Å. There are no classical hydrogen bonds, although intramolecular C—H···N and intermolecular C—H···π(arene) interactions influence the crystal-structure packing.

Comment

Organic conductors are currently an important research area in materials chemistry (Martin *et al.*, 1997; Yamashita & Tomura, 1998), with special interest in the interaction of π-deficient and π-excessive materials in 1:1 complexes, *e.g.* TCNQ/TTF, where TCNQ is tetracyanoquinodimethane and TTF is tetrathiafulvalene.

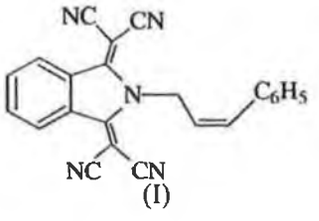

(I)

The bond lengths and angles in the heterocyclic ring of the title compound, (I) (Fig. 1), are similar to those reported previously in related systems (McNab *et al.*, 1997; Brady *et al.*, 1998; Gallagher & Murphy, 1999; Brady & Gallagher, 2000). For TCNQ (tetracyanoquinodimethane) systems (280 examples), the average exocyclic Csp^2=Csp^2 and Csp^2—Csp^1 bond lengths are 1.392 (17) and 1.427 (10) Å, respectively; thus, in (I), the C6*A*—C7*A*, C6*A*—C8*A*, and C6*B*—C7*B* and C6*B*—C8*B* bond lengths in the range 1.425 (3)–1.436 (3) Å are normal (Orpen *et al.*, 1994). The four nitrile C≡N values are from 1.144 (2) to 1.146 (2) Å, which compare with the average C≡N dimension from the literature, 1.144 (8) Å (Orpen *et al.*, 1994). The exocyclic indolinyl ring C=C bond lengths are 1.372 (2) and 1.374 (2) Å, which are longer than typical double bonds. The four remaining exocyclic indolinyl cyano C—C bond lengths are in the range 1.425 (3)–1.436 (3) Å and similar

DOI: 10.1107/S1600536801002598

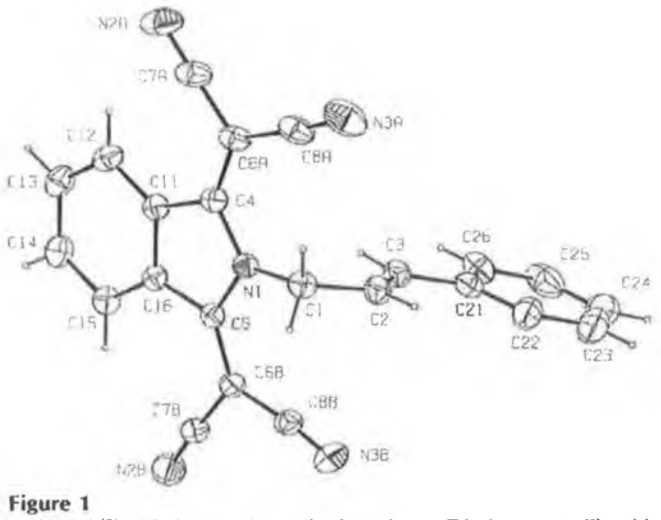

Figure 1
A view of (I) with the atomic numbering scheme. Displacement ellipsoids are depicted at the 30% probability level.

to previously reported values. The angles which the C(C≡N)$_2$ groups make with the C_4N ring are 7.01 (10) (C6*A*) and 2.33 (10)° (C6*B*), demonstrating a small twist from planarity about the C4—C6(*A*/*B*) bonds.

The hydrogen bonding in (I) is dominated by intramolecular C—H···N interactions and close contacts (details in Table 2). There are two intramolecular C(arene)—H···π(C≡N) interactions with C12—H12···N2*A* and C15—H15···N2*B* C···N distances of 3.390 (3) and 3.390 (2) Å, respectively. A C1—H1*B*···N3*A* intramolecular contact is present [C1···N3*A* 3.401 (2) Å and C—H···N 139°]. A C—H···π(arene) interaction is also present, C14—H14···*Cg*1, where *Cg*1 is the centroid of {C21–C26}^{i} [symmetry code: (i) $\frac{1}{2}-x, \frac{1}{2}+y, \frac{1}{2}-z$; details in Table 2]. The closest C14···C26^i contact distance is 3.696 (2) Å with a C14—H14···*Cg*1 angle of 121°.

Experimental

The title compound was prepared by the 5 d reaction under argon of DIAD (diisopropylazodicarboxylate) (0.37 g, 1.9 mmol), triphenylphosphine (0.49 g, 1.9 mmol), 2,2′-(isoindolin-1,3-diylidene)bispropanedinitrile (0.25 g, 1.9 mmol) (Farbenfabriken Bayer Aktiongesellschaft, 1968), cinnamyl alcohol (0.25 g, 1.9 mmol) in 40 ml tetrahydrofuran. 2,2′-(Cinnamylisoindolin-1,3-diylidene)bispropanedinitrile, (I), was isolated as an orange crystalline material after column chromatography (m.p. 469–471 K uncorrected). IR (KBr, cm^{-1}): 3049, 2372, 2335, 2224, 1563, 1465, 1407, 1228, 1146, 1109, 983, 775, 723; UV–Vis (CH_3CN) $\lambda_{max}(\varepsilon)$: 552 (5250), 459 (6667), 414 (38333), 392 (39167), 249 (47083) nm; ^{1}H NMR (400 MHz, δ, $CDCl_3$): 8.75 (*m*, 2H, aromatic), 7.85 (*m*, 2H, aromatic), 7.37 (*m*, 2H, aromatic), 7.30 (*m*, 3H, aromatic), 6.50 (*d*, *J* = 16 Hz, 1H), 6.25 (*m*, 1H), 5.50 (*m*, 2H); ^{13}C NMR (δC, $CDCl_3$): 156.8, 135.0, 134.8, 134.0, 130.9, 128.8, 128.7, 126.9, 126.0, 120.5, 113.1, 112.3, 62.1, 47.8.

Crystal data

$C_{23}H_{13}N_5$	D_x = 1.309 Mg m^{-3}
M_r = 359.38	Mo $K\alpha$ radiation
Monoclinic, $P2_1/n$	Cell parameters from 33 reflections
a = 14.3872 (18) Å	θ = 7.1–20.5°
b = 8.2696 (10) Å	μ = 0.08 mm^{-1}
c = 16.1442 (15) Å	T = 296 (1) K
β = 108.327 (7)°	Block, orange
V = 1823.4 (4) Å^3	0.43 × 0.38 × 0.28 mm
Z = 4	

Data collection

Bruker *P*4 diffractometer	$h = -1 \rightarrow 17$
ω–2θ scans	$k = -1 \rightarrow 10$
4331 measured reflections	$l = -19 \rightarrow 18$
3367 independent reflections	3 standard reflections
2630 reflections with $I > 2\sigma(I)$	every 197 reflections
R_{int} = 0.012	intensity decay: 2%
θ_{max} = 25.5°	

Refinement

Refinement on F^2	$w = 1/[\sigma^2(F_o^2) + (0.0529P)^2 + 0.3178P]$ where $P = (F_o^2 + 2F_c^2)/3$
$R[F^2 > 2\sigma(F^2)]$ = 0.042	$(\Delta/\sigma)_{max} < 0.001$
$wR(F^2)$ = 0.112	$\Delta\rho_{max}$ = 0.25 e Å^{-3}
S = 1.06	$\Delta\rho_{min}$ = −0.16 e Å^{-3}
3367 reflections	
253 parameters	
H-atom parameters constrained	

Table 1
Selected geometric parameters (Å, °).

N1—C1	1.469 (2)	C1—C2	1.495 (2)
N1—C4	1.386 (2)	C2—C3	1.319 (2)
N1—C5	1.388 (2)	C3—C21	1.471 (2)
N2*A*—C7*A*	1.145 (2)	C4—C6*A*	1.374 (2)
N3*A*—C8*A*	1.146 (2)	C4—C11	1.460 (2)
N2*B*—C7*B*	1.144 (2)	C5—C6*B*	1.372 (2)
N3*B*—C8*B*	1.145 (2)	C5—C16	1.461 (2)
C1—N1—C4	125.99 (12)	N1—C5—C6*B*	125.80 (14)
C1—N1—C5	123.11 (12)	N1—C4—C11	107.12 (12)
C4—N1—C5	110.82 (12)	N1—C5—C16	106.81 (12)
N1—C1—C2	113.84 (13)	N2*A*—C7*A*—C6*A*	176.3 (2)
C1—C2—C3	126.34 (15)	N3*A*—C8*A*—C6*A*	175.3 (2)
C2—C3—C21	126.82 (16)	N2*B*—C7*B*—C6*B*	175.81 (18)
N1—C4—C6*A*	126.02 (15)	N3*B*—C8*B*—C6*B*	173.41 (18)
C4—N1—C1—C2	−102.16 (17)	C1—C2—C3—C21	−174.28 (16)
C5—N1—C1—C2	81.50 (18)	C2—C3—C21—C22	−1.5 (3)
N1—C1—C2—C3	6.6 (2)	C2—C3—C21—C26	176.66 (17)

Table 2
Hydrogen-bonding geometry (Å, °).

*Cg*1 is the centroid of {C21–C26}^{i}.

D—H···*A*	*D*—H	H···*A*	*D*···*A*	*D*—H···*A*
C1—H1*B*···N3*A*	0.97	2.61	3.401 (2)	139
C12—H12···N2*A*	0.93	2.59	3.390 (3)	145
C12—H12···C7*A*	0.93	2.45	3.019 (3)	119
C15—H15···N2*B*	0.93	2.59	3.390 (2)	145
C15—H15···C7*B*	0.93	2.46	3.015 (2)	119
C14—H14···*Cg*1^i	0.93	3.20	3.984 (2)	143

Symmetry code: (i) $\frac{1}{2}-x, \frac{1}{2}+y, \frac{1}{2}-z$.

In (I), all H atoms bound to C atoms were treated as riding, with *SHELXL*97 (Sheldrick, 1997) defaults for C—H lengths and with U_{iso}(H) = 1.5U_{eq}(C) for methylene H atoms and 1.2U_{eq}(C) for the remainder. Examination of the structure with *PLATON* (Spek, 1998) showed that there were no solvent-accessible voids in the crystal lattice.

Data collection: *XSCANS* (Bruker, 1994); cell refinement: *XSCANS*; data reduction: *XSCANS*; program(s) used to solve structure: *SHELXS*97 (Sheldrick, 1997); program(s) used to refine structure: *NRCVAX*96 (Gabe *et al.*, 1989) and *SHELXL*97 (Sheldrick, 1997); molecular graphics: *ORTEP*III (Burnett & Johnson, 1996) and *PLATON* (Spek, 1998); software used to prepare material for publication: *NRCVAX*96, *SHELXL*97 and *WordPerfect* macro *PREP*8 (Ferguson, 1998).

JFG. thanks Dublin City University for the purchase of a Bruker *P*4 diffractometer.

References

Brady, F. & Gallagher, J. F. (2000). *Acta Cryst.* C**56**, 1407–1410.
Brady, F., Gallagher, J. F. & Kenny, P. T. M. (1998). *Acta Cryst.* C**54**, 1523–1525.
Burnett, M. N. & Johnson, C. K. (1996). *ORTEP*III. Report ORNL-6895. Oak Ridge National Laboratory, Tennessee, USA.
Bruker (1994). *XSCANS*. Version 2.2. Bruker AXS Inc., Madison, Wisconsin, USA.
Farbenfabriken Bayer Aktiongesellschaft (1968). French Patent No. 1537299.
Ferguson, G. (1998). *PREP*8. University of Guelph, Canada.
Gabe, E. J., Le Page, Y., Charland, J.-P., Lee, F. L. & White, P. S. (1989). *J. Appl. Cryst.* **22**, 384–387.
Gallagher, J. F. & Murphy C. (1999). *Acta Cryst.* C**55**, 2167–2169.
Martin, N., Segura, J. L. & Seoane, C. (1997). *J. Mater. Chem.* **7**, 1661–1676.
McNab, H., Parsons, S. & Shannon, D. A. (1997). *Acta Cryst.* C**53**, 1098–1099.
Orpen, A. G., Brammer, L., Allen, F. H., Kennard, O., Watson, D. G. & Taylor, R. (1994). *Structure Correlation*, Vol. 2, edited by H.-B. Bürgi & J. D. Dunitz. Weinhelm, Germany: VCH Publishers.
Sheldrick, G. M. (1997). *SHELXS*97 and *SHELXL*97. University of Göttingen, Germany.
Spek, A. L. (1998). *PLATON*. University of Utrecht, The Netherlands.
Yamashita Y. & Tomura, M. (1998). *J. Mater. Chem.* **8**, 1933–1944.

Appendix 5

Acta Crystallographica Section C
Crystal Structure Communications
ISSN 0108-2701

2,2′-[2,3-Dihydro-2-(prop-2-enyl)-1*H*-isoindole-1,3-diylidene]bis(propanedinitrile)–tetrathiafulvalene (1/1), TCPI–TTF[1]

Colm Crean, John F. Gallagher* and Albert C. Pratt

School of Chemical Sciences, Dublin City University, Dublin 9, Ireland
Correspondence e-mail: john.gallagher@dcu.ie

Received 15 October 2001
Accepted 17 October 2001
Online 22 December 2001

The title complex, $C_{17}H_9N_5{\cdot}C_6H_4S_4$, contains π-deficient bis(dinitrile) and TTF molecules stacked alternately in columns along the *a*-axis direction; the interplanar angle between the TTF molecule and the isoindolinyl $C_4N[C(CN)_2]_2$ moiety is 1.21 (4)°. The *N*-allyl moiety in the TCPI molecule is oriented at an angle of 87.10 (10)° with respect to the five-membered C_4N ring, and the four C≡N bond lengths range from 1.134 (3) to 1.142 (3) Å, with C—C≡N angles in the range 174.3 (3)–176.9 (2)°. In the TTF system, the S—C bond lengths are 1.726 (3)–1.740 (3) and 1.751 (2)–1.763 (2) Å for the external S—C(H) and internal S—C(S) bonds, respectively.

Comment

Organic conductors are currently an important research area in materials science (Martin *et al.*, 1997; Yamashita & Tomura, 1998; Bryce, 2000), of which the organic metal system TTF–TCNQ is exemplary (TCNQ is tetracyanoquinodimethane). Such complexes can be divided into (i) donor–acceptor (*D*–*A*) systems derived from closed-shell electron donor and acceptor organic molecules and (ii) radical salts comprising a radical ion of an organic donor or acceptor molecule and a closed-shell counter-ion. Our interest is in the former type of *D*–*A* complexes and in the interaction of π-deficient and π-excessive materials in 1:1 complexes, *e.g.* TCNQ–TTF, with the purpose of studying weak interactions. We report herein the crystal structure of 2,2′-[2,3-dihydro-2-(prop-2-enyl)-1*H*-isoindole-1,3-diylidene]bis(propanedinitrile)–tetrathiafulvalene (1/1), TCPI–TTF, (I) (Fig. 1).

The bond lengths and angles in the heterocyclic ring of TCPI are similar to those reported in the molecular structure of 2,2′-(cinnamylisoindoline-1,3-diylidene)bis(propanedinitrile), (II) (Crean *et al.*, 2001). As TCPI analogues are rare, an analysis of TCNQ molecules, (III), for comparison purposes was undertaken using the April 2001 ConQuest 1.2 version of the Cambridge Structural Database (CSD; Allen & Kennard, 1993). In TCNQ systems (280 examples, 401 hits), the mean exocyclic $Csp^2{=}Csp^2$ and $Csp^2{-}Csp$ bond lengths are 1.394 (range 1.33–1.45 Å) and 1.425 Å (range 1.36–1.55 Å), respectively (full details deposited). In (I), the exocyclic indolinyl ring C=C bond lengths C4=C6*A* and C5=C6*B*

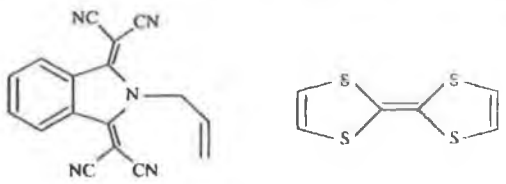

(I)

are 1.372 (3) and 1.374 (3) Å, respectively, and longer than typical double bonds; the C6*A*—C7*A*/C6*A*—C8*A* and C6*B*—C7*B*/C6*B*—C8*B* bond lengths are in the range 1.430 (3)–1.440 (3) Å and similar to those reported for (II) (Crean *et al.*, 2001) and found in the CSD (Allen & Kennard, 1993). The four nitrile C≡N values range from 1.134 (3) to 1.142 (3) Å and are comparable with the average literature C≡N length of 1.144 (8) Å (Orpen *et al.*, 1994). The angles which the $C(C{\equiv}N)_2$ groups make with the C_4N ring are 7.56 (10) (C6*A*) and 6.57 (10)° (C6*B*), demonstrating a small twist from coplanarity about the C4—C6*A*/C5—C6*B* bonds, and are similar to the values of 7.01 (10) and 2.33 (10)° in (II). The *N*-allyl moiety is oriented at an angle of 87.10 (10)° to the C_4N heterocyclic ring, with bond lengths along the N1—C1—C2=C3 group of 1.471 (2), 1.496 (3) and 1.296 (3) Å, which are analogous to the values of 1.469 (2), 1.495 (2) and 1.319 (2) Å in (II) (Crean *et al.*, 2001); the C=C bond length is shorter in (I). A search for $N{-}CH_2{-}CH{=}CH_2$ systems in the CSD (Allen & Kennard, 1993) with the terminal C=C atoms limited to three-coordination, yielded 109 examples (151 hits) and gave mean bond lengths of 1.476, 1.480 and 1.275 Å, and angles of 112.9 and 126.6° along the chain.

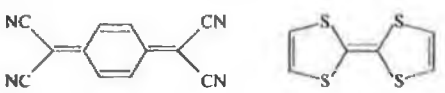

(III) (IV)

The S—C bond lengths in the TTF molecule of (I) are in the range 1.726 (3)–1.740 (3) Å for the external S—C(H) and 1.751 (2)–1.763 (2) Å for the internal S—C(S) bonds. The mean CSD value is 1.735 Å for TTF systems, (IV) (91 entries, 164 examples), for all of the *exo*/*endo*-C—S bond lengths. The C=C bond lengths of 1.344 (3) and 1.314 (4)/1.325 (4) Å (*exo*) are shorter than the CSD values of 1.37 and 1.34 Å. This suggests that the TTF and TCPI molecules experience little perturbation on forming the TCPI–TTF 1:1 complex.

The hydrogen-bonding in (I) is dominated by intramolecular C—H···N interactions and close contacts (details are given in Table 2). This results in angles at C6*A* and C6*B* of 121.10 (17)/127.01 (18) and 120.75 (18)/127.29 (19)°, respectively; the smaller angle reflects the favourable effect of the

[1] TCPI and TTF are abbreviations for 2,2′-(allylisoindolin-1,3-diylidene)bis(propanedinitrile) and tetrathiafulvalene, respectively.

  DOI: 10.1107/S0108270101017632

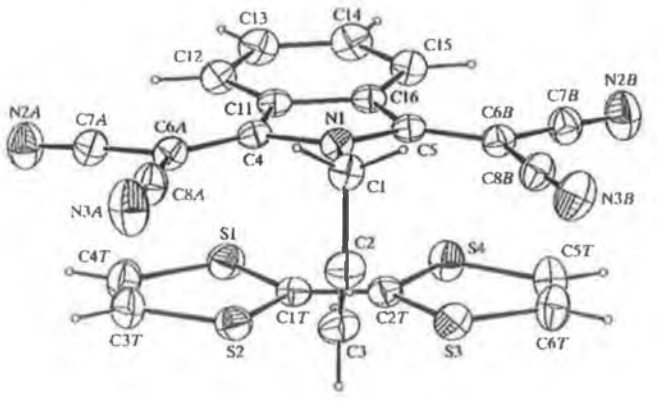

Figure 1
A view of (I) with the atomic numbering scheme. Displacement ellipsoids are drawn at the 30% probability level.

intramolecular C12—H12···*C7A*≡N2*A* and C15—H15···*C7B*≡N2*A* interactions in the TCPI system. This difference is also present in (II), with an average difference of 7° between the two $Csp^2{=}Csp^2{-}Csp$ angles. TTF and the TCPI isoindolinyl moiety $C_4N[C(CN)_2]_2$ are essentially coplanar [1.21 (4)°] and stack in an alternate fashion along the *a*-axis direction, with a mean interplanar spacing between the ligands of *ca* 3.5 Å. Columns of $[TCPI{-}TTF]_n$ molecules are linked by two weak (TTF)C—H···N interactions (Table 2). A close N3*A*···S2^{iii} contact is also present [symmetry code: (iii) $-x, 1-y, 1-z$].

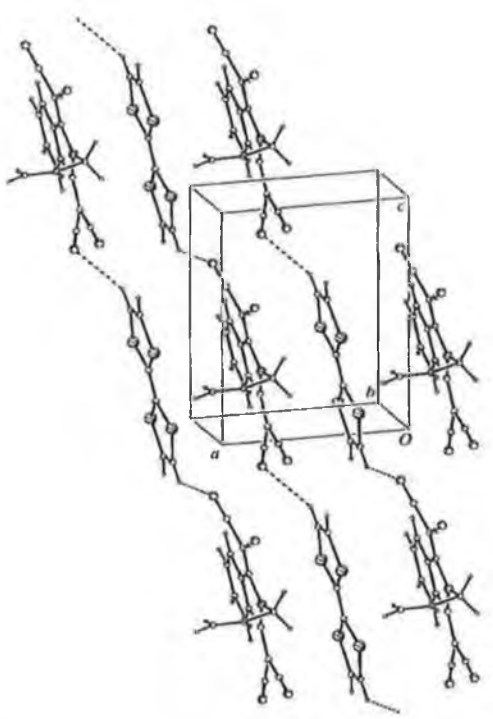

Figure 2
A view of the interactions and packing in the crystal structure of (I).

A CSD search using ConQuest (Version 1.2; Allen & Kennard, 1993) for molecular systems containing the TTF group and bis(propanedinitrile) ligands revealed several related structures, including 2,5-bis(dicyanomethylene)-thieno[3,4-*b*]pyrazine–TTF (1/1) (CSD refcode PUMVOI; Suzuki *et al.*, 1998), bis(tetracyano-3,5-diimino-3,5-dihydropyrrolizinide-*N*,*N*′)nickel(II)–TTF–THF (1/1/2) (SOLGUV; Bonamico *et al.*, 1991) and pentakis[bis(ethylenedioxy)TTF]-tris(dicyanomethylene)cyclopropandiide acetonitrile solvate (TOKXUM; Horiuchi *et al.*, 1996).

Experimental

For the synthesis of TCPI, diisopropylazodicarboxylate (0.37 g, 1.9 mmol) and triphenylphosphine (0.49 g, 1.9 mmol) were shaken together in tetrahydrofuran (40 ml) for 30 s. Allyl alcohol (0.2 g, 3.4 mmol) was added and the mixture was allowed to stand for 2 min, then 2-(3-dicyanomethylene-2,3-dihydroisoindol-1-ylidene)malononitrile (0.50 g, 2.1 mmol) was added. The reaction mixture was sealed under argon and allowed to stand at ambient temperature for one week. The solvent was removed and the residue subjected to chromatography. TCPI was isolated as a green solid (m.p. 240–242 K). Analysis for $C_{17}H_9N_5$, calculated: C 72.08, H 3.20, N 24.72%; found: C 71.83, H 3.28, N 24.60%. IR (KBr, cm^{-1}): 3106, 2222, 1560, 1459, 1332, 1222, 1162, 1111, 783. UV–vis [CH_3CN, λ_{max} nm (ε)]: 414 (35589), 391 (35522), 291 (9394), 279 (10303), 269 (10202), 243 (19966). ^{1}H NMR (400 MHz, δ, $CDCl_3$), 8.74 (*m*, 2H, aromatic), 7.85 (*m*, 2H, aromatic), 6.05 (*m*, 1H), 5.50 (*d*, J = 10.4 Hz, 1H), 5.35 (*s*, 2H), 5.05 (*d*, J = 17.2 Hz, 1H). ^{13}C NMR (δC, DMSO): 157.81 [C=C(CN)$_2$], 135.04 132.60, 125.30 (aromatic C), 114.52, 113.27 (CN), 60.60 [C=C(CN)$_2$], 131.30, 116.69, 48.78 (*N*-allyl).

For the synthesis of the TCPI–TTF complex, TCPI (0.05 g, 0.2 mmol) and TTF were added to acetonitrile (15.0 ml). The mixture was heated under reflux until all the solid material had dissolved. The resulting green solution was allowed to cool to ambient temperature and the TCPI–TTF (1/1) complex crystallized from solution as dark-green needles. The needles were isolated by filtration and recrystallized from acetonitrile to give black–green needles (0.04 g, 41.0%; m.p. 169–172 K). Analysis for $C_{17}H_9N_5{\cdot}C_6H_4S_4$, calculated: C 56.65, H 2.69, N 14.36, S 26.30%; found: C 56.61, H 2.62, N 14.24, S 25.11%. IR (KBr, cm^{-1}): 2218, 1551, 1472, 1327, 1145, 975, 651.

Crystal data

$C_{17}H_9N_5{\cdot}C_6H_4S_4$	D_x = 1.449 Mg m^{-3}
M_r = 487.62	Mo $K\alpha$ radiation
Monoclinic, $P2_1/c$	Cell parameters from 25 reflections
a = 7.3982 (11) Å	θ = 5.5–19.9°
b = 31.854 (5) Å	μ = 0.45 mm^{-1}
c = 9.516 (2) Å	T = 294 (1) K
β = 94.608 (17)°	Needle, black–green
V = 2235.3 (7) Å^3	0.50 × 0.50 × 0.35 mm
Z = 4	

Data collection

Bruker AXS *P4* diffractometer	R_{int} = 0.018
ω scans	θ_{max} = 28.0°
Absorption correction: ψ scan (North *et al.*, 1968)	$h = -1 \rightarrow 9$
T_{min} = 0.806, T_{max} = 0.860	$k = -42 \rightarrow 1$
5764 measured reflections	$l = -12 \rightarrow 12$
5366 independent reflections	3 standard reflections
4247 reflections with $I > 2\sigma(I)$	every 296 reflections
	intensity decay: 1%

Refinement

Refinement on F^2	$w = 1/[\sigma^2(F_o^2) + (0.0586P)^2 + 0.6527P]$ where $P = (F_o^2 + 2F_c^2)/3$
$R[F^2 > 2\sigma(F^2)] = 0.045$	$(\Delta/\sigma)_{max} = 0.001$
$wR(F^2) = 0.121$	$\Delta\rho_{max} = 0.71$ e Å^{-3}
$S = 1.09$	$\Delta\rho_{min} = -0.38$ e Å^{-3}
5366 reflections	
289 parameters	
H-atom parameters constrained	

Table 1
Selected geometric parameters (Å, °).

S1—C1*T*	1.751 (2)	C1*T*—C2*T*	1.344 (3)
S1—C4*T*	1.740 (3)	C3*T*—C4*T*	1.314 (4)
S2—C1*T*	1.763 (2)	C5*T*—C6*T*	1.325 (4)
S2—C3*T*	1.733 (3)	N1—C1	1.471 (2)
S3—C2*T*	1.760 (2)	N1—C4	1.385 (2)
S3—C6*T*	1.731 (3)	N1—C5	1.382 (2)
S4—C2*T*	1.761 (2)	C1—C2	1.496 (3)
S4—C5*T*	1.726 (3)	C2—C3	1.296 (3)
N1—C1—C2	112.65 (17)	C1—C2—C3	126.6 (2)

Table 2
Hydrogen-bond parameters and contact geometry (Å, °).

D—H···*A*	*D*—H	H···*A*	*D*···*A*	*D*—H···*A*
C12—H12···N2*A*	0.93	2.60	3.391 (3)	143
C12—H12···C7*A*	0.93	2.47	3.027 (3)	118
C15—H15···N2*B*	0.93	2.61	3.399 (3)	144
C15—H15···C7*B*	0.93	2.47	3.020 (3)	118
C4*T*—H4*T*···N2*B*^{i}	0.93	2.63	3.479 (3)	152
C6*T*—H6*T*···N2*A*^{ii}	0.93	2.63	3.273 (3)	127

Symmetry codes: (i) $1 + x, y, 1 + z$; (ii) $x, y, z - 1$.

The title compound crystallized in the monoclinic system; space group $P2_1/c$ was assumed from the systematic absences and confirmed by the analysis. All H atoms were allowed for as riding atoms, with C—H distances in the range 0.93–0.97 Å, using *SHELXL97* (Sheldrick, 1997) defaults.

Data collection: *XSCANS* (Siemens, 1994); cell refinement: *XSCANS*; data reduction: *XSCANS*; program(s) used to solve structure: *SHELXS97* (Sheldrick, 1997); program(s) used to refine structure: *SHELXL97* (Sheldrick, 1997); molecular graphics: *ORTEP*III (Burnett & Johnson, 1996) and *PLATON* (Spek, 1998); software used to prepare material for publication: *SHELXL97* and *WordPerfect* macro *PREP8* (Ferguson, 1998).

JFG thanks the Research and Postgraduate Committee of Dublin City University for research funding and the School of Chemical Sciences for the purchase of a Bruker *P4* diffractometer.

Supplementary data for this paper are available from the IUCr electronic archives (Reference: SK1518). Services for accessing these data are described at the back of the journal.

References

Allen, F. H. & Kennard, O. (1993). *Chem. Des. Autom. News*, **8**, 1, 31–37.
Bonamico, M., Fares, V., Flamini, A. & Poli, N. (1991). *Inorg. Chem.* **30**, 3081–3087.
Bryce, M. R. (2000). *J. Mater. Chem.* **10**, 589–598.
Burnett, M. N. & Johnson, C. K. (1996). *ORTEP*III. Report ORNL-6895. Oak Ridge National Laboratory, Tennessee, USA.
Crean, C., Gallagher, J. F. & Pratt, A. C. (2001). *Acta Cryst.* E**57**, o236–o238.
Ferguson, G. (1998). *PREP8*. University of Guelph, Canada.
Horiuchi, S., Yamochi, H., Saito, G., Sakaguchi, K. & Kusunoki, M. (1996). *J. Am. Chem. Soc.* **118**, 8604–8622.
Martin, N., Segura, J. L. & Seoane, C. (1997). *J. Mater. Chem.* **7**, 1661–1676.
North, A. C. T., Phillips, D. C. & Mathews, F. S. (1968). *Acta Cryst.* A**24**, 351–359.
Orpen, A. G., Brammer, L., Allen, F. H., Kennard, O., Watson, D. G. & Taylor, R. (1994). *Structure Correlation*, Vol. 2. edited by H.-B. Bürgi & J. D. Dunitz. Weinheim, Germany: VCH Publishers.
Sheldrick, G. M. (1997). *SHELXS97* and *SHELXL97*. University of Gottingen, Germany.
Siemens (1994). *XSCANS*. Version 2.2. Siemens Analytical X-ray Instruments Inc., Madison, Wisconsin, USA.
Spek, A. L. (1998). *PLATON*. University of Utrecht, The Netherlands.
Suzuki, K., Tomura, M. & Yamashita, Y. (1998). *J. Mater. Chem.* 8, 1117–1119.
Yamashita, Y. & Tomura, M. (1998). *J. Mater. Chem.* **8**, 1933–1944.